UNIVERSITY OF
LIVERPOOL

# Conversion of glycerol to value-added chemicals using multifunctional catalysts

Thesis submitted in accordance with the requirements of the University of Liverpool for the degree of Doctor in Philosophy

by

Abdullah Mohammed A. Alhanash

December 2010

# Abstract


## "Conversion of glycerol to value-added chemicals using multifunctional catalysts"

**PhD thesis by Abdullah M. Alhanash**

The aim of this thesis is to investigate the use of multifunctional catalysts for liquid-phase hydrogenolysis of glycerol to 1,2- and 1,3-propanediols (PDO) and the gas-phase dehydration of glycerol to acrolein. These chemicals are important industrial intermediates and currently produced from petroleum derivatives. The study involves the preparation, characterisation and testing of two different classes of solid acids as supports. $Cs_{2.5}H_{0.5}PW_{12}O_{40}$ (CsPW) is well-known as a water-insoluble strong Brønsted acid with high thermal stability (≥500 °C). The in-house made hydrated niobium oxide ($Nb_2O_5$) is also a water-tolerant, relatively strong acid possessing both Lewis and Brønsted sites and high thermal stability. CsPW and $Nb_2O_5$ were doped with Ruthenium, platinum, rhodium and palladium metals using impregnation method. Catalysts under study were characterised by number of physical and chemical techniques such as nitrogen physisorption, TGA, $NH_3$ adsorption calorimetry, XRD, FTIR and hydrogen chemisorption.

The 5%Ru/CsPW is an active bifunctional catalyst for the one-pot hydrogenolysis of glycerol in liquid phase, providing 96% selectivity to 1,2-PDO at 21% conversion of glycerol at 150 °C and a very low hydrogen pressure of 5 bar. Rhodium catalyst, 5%Rh/CsPW, although less active, shows considerable selectivity to 1,3-PDO (7%), with 1,2-PDO being the main product (65%). 5%Ru/$Nb_2O_5$ also exhibits good activity at similar conditions where 29% conversion of glycerol and 69% selectivity of 1,2-PDO were achieved. Acetol, 1- and 2-propanol, ethylene glycol, ethanol and methane were found amongst by-products. CsPW and $Nb_2O_5$ themselves are not active in the formation of 1,2-PDO, providing only traces of acetol. In the absence of hydrogen, 1,2-PDO and acetol were obtained in the presence of Ru on both catalysts; in this system, $H_2$ is supplied by the liquid phase reforming of glycerol. These results indicate that the reaction probably occurs via dehydrogenation of glycerol to glyceraldehyde followed by dehydration to 2-hydroxyacrolein and further hydrogenation to yield 1,2-PDO.

CsPW, possessing strong Brønsted acid sites, is an active catalyst for the dehydration of glycerol to acrolein in the gas-phase process at 275 °C and 1 bar pressure. The initial glycerol conversion amounts to 100% at 98% acrolein selectivity, however, this decreases significantly with the time on stream (40% after 6 h) due to catalyst coking, without impairing acrolein selectivity. Doping CsPW with platinum group metals (PGM) (0.3–0.5%) together with co-feeding hydrogen improves catalyst stability to deactivation, while maintaining a high selectivity to acrolein. The enhancing effect of PGM was found to increase in the order: Ru ≈ Pt < Pd. The catalyst 0.5%Pd/CsPW gives 96% acrolein selectivity at 79% glycerol conversion, with a specific rate of acrolein production of 23 mmol $h^{-1}$ $g_{cat}^{-1}$ at 275 °C and 5 h time on stream, exceeding that reported previously for supported heteropoly acids (5–11 mmol $h^{-1}$ $g_{cat}^{-1}$ per total catalyst mass). Evidence is presented regarding the nature of acid sites required for the dehydration of glycerol to acrolein, supporting the importance of strong Brønsted sites for this reaction.

# Publications

## Published papers

1- Abdullah Alhanash, Elena F. Kozhevnikova, Ivan V. Kozhevnikov., Hydrogenolysis of glycerol to propanediol over Ru-polyoxometalate bifunctional catalyst, Catal. Lett. 120 (2008) 307.

2- Abdullah Alhanash, Elena F. Kozhevnikova, Ivan V. Kozhevnikov., Gas-phase dehydration of glycerol to acrolein catalysed by caesium heteropoly salt, Appl. Catal. A 378 (2010) 11.

## Poster presentations

1- Abdullah Alhanash, Elena F. Kozhevnikova, Ivan V. Kozhevnikov., Hydrogenolysis of glycerol to propanediol over Ru-polyoxometalate bifunctional catalyst, Poster Day, University of Liverpool, March 2008.

2- Abdullah Alhanash, Elena F. Kozhevnikova, Ivan V. Kozhevnikov., Hydrogenolysis of glycerol to propanediol over Ru-polyoxometalate bifunctional catalyst, The Saudi International Innovation Conference, Leeds, 9-10 June 2008.

3- Abdullah Alhanash, Elena F. Kozhevnikova, Ivan V. Kozhevnikov, Hydrogenolysis of glycerol to propanediol over Ru-polyoxometalate bifunctional catalyst, The 14$^{th}$ International Congress on Catalysis, Seol, South Korea, 13-17 July 2008.

4- Abdullah Alhanash, Elena F. Kozhevnikova, Ivan V. Kozhevnikov, Gas-phase dehydration of glycerol to acrolein over Cs salt of 12-phosphotungstic acid, The 42$^{nd}$ IUPAC Congress, Glasgow, UK, 2-7 August 2009.

## Oral Presentation

1- Abdullah Alhanash, Elena F. Kozhevnikova, Ivan V. Kozhevnikov., Hydrogenolysis of glycerol to propanediol by multifunctional catalysts, the 21st North American Catalysis Society Meeting, San Francisco, USA, 7-12 June 2009.

# Acknowledgements

I would like to express my sincere gratitude to my main supervisor Prof. Ivan V. Kozhevnikov for his invaluable guidance and support throughout the whole course of my study. I am indebted to him for the knowledge and experience that he provided me with that have been fundamental to the success of my PhD project.

My deepest appreciation is forwarded to Dr. Elena F. Kozhevnikova for her kind and endless assistance with experimental work. Thanks very much indeed for her standing with me to solve many technical problems during my laboratory work.

I wish to greatly acknowledge and thank my past and present group members, Ali Alsalme, Fahd Al-Wadaani, Robert Hetterly, Mshari Alotaibi, Maria Tsiamtsouri and Edidiong Dianabasi for their valuable discussions, comments and friendship.

Special thanks are due to laboratory technicians, Moya McCarron, Stephen Apter, Allan Mills and Charles Clavering for the analytical services. Thanks also to Gary Evans and Maria Tsiamtsouri for their help with the XRD experiments.

The scholarship and financial support I received from King Khalid University, Abha, Saudi Arabia are gratefully acknowledged. Extended appreciation goes to the Saudi Arabian Cultural Bureau in the UK for taking the responsibility for my scholarship in the United Kingdom.

I owe my love and respect to my wife, Sarah Alahmed, and my children, Mohammed, Tameem and Husam. Your everlasting love, patience and encouragement have been the secret of my success. Your constant support gave me the strength and courage to complete this project successfully.

Last but definitely not the least, heartfelt thanks to my beloved mother, Rahmah Alsadani, my father Mohammed Alhanash and my brothers and sisters for

always being on my side throughout my life and career. The sacrifices they made, love and patience they displayed have been great motivation to achieve my long-term goals.

# List of abbreviations

| | |
|---|---|
| APR | Aqueous Phase Reforming. |
| BET | Brunauer-Emett-Teller. |
| CsPW | Caesium salt ($Cs_{2.5}$) of phosphotungstic acid ($H_3PW_{12}O_{40}$). |
| CsSiW | Caesium salt ($Cs_{3.5}$) of silicotungstic acid ($H_4SiW_{12}O_{40}$). |
| C | Carbon. |
| DSC | Differential Scanning Calorimetry. |
| DTG | Derivative Thermogravimetric. |
| D | Metal Dispersion. |
| DRIFT | Diffuse Reflectance Infrared Fourier. |
| EG | Ethylene glycol. |
| FTIR | Fourier Transform Infrared. |
| GC | Gas Chromatography. |
| HPA | Heteropoly Acid. |
| ICP | Inductively Coupled Plasma. |
| MS | Mass Spectroscopy. |
| PDO | Propanediol. |
| PGM | Platinum Group Metals |
| PO | Propanol. |
| POMs | Polyoxometalates. |
| TCD | Thermal Conductivity Detector. |
| TGA | Thermogravimetric Analysis. |
| TOF | Turnover Frequency. |
| UV | Ultraviolet. |
| WHSV | Weight Hourly Space Velocity. |
| XRD | X-ray Diffraction. |

# Content

# 1. Introduction

## 1.1 Glycerol

Glycerol is a tri-basic alcohol and named 1,2,3-propanetriol (Scheme 1.1). It was discovered in 1779 by the chemist Carl Wilhelm Scheele and has been used widely as a chemical for more than two centuries. The name glycerol is derived from the Greek word for sweet, "glykos", and the term glycerine is also used in the literature. Glycerol has unique combination of chemical and physical properties (Table 1.1, Scheme 1.1), which makes it one of the most versatile and valuable chemicals [1]. Physically, it is a colourless, viscous liquid with high-boiling point (290 °C). It is very soluble in water, alcohols and other solvents such as ether and dioxane. Its ability to absorb moisture from the atmosphere, and the nontoxic nature enables glycerol to meet certain requirements of food and the cosmetics industry. Among its distinctive characteristics are low vapour pressure and antifreeze properties.

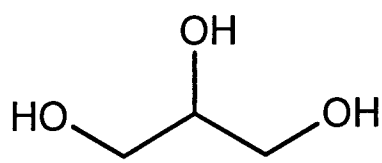


**Scheme 1.1** Structure of glycerol.

Chemically, glycerol consists of three carbon atoms accommodating three hydroxyl groups (Scheme 1.1), which are responsible for its high solubility in water and its hygroscopic nature. Glycerol is very stable under normal conditions and compatible with many other chemicals.

**Table 1.1** Physicochemical properties of glycerol [2].

| | |
|---|---|
| Chemical formula | $C_3H_5(OH)_3$ |
| Molecular mass | 92.09 g $mol^{-1}$ |
| Density | 1.261 g $cm^{-3}$ |
| Vapour pressure | 0.0025 mmHg (50 °C) |
| Boiling point | 290 °C |
| Melting point | 18.17 °C |
| Freezing point | -46.5 °C (66.7% glycerol aqueous solution) |

Due to its chemical stability, glycerol, like other alcohols, is an attractive solvent in many catalytic and non-catalytic organic reactions. As a highly functionalised molecule, glycerol can undergo many chemical transformations to produce a wide range of chemicals. This particular advantage of glycerol makes it a basic building block for the chemical industry [1, 3, 4].

### 1.1.1 Production of glycerol

Glycerol is available in nature in the form of fatty acid esters and also as an important intermediate in the metabolism of living organisms. Traditionally, glycerol can be obtained as a by-product in saponification process in which fats and oils are hydrolysed in the presence of a base to yield glycerol and soap. Up to 90% of glycerol is obtained by the production of fatty acids via the hydrolysis of fatty acid methyl esters and methanolysis of plant and animal fats (both of which are triglycerides) (Scheme 1.2) [3-5].

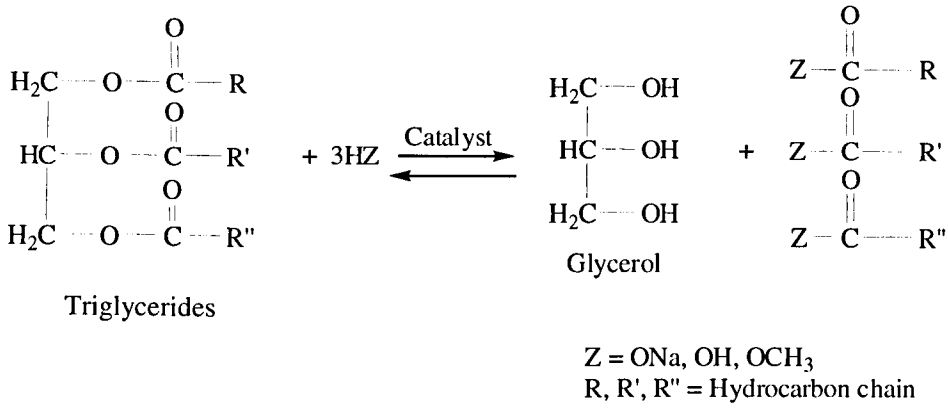


**Scheme 1.2** Production of glycerol from fats and oils.

Glycerol can be synthesised by microbial fermentation. This process has been known for 150 years, and was used on a commercial scale during World War 1. A number of microorganisms were used to produce glycerol by fermentation, including yeasts such as *Saccharomyces cerevisiae*, *Candida magnolia*, bacteria such as *Bacillus subtilis* and algae such as *Dunaliella tertiolecta* [6]. Glycerol has been chemically produced by oxidation or chlorination of petroleum-based propylene, but this route is less attractive for industrial use due to the decreasing availability of propylene and environmental and economical concerns [7]. The production of glycerol from the above processes contributes significantly to the total volume of glycerol production worldwide. However, a new trend in the production of glycerol has emerged in recent years following the development of biodiesel production.

The development of industrial processes to utilise economically and efficiently renewable bioresources for the production of fuels and chemicals is inevitable for several reasons. Among these are the depletion of fossil fuels, pollution caused by the continuous increase of energy demands and the instability and increase of crude oil

prices. Various processes have been developed to convert biomass and biomass-derived molecules into liquid fuels and chemicals [8].

One such process is the production of biodiesel. Biodiesel has become an attractive substitute for fossil fuel and has proved its efficiency as a fuel for diesel engines, being renewable and clean. Therefore, the biodiesel market is expected to grow rapidly to meet the renewable energy demands and the new European Directive target of 5.75% volume of biofuels in the transport sector by 2010 [9]. Biodiesel, a term for fatty acid methyl esters, is produced by transesterification of plant oils and animal fats (Scheme 1.2). Glycerol is the main by-product at a rate of 1 mol of glycerol for every 3 mol of methyl esters synthesised, approximately 10% of the total product by mass [10]. Although, the global production of biodiesel is limited, a large amount of glycerol is available and thus the price of glycerol has sharply declined. This creates new opportunities for glycerol to be one of the top 12 building-block chemicals that can be derived from plant sources, and hence to play an important role in the future biorefineries [11].

### 1.1.2 Traditional uses of glycerol

Due to its unique combination of physical and chemical properties, glycerol is already used in many applications and has over 1500 known uses. For example, it is commonly used in food and beverages as a humectant, a solvent and a preservative. Glycerol is also widely used in drugs and pharmaceuticals as a solvent, a moistener, a humectant and a bodying agent. In addition, glycerol is a major ingredient in cosmetics and other toiletries and is an active agent in tobacco, surface coating resins, paper and

printing, lubrication, textiles and urethane polymers, amongst other things [1, 3, 12]. However, the expansion of glycerol use in these areas is limited and thus finding new uses for glycerol, consisting of high value-added products, is vitally needed in order to improve the economy of the whole biodiesel process and provide a bio-sustainable resource for the production of energy, chemicals and materials (one of the key issues of sustainable development) [4, 13].

### 1.1.3 From glycerol to value-added chemicals

Scientists and research-led institutions worldwide have reacted strongly to the increased availability of glycerol, supported by large amounts of funding from government and industry. Therefore, new processes to convert glycerol into valuable chemicals are being developed. A number of comprehensive reviews have reported a series of novel catalytic processes that produce useful chemicals from glycerol [3, 4, 8, 12].

The traditional applications of glycerol were based on its physical properties and chemical stability, sometimes with a simple chemical modification. Until recently, complex functionalisation of the glycerol molecule was economically restricted. Now, glycerol is both cheap and readily available; therefore, more complex conversions of glycerol into useful chemicals become economically viable.

Glycerol's multifunctional structure enables a large number of catalytic processes to be carried out to form enormous amounts of valuable commodity chemicals (Scheme 1.3) such as dihydroxyacetone (DHA), glyceric acid, hydroxypyruvic acid [3],

glycerol tertiary butyl ether (GTBE), monoglycerides, glycerol carbonate, acrolein [4], 1,2- and 1,3-propanediol (PDO).

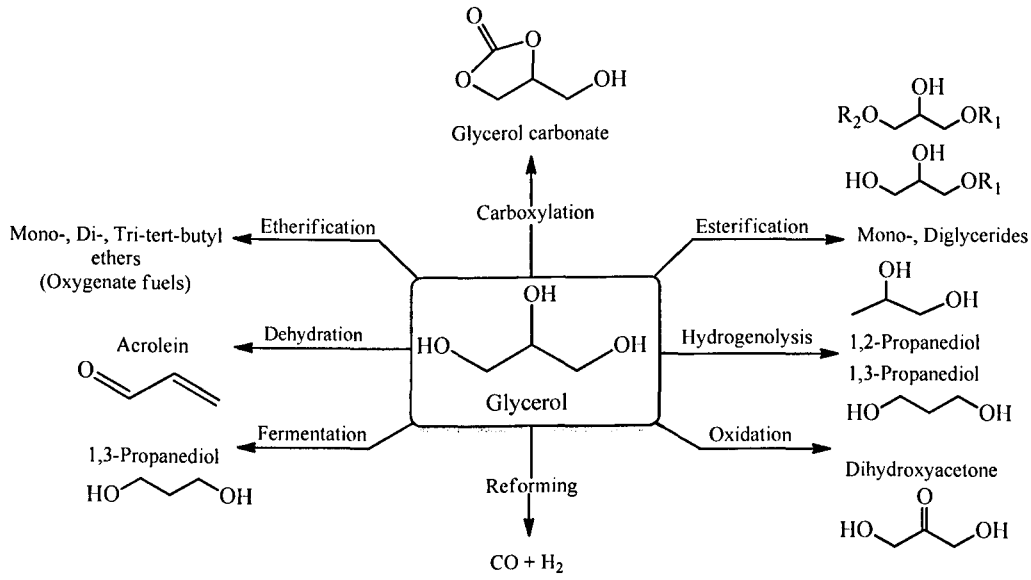


**Scheme 1.3** Possible conversion of glycerol into useful chemicals.

Further possible application of glycerol is its conversion to synthesis gas ($H_2$ and CO), which is essential for the production of fuels and chemicals, such as methanol [14]. This process is one of the major achievements of the new chemical conversions of glycerol. There are several processes to produce synthesis gas from glycerol, such as steam reforming, aqueous phase reforming and gasification in supercritical water [5].

Reduction of glycerol is a topic of great industrial importance. The main products formed from this process are 1,2-propanediol (1,2-PDO) and 1,3-propanediol (1,3-PDO), which are useful commodity chemicals and also valuable starting materials in the synthesis of polymers. These compounds are commercially produced from petroleum derivatives and thus the hydrogenolysis of glycerol to propanediols is an

attractive alternative to the existing petroleum-based processes. This process is discussed in more detail Section 1.1.6.

Acrolein is an important intermediate for the chemical and agricultural industries and is currently produced by the oxidation of petroleum-derived propene. Therefore, the development of an alternative environmentally benign process for acrolein production based on the biomass-derived glycerol is another attractive process in the utilisation of glycerol. This process is also discussed in Section 1.1.7.

## 1.1.4 Current production of 1,2-propanediol

1,2-Propanediol (1,2-PDO) is an important commodity chemical, with a 4% annual market growth. It is used in polyester resins, liquid detergents, pharmaceuticals, cosmetics, tobacco humectants, flavours and fragrances, personal care, paints, animal feed, antifreeze, etc. It is commercially produced from petroleum derivatives by the hydration of propylene oxide derived from propylene, by either the chlorohydrin process or the hydroperoxide process (Scheme 1.4).

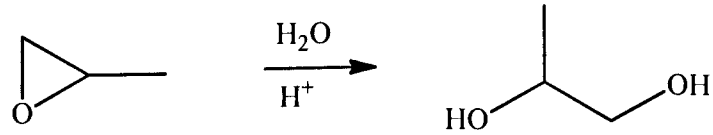


Propylene oxide 1,2-Propanediol

**Scheme 1.4** 1,2-PDO production from petroleum derivative.

There has been a high demand for 1,2-PDO as an antifreeze and de-icing agent, due to growing concerns over the toxicity of ethylene glycol-based products [15]. The

use of raw petroleum materials for the production of 1,2-PDO is less favourable to consumers, and thus a process using renewable feedstock to produce 1,2-PDO needs to be developed.

### 1.1.5 Current production of 1,3-propanediol

1,3-Propanediol (1,3-PDO) is a chemical intermediate that is mainly used in the manufacture of polyester fibres, films and coatings. It is also copolymerised with terephthalic acid, in order to produce DuPont SORONA® polyester and Shell's CORTERRA®, which are both used in the manufacture of carpets and textile fibres exhibiting unique chemical resistance, light stability, elastic recovery and dyeability [16, 17]. 1,3-PDO is currently produced from petroleum derivatives, such as ethylene oxide (the Shell process) and acrolein (the Degussa-DuPont Process) (Scheme 1.5) [17]. The microbial production of 1,3-PDO is currently being developed by DuPont-Genencor in order to produce 1,3-PDO using glucose as a feedstock [18].

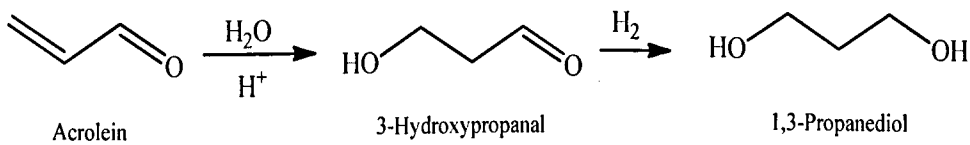


Acrolein-based process (Degussa-DuPont)

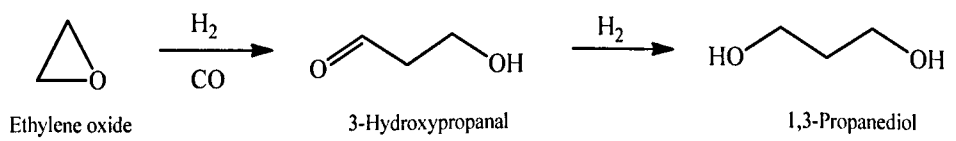


Hydrocarbonylation of ethylene oxide (Shell)

**Scheme 1.5** 1,3-PDO synthesis from petroleum derivatives.

The main disadvantages of these commercial processes are the high pressure required for hydroformylation and hydrogenation, the use of an aromatic solvent in the first steps, the hazardous nature of acrolein and the low conversion efficiency of the acrolein process. Thus, alternative routes for producing 1,3-PDO using other chemical sources (particularly renewable sources) are highly desirable.

### 1.1.6 Alternative routes to 1,2-PDO and 1,3-PDO from glycerol

The availability and low price of glycerol make it an attractive renewable feedstock for producing a wide range of value-added chemicals. The selective hydrogenolysis of glycerol to 1,2-PDO and 1,3-PDO has emerged and thus attracted significant attention as an alternative to the existing petroleum-based processes. The reduction of glycerol in the presence of metallic catalysts and hydrogen has long been known. Scheme (1.6) summarises the overall conversion of glycerol to propylene glycols and ethylene glycol.

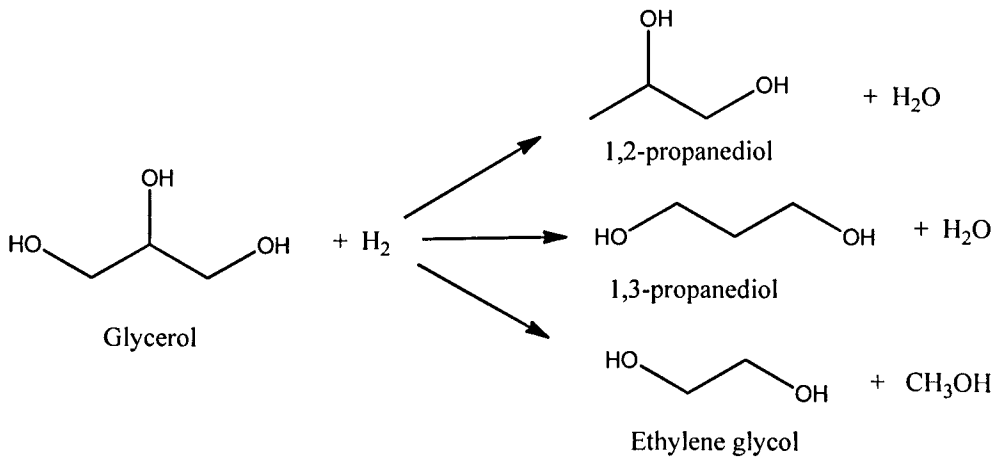


**Scheme 1.6** Glycerol reduction to propylene glycols and ethylene glycol.

Traditionally, alcohols are stable and do not readily react under normal hydrogenating conditions. Moreover, they can be used as solvents in hydrogenation reactions. Thus, the conventional hydrogenation catalysts, such as nickel, ruthenium and palladium, are not readily active when applied to catalytic C–OH cleavage, i.e hydrogenolysis of glycerol. This can be seen from the harsh conditions (200-300°C, 150-318 bars of $H_2$) at which glycerol reduction was carried out in early publications and patents [19, 20]. It was found from the reaction products that the process is a multi-stage one rather than a single reduction step. The term hydrogenolysis has been used to describe this reaction in practically all relevant publications and, in terms of the process of glycerol hydrogenolysis, it means that a C-O bond is broken and an H is inserted in its place. This process has long been established [21-24].

The fundamental chemistry and mechanism of glycerol hydrogenolysis has to be understood for the development of glycerol hydrogenolysis technology. Preliminary investigations of glycerol hydrogenolysis into propylene glycols have shown that hydroxyacetone (acetol) was among the reaction products, indicating that it could be an intermediate in the hydrogenolysis process. The presence of 1,2- and 1,3-propanediols as the main hydrogenolysis products indicates that they are formed through different intermediates.

The dehydration of the alcohol group is a well-known process that occurs when alcohol is heated with concentrated $H_2SO_4$ (Equation 1.1), producing the corresponding alkene [25].

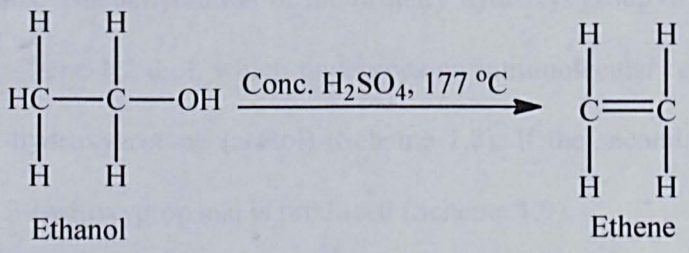


Ethanol Ethene

This is an elimination reaction which follows the E1 or E2 mechanism. The first step is the protonation of the OH group followed by loss of $H_2O$ (a good leaving group). The reaction intermediate is a carbenium ion that loses $H^+$ in the presence of water, which acts as a base (Scheme 1.7). The order of stabilities of carbenium ions are $[R_3C]^+ > [R_2CH]^+ > [RCH_2]^+$ (R = alkyl substituent), which implies that tertiary alcohols undergo dehydration more readily than secondary or primary alcohols. The nature R plays an important role in the overall reaction mechanism, however, the initial stages are common in many alcohol reactions [25, 26].

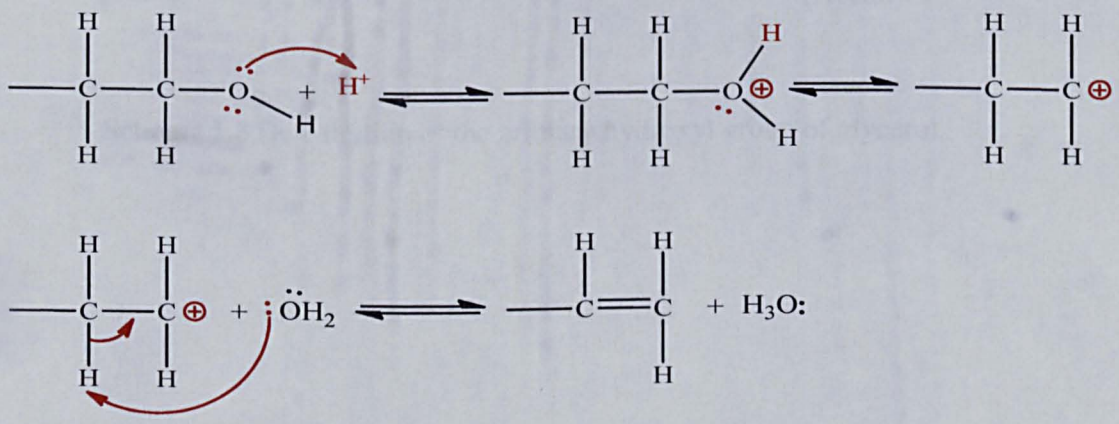

**Scheme 1.7** The mechanism of alcohol dehydration.

Although glycerol is an alcohol, its dehydration is rather complicated. Considering the nature of glycerol, when the dehydration reaction takes place, the internal or terminal hydroxyl group can be attacked, depending on the catalytic system and reaction conditions. The dehydration of the primary hydroxyl group of the glycerol molecule forms prop-2-ene-1,2-diol, which undergoes an intramolecular rearrangement to finally produce 2-hydroxyacetone (acetol) (Scheme 1.8). If the secondary hydroxyl group is dehydrated, 3-hydroxypropanal is produced (Scheme 1.9).

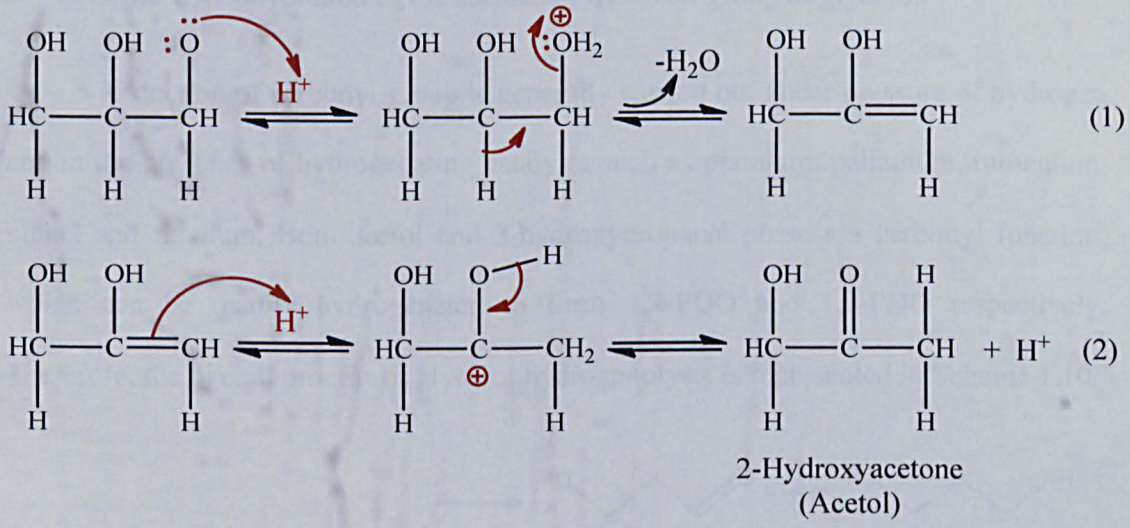


**Scheme 1.8** Dehydration of the primary hydroxyl group of glycerol.

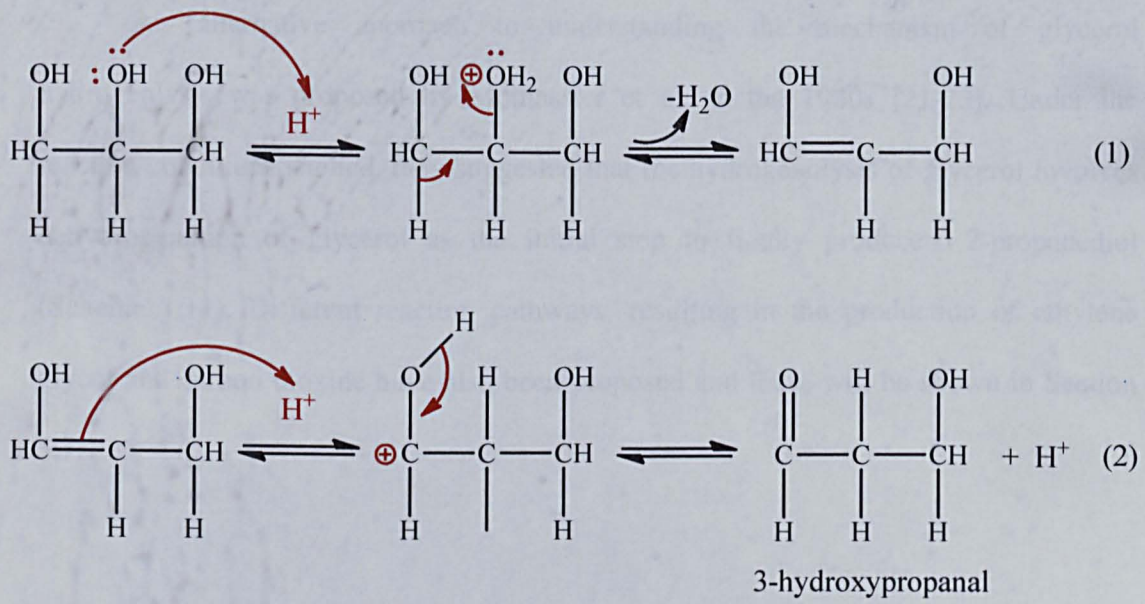


**Scheme 1.9** Dehydration of the secondary hydroxyl group of glycerol.

Reduction of carbonyl group is generally carried out under pressure of hydrogen and in the presence of hydrogenating catalysts such as platinum, palladium, ruthenium, nickel and rhodium. Both acetol and 3-hydroxypropanal possess a carbonyl function, which can be readily hydrogenated to form 1,2-PDO and 1,3-PDO respectively. Therefore, the overall process of glycerol hydrogenolysis is represented in Scheme 1.10:

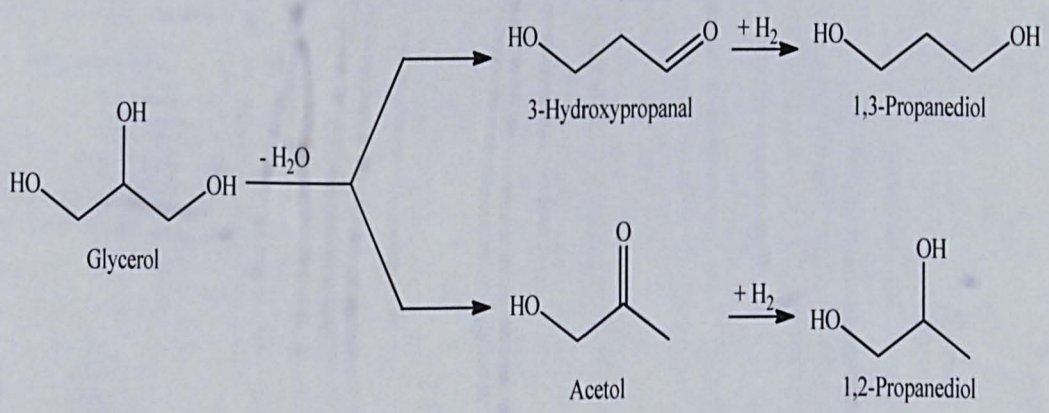


**Scheme 1.10** Hydrogenolysis of glycerol (dehydration + hydrogenation) to 1,2-PDO and1,3-PDO.

An alternative approach to understanding the mechanism of glycerol hydrogenlysis was proposed by Montassier et al. in the 1980s [21-23]. Under the reaction conditions studied, they suggested that the hydrogenolysis of glycerol involves dehydrogenation of glycerol as the initial step to finally produce 1,2-propanediol (Scheme 1.11). Different reaction pathways, resulting in the production of ethylene glycol and carbon dioxide have also been proposed and these will be shown in Section 5.7.

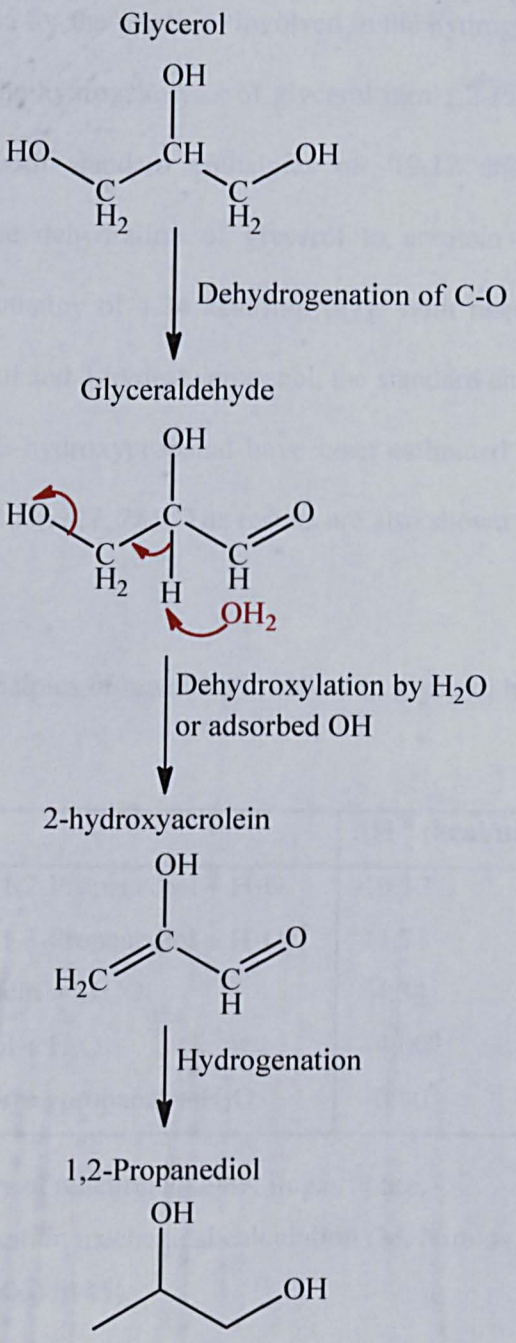


**Scheme 1.11** Hydrogenolysis of glycerol through initial dehydrogenation[23].

Thermodynamic data for the reactions involved in the hydrogenolysis of glycerol are shown in Table 1.2.. The hydrogenolysis of glycerol into 1,2-PDO and 1,3-PDO is an exothermic reaction, with standard enthalpies of -19.12 and -11.71 kcal/mol, respectively. The gas-phase dehydration of glycerol to acrolein is an endothermic reaction with a standard enthalpy of 4.34 kcal/mol [27]. With respect to the possible reaction intermediates, acetol and 3-hydroxypropanal, the standard enthalpies of glycerol dehydration to acetol and 3-hydroxypropanal have been estimated theoretically using quantum mechanical calculation [27, 28]. The results are also shown in Table 1.2.

**Table 1.2** The standard enthalpies of reactions involved in glycerol hydrogenolysis [28-30].

| **Reaction** | **$\Delta H^{\circ a}$ (kcal/mol)** |
|---|---|
| Glycerol + $H_2$ → 1,2-Propanediol + $H_2O$ | -19.12 |
| Glycerol + $H_2$ → 1,3-Propanediol + $H_2O$ | -11.71 |
| Glycerol → Acrolein + $2H_2O$ | 4.34 |
| Glycerol → Acetol + $H_2O$ | -4.00[b] |
| Glycerol → 3-Hydroxypropanal + $H_2O$ | -0.80[b] |

a) Standard enthalpy of reaction at 298K in gas phase.

b) Estimated by quantum mechanical calculation (M. Nimlos et al. J. Phys. Chem. A 110 (2006) 6145).

### 1.1.6.1 Catalysis for glycerol hydrogenolysis to propanediols

Catalysis is vital for modern industry: approximately 90% of chemicals and materials are produced using catalysts, at one stage or more of the catalytic process. Glycerol possesses a rich functionality that can be tailored to several reaction pathways

in order to create many diverse chemicals. Thus, catalysis is a key factor in the 'green' utilisation of glycerol. Catalysis also plays a crucial role in the hydrogenolysis of glycerol to propanediols. A great number of homogeneous, heterogeneous and bio-catalysts have been considered for the purpose of glycerol hydrogenolysis.

### 1.1.6.1.1 Homogeneous and bio-catalysts

The hydrogenolysis of glycerol into propanediols has been tested in the presence of a number of homogenous metal complex catalysts. Catalytic systems based on $Rh(CO)_2(acac)$ and $H_2WO_4$ in N-methyl-2-pyrrolidone (NMP) has been successfully employed achieving 21% conversion at 200 °C and 320 bar pressure, 1,3-PDO and 1,2-PDO were produced with 20% and 23% yield respectively [31]. Ruthenium complex has also been tested for the catalytic hydrogenolysis of glycerol in sulfolane under mild conditions (50 bar, 110 °C); however, very low yields of the desirable products were obtained (<5%) [32]. A process using homogeneous palladium complex in water-sulfolane mixture has been developed by Shell Oil Company [3]. 1-Propanol, 1,2-PDO and 1,3-PDO were obtained after 10 h reaction time with selectivities of 47%, 22%, and 31% respectively.

In order to increase the selectivity to 1,3-PDO, Wang et al. used *p*-toluenesulfonic acid as a catalyst, in the presence of a protection group. The process consisted of four steps, namely the acetalisation of glycerol with beznaldehyde, the tosylation of the resulting compound and further hydrolysis and hydrogenolysis, which led to 1,3-PDO, with an overall yield of 72% [33]. As expected, the use of homogeneous catalysts has shown greater control over product selectivity. Therefore, the selectivity of the more valuable 1,3-PDO was higher than that achieved with heterogeneous systems.

However, the use of homogeneous catalysts requires the addition of solvents, which is unfavourable due to environmental concerns and the costs associated with the separation processes.

Some enzymes have been examined in order to determine their capacity to convert glycerol to 1,3-PDO. A number of different bacteria were able to ferment glycerol with sufficient results; *Bacillus, Klebsiella, Citrobacter, Enterobacter, Clostridium Butyricum* and *Lactacillus* [18]. One example of a technology that uses bacteria to produce 1,3-PDO is the process developed by Genencor International and DuPont, in which glycerol is fermented to 1,3-PDO with recombinant *Escherivhia coli* [5].

#### 1.1.6.1.2 Heterogeneous catalysts for liquid-phase hydrogenolysis of glycerol

Several patents and papers have disclosed glycerol hydrogenolysis using various heterogeneous catalysts such as copper and zinc catalysts [34], sulfided ruthenium on carbon [35] and catalysts containing cobalt, copper, manganese molybdenum, and inorganic polyacid to obtaine 95% yield of 1,2-PDO at 250 bar and 250 °C [36].

These initial data have shown that the overall reaction is influenced by various reaction parameters, such as catalysts, metals, solvents, pressure, temperature, glycerol concentration and reaction time. Hence, in order to obtain the optimum conversion of glycerol and product selectivity, complex conditions and catalytic systems are needed.

### 1.1.6.1.2.1 Synthesis of 1,2-PDO using copper-containing catalysts

Suppes et al. studied low-pressure hydrogenolysis of glycerol to 1,2-PDO using nickel, palladium, platinum, copper and copper-chromite catalysts [20, 37]. 80% wt glycerol aqueous solution was used and copper-chromite was identified as the most active catalyst leading to 73% yield of 1,2-PDO at moderate conditions of 14 bar and 200 °C. This process was distinctive over the traditional processes that use more severe conditions. The reaction was carried out in two steps (Scheme 1.12): (1) the dehydration step in which pure acetol (1-hydroxyacetone) as a reactive intermediate was obtained from glycerol at atmospheric pressure and 200 °C, and (2) the hydrogenation step, when acetol was hydrogenated to 1,2-PDO at the same reaction temperature and at 14 bar hydrogen pressure.

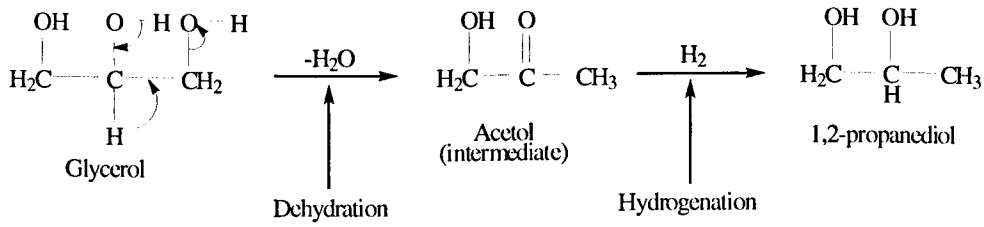


**Scheme 1.12** Reaction mechanism for glycerol conversion to 1,2-PDO on copper-chromite [20].

Lui et al. reported that the co-precipitated Cu-ZnO catalyst effectively catalyses glycerol hydrgenoylysis to 1,2-PDO at 180 - 240 °C, pH 12, and 42 bar. 40% glycerol conversion and 77% 1,2-PDO selectivity were achieved. The acidic ZnO itself showed only dehydration products (acetol and glycidol) whereas CuO gave high selectivity to 1,2-PDO with low conversion of glycerol. Therefore, higher glycerol conversion can be

obtained with the Cu-ZnO catalysts containing combined acid and hydrogenation functions. The authors suggested that the reaction proceeds most likely via bifunctional pathway which includes glycerol dehydration to acetol and glycidol intermediates on acidic ZnO surfaces followed by their hydrogenation on Cu surfaces. This is consistent with the results reported by Suppes et al. using copper-chromite catalyst (Scheme 1.12) [20, 37]. Small ZnO and Cu particles were found to be formed at higher pH values (e.g. at pH = 12), leading to higher conversions and selectivities of 1,2-PDO. The high pH values did not show any effect on the bifunctional pathway but affected the catalyst structure preventing the aggregation of catalyst particles.

Although identified as the most effective catalyst for glycerol reaction to 1,2-PDO, the copper-chromite catalyst and other chromium containing catalysts raise environmental concerns. Therefore, the preparation of copper, the active component in all copper containing catalysts, chromium-free catalysts is attracting significant attention recently. Xia et al. reported that $CuO/SiO_2$ catalyst prepared by precipitation-gel (PG) method was efficient in the hydrogenolysis of glycerol, and featured much higher activity and stability than the same catalyst prepared by the convenient impregnation method (IM) [38]. 73% conversion of glycerol and 94% 1,2-PDO selectivity were achieved using pre-reduced PG catalyst at reaction conditions: 80% glycerol aqueous solution, 90 bar $H_2$, 200 °C and 12 h. Based on the characterisation data, it was explained that the high performance of the PG catalyst could be due to a much small particle size and high dispersion of copper species with strong metal-support interaction and high resistance to sintering. The $Cu^0$ formed during the pre-reduction treatment and/or generated in situ during the reaction is believed to be the active site for glycerol reaction; and high copper surface area leads to high reactivity. The $Cu^+$ species formed

during the pre-reduction treatment that may be catalytically inactive in glycerol reaction, is suggested to help inhibit the sintering of active phases during the reaction. The reaction is likely to proceed via a metallic copper, and the in situ generated acid sites catalyses the dehydration of glycerol to form acetol, which is subsequently hydrogenated to 1,2-propanediol over copper surface [38].

To improve the efficiency of active Cu component for glycerol hydrogenolysis, Cu was doped using various supports including $\gamma$-$Al_2O_3$, HZSM-5, HY, H$\beta$ [39]. Cu/ $\gamma$-$Al_2O_3$ exhibited the best catalytic activity, with 50% glycerol conversion, and 96% selectivity at 220 °C, 15 bar, 10 h. Pre-reduction of catalyst at 300 °C in hydrogen was necessary to generate Cu active sites for higher catalytic activity, similar to that reported previously [20, 38]. Partial deactivation of the catalyst was observed.

Rode et al. introduced a non-chromium Cu:Al nano catalyst, prepared by simultaneous co-precipitation, for liquid phase hydrogenolysis of glycerol to 1,2-PDO [40]. The maximum conversion obtained was 76% with 89% selectivity to 1,2-PDO, at 240 °C 70 bar $H_2$, 5 h, 100 mL of 20% glycerol aqueous solution. The major by-product was EG which is favoured at high temperatures. The authors explained that the high performance of the Cu:Al nano catalyst for glycerol hydrogenolysis is probably due to the following two reasons. (1) The higher acidic sites as shown by ammonia TPD results, leading to faster dehydration of glycerol to form acetol, as proposed that alumina-supported copper as well as pure copper were effective catalysts for the dehydration of glycerol to acetol under inert conditions [41]. (2) Acetol formed undergoes a fast hydrogenation to 1,2-PDO, catalysed by nano sized $Cu^0$, which is stabilised due to the inhibition of sintering by $Cu^+$, the presence of which is evidenced by the XRD pattern, in agreement with that reported by Xia et al. [38, 40].

More recently, Wang et al. investigated the catalytic properties of supported Cu/SBA-15 catalyst prepared by the ion-exchange method for the hydrogenolysis of glycerol in fixed-bed tubular reactor [42]. For 1%Cu/SBA-15 catalyst, 96% conversion of glycerol and 92% selectivity of 1,2-PDO were reached at 250 °C, 40 bar, LHSV 0.8 $h^{-1}$, 80% glycerol aqueous solution and 7 h reaction time. The catalytic performance of 1%Cu/SBA-15 catalyst remained constant during 20 h time-on-stream, indicating the higher stability of this catalyst. The relatively large specific area of SBA-15 support could result in a better dispersion of Cu species and lead to the formation of active and durable Cu species against sintering [42].

Zheng et al. carried out glycerol hydrogenolysis to 1,2-PDO over CuO/MgO catalysts prepared by impregnation and coprecipitation at 180 °C and 30 bar $H_2$ [43]. It has been found that the 15%Cu/MgO catalyst prepared by coprecipitation had the best activity. The conversion of glycerol and the selectivity of 1,2-PDO over 15%Cu/MgO reached 72.0% and 97.6%, respectively. And the conversion of glycerol was further increased to 82.0% when small amount of NaOH was added to the reaction mixture. Characterization results revealed that the activity of the prepared catalysts depends strongly on the particle size of both Cu and MgO. Catalysts that have smaller sized Cu and MgO particles are more active for glycerol hydrogenolysis. This is consistent with all reported copper supported catalysts [38, 42].

### 1.1.6.1.2.2 Synthesis of 1,2-PDO using supported noble metal catalysts

Tomishige et al. reported that the combination of Ru/C and cation exchange resins, such as Amberlyst-15, exhibit higher activity in glycerol hydrogenolysis under mild conditions (120 °C, 40-80 bar) than other metal-acid bifunctional catalysts such as zeolites, sulphated zirconia, $H_2WO_4$ and liquid $H_2SO_4$ and HCl [44-46]. However, catalyst performance was rather low: 1,2-PDO together with 1,3-PDO were obtained with 55 and 5% selectivity, respectively, at 13% glycerol conversion. In this system, Rh/C also exhibited some catalytic activity and higher selectivity to 1,3-PDO, whereas Pd/C and Pt/C were practically inactive. Acetol was observed over Ru/C + Amberlyst 15 under standard reaction conditions, however, at a very low yield (0.01%). Therefore, acetol is suggested to be an intermediate for glycerol hydrogenolysis to 1,2 and 1,3-PDO. The hydrogenation of acetol over Ru/C, Rh/C, Pt/C and Pd/C selectively forms 1,2-PDO with no degradation reaction of acetol. The order of hydrogenation activity was Ru/C > Rh/C > Pt/C > Pd/C. In the absence of Ru/C, no hydrogenolysis products were obtained, however, about 0.1% yield of acetol formation was observed. Using Ru/C in the absence of Amberlyst, 1,2- and 1,3-PDO were obtained with a considerable yield. 1- and 2-propanol (1-PO, 2-PO), ethylene glycrol (EG), methanol and methane were among reaction side-products. The activity of reaction products was investigated under reaction conditions. The reactivity order was 1,3-PDO > EG > 1,2-PDO. On the basis of the above results, general mechanism shown in scheme 1.13 was proposed.

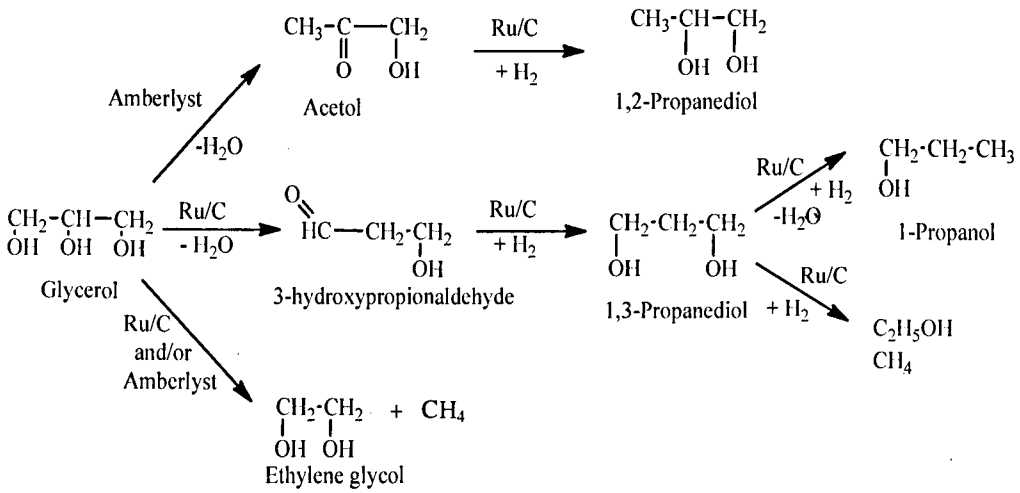


**Scheme 1.13** Reaction scheme of glycerol hydrogenolysis and degradation reaction using Ru/C + Amberlyst-15 [44].

Ru/C prepared using active carbon with low surface area (~ 250 $m^2/g$) and $Ru(NO)(NO_3)_3$ precursor treated with Ar flow at the appropriate temperature enhanced the conversion of glycerol and 1,2-PDO selectivity compared to the commercially available Ru/C. It was also found that the rate of formation of 1,2-PDO was remarkably enhanced by the addition of Amberlyst whereas 1,3-PDO + 1-PO + 2-PO formation rates were not influenced by the addition of Amberlyst. This indicates that 1,2-PDO can be formed via glycerol dehydration to acetol catalysed by Amberlyst and the subsequent hydrogenation of acetol to 1,2-PDO catalysed by Ru/C. In contrast, 1-PO and 2-PO can be obtained from 1,3-PDO over Ru/C (Scheme 1.13) [45].

The activity of Ru/C + Amberlyst-15 system decreased significantly at higher reaction temperatures. This was explained by the poisoning of Ru/C with sulphur compounds such as $SO_2$ and $H_2S$, which are formed by the thermal decomposition of the resin. Therefore, this process is limited by the highest operation temperature of the ion-

exchange resin. The use of home-made Ru/C and heat-resistant Amberlyst-70, whose highest operating temperature is 190 °C, greatly increased glycerol conversion from 13% to 48% and selectivity of 1,2-PDO from 55% to 70% [44].

Amberlyst itself was not active for the dehydration of glycerol to acetol though it was suggested to be the hydrogenolysis reaction intermediate. With copper-chromite, acetol proved to be the reaction intermediate as it was selectively formed in the absence of hydrogen with no hydrogenolysis products. Ru/C itself was active under reaction conditions with considerable selectivity to 1,2-PDO.

Various supported catalysts (metal: Rh, Ru, Pt, Pd support: active carbon, $SiO_2$, $Al_2O_3$) have been investigated by Tomishige et al. under reaction conditions similar to that of the Ru/C + Amberlyst system [47]. Pd and Pt exhibited low activity with supports. It was also found that $Rh/SiO_2$ is much more active than $Rh/Al_2O_3$ and Rh/C. This was explained by reduction of Rh species under reduction pre-treatment; therefore the active metallic species of Rh is more abundant over $SiO_2$ support. However, the reduction of Ru species on $SiO_2$ and $Al_2O_3$ occurred above the reduction pretreatment and reaction temperature (120 °C) meaning that the Ru active species is not formed which could explain the low activity of Ru/ $SiO_2$ and $Ru/Al_2O_3$.

$Rh/SiO_2$ exhibited higher activity and selectivity to hydrogenolysis products (1,2-PDO, 1,3-PDO, 1-PO, 2-PO) in the reaction of glycerol under hydrogen than Ru/C. Under higher $H_2$ pressure and higher glycerol concentration, $Rh/SiO_2$ was more effective than Ru/C. From previous work, the addition of Amberlyst to Ru/C promoted glycerol conversion and the total hydrogenolysis product yield, in particular, 1,2-PDO. On the other hand, the addition of Amberlyst to $Rh/SiO_2$ enhanced glycerol conversion and hydrogenolysis product yields, however, 1-PO formation was promoted most

significantly. Therefore, the reaction route of glycerol hydrogenolysis on $Rh/SiO_2$ can be different from that of Ru/C shown in Scheme 1.13. Glycerol reaction may proceed mainly from 1,3-PDO on Ru/C, while propanols can be formed from consecutive reaction of 1,2-PDO on $Rh/SiO_2$.

Davis and co-workers studied hydrogenolysis of glycerol over carbon-supported Ru, Pt, and bimetallic PtRu and AuRu catalysts [48, 49]. Ru/C and Pt/C were examined, the effects of NaOH and CaO additions on the reaction rates were studied and the overall reaction routes were studied. The addition of both NaOH and CaO improved the rate of glycerol hydrogenolysis over both catalysts; however, the improvement was greater with Pt/C than Ru/C. Under neutral conditions, Ru favours the formation of ethylene glycol over propylene glycol. The results supported the mechanism presented in Scheme 1.11 in which metal-catalysed glycerol dehydrogenation is the first step. A more detailed mechanism was proposed to account for the results of their study [48, 49].

Zhanping Li et al. reported that Re ($Re_2(CO)_{10}$) possesses high promoting effects on the catalytic performance of Ru/C, $Ru/Al_2O_3$ and $Ru/ZrO_2$ in glycerol hydrogenolysis [50]. Conversion of glycerol and 1,2-PDO selectivity increased upon the addition of Re, whereas the selectivity to EG decreased, suggesting that Re may inhibit the degradation reaction of glycerol.

An investigation into the effect of catalyst preparation conditions, reduction temperature and support on the hydrogenolysis of glycerol to propanediols was carried out by Xianjun Li et al [51]. It has been revealed that the catalytic activity of tested supports in the presence of Ru increases in the order $SiO_2$ < NaY < $\gamma$-$Al_2O_3$ < C < $TiO_2$. Interestingly, the Ru particle sizes of the catalysts before reaction decrease in the order $Ru/SiO_2$ > Ru/NaY > $Ru/\gamma$-$Al_2O_3$ > Ru/C > $Ru/TiO_2$, which is consistent with their

increasing activity with respect to the support. This indicates that the hydrogenolysis of glycerol is more active on small metal particles [51], in good agreement with the results reported by Tomishige et al [46]. The difference in Ru particle size on different supports can be related to the intrinsic property of the support as shown in previous studies [51]. Different supports have also shown remarkable effects on the selectivity of the desirable products. The selectivity of 1,2-PDO was significantly higher over $Ru/SiO_2$, Ru/NaY, $Ru/\gamma\text{-}Al_2O_3$ and Ru/C than EG. However, $Ru/TiO_2$ catalyst favoured the production of EG over 1,2-PDO under tested conditions (180 °C, 50 bar). Increasing the reduction temperature from 200 to 500 °C resulted in a decrease in catalyst activity accompanied by a decline in 1,2-PDO selectivity and an increase in EG selectivity. This remarkable effect was explained by: (1) the growth in the Ru particle size caused by heating treatment; (2) the strong metal-support interaction (SMSI) which results in partial covering of Ru metal particles by $Ti_2O_3$ species especially above 300 °C [51].

Regarding the reaction mechanism, the results show that the support in the presence of metal influences the reaction routes. In presence of supports, acetol was not observed, indicating that the glyceraldehyde route proposed by Montassier et al. [22] is most likely. In this mechanism, the metal site (Ru) catalyses both hydrogenation and dehydrogenation reactions in the whole process.

### 1.1.6.1.2.3 Synthesis of 1,2-PDO using supported non-noble metal catalysts

Ni-based catalysts have been successfully employed for a number of chemical reactions such as hydrogenation and hydrogen production from aqueous phase reforming of oxygenated hydrocarbons [52-55]. A Raney Ni catalyst has been employed for selective hydrogenolysis of glycerol to 1,2-PDO [56]. The catalyst was active at 190 °C and 10 bar of $H_2$ providing 79% 1,2-PDO selectivity at 32% conversion of glycerol. Ethanol and $CO_2$ were observed as by-products and no solvents or promoters were required. No 1,3-PDO or low alcohols were formed indicating that the second glycerol OH may not be reactive under these conditions, unlike the competitive formation of 1,2-PDO and 1,3-PDO in other systems.

Ni has been further investigated using zeolite and active carbon as supports [57, 58]. Ni/NaX catalyst has been found efficient in glycerol hydrogenolysis to 1,2-PDO and the acidity of zeolite support strongly influences the conversion and selectivity of the catalyst [57]. At 200 °C, under 60 bar $H_2$ and after 10 h the conversion reached 86% with 94% selectivity for 1,2-PDO. Trace amounts of acetol were detected, therefore, the proposed reaction pathway for glycerol hydrogenolysis over Ni/NaX is suggested to be via acetol intermediate, followed by hydrogenation over Ni surface to form 1,2-PDO. However, no data is available for the activity of zeolite support in the absence of Ni in this study. Other acidic supports [51] were not active for acetol formation in the absence of metals, therefore, NaX support is likely to behave similarly in the absence of Ni catalyst, implying that the reaction may proceed via glyceraldehyde intermediate.

Ni/AC (active carbon), reduced in the presence of carbon at 500 °C under $N_2$ flow and further treated with $KBH_4$ (denoted Ni/AC-CB), has shown greater performance compared to $H_2$ reduced catalyst [58]. Ni/AC-CB catalyst gave 43% glycerol conversion and 76% selectivity for 1,2-PDO at 200 °C under 50 bar $H_2$ after 6 h. The high activity of this catalyst was explained by the synergy effect of hydrogenation centre and the acidity generated from the variation of oxygen-containing surface group (OSGs). The carbothermal reduction was suggested to form metallic Ni and generate large amount of (OSGs) which could lead to higher dispersion of Ni. The treatment of $KBH_4$ increased the acidity of the catalyst, as confirmed by $NH_3$-TPD study, by reducing carbonyl groups of (OSGs) to phenolic hydroxyls, which represent the acid sites of active carbon [58]. This paper concludes that the synergetic effect of metal and acidity function enhances the catalytic performance.

Bifunctional Co/MgO catalyst has been investigated for 1,2-PDO synthesis via glycerol hydrogenolysis [59]. Low 1,2-PDO selectivity (42%) at 45% glycerol conversion was achieved using calcination temperature of 600 °C. At lower calcination temperatures, poor glycerol conversion took place. The high calcination temperatures (e.g. 600 °C) greatly strengthen the interactions between $Co_3O_4$ and MgO promoting the formation of $MgCo_2O_4$ spinel and Mg–Co–O solid solution, which decreases the reducibility of cobalt oxides. However, this strong interaction prevents the aggregation of Co particles in the resulting Co/MgO catalyst under glycerol hydrogenolysis conditions, showing a much higher activity and stability. The glycerol reaction has been proposed to take place via dehydrogenation step to form glyceraldehyde and/or pyruvaldehyde intermediates over the basic sites of $Mg(OH)_2$, which is formed under

reaction conditions. The hydrogenation of these intermediates to 1,2-PDO is catalysed by Co particles. This mechanism is consistent with that reported by Davis et al [48, 49], which states the dehydrogenation of glycerol to glyceraldehyde and/or pyruvaldehyde in basic conditions.

### 1.1.6.1.3 Heterogeneous catalysts for gas-phase synthesis of 1,2-PDO

The gas phase hydrogenolysis of glycerol to value-added products has recently been conducted by several research groups [41, 60-62]. The gas phase process has shown the ability to overcome some of the difficulties of the liquid-phase process. These include discontinuous operation, use of solvents, high hydrogen pressure and catalyst separation from slurry phase reactors.

Suppes et al. have carried out gas phase conversion of glycerol to 1,2-PDO in low-pressure packed-bed reactor using copper-chromite catalyst [60]. The effect of reaction parameters such as gas feed, reaction temperature, catalyst loading and hydrogen feed rate have been investigated. Higher yields of 1,2-PDO were obtained at higher hydrogen feed rates whereas temperatures higher than 220 °C resulted in undesired by-product formation. 100% conversion of glycerol and single-pass yields of 1,2-PDO >50% were achieved in the temperature range of 220 - 230 °C at atmospheric pressure with a hydrogen feed of 5 ml/min, 1160 g of catalyst and 2.5% glycerol solution. In this process, a two-step mechanism to produce 1,2-PDO via acetol intermediate was proposed and validated (Scheme 1.12).

Zeng et al. have successfully demonstrated continuous production of 1,2-PDO by selective hydrogenolysis of solvent-free glycerol in a fixed-bed reactor using $Cu/ZnO/Al_2O_3$ [61]. At 190 °C and 6.4 bar $H_2$, almost 100% conversion of glycerol was

achieved with 1,2-PDO selectivity up to 92%. In another work reported by Yokota et al., copper metal catalysts provide an active site for the dehydration of glycerol and other triols and diols to afford the corresponding hydroxyketones [41]. Alumina-supported copper showed the best catalytic activity with hydroxylacetone (acetol) selectivity of > 90 mol% at ambient pressure of nitrogen and 250 °C.

These initial data reveals that by using copper-containing catalysts in the gas phase, 12-PDO can be formed from glycerol via acetol intermediate with great selectivity at high glycerol conversion. This is similar to reaction mechanism reported using copper-containing catalysts in liquid phase hydrogenolysis of glycerol. The catalyst deactivation, however, is a major problem.

### 1.1.6.1.4 Heterogeneous catalysts for liquid-phase synthesis of 1,3-PDO

Chaminand et al. carried out the hydrogenolysis of glycerol using Pd, Cu, and Rh supported on ZnO, C and alumina at 80 bar pressure at 180 °C in the presence of solvents (water, sulfolane, dioxane) and additives ($H_2WO_4$) [16]. To improve the selectivity to 1,3-PDO , the reaction was conducted with Rh catalysts and tungstic acid was added to the reaction medium. The authors obtained the best conversion and selectivity to 1,3-PDO (1,3-PDO/1,2-PDO = 2) when using sulfolane as a reaction medium.

Sazaki et al. have reported a breakthrough in the formation of 1,3-PDO using $Pt/WO_3/ZrO_2$ [63]. High yields of 1,3-PDO up to 24% were obtained at 170 °C, 80 bar, 18 h in the presence of DMI (1,3-dimethyl-2-imidazolidinone) as a stable solvent.

Furthermore, $Pt/WO_3/ZrO_2$ catalyst prepared by sequential impregnation of $WO_3$ and then Pt on $ZrO_2$ showed the best result. When these catalysts, $Pt/WO_3$, $Pt/ZrO_2$, $WO_3/ZrO_2$ were used separately or in combination no great activity was observed. Therefore, it is not plausible to assume that the reaction mechanism is a bifunctional system where acid sites and Pt metal sites play separate roles. Additional studies are necessary to address mechanistic considerations [63].

The central hydroxyl group of glycerol is more active than the terminal ones but it is less accessible due to the steric hindrance, which restricts its reactivity in heterogeneous catalysis. Therefore, the use of solvent seems to play an important role in the activation of the central hydroxyl group which its substitution with hydrogen forms 1,3-PDO.

Weimiao et al. studied the effect of different solvents for the dehydroxlation of glycerol to 1,3-PDO over $Pt/WO_3/ZrO_2$ catalyst [64]. It has been found that protic solvents such as water and ethanol favour the formation of 1,3-PDO from glycerol. They suggested that portic solvents, such as water and ethanol, are ionised to form protons by the surface acid sites of the $Pt/ WO_3/ZrO_2$ catalyst, and this facilitates the transfer of formed protons to act as a Brønsted acid in the liquid reaction. These free protons can overcome the steric hindrance to the central hydroxyl group in glycerol, leading to almost the same accessibility for the activation as the terminal hydroxyl group. When protons have the same accessibility to all three hydroxyl groups in glycerol, the central OH is easier to activate, according to proton affinity data reported by Nimlos et al. [65]. This could explain the higher selectivity for 1,3-PDO in ethanol and water than that in DMI and sulfolane [64]. It was also shown that binary (protic-aprotic) solvent has a synergetic solvent effect on the selective dehydroxylation of glycerol to 1,3-PDO. When

using DMI-water as a solvent, the selectivity of 1,3-PDO increased as water content increased. The best selectivity of 1,3-PDO (34%) was obtained when using DMI-water (50% water content) with 32% glycerol conversion. In contrast, 1,2-PDO selectivity decreased as water content increased reaching the minimum value of 6.4% at a water content of 75%. It was also noted that the acid strength of the catalyst is a key factor in the selectivity of 1,3-PDO. A stronger acid strength could lead to an activation of all three hydroxyl groups in glycerol producing more 1,2-PDO.

Remarkable progress in the hydrogenolysis of glycerol to 1,3-PDO has been made recently by Tomishige and co-workers [66]. The active catalyst uder investigation was rhenium-oxide-modified supported iridium nanoparticles on silica (Ir-$ReO_x/SiO_2$), which formed 1,3-PDO with selectivity of up to 63% at an initial stage. The yield of 1,3-PDO reaches 38% at 81% conversion of glycerol, under the following reaction conditions: 20% glycerol aqueous solution, 80 bar $H_2$, Re/Ir = 1, 120 °C for 24 h, sulforic acid ($H^+$/Ir = 1). Under these conditions, the reactivity of alcohols decreases in the following order: 1,2-PDO ≥ glycerol > 1,3-PDO ≈ 2,3-butanediol ≈ propanols. The characterisation of the catalyst along with reactivity results of alcohols suggests that 1,3-PDO is formed via the attack of active hydrogen species on iridium metal to 1-glyceride species presented on the oxidised rhenium cluster.

### 1.1.6.1.5 Heterogeneous catalysts for gas-phase synthesis of 1,3-PDO

Conversion of glycerol into 1,3-PDO in the vapour phase has been conducted recently using Cu-$H_4SiW_{12}O_{40}/SiO_2$ [30]. At 210 °C, 5.4 bar of $H_2$ and 83% glycerol conversion, the selectivity of 1,3-PDO reached 32%, together with 22% selectivity of

1,2-PDO. In the presence of $H_4SiW_{12}O_{40}/SiO_2$, acrolein, the dehydration products of 3-hydroxypropanal, was the main product and no 1,3-PDO was detected. With $Cu/SiO_2$ catalyst, very small amounts of 1,3-PDO and acrolein were seen and 1,2-PDO and acetol were the major products, consistent with copper-containing catalysts which are active for 1,2-PDO formation in both gas and liquid phase. Therefore, it has been suggested that the 1,3-PDO formation takes place through bifunctional catalysis: dehydration of glycerol to 3-hydroxypropanal on the acid sites of $H_4SiW_{12}O_{40}$ followed by hydrogenation of 3-hydroxypropanal to 1,3-PDO on copper metal, whilst 1,2-PDO is mainly obtained on copper metal via acetol route.

### 1.1.6.1.6 Conclusions

As outlined above, two possible main mechanisms for the hydrogenolysis of glycerol have been proposed: (1) acetol route (Scheme 1.12) and (2) glyceraldehyde route (Scheme 1.11). The acetol route has been validated for copper-containing catalysts such as copper-chromite and Cu/ZnO, where acetol is selectively obtained initially in a high yield in the absence of hydrogen and the subsequent hydrogenation of acetol selectively forms 1,2-PDO. Ru shows a superior activity compared to other metals such as Rh, Pt and Pd for the hydrogenolysis of glycerol under neutral, acidic and basic conditions. In the absence of Ru, only traces of acetol and no 1,2-PDO were obtained indicating that, in the presence of Ru doped acidic supports, the hydrogenolysis of glycerol may proceed via glyceraldehyde route including glycerol dehydrogenation over Ru sites (Scheme 1.11).

1,2-PDO has been the main product in most of catalytic heterogeneous processes so far. Achieving high selectivity of the more valuable product, 1,3-PDO, remains a challenge. Rh metal, oxides of group 6 and 7 and polar solvents seem to have positive influence upon 1,3-PDO formation.

Copper-chromite system has shown high conversion of glycerol and 1,2-PDO selectivity with clear understanding of the reaction route through acetol intermediate. However, with Ru-based catalysts, improvements of glycerol conversion and propanediol selectivity are still required. Kinetic and mechanistic data also need to be gathered for deep understanding of how the reaction proceeds in the presence of Ru-supported catalysts.

As the reaction appears to be influenced by different reaction parameters such as temperature, hydrogen pressure, catalyst preparation conditions, glycerol concentration, reaction media, etc, more focus on the optimisation of reaction parameters is required.

### 1.1.7 Alternative route for acrolein synthesis from glycerol

#### 1.1.7.1 Acrolein current production

Acrolein is an unsaturated aldehyde, a highly toxic, flammable material with extreme lacrimatory properties. At room temperature, acrolein is a volatile liquid and its solubility in water is limited. Acrolein has been produced commercially since 1938. It is an important bulk chemical used as feedstock for the production of acrylic acid, pharmaceuticals and for fibre treatments, amongst other things. Acrolein is currently manufactured using propylene oxidation or petroleum-derived propane. The catalytic selective oxidation of propylene into acrolein has been extensively investigated since the

1960s and a number of bulk metal oxide catalysts have been selected for this purpose (Scheme 1.14) [67]. Propane is also considered a source for acrolein synthesis but is still below commercial applications due to the low acrolein yield [68].

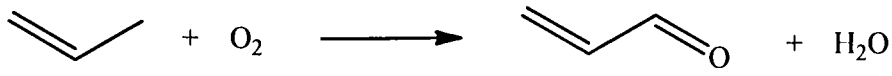


Propylene acrolein

**Scheme 1.14** Production of acrolein by partial oxidation of propylene.

### 1.1.7.2 Liquid phase dehydration of glycerol to acrolein

Acrolein can also be obtained from glycerol, via acid-catalysed dehydration in the gas or liquid phase [69]. The development of an alternative environmentally-benign process for the production of acrolein, based on biomass-derived glycerol as a sustainable feedstock, is a real challenge. The dehydration of glycerol to produce acrolein has been known since the nineteenth century [3, 4, 69] and there have been a number of studies on acrolein production through the dehydration of glycerol using homogenous, heterogeneous and bio-catalysts.

It has long been known that the decomposition of glycerol occurs at high temperatures, producing acrolein, water and some by-products. However, in order to obtain acrolein in a high yield at moderate temperatures, an acid catalyst is needed. In homogeneous system, Ramayya et al. reported that 84% acrolein selectivity can be obtained at 40% conversion of glycerol by adding 5 mM $H_2SO_4$ to water at 300 – 350 °C and 345 bar [70]. Antal et al. showed that a high reaction temperature is needed for the dehydration of glycerol in water: a low glycerol conversion (1%) was obtained without

any acrolein formed when the reaction was conducted at 250 °C and 345 bar pressure [71]. These (near-) supercritical conditions, especially when using an acid catalyst, create serious corrosion problems, which require expensive corrosion-resistance materials. Ott et al. investigated the dehydration of glycerol in supercritical water, using zinc sulphate as the catalyst [72]. This choice of zinc sulphate, which is not acidic enough to promote the reaction, was to limit the corrosion caused by water and acids under supercritical conditions. They claimed that the supercritical conditions were not optimal for the reaction, as near-critical water exhibited better conversion and selectivity than supercritical water (50% and 75% respectively) [72]. This can be explained by the degradation of acrolein at high temperatures once it is formed. Lehr et al. reported 59% glycerol conversion, with 60% acrolein selectivity using $ZnSO_4$ as a catalyst in supercritical water [73].

Catalytic processes using homogeneous or heterogeneous catalysts under (near-) supercritical conditions for glycerol dehydration seem difficult to scale up to an industrial level due to the complex experimental set-up, the extreme corrosive medium and high pressure and temperature. Due to the technical and environmental problems associated with the use of homogenous and biocatalysts, heterogeneous catalysts are more attractive.

### 1.1.7.3 Gas-phase dehydration of glycerol to acrolein

There are a number of patents concerning the gas phase dehydration of glycerol. An early study by Schering-Kahlbaum AG reported a 75% acrolein yield in the glycerol dehydration process using lithium phosphate as a catalyst at 400 - 420 °C [69]. In the early 1990s, Neher et al. filed two patents claiming a full conversion of 10-40% glycerol aqueous solution at 300°C over alumina-supported phosphorous acid with selectivity of acrolein up to 75% [74, 75]. Dubois et al. patented their work on the dehydration of glycerol over different types of solid acid catalysts, such as zeolites, nafion, heteropoly acids and acid-impregnated metal oxides [76, 77]. Solid acid catalysts, including sulphates, phosphates and zeolites, have been examined for glycerol gas phase dehydration [78-80]. Several acid catalysts, such as HZSM-5, HY zeolite, supported mineral acids and heteropoly acids, have been reported by Degussa to be active in the gas-phase dehydration of glycerol to acrolein: a yield of up to 75% upon the complete conversion of glycerol was achieved [79]. Chai et al. demonstrated that $Nb_2O_5$ and sulphate zirconia are active catalysts; however, catalyst deactivation was observed [81]. Supported heteropoly acids have been found to be effective catalysts. Their catalytic activity was significantly affected by the type of heteropoly acid and the size of the mesopres in the silica support [82]. Martin et al. investigated different types of supported heteropoly acids, and silicotungstic acid supported on alumina and aluminosilicate showed complete conversion of glycerol and great catalyst stability, with 75% acrolein yield at 275°C [83].

The dehydration of glycerol has also been conducted in the gas phase using zeolite ZSM-5. The highest yield of acrolein (60%) was obtained at 350°C [84]. More

recently, $ZrO_2$-supported 12-tungstophosphric acid (12-$H_3PW_{12}O_{40}$, HPW) exhibited significantly higher activity and stability in acrolein formation than those on silica, due to retaining the HPW Keggin structure in highly-dispersed states in HPW/$ZrO_2$ [37, 41]. Suppes et al. studied the dehydration of glycerol with the $H_3PO_4$/activated carbon catalyst and observed acrolein yields of up to 67% at 80% glycerol conversion and 260°C and 0.85 bar [5]. As much steam is present in the gas flow, the catalyst should have good water tolerance. The catalyst efficiency in acrolein synthesis is enhanced with increasing catalyst acidity [3, 4, 69]. Supported Keggin heteropoly acids, possessing very strong Brønsted acidity, are amongst the most efficient catalysts for glycerol-to-acrolein conversion in the gas phase [83, 85-87]. In particular, with 12-tungstosilicic acid, $H_4SiW_{12}O_{40}$ possessing a higher water tolerance than other Keggin heteropoly acids, acrolein yields of ≥80% have been achieved at an optimum temperature of 275°C [85].

With regards to the reaction mechanism, the dehydration of glycerol on acid catalysts is suggested to proceed through the formation of 3-hydroxypropanal, with 1-hydroxyacetone (acetol) formed as a relatively stable by-product (Scheme 1.15) [69, 84, 85, 87, 88]. Acetol is the main product (>90% selectivity) in the gas-phase dehydration of glycerol on mixed-oxide catalysts, such as copper chromite [37] and supported metal catalysts, e.g., Cu/$Al_2O_3$ [41]. This may indicate that Lewis acid sites and metal sites are important for the formation of acetol, whereas the formation of 3-hydroxypropanal, followed by its dehydration to acrolein, is favoured in the presence of strong Brønsted acid site

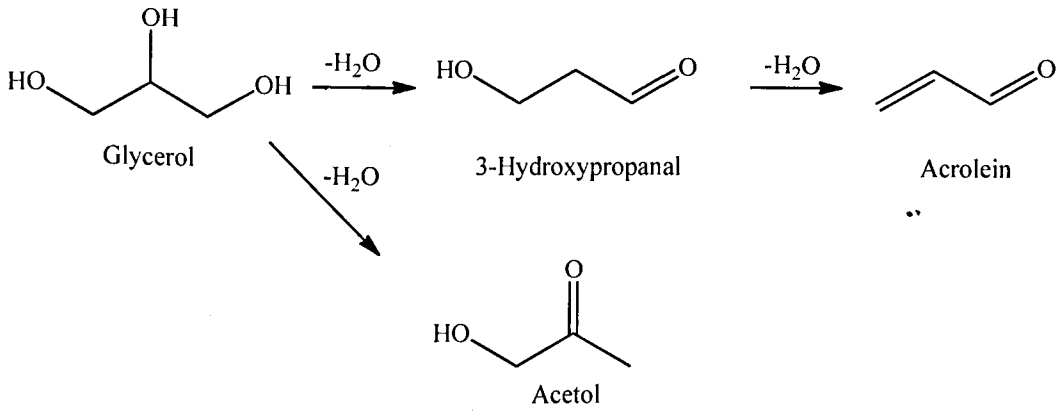


**Scheme 1.15** Dehydration of glycerol over acid catalysts.

A major drawback to the gas-phase dehydration of glycerol on acid catalysts is the high possibility of catalyst deactivation due to extensive coke deposition on the catalyst surface and the difficulty of the direct use of the crude glycerol obtained from biodiesel production [69]. Catalyst regeneration through the combustion of coke has been attempted [69], either in-situ continuously [89, 90] or ex-situ periodically [91], although with limited success. Glycerol dehydration using a fluidised catalyst bed, with a catalyst circulation between the reactor and regenerator similar to the fluidised catalytic cracking process, has been demonstrated [84]. It should be noted that the regeneration of heteropoly acid catalysts by the combustion of coke is difficult due to relatively low thermal stability [92].

## 1.2 Heteropoly acids (HPA)

Heteropolyanions are polyoxometalate anions consisting of nanosized metaloxygenclusters. Today, polyoxometalate (POM) chemistry is a fast-growing area of material science. Unique physicochemical properties and multifunctionality of POMs can be tuned and exploited for the synthesis of new materials. The enormous volume of literature over the past years has led to a deep understanding of the fundamental chemistry of POM and resulted in numerous applications. Hill, in collaboration with leading experts in the field, organised a special issue of Chemical Reviews outlining the history, developments and applications of POMs in many areas [93].

Chemically, POMs are a part of the large group of nanosized metal-oxygen cluster anions. Two types of POMs can be distinguished, based on their chemical composition: isopoly anions and heteropoly anions. These anions have the following general formula:

$[M_mO_y]^{p-}$ isopoly anions

$[X_xM_mO_y]^{q-}$ $(x \leq m)$ heteropoly anions

where M is an addenda or poly atom (M= $V^{5+}$, $Mo^{6+}$, $Nb^{5+}$, $W^{6+}$) and X is a heteroatom (in some cases a central atom) (X= $P^{5+}$, $Si^{4+}$, $Ge^{4+}$, $B^{3+}$, etc). The most frequently used addenda atoms are molybdenum (VI) or tungsten (VI), as a result of the favourable combination of ionic radius and charge and the accessibility of empty d orbitals for metal-oxygen $\pi$ bonding [94]. These anions are formed by a self-assembly process in an aqueous acidic solution, as shown in the equations below [94]:

$$8H^+ + 7WO_4^{2-} \longrightarrow [W_7O_{24}]^{6-} + 4H_2O$$

$$23H^+ + HPO_4^{2-} + 12MoO_4^{2-} \longrightarrow [PMo_{12}O_{40}]^{3-} + 12H_2O$$

One of the key properties of heteropolyanions is that they can be isolated as solids when coupled with an appropriate counteraction, for example $H^+$, alkali metal cation, $NH_4^+$, etc. The hydrogen (acidic) forms of heteropoly anions are called heteropoly acids (HPAs), and some structural types of heteropoly acids and related polyoxometalates have been identified, such as Well-Dawson, Anderson-Evans and Keggin structure.

### 1.2.1 The Keggin structure

According to statistics, 80-85% of patent applications concerning polyoxometalates are related to catalysis [95]. The majority of patents and publications in the literature are related to the Keggin compounds and their derivatives, which is, to a large extent, attributed to their stability and availability [96]. Most typical Keggin type heteropoly acids, such as $H_3PW_{12}O_{40}$, $H_4SiW_{12}O_{40}$, $H_3PMo_{12}O_{40}$ and $H_4SiMo_{12}O_{40}$, are commercially available. They are typically represented by the formula $[XM_{12}O_{40}]^{x-8}$, where X is the heteroatom, x is its oxidation state and M is the addenda atom (usually $Mo^{6+}$ or $W^{6+}$).

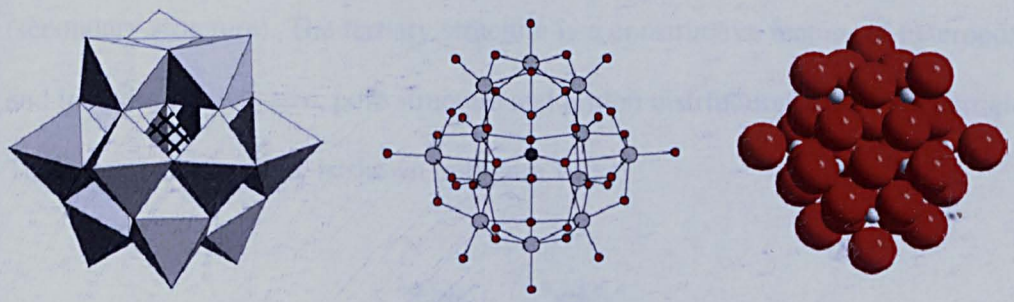

**Figure 1.1** The Keggin structure of the $[XM_{12}O_{40}]^{x-8}$ anion (α-isomer): polyhedral (left), ball-and- stick (middle) and space-filling (right) representations [97].

The Keggin anion (Fig. 1.1) has a diameter of ca. 1.2 nm and is composed of a central tetrahedron $XO_4$ surrounded by 12 edge- and corner-sharing metal-oxygen octahedra $MO_6$ [1,18]. The octahedra are arranged in four $M_3O_{13}$ groups and each group is formed by three octahedral sharing edges and a common oxygen atom, which is also shared with the central tetrahedron $XO_4$. The total assemblage contains 40 close-packed oxygen atoms, and the oxygens in the structure are of four types:

- twelve terminal M=O;
- twelve edge-bridging angular M-O-M shared by the octahedra within a $M_3O_{13}$ group;
- twelve corner-bridging quasi-linear M-O-M, connecting two $M_3O_{13}$ groups;
- four internal X-O-M.

These oxygens can be differentiated using $^{17}O$ NMR and infrared techniques [1]. The M-O and X-O bonds exhibit characteristic infrared bands in the range of 500-1100 $cm^{-1}$ [1].

HPAs commonly exist as ionic crystals in their solid state (sometimes amorphous) and are composed of large polyanions (primary structure), cations, water crystallisation and other molecules contained within a three-dimensional arrangement

(secondary structure). The tertiary structure is a constructive feature of heteropoly acids and includes particle size, pore structure and proton distribution within the particles [59]. This structural hierarchy is shown in Figure 1.2:

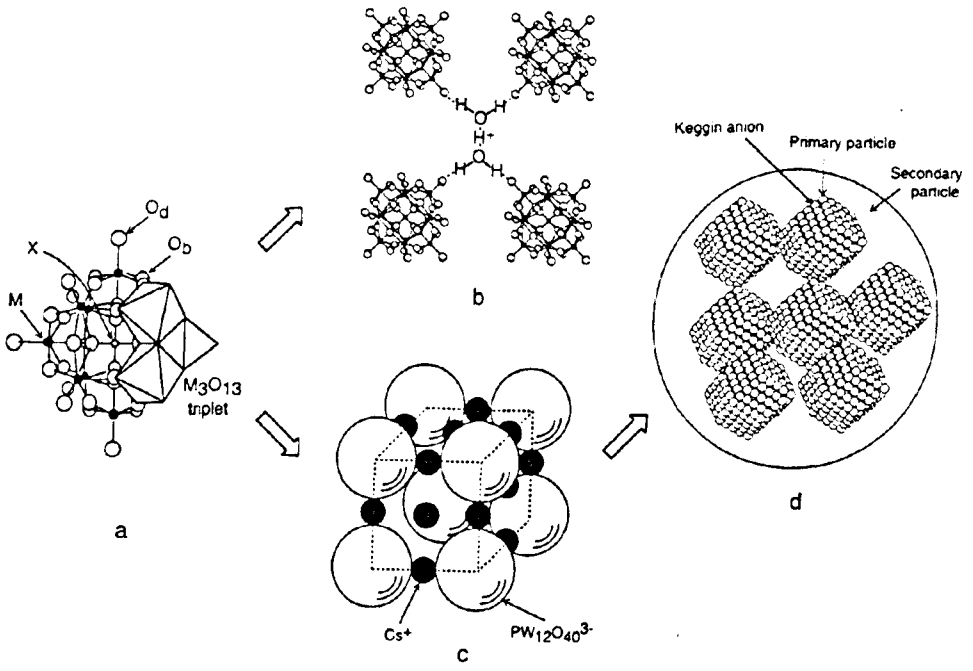


**Figure 1.2** Primary, secondary, and tertiary structures of heteropoly compounds: (a) primary structure (Keggin structure, $XM_{12}O_{40}$); (b) secondary structure ($H_3PW_{12}O_{40}\cdot 6H_2O$); (c) secondary structure ($Cs_3PW_{12}O_{40}$ unit cell); (d) tertiary structure of bulk $Cs_{2.5}HPW_{12}O_{40}$ [5].

## 1.2.2 Acidity and stability of HPA

### 1.2.2.1 Acidity in solution

Many heteropoly acids, such as the Keggins, are strong Brønsted acids and their acid properties have been well-established in solutions as well as in the solid state [96]. The protons present in the bulk and on the surface are distinguished. The characterisation of the proton sites of HPAs is an important step in understanding the catalytic activity of heteropoly acids.

**Proton structure**

Thorough proton characterisation has been carried out for the bulk heteropoly acids, in particular for the strongest acid $H_3[PW_{12}O_{40}]$, but surface proton sites have been less thoroughly characterised. Two types of protons have been identified in solid heteropoly acids: (i) hydrated protons and (ii) non-hydrated protons (Figure 1. 3) [96, 98].

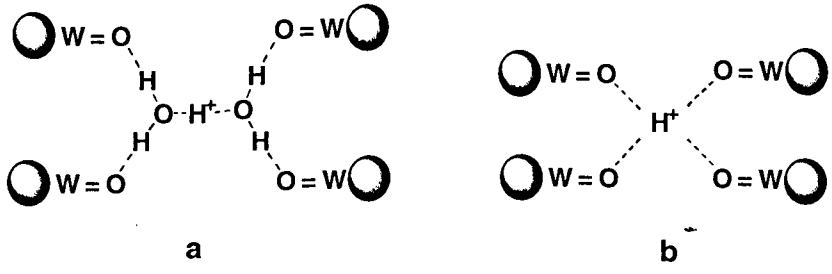


**Figure 1.3** Schematic structure of (a) bulk proton sites in $H_3[PW_{12}O_{40}].6H_2O$ and (b) anhydrous $H_3[PW_{12}O_{40}]$ [94].

The hydrated protons are highly mobile and are responsible for the extremely high proton conductivity of crystalline heteropoly acid hydrates. The non-hydrated protons are much less mobile and are thought to be localised on the peripheral oxygens of the polyanion [94].

**Heteropoly acids in solution**

The Keggin heteropoly acids, such as $H_3PW_{12}O_{40}$, $H_4SiW_{12}O_{40}$ and $H_3PMo_{12}O_{40}$, are strong acids. Protons are dissociated completely from the structures in aqueous solutions. HPAs have a very high solubility in polar media, such as water, alcohol, etc. However, they are insoluble in non-polar solvents, such as benzene and hydrocarbons. The acid properties of HPAs have been characterised in terms of dissociation constants and Hammett acidity function [94].

Heteropoly acids have been found to be much stronger acids than $H_2SO_4$, HBr, HCl, $HNO_3$, and $HClO_4$ [94]. The greater acid strength of heteropoly acids is explained by the fact that in heteropoly anions the negative charge of a similar value is spread over much larger anions than those formed from mineral acids. Hence, the electrostatic interaction between a proton and an anion is much weaker for heteropoly acids than for mineral acids. An additional important factor is the possibility of the dynamic delocalisation of the charge or electron. The change in the charge caused by deprotonation may be spread over the entire polyanion unit [94]. With regards to the acid strength of heteropoly acids, the following order has been reported for the acetone solution [94]:

$$H_3PW_{12}O_{40} > H_4SiW_{12}O_{40} \approx H_3PMo_{12}O_{40} > H_4PMo_{11}VO_{40}$$

### 1.2.2.2 Acidity of solid HPA

As established by the IR spectroscopy of adsorbed pyridine, solid heteropoly acids possess pure Brønsted acidity. Compared to conventional solid acids, such as $SiO_2$-$Al_2O_3$, $H_3PO_4/SiO_2$ and H-X and H-Y zeolites, heteropoly acids, such as $H_3PW_{12}O_{40}$ in its solid state, have stronger acidity and hence higher catalytic activity. As found by the temperature-programmed desorption (TPD) of ammonia, the acid strength of crystalline heteropoly acids decreases in the following order:

$$H_3PW_{12}O_{40} > H_4SiW_{12}O_{40} \geq H_3PMo_{12}O_{40} > H_4SiMo_{12}O_{40}$$

## 1.2.3 Stability of HPA

### 1.2.3.1 Stability in solution

The hydrolytic stability of heteropoly anions is of particular interest. The stability of heteropoly anions in aqueous solution depends on pH values [94]. Generally, the stability of 12-heteropoly anions towards hydrolysis in an aqueous solution decreases in the order of addenda atoms [94]:

$$W\ (VI) > Mo\ (VI) > V\ (V).$$

The stability of heteropoly compounds is greatly influenced by the nature of the central atom (heteroatom) of the primary structure. Generally, the stability decreases in the following series of central atoms [31]:

$$Si^{4+} > Ti^{4+}, Zr^{4+} > Ge^{4+} > P^{5+} > As^{5+}.$$

Keggin, Wells-Dawson and other types of heteropoly anions form lacunary (defect) species in solution at an appropriate pH [1,31]. The lacunary anions have one or

more vacancies created by the loss of addenda atom(s) from the structure. For example, $PW_{12}O_{40}^{3-}$ forms the lacunary anion $PW_{11}O_{39}^{7-}$ at pH 2 in aqueous solution:

$$PW_{12}O_{40}^{3-} \leftrightarrows PW_{11}O_{39}^{9-} + W(VI)$$

The lacunary anion is stable until pH ~ 8, then further degrades to give the trivacant lacunary species $PW_9O_{34}^{9-}$. In organic media, the stability of polyoxometalates species increases compared to in aqueous solutions [94]

### 1.2.3.2 Thermal stability of solid HPA

HPAs possess a relatively high thermal stability that makes them useful for heterogeneous catalytic reactions (which often occur at high temperatures). Generally, Keggin-type heteropoly compounds are the most stable amongst the various polyoxometalates.

The decomposition temperature (°C) for the most typical Keggin heteropoly acids, as estimated from TGA, decreases in the following order [94]:

$H_3PW_{12}O_{40}$ > $H_4SiW_{12}O_{40}$ > $H_3PMo_{12}O_{40}$ > $H_4SiMo_{12}O_{40}$

465 445 375 350

The decomposition temperature of $H_3PW_{12}O_{40}$ is 465 °C and thus it has the highest thermal stability among Keggin-type heteropoly acids [94].

## 1.2.4 Heterogeneous acid catalysis by HPA

HPAs have been the core of numerous catalytic applications, including acid and redox catalysts, in both homogeneous and heterogeneous systems. Heterogeneous acid catalysis by HPAs is of great importance for 'green' chemical synthesis and sustainable development [97, 99]. As crystalline HPAs have a very low surface area (1-5 $m^2 g^{-1}$) and low porosity (<0.1 $cm^3g^{-1}$), it is rather difficult to use bulk HPAs in heterogeneous systems. Therefore, HPAs are supported on inert porous supports that have a larger surface area, such as silica [96]. The acidity and the catalytic activity of supported HPAs depend on the type of carrier, the HPAs' loading and the conditions of pre-treatment. Typical supports are $SiO_2$, active carbon and acidic ion-exchange, and the most widely used is $SiO_2$ [94, 100]. Silica supported $H_3[PW_{12}O_{40}]$ (HPW) has frequently been characterised in terms of acid strength and it was revealed that the acidity of supported HPW is weaker than that of bulk HPW and can be increased by increasing HPW loadings [101, 102]. Many catalytic processes have been successfully carried out using supported HPAs and examples can be found in several review articles [94, 101, 103].

The substitution of $H^+$ in the acidic form of HPAs with small cations such as $Li^+$, $Na^+$ and $Ag^+$, exhibits interesting effects on surface area and pore structure. The resulting salts resemble the parent heteropoly acids: they are soluble in water, nonporous, and possess a low surface area $\leq$ 10 $m^2g^{-1}$. In contrast, salts with large monovalent cations, such as $NH_4^+$, $Cs^+$, $K^+$, etc., are water insoluble, have a microporous/mesoporous structure and have surface areas over 100 $m^2g^{-1}$.

$Cs_{2.5}H_{0.5}$ $[PW_{12}O_{40}]$ shows the highest acidity and catalytic activity for various reactions in the liquid and gas phase and hence it has been extensively studied and characterised [100, 101, 103]. As the Cs content ($x$ in $Cs_xH_{3-x}PW_{12}O_{40}$) increases, the number of surface protons decreases at first but greatly increases when the Cs content exceeds 2 and shows the highest surface acidity at $x$ = 2.5, which is due to the sharp increase in the surface area. When $x$ increases from 2.5 to 3.0, the formal concentration of protons becomes low or zero and the number of surface protons decreases greatly.

Misono et al. [101] demonstrated that there are three different types of catalysis by solid HPAs: surface type, pseudo-liquid (bulk type I) and bulk type II (Figure 1.4). Surface-type catalysis (a) represents the ordinary heterogeneous catalysis, which takes place on the solid surface (two dimensional reaction fields on outer surface and pore wall). Bulk-type (b, c) catalysis shows that the reaction fields are three-dimensional in contrast to surface-type catalysis.

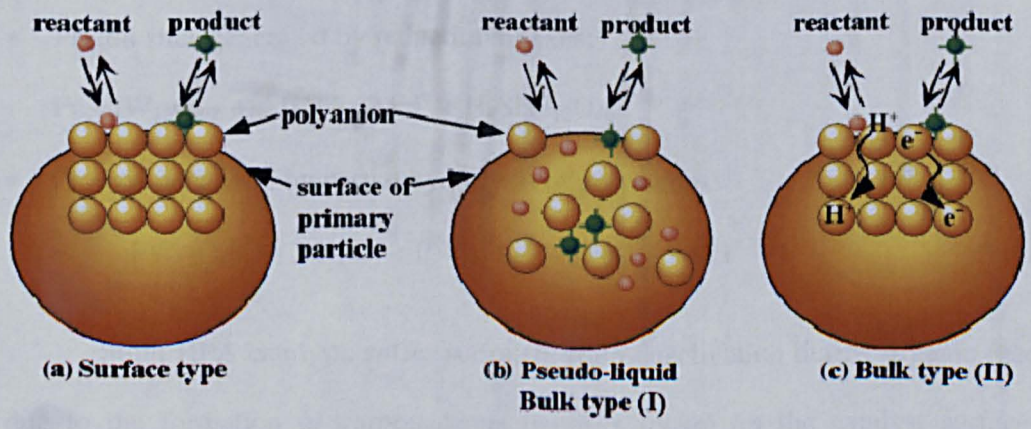


**Figure 1.4** Three types of catalysis for solid heteropoly compounds: (a) surface type (b) pseudoliquid: bulk type (I), (c) bulk type (II).

Acidity, basicity and pseudo-liquid behaviour are the principal factors governing the acid catalysis of solid HPAs. The acidic properties are mainly controlled by:

- the structure and composition of the heteropoly anion itself;
- the countercations;
- the dispersion on supports.

The secondary and tertiary structures are also affected by these factors. Bulk and supported heteropoly acids and salts are used as catalysts in heterogeneous acid-catalysed reactions. Several types of acid sites are present in these catalysts [5]:

- Proton sites in heteropoly acids (e.g. $H_3PW_{12}O_{40}$).
- Proton sites in acidic salts (e.g. $Cs_{2.5}H_{0.5}PW_{12}O_{40}$).
- Lewis acid sites in salts (metal countercations, e.g. in $La^{III}PMo_{12}O_{40}$).
- Proton sites generated by dissociation of coordinated water:

$$Ln(H_2O)_n^{3+} \rightarrow Ln(H_2O)_n(OH)^{2+} + H^+$$

- Proton sites generated by reduction of salts:

$$Pd_2SiW_{12}O_{40} + 4\,[H] \rightarrow 2\,Pd^0 + H_4SiW_{12}O_{40}$$

- Protons generated by partial hydrolysis of polyanions:

$$PW_{12}O_{40}^{3-} + 2\,H_2O \rightarrow PW_{11}O_{39}^{7-} + [WO_3] + 4\,H^+$$

Solid HPA catalysts suffer seriously from deactivation during organic reactions, due to the formation of carbonaceous deposits (coke) on the catalyst surface [94]. Burning coke at 500-550$^{o}$C, which is generally used in the case of aluminosilicates and zeolites, is not applicable to HPAs because they are not thermally stable at such high

temperatures. It has been shown that supporting HPA on a carrier inhibits the formation of coke, whilst bulk HPAs, with their strong acid sites and low surface area, coke more rapidly [94].

## 1.3 Niobium compounds

### 1.3.1 Introduction

Niobium (Nb), with an atomic number of 41 and a relative atomic mass of 92.9, belongs to the VA group in the periodic table and is a shiny silvery metal with a typical metallic bcc structure [104]. In its purest state, niobium is a soft and ductile metal and the presence of impurities hardens it. It is used in the manufacture of alloys as an additive, due to its corrosion resistance, and is also used in the electronics industry. This behaviour, along with a small difference in the electronegativity and ionic radius between niobium and its neighbours (V, Zr, Mo) has motivated much research and development of niobium compounds in the last 20 years [105, 106].

Niobium exhibits special properties not shown by the compounds of neighbouring elements and hence has been known as an attractive compound for various applications [107]. One of the major applications for niobium materials is heterogeneous catalysis: materials such as niobium pentoxide ($Nb_2O_5$), niobic acid ($Nb_2O_5.nH_2O$), niobium phosphate ($NbOPO_4$), niobium layered compounds ($K_4Nb_6O_{17}$, $HCa_2Nb_3O_{10}$, etc.) and mixed oxides containing niobia ($Nb_2O_5$-$SiO_2$, $Nb_2O_5$-$AI_2O_5$, $Nb_2O_5$-$TiO_2$, $Nb_2O_5$-$V_2O_5$, etc.) have demonstrated excellent activities

as promoters and supports of catalysts and as unique solid acid catalysts, selective oxidation catalysts and photosensitive catalysts for many catalytic processes [105, 108]. Reviews by Tanabe [105, 108], and Tanabe and Okazaki [107] in 1995 described the catalytic applications of niobium compounds.

### 1.3.2 Niobium oxide (niobic acid, $Nb_2O_5.nH_2O$)

Niobic acid ($Nb_2O_5.nH_2O$) has attracted great interest as a catalyst due to its strong acidity, which can be preserved in polar liquids and at high operation temperatures [104, 109]. It has been used as a water-tolerant solid acid catalyst for various water-involving reactions, such as esterification, hydrolysis, dehydration and hydration [105]. Niobium oxide compounds generally possess an octahedrally co-ordinated $NbO_6$ structural unit that is distorted to different extents, depending on whether the octahedra are corner or edge-shared [110, 111]. Occasionally, $NbO_7$ and $NbO_8$ units can also be found in niobium oxide phases. The highly distorted $NbO_6$ octahedra possess Nb=O bonds and are associated with Lewis acid sites. In contrast, the slightly distorted $NbO_6$ octahedra and the $NbO_7$ and $NbO_8$ groups only possess Nb-O bonds and are associated with Brønsted acid sites [112, 113].

Hydrated niobium oxide ($Nb_2O_5.nH_2O$, niobic acid) has a strong acidity ($H_o$ = -5.6 ~ -8.2) [114, 115]. Generally, hydrated niobium oxide crystallises at 580°C and its strong acidity disappears when it is heated to temperatures higher than 500°C. $Nb_2O_5.nH_2O$ possesses both Lewis acid sites (whose number increases with increasing pre-treatment temperatures up to 500°C and then decreases at higher temperatures) and Brønsted acid sites (which are most abundant at 100°C and decrease in number at higher

temperatures) on its surface [116]. To summarise, hydrated niobium oxide possesses distinctive features, a large surface area, strong acidity that can be maintained in polar media, stability at high temperatures and reducing conditions.

## 1.4 Multifunctional catalysis

### 1.4.1 Cascade processes

Chemical processes in the living cells demonstrate an outstanding efficiency, with 100% selectivity to desirable products and complete conversion of reactants in multistep cascade reactions without intermediate separations (Figure 1.5). In synthetic organic chemistry, the conventional step-by-step processes, in which intermediates are separated after each step (Figure 1.6), produce large amounts of waste, require a long operation time, require vast amounts of energy and hence have a high cost. Furthermore, increasing public concern about environmental protection at a time of increasing worldwide need for chemical products makes it necessary for environmentally-friendly processes to be introduced [117-119].

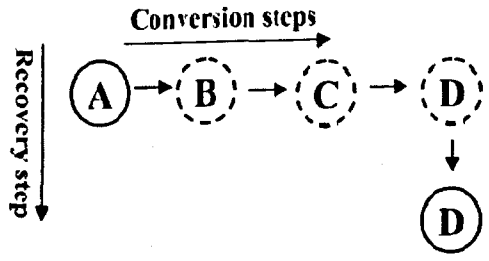


**Figure 1.5** One stage organic synthesis in the cells of organisms involves a combination of reaction steps without the need for intermediate recovery [117].

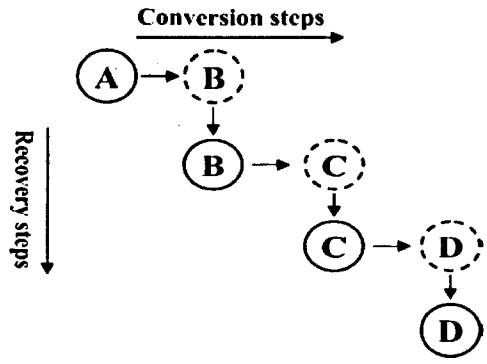


**Figure 1.6** Multistage organic synthesis in a traditional chemical process which needs a recovery step after each conversion step [117].

The cascade process that takes place in living cells is the most attractive alternative to the conventional step-by-step process due to its potential for overcoming most of the drawbacks mentioned above in the traditional multistep process. In addition, in the cascade process, thermodynamic barriers can be overcome, in order to obtain the desired product when the intermediates are highly energetic, as seen in Figure 1.7 [117].

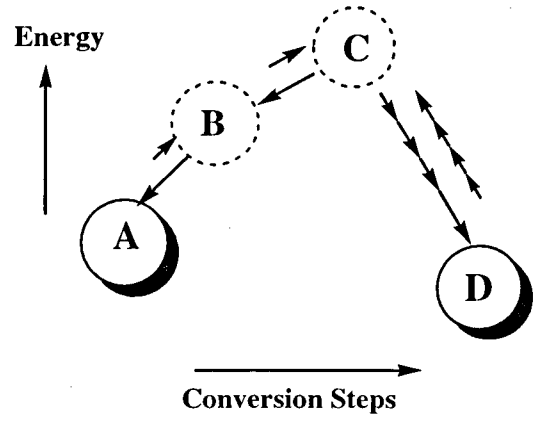


**Figure 1.7** The ability of the cascade process to overcome thermodynamic barriers in multistep synthesis [117].

A considerable number of cascade reactions have been reported involving a variety of combinations of enzymes and homogeneous and heterogeneous or uncatalysed organic chemical reactions [117]. These have been classified into three categories, according to the type of catalyst involved:

1. Bio-bio catalytic cascade transformations, where enzymes work together under reaction conditions.
2. Bio-chemo catalytic cascade transformations, where enzyme and metal catalysts react simultaneously in a one-step synthesis.
3. Chemo-chemo catalytic cascade transformations, where two or more catalytic active sites work synergistically in a one-step conversion without intermediate recovery.

The replacement of the step-by-step processes in organic synthesis by the one-pot syntheses has recently come into practice with a few examples, such as the synthesis of the drug sertraline by Pfizer [117]. Cascade conversion has also been employed in organic transformation with the use of organometallic complexes as catalysts (for further details, see [118, 120]).

## 1.4.2 Multifunctional catalysis in cascade processes

There are certain requirements for the implementation of cascade processes in organic synthesis, such as appropriate reactor design, medium engineering and new catalytic methods [117]. Multifunctional catalysts are catalysts containing two or more different catalytic functions, acting simultaneously to facilitate a sequence of catalytic reactions in the one-pot system. Multifunctional catalysis can be considered as one of

the most important catalytic methods introduced in the chemical industry, along with the use of cascade synthetic processes [121]. They have been widely used in many industrial processes, such as the hydroisomerisation of $C_5$-$C_6$ alkanes, in the production of intermediates and fine chemicals [122, 123].

Multifunctional catalysts have been successfully used in the cascade conversions of organic molecules. Much of the research regarding heterogeneous multifunctional catalysis has focused on developing catalysts consisting of transition metals supported on an active support possessing acidic and/or basic sites for multistep reactions. Early studies, such as that by Weisz and Swelgler, featured a catalyst made up of a mixture of silica and alumina, with platinum supported on a high surface area. Carbon was also employed, in order to improve the efficiency of the hydrocracking of n-dodecane to yield a mixture of $C_3$-$C_8$ hydrocarbons [124]. Similar transition metal-supported multifunctional catalysts proved to be active for the isomerisation of paraffins, the hydroisomerisation of napthenes and the hydrogenative cracking of paraffins [125-128].

### 1.4.3 Metal/heteropolyacid multifunctional catalysts

Among HPA compounds, the acidic cesium salt, $Cs_{2.5}H_{0.5}PW_{12}O_{40}$, exhibits strong solid acidity and is present as fine particles possessing a relatively high surface area and mesopores. This salt is insoluble in water and various organic solvents and is thus utilised as an effective solid acid catalyst in solid-liquid and solid-gas reaction systems [101]. Another feature of Cs salt is its hydrophobic surface [129]. Cs salt and other supported HPAs allow considerable alteration of their texture and can be modified to introduce another chemical function, e.g., a metal function. Therefore, they have been

widely employed as acidic supports as part of a metal-supported multifunctional catalyst to effect multistep reactions involving organic fine chemicals.

A number of multistage chemical processes have been run using metal/HPAs as active catalysts. The one-stage oxidation of ethylene to acetic acid has been commercialised by the Japanese company *Showa Denko Co. Ltd* (10000 ton $yr^{-1}$) and combines a Keggin type HPA catalyst and Pd [130]. Se or Te is added to Pd to suppress complete oxidation to $CO_2$. Pd/Pt supported $Cs_{2.5}PW_{12}O_{40}$ has been employed in the isomerisation of n-alkanes ($C_4$-$C_7$). The reaction occurs through an acid-metal bifunctional mechanism [131]. The bifunctional catalyst system involving palladium and $H_3PW_{12}O_{40}$ supported on $SiO_2$ has been introduced for the one-step synthesis of menthol from citronellal [132]. The reaction involves two reaction steps: (i) the cyclisation of citronellal in order to form isopulegol occurring on acid sites of HPA and (ii) the subsequent hydrogenation of the C=C bond in isopulegol over Pd(0) particles, resulting in the formation of the desired product menthol. Pd-doped $Cs_{2.5}PW_{12}O_{40}$ is an active bifunctional catalyst for the one-pot hydrogenation of acetone to methyl isobutyle ketone (MIBK) [133]. MIBK forms in three steps: acetone condensation to diacetone alcohol (DA) on acid sites, acid-catalysed dehydration of DA to mesityl oxide (MO), and hydrogenation of the C=C bond of MO on Pd sites to MIBK.

### 1.4.4 Metal/niobium oxide multifunctional catalysts

Hydrated niobium oxide, $Nb_2O_5.nH_2O$, is known to be a strong, water tolerant solid acid, exhibiting high catalytic activity and selectivity for the hydration of alkenes, dehydration of alcohols, esterification of carboxylic acids with alcohols, and

condensation of butylaldehyde. Niobium oxide has been used as an oxide support for metals, such as Ru, Rh, Ni, and metal oxides, providing both acid and metal functions for catalytic reactions [105, 134]. $Pd/Nb_2O_5$ catalyst showes high activity and selectivity for MIBK formation and also demonstrates good durability for the one-step synthesis of MIBK. Furthermore, this catalyst is highly resistant to water in acetone. It is bifunctional: the acid site on niobic acid catalyses the condensation of acetone to mesityl oxide and the palladium metal deposited on the catalyst surface hydrogenates mesityl oxide to MIBK [135].

Pt supported on niobium-based solid acids has been applied as a bifunctional catalyst in the aqueous-phase dehydration and hydrogenation of sorbitol to alkanes at temperatures close to 257 °C and pressure of 54 bar [136]. In this process, niobium-based catalysts exhibited a superior reactivity compared to silica-alumina based catalysts: 50% and 20% yields of sorbitol to alkanes respectively. The high activity of niobium-based materials is reported to be due to the co-ordination environment of the niobium acid centre [136].

## 1.5 Objectives of our study and thesis outline

Glycerol is expected to play an important role in the future biorefinaries. Significant research has been focused on the conversion of glycerol by catalytic processes, such as reforming, oxidation, hydrogenolysis, esterification and etherification. 1,2- and 1,3-propanediols are important commodity chemicals and are currently produced from petroleum derivatives by chemical catalysis. However, these diols can be alternatively produced through glycerol hydrogenolysis. Acrolein is also an important

intermediate for the chemical and agricultural industries and is currently produced by the oxidation of petroleum-derived propene. It can also be obtained from glycerol via acid-catalysed dehydration in the gas or liquid phase.

The results reported so far for liquid-phase glycerol hydrogenolysis and the mechanisms proposed so far imply that this process is a multistage one (dehydration + hydrogenation) or (dehydrogenation + dehydroxylation + hydrogenation). Therefore, bifunctional acid/hydrogenation catalysis should be an effective candidate to carry out glycerol hydrogenolysis in one-pot system. Glycerol dehydration to acrolein has been reported to occur in two dehydration steps and requires the presence of strong and water-tolerant solid acids.

From the previous research efforts, it is apparent that there are several important challenges associated with liquid-phase glycerol hydrogenolysis, as well as gas-phase dehydration of glycerol, which need to be addressed. These are the use of high temperature and pressure, dilute solutions, the low conversion and selectivity towards propanediols, the catalyst stability, the optimisation of metal and acid functions and the lack of mechanistic understanding.

Acidic cesium heteropoly salt, $Cs_{2.5}H_{0.5}PW_{12}O_{40}$, exhibits strong acidity, and relatively high surface area. This salt is insoluble in water and various organic solvents and is thus utilised as an effective solid acid catalyst in solid-liquid and solid-gas reaction systems. Another feature of the Cs salt is its hydrophobic surface. Cs salt and supported HPAs allow for considerable alteration of their texture and thus can be modified to introduce another chemical function, e.g., metal function.

Hydrated niobium oxide, $Nb_2O_5.nH_2O$, is known as a strong solid acid, exhibiting high catalytic activity and selectivity for various reactions in which water is a product or solvent. It also possesses a high surface area, which facilitates its use as a support for metals, such as Ru, Rh, Ni, and metal oxides, providing both acid and metal functions for catalytic reactions.

A number of metals, either in their metal or oxide state, have been found active for C=C and C=O hydrogenation in the hydrogenolysis of glycerol. These include Ni, Cu, Pd, Pt, Ru and Rh. However, with regards to the acid-metal catalysed hydrogenolysis of glycerol, Ru is superior to other metals for C-O cleavage and hence is more selective to 1,2-PDO. Rh favors the formation of 1,3-PDO, but 1,2-PDO still being the predominant product.

The aim of this work is to investigate the use of multifunctional catalysts for the conversion of glycerol to value-added chemicals. This will be conducted by the preparation of two classes of solid acid/metal bifunctional catalysts, (1) cesium salt of tungstophosphoric acid, $Cs_{2.5}H_{0.5}PW_{12}O_{40}$ (CsPW), and (2) hydrated niobium oxide, ($Nb_2O_5$) using literature procedures. These two catalysts are impregnated with Ru and Rh metals, known to be active for glycerol hydrogenolysis. Other metals such as Pd and Pt will be prepared for comparison. The characterisation of catalyst physical and chemical properties will be carried out by different techniques, including nitrogen adsorption for catalyst texture, thermogravimetric analysis (TGA) for thermal stability, infrared spectroscopy (IR), X-ray diffraction (XRD) for catalyst structure. The bifunctionality of the prepared catalysts will confirmed using hydrogen chemisorption experiment. Differential scanning calorimetry (DSC) and infrared spectroscopy (IR) will be used to characterise the acidic properties of catalysts.

The bifunctional catalysts possessing both acid and metal sites will be investigated for their activity towards the one-step conversion of glycerol to 1,2- and 1,3-propanediols in the liquid phase. The effect of different reaction parameters such as temperature, pressure, time, etc. will be studied in order to establish the optimum conditions. The effect of acid and metal functions on the conversion, product selectivity and the reaction mechanism will be discussed.

The gas-phase dehydration of glycerol will also be investigated using cesium salt of tungstophosphoric acid, $Cs_{2.5}H_{0.5}PW_{12}O_{40}$. We also attempt to enhance catalyst lifetime and reduce coke deposition by doping CsPW with platinum group metals (PGM), such as Ru, Pd and Pt, and co-feeding hydrogen to the reaction system.

**In Chapter 1**, Introduction to glycerol synthesis and application, heteropoly acids, niobic acid and multifunctional catalysis is presented. The up-to-date literature for glycerol hydrogenolysis and glycerol dehydration is also covered.

**In Chapter 2,** a description of the preparation methods used for the catalyst synthesis is given. The techniques used for catalyst characterisation along with the liquid and gas phase catalyst reaction testing procedures are also described.

**In Chapter 3**, the results of catalyst characterisation are described and information about the structure and physicochemical properties of the fresh and spent catalysts is provided.

**In Chapter 4,** the catalytic activity of metal (Ru, Rh) doped CsPW catalyst is investigated in liquid-phase glycerol hydrogenolysis. The effects of reaction temperature, glycerol concentration, metal loading, hydrogen pressure and reaction time on glycerol conversion and product selectivity are studied to arrive at optimum conditions. The mechanistic implications of the results obtained are disclosed.

**In Chapter 5,** the catalytic performance of metal (Ru, Rh) doped $Nb_2O_5$ catalyst is examined. The effects of reaction parameters on glycerol conversion and product selectivity are studied to reach the optimal reaction conditions. The mechanistic implications of the results obtained are discussed.

**In Chapter 6,** the dehydration of glycerol is performed in gas phase in the presence of $Cs_{2.5}H_{0.5}PW_{12}O_{40}$ catalyst to obtain acrolein under mild conditions. The effects of platinum group metals (PGM), such as Ru, Pd and Pt doped $Cs_{2.5}H_{0.5}PW_{12}O_{40}$ in the presence of hydrogen, on glycerol conversion, product selectivity and catalyst lifetime are investigated.

**Chapter 7** gives conclusions regarding the results from the catalytic study and characterisation of the catalysts. It also summarises the contribution of our results to understanding the chemistry of glycerol hydrogenolysis and dehydration processes.

## Reference


[1] M. Pagliaro, M. Rossi, Future of Glycerol: New Usages for a Versatile Raw Material, RSC: Green Chemistry (2008).

[2] D. R. Lide, CRC Handbook of Chemistry and Physics (2003).

[3] C. H. C. Zhou, J. N. Beltramini, Y. X. Fan, G. Q. M. Lu, Chem. Soc. Rev. 37 (2008) 527.

[4] Y. G. Zheng, X. L. Chen, Y. C. Shen, Chem. Rev. 108 (2008) 5253.

[5] A. Behr, J. Eilting, K. Irawadi, J. Leschinski, F. Lindner, Green Chem. 10 (2008) 13.

[6] Z. X. Wang, J. Zhuge, H. Y. Fang, B. A. Prior, Biotechnol. Adv. 19 (2001) 201.

[7] E. Jungermann, N. O. V. Sonntag, Glycerine: A Key Cosmetic Ingredient (1991) 64.

[8] G.W. Huber, S. Iborra, A. Corma, Chem. Rev. 106 (2006) 4044.

[9] E.U. PARLIAMENT, The promotion of the Use of Biofuels or Other Renewable Fuels for Transport, Official Journal of the European Union, 8 May 2003.

[10] M. Pargliaro, R. Ciriminna, H. Kimura, M. Rossi, C. Della Pina, Angew. Chem. Int. Ed. 46 (2007) 4434.

[11] Top Value added chemicals from biomass, US Depatment of Energy (USDOE). T. Werpy and G. Petersen, Vol. 1 (2004).

[12] M. Pagliaro, R. Ciriminna, H. Kimura, M. Rossi, C. Della Pina, Angew. Chem. Int. Ed. 46 (2007) 4434.

[13] A. J. Ragauskas, C. K. Williams, B. H. Davison, G. Britovsek, J. Cairney, C.A. Eckert, W. J. Frederick, J. P. Hallett, D. J. Leak, C. L. Liotta, J.R. Mielenz, R. Murphy, R. Templer, T. Tschaplinski, Science. 311 (2006) 484.

[14] R. R. Soares, D. A. Simonetti, J. A. Dumesic, Angew. Chem. Int. Ed. 45 (2006) 3982.

[15] A. Corma, S. Iborra, A. Velty, Chem. Rev. 107 (2007) 2411.

[16] J. Chaminand, L. Djakovitch, P. Gallezot, P. Marion, C. Pinel, C. Rosier, Green Chem. 6 (2004) 359.

[17] C. Zhou, J.N. Beltramini, Y. Fan, G. Q. Lu, Chem. Soc. Rev. 37 (2008) 527.

[18] S. Papanikolaou, P. Ruiz-Sanchez, B. Pariset, F. Blanchard, M. Fick, J. Biotechnol. 77 (2000) 191.

[19] B. Casale, A. M. Gomez, US Patent 5,276,181, 1994.

[20] M. A. Dasari, P. P. Kiatsimkul, W. R. Sutterlin, G.J. Suppes, Appl. Catal. A 281

(2005) 225.

[21] D. K. Sohounloue, C. Montassier, J. Barbier, React. Kinet. Catal. Lett. 22 (1983) 391.

[22] C. Montassier, D. Giraud, J. Barbier, J. P. Boitiaux, Bull. Soc. Chim. Fr. (1989) 148.

[23] C. Montassier, D. Giraud, J. Barbier, Stud. Surf. Sci. Catal. 41 (1988) 165.

[24] R. A. Sheldon, H.v. Bekkum (Eds.), Fine Chemicals Through Heterogeneous Catalysis, Wiley-VCH, Weinbeim 2001.

[25] T. A. Geissman, Principles of Organic Chemistry, (3rd ed) W. H. Freeman and Company, San Francisco and London 1968.

[26] W. H. Brown, C.S. Foote, Organic Chemistry, (2nd ed) Saunders College Pblishing 1998.

[27] M. R. Nimlos, S. J. Blanksby, X. H. Qian, M. E. Himmel, D.K. Johnson, J. Phys. Chem. A. 110 (2006) 6145.

[28] J. Espinosa-Garcia, S. Dobe, J. Mol. Struct. THEOCHEM. 713 (2005) 119.

[29] Yaws. CL, Li B, Nijhawa S, Hopper J, P. P, In: Y. CL (Ed.) Chemical properties handbook, McGraw-Hill, New York, 1999.

[30] L. Huang, Y. L. Zhu, H. Y. Zheng, G. Q. Ding, Y. W. Li, Catal. Lett. 131 (2009) 312.

[31] M. Schlaf, Dalton Trans. (2006) 4645.

[32] M. Schlaf, P. Ghosh, P. J. Fagan, E. Hauptman, R. M. Bullock, Angew. Chem. Int. Ed. 40 (2001) 3887.

[33] K. Y. Wang, M. C. Hawley, S. J. DeAthos, Ind. Eng. Chem. Res. 42 (2003) 291.

[34] B. Casale, A. M. Gomez, US Pat., 5,214,219 (1993).

[35] B. Casale, A.M. Gomez, US Pat. 5,276,181 (1994).

[36] S. Ludwig, E. Manfred, US Pat. 5,616,817 (1997).

[37] C. W. Chin, M. A. Dasari, G. J. Suppes, W. R. Sutterlin, AIChE J. 52 (2006) 3543.

[38] Z. W. Huang, F. Cui, H. X. Kang, J. Chen, X. Z. Zhang, C. G. Xia, Chem. Mater. 20 (2008) 5090.

[39] L. Y. Guo, J. X. Zhou, J. B. Mao, X. W. Guo, S. G. Zhang, Appl. Catal. A 367 (2009) 93.

[40] R. B. Mane, A. M. Hengne, A. A. Ghalwadkar, S. Vijayanand, P. H. Mohite, H. S. Potdar, C. V. Rode, Catal. Lett. 135 (2010) 141.

[41] S. Sato, M. Akiyama, R. Takahashi, T. Hara, K. Inui, M. Yokota, Appl. Catal. A 347 (2008) 186.

[42] J. Zheng, W. C. Zhu, C. X. Ma, Y. Z. Hou, W. X. Zhang, Z. L. Wang, Reaction Kinetics Mechanisms and Catalysis. 99 (2010) 455.

[43] Z. Yuan, J. Wang, L. Wang, W. Xie, P. Chen, Z. Hou, X. Zheng, Bioresour. Technol. 101 (2010) 7088.

[44] T. Miyazawa, S. Koso, K. Kunimori, K. Tomishige, Appl. Catal. A 329 (2007) 30.

[45] T. Miyazawa, S. Koso, K. Kunimori, K. Tomishige, Appl. Catal. A 318 (2007) 244.

[46] T. Miyazawa, Y. Kusunoki, K. Kunimori, K. Tomishige, J. Catal. 240 (2006) 213.

[47] I. Furikado, T. Miyazawa, S. Koso, A. Shimao, K. Kunimori, K. Tomishige, Green Chem. 9 (2007) 582.

[48] E. P. Maris, R. J. Davis, J. Catal. 249 (2007) 328.

[49] E. P. Maris, W. C. Ketchie, M. Murayama, R. J. Davis, J. Catal. 251 (2007) 281.

[50] L. Ma, D. H. He, Z. P. Li, Catal. Commun. 9 (2008) 2489.

[51] J. Feng, H. Y. Fu, J. B. Wang, R. X. Li, H. Chen, X. J. Li, Catal. Commun. 9 (2008) 1458.

[52] Y. G. He, M. H. Qiao, H. R. Hu, J. F. Deng, K. N. Fan, Appl. Catal. A 228 (2002) 29.

[53] A. Nieto-Marquez, S. Gil, A. Romero, J.L. Valverde, S. Gomez-Quero, M. A. Keane, Appl. Catal. A 363 (2009) 188.

[54] G. W. Huber, J. W. Shabaker, J. A. Dumesic, Science. 300 (2003) 2075.

[55] R. R. Davda, J. W. Shabaker, G. W. Huber, R. D. Cortright, J.A. Dumesic, Appl. Catal. B 56 (2005) 171.

[56] A. Perosa, P. Tundo, Ind. Eng. Chem. Res. 44 (2005) 8535.

[57] J. Zhao, W.Q. Yu, C. Chen, H. Miao, H. Ma, J. Xu, Catal. Lett. 134 (2010) 184.

[58] W. Q. Yu, J. Xu, H. Ma, C. Chen, J. Zhao, H. Miao, Q. Song, Catal. Commun. 11 (2010) 493.

[59] X. H. Guo, Y. Li, R. J. Shi, Q. Y. Liu, E. S. Zhan, W. J. Shen, Appl. Catal. A 371 (2009) 108.

[60] C. W. Chiu, A. Tekeei, W. R. Sutterlin, J. M. Ronco, G. J. Suppes, AIChe J. 54 (2008) 2456.

[61] L. Huang, Y. L. Zhu, H. Y. Zheng, Y. W. Li, Z. Y. Zeng, J. Chem. Technol. Biotechnol. 83 (2008) 1670.

[62] M. Akiyama, S. Sato, R. Takahashi, K. Inui, M. Yokota, Appl. Catal. A 371 (2009) 60.

[63] T. Kurosaka, H. Maruyama, I. Naribayashi, Y. Sasaki, Catal. Commun. 9 (2008) 1360.

[64] L.F. Gong, Y. Lu, Y.J. Ding, R. H. Lin, J. W. Li, W. D. Dong, T. Wang, W. M. Chen, Chin. J. Catal. 30 (2009) 1189.

[65] M. R. Nimlos, S. J. Blanksby, X. H. Qian, M. E. Himmel, D. K. Johnson, J. Phys. Chem. A. 110 (2006) 6145.

[66] Y. Nakagawa, Y. Shinmi, S. Koso, K. Tomishige, J. Catal. 272 (2010) 191.

[67] C. L. Zhao, I. E. Wachs, Catal. Today. 118 (2006) 332.

[68] M. M. Lin, Appl. Catal. A 207 (2001) 1.

[69] B. Katryniok, S. Paul, M. Capron, F. Dumeignil, ChemSusChem. 2 (2009) 719.

[70] S. Ramayya, A. Brittain, C. Dealmeida, W. Mok, M. J. Antal, Fuel. 66 (1987) 1364.

[71] M. J. AntalJr, W. S. L. Mok, G. N. Richards, Carbohydr. Res. 199 (1990) 111-115.

[72] L. Ott, M. Bicker, H. Vogel, Green Chem. 8 (2006) 214.

[73] V. Lehr, M. Sarlea, L. Ott, H. Vogel, Catal. Today. 121 (2007) 121.

[74] A. Neher, T. Hass, A. Dietrich, H. Klenk, W. Girke, Degussa DE 4238493 (1994).

[75] A. Neher, T. Hass, A. Dietrich, H. Klenk, W. Girke, Degussa. DE 4238493 (1994).

[76] J.-L. Dubois, C. Duquenne, W. Hoelderich, J. Kervennal, Arkema. WO 2006087084 (2006).

[77] J.-L. Dubois, C. Duquenne, Arkema. WO 2006087083 (2006 ).

[78] H. Adkins, W. H. Hartung, Org. Synth. Coll. . 1 (1941) 15.

[79] A. Neher, T. Haas, D. Arntz, H. Klenk, W. Girke, U.S. patent 5387 720 (1995).

[80] E. Schwenk, M. Gehrke, F. Aichner, U.S. patent 1916 743 (1933).

[81] S. H. Chai, H. P. Wang, Y. Liang, B.Q. Xu, J. Catal. 250 (2007) 342.

[82] E. Tsukuda, S. Sato, R. Takahashi, T. Sodesawa, Catal. Commun. 8 (2007) 1349.

[83] H. Atia, U. Armbruster, A. Martin, J. Catal. 258 (2008) 71.

[84] A. Corma, G.W. Huber, L. Sauvanauda, P. O'Connor, J. Catal. 257 (2008) 163.

[85] E. Tsukuda, S. Sato, R. Takahashi, T. Sodesawa, Catal. Commun. 8 (2007) 1349.

[86] S. H. Chai, H. P. Wang, Y. Liang, B. Q. Xu, Green Chem. 10 (2008) 1087.

[87] S. H. Chai, H. P. Wang, Y. Liang, B.Q. Xu, Appl. Catal. A 353 (2009) 213.

[88] W. Suprun, M. Lutecki, T. Haber, H. Papp, J. Mol. Catal. A 309 (2009) 71.

[89] J. L. Dubois, C. Duquenne, W. Hoelderich, J. Kervennal, WO 2006087084 (2006).

[90] H. Kasuga, M. Okada, JP 2008137950 (2008).

[91] Y. Arita, H. Kasuga, M. Kirishiki, JP 2008110298 (2008).

[92] I. V. Kozhevnikov, J. Mol. Catal. A 305 (2009) 104-111.

[93] C. L. Hill, Chem. Rev. 98 (1998) 1.

[94] I. V. Kozhevnikov, Catalysts For Fine Chemical Synthesis, Catalysis by Polyoxometalates Wiley 2002.

[95] D. E. Katsoulis, Chem. Rev. 98 (1998) 359.

[96] I. V. Kozhevnikov, Catalysts for Fine Chemical Synthesis: Catalysis by Polyoxometalates, Wiley Cheichester, England, 2002.

[97] I. V. Kozhevnikov, J. Mol. Catal. A 262 (2007) 86.

[98] I. V. Kozhevnikov, Chem. Rev. 98 (1998) 171.

[99] M. N. Timofeeva, Appl. Catal. A 256 (2003) 19.

[100] T. Okuhara, N. Mizuno, M. Misono, Adv. Catal. 41 (1996) 113.

[101] M. Misono, Chem. Commun. (2001) 1141.

[102] E. F. Kozhevnikova, I. V. Kozhevnikov, J. Catal. 224 (2004) 164.

[103] N. Mizuno, M. Misono, Chem. Rev. (Washington, DC, U. S.). 98 (1998) 199.

[104] I. Nowak, M. Ziolek, Chem. Rev. 99 (1999) 3603.

[105] K. Tanabe, Catal. Today. 78 (2003) 65.

[106] K. Tanabe, Catal. Today. 28 (1996) 1.

[107] K. Tanabe, S. Okazaki., Appl. Catal A 133 (1995) 191.

[108] K. Tanabe, Catal. Today. 8 (1990) 1.

[109] K. Tanabe, S. Okazaki, Appl. Catal. A 133 (1995) 191.

[110] J. M. Jehng, I. E. Wachs, Chem. Mater. 3 (1991) 100.

[111] I. E. Wachs, L. E. Briand, J. M. Jehng, L. Burcham, X. T. Gao, Catal. Today. 57 (2000) 323.

[112] J. Jehng, I. E. Wachs, Catal. Today. 8 (1990) 37.

[113 J. M. Jehng, I. E. Wachs, J. Phys. Chem. 95 (1991) 7373.

[114] K. Tanabe, Mater. Chem. Phys. 17 (1987) 217.

[115] M. Ziolek, Catal. Today. 78 (2003) 47.

[116] T. Iizuka, K. Ogasawara, K. Tanabe, Bull. Chem. Soc. Jpn. 56 (1983) 2927.

[117] A. Bruggink, R. Schoevaart, T. Kieboom, Org. Process Res. Dev. 7 (2003) 622.

[118] J. C. Wasilke, S. J. Obrey, R. T. Baker, G. C. Bazan, Chem. Rev. 105 (2005) 1001.

[119] D. E. Fogg, E. N. dos Santos, Coord. Chem. Rev. 248 (2004) 2365.

[120] J. M. Lee, Y. Na, H. Han, S. Chang, Chem. Soc. Rev. 33 (2004) 302.

[121] B. Cornils, W. A. Herrmann, R. Schlogl, C.-H. Wong (Eds.), Catalysis from A to Z : A Concise Encyclopedia, Wiley-VCH, New York, 2000.

[122] N. Lavaud, P. Magnoux, F. Alvarez, L. Melo, G. Giannetto, M. Guisnet, J. Mol. Catal. A 142 (1999) 223.

[123] G. C.A. Schuit, B. C. Gates, Chemtech. 13 (1983) 693.

[124] P. B. Weisz, E. W. Swegler, J. Phys. Chem. 59 (1955) 823.

[125] F. G. Ciapetta, J. B. Hunter, Ind. Eng. Chem. 45 (1953) 155.

[126] F. G. Ciapetta, J. B. Hunter, Ind. Eng. Chem. 45 (1953) 147.

[127] V. Haensel, G.R. Donaldson, Ind. Eng. Chem. 43 (1951) 2102.

[128] H. Heinemann, G. A. Mills, J. B. Hattman, F. W. Kirsch, Ind. Eng. Chem. 45 (1953) 130.

[129] T. Nakato, M. Kimura, S. Nakata, T. Okuhara, Langmuir. 14 (1998) 319.

[130] K. Sano, H. Uchida, S. Wakabayashi, Catalysis Surveys from Japan. 3 (1999) 55.

[131] K. Na, T. Okuhara, M. Misono, J. Catal. 170 (1997) 96.

[132] K. A. D. Rocha, P. A. Robles-Dutenhefner, E. M. B. Sousa, E. F. Kozhevnikova, I. V. Kozhevnikov, E. V. Gusevskaya, Appl. Catal. A 317 (2007) 171.

[133] R. D. Hetterley, E. F. Kozhevnikova, I. V. Kozhevnikov, Chem. Commun. (2006) 782.

[134] J. M. Jehng, A. M. Turek, I. E. Wachs, Appl. Catal.A 83 (1992) 179-200.

[135] Y. Higashio, T. Nakayama, Catal. Today. 28 (1996) 127.

[136] R. M. West, M. H. Tucker, D. J. Braden, J. A. Dumesic, Catal. Commun. 10 (2009) 1743.

# 2. Experimental

## 2.1 Introduction

This chapter describes the experimental methods that were used in this study for the preparation of bifunctional (metal/acid) catalysts. The experimental set up for the reaction studies in gas and liquid phase are then illustrated. The catalyst characterisation techniques which have been used to determine surface and porosity of catalysts, metal content and catalyst stability are detailed. The analytical approaches by which reaction products were detected and identified, and the conversion and product selectivity calculated, are explained.

## 2.2 Materials

The materials consumed within this study are listed in Table 2.1.

**Table 2.1** Chemicals used in this study.

| Material | Supplier |
|---|---|
| $RuCl_3$ . $xH_2O$ (99.98%) | Aldrich |
| $H_2PtCl_6$.x $H_2O$ (99%) | |
| $RhCl_3$ . $xH_2O$ (99.98%) | |
| $Pd(OAc)_2$ (99%) | |
| $H_3PW_{12}O_{40}.xH_2O$ (HPW) | |
| $H_4SiW_{12}O_{40}.xH_2O$ (HSiW) | |
| Acetol (90%) | |
| $Cs_2CO_3$ (99%) | |
| Niobium (V) chloride (99%) | |
| Niobium oxide (>99.5%) | |
| n-Butanol (99.5%) | |
| Glycerol (99+%) | Alfa Aesar |
| Ethanol (99.9%) | MERCK KGaA |
| Acrolein | Acros Organics |
| $N_2$, $H_2$ and He gases | BOC |

## 2.3 Catalyst preparation

### 2.3.1 Preparation of $Cs_{2.5}H_{0.5}PW_{12}O_{40}$ (CsPW)

$Cs_{2.5}H_{0.5}PW_{12}O_{40}$ (CsPW) was prepared as a white crystalline powder as described in the literature [1, 2]. The preparation was carried out by adding dropwise an aqueous solution of $Cs_2CO_3$ (0.47 M) to an aqueous solution of $H_3PW_{12}O_{40}.xH_2O$ (0.75 M) at room temperature according to Equation 1. The precipitate was aged for 24 hrs at room temperature, followed by evaporation at 45°C in vacuum. The material obtained was calcined at 150°C for 1.5 hr in vacuum. The surface area was then measured using the Brunauer Emmett and Teller (BET) method to ensure a high surface area of between 110-140 $m^2/g$ as an indication of the correct elemental composition and the optimum preparation and aging times.

$$H_3PW_{12}O_{40} + 1.25Cs_2CO_3 \rightarrow Cs_{2.5}H_{0.5}PW_{12}O_{40} + 1.25CO_2 + 1.25H_2O\ [3] \quad (2.1)$$

### 2.3.2 Preparation of Ru, Rh, Pt and Pd doped CsPW

(0.5-10 wt%) Ru/CsPW was prepared by wet impregnation method. 0.1M of $RuCl_3$ aqueous solutions was initially prepared. Then CsPW, a solid white powder, was stirred with Ru aqueous solution at room temperature for 24 hrs, followed by drying in a rotary evaporator at 60°C. The reduction of Ru (III) to Ru metal was carried out by exposing the solid material to $H_2$ flow at 250°C for 2 hrs. The dark catalyst obtained was stored in a desiccator over $P_2O_5$. The same procedure was followed for the preparation of 5%Rh/CsPW using $RhCl_3$ as a metal precursor.

0.5% Pd/CsPW catalyst was synthesised by stirring CsPW with 0.1 M benzene solution of $Pd(OAc)_2$ for 1 h at room temperature. The resultant brown precipitate was isolated by low pressure evaporation using a rotary evaporator at 25 °C [4].

After drying in vacuum at 150 °C and subsequent grinding, the $Pd/Cs_{2.5}PW$ material was reduced in a furnace in $H_2$ flow at 250 °C for 2 h leaving the grey crystalline bifunctional catalyst.

0.3%Pt/ $Cs_{2.5}PW$ was similarly prepared using $H_2PtCl_6.x\ H_2O$ solution as a metal precursor. The slurry was then left to stir for 24 hr at room temperature. The precipitate was isolated by low pressure evaporation using a rotary evaporator at 25 °C, dried in vacuum at 150 °C and finally reduced in $H_2$ flow at 250 °C for 2 h.

### 2.3.3 Preparation of niobic acid ($Nb_2O_5.nH_2O$)

Niobic acid (hydrous niobium oxide, $Nb_2O_5.nH_2O$) was prepared by dissolving 5 g of $NbCl_5$ powder into 10 ml of ethanol to obtain a colourless solution. Then, $NbCl_5$ solution was added dropwise into 200 ml of ammonium hydroxide (0.3 M) resulting in a white precipitate of niobic acid which was stirred at room temperature for 2 h. The white precipitate was washed with distilled water many times until chloride free, dried in oven at 100°C for 3 h and then kept in desiccator.

### 2.3.4 Preparation of 5%Ru/$Nb_2O_5$ and Rh/$Nb_2O_5$

The same procedure as that applied in section 2.2.2 was applied for doping $Nb_2O_5$ with 5%Ru and 5%Rh.

### 2.3.5 Preparation of silica-supported $H_3PW_{12}O_{40}$ (HPW)

Silica-supported $H_3PW_{12}O_{40}$ catalysts, $HPW/SiO_2$, comprising of 20% HPW was prepared by impregnation as described elsewhere [4]. A suspension of 6-8 g

Aerosil 300 silica in 60-80 ml aqueous solution, containing a certain amount of HPW, was stirred in a stoppered glass vessel for 3-4 h and kept overnight at room temperature for ageing, followed by drying at 45°C /24 Torr using a rotary evaporator.

### 2.3.6 Preparation of Pd doped silica-supported HPW

0.5% Pd-doped 20% HPW/$SiO_2$, was prepared by impregnating Aerosil 300 silica by a 0.02 M solution of $PdCl_2$ in 3 M aqueous HCl, followed by drying in a rotary evaporator and reduction of Pd(II) to Pd(0) by a hydrogen flow at 250°C for 2 h [5]. The sample was washed with water until chloride free ($AgNO_3$), then 20 wt % HPW was loaded by the impregnation method described above.

### 2.3.7 Preparation of $Zn^{II}$ –$Cr^{III}$ mixed oxide

The literature procedure [6] was used for the preparation of Zn-Cr mixed oxide (atomic ratio 1:1). 0.2 M of aqueous solution of $Zn(NO_3)_2.6\ H_2O$ and $Cr(NO_3)_3.9H_2O$ were prepared, stirred and heated to 70 °C with stirring. The coprecipitation of Zn-Cr hydroxides were obtained by adding 10%wt aqueous ammonium hydroxide dropwise to the stirred mixture of zinc and chromium nitrates. The temperature was kept at 70°C during the preparation. The pH of the mixture was monitored and when it reached 7-7.5, the precipitate was left to age for 3 h at 70°C. The precipitate was then filtered, washed with deionised water to remove ammonia, and dried in air at 100-110°C overnight. The amorphous Zn-Cr (1:1) mixed oxide was obtained by calcination of the resulting Zn-Cr hydroxides at 300°C for 5 h under nitrogen flow. The material was ground into powder with particle size of 90-180 μm.

### 2.3.8 Preparation of Pd doped Zn-Cr mixed oxide

The Pd-doped catalysts were prepared by impregnating Zn–Cr oxide with a 0.02 M solution of $Pd(OAc)_2$ in benzene at room temperature, followed by evaporation of the solvent in a rotary evaporator and subsequent reduction of $Pd^{II}$ to $Pd^0$ in a hydrogen flow at 250 °C for 2 h. The catalysts were stored in a desiccator over $P_2O_5$.

### 2.3.9 Preparation of $Cs_{3.5}H_{0.5}SiW_{12}O_{40}$ (CsSiW)

The acidic salt $Cs_{3.5}H_{0.5}SiW_{12}O_{40}$ (CsSiW) was prepared using a similar method used for CsPW by adding dropwise the required amount of aqueous cesium carbonate (0.47 M) to aqueous solution of $H_4SiW_{12}O_{40}$ (0.75 M) at 40°C with stirring [2]. The precipitate obtained was aged in aqueous mixture for 48 h at room temperature and dried using a rotary evaporator at 45°C.

Similar to 5%Ru/CsPW, 5%Ru doped CsSiW was synthesised as described in section 2.2.2.

## 2.4 Catalyst characterisation techniques

### 2.4.1 Inductively coupled plasma atomic emission spectroscopy (ICP-AES)

Inductively coupled plasma atomic emission spectroscopy is one of the analytical atomic spectroscopic techniques which uses plasma as an excitation source. Plasmas containing a high proportion of electrons and ions are created by heating a gas such as argon above 6000 K. Two different plasma emission sources

have been described in analytical chemistry textbooks- the direct-current plasma source (DCP) and the inductively coupled plasma (ICP) [7].

In ICP-AES, the sample is dissociated into its constituent atoms or ions. They emit light at a characteristic wavelength by their excitation to a higher energy level. The radiation from the plasma goes through a slit and is subsequently dispersed by a concave reflection grating. The sample wavelength reaches a series of exit slits which separate the selected emission lines for specific elements. The light from each exit slit is focussed to fall on the cathode of a photomultiplier tube, one for each spectral line separated. The voltages obtained on the photomultiplier are proportional to the concentrations of the elements in the sample [7]. ICPA-AES can detect a great number of elements in a wide range of concentrations [7].

ICP spectroscopy was used in this study to determine tungsten and phosphorus content in $Cs_{2.5}PW$. Experiments were carried out on a Spectro Ciros emission spectrometer available in the Department of Chemistry at Liverpool University.

## 2.4.2 Thermogravimetric analysis (TGA)

The aim of thermogravimetric analysis is to investigate changes that accompany the increase in sample temperature. The changes in sample weight may be a result of a physical transformation or chemical reaction or even the decomposition of the sample which includes volatile components such as water..

For instrumental requirements, it is important to provide a sensitive balance with a sample container which should be located inside a furnace whose temperature can be easily controlled and programmed for change. Software to collect data and

represent curves is also required. Typical TGA curves show the changes in sample weight as a function of temperature or time. A derivative thermogravimetric weight loss curve (DTG) can be used to show the point at which the weight loss becomes most apparent. This technique was used in this study to determine the water content in materials used in catalyst synthesis in order for the correct amount of reactants to be used. The technique was also employed to measure the thermal stability of the catalysts under study.

A Perkin Elmer TGA 7 instrument was used to perform the thermogravimetric experiments using a heating rate of either 10 or 20 °C per minute to raise the temperature from room temperature to 700 °C, under a nitrogen gas flow.

### 2.4.3 Surface area and pore size measurements

Adsorption measurements are carried out for a variety of purposes. Determination of the surface area and the pore texture for heterogeneous catalysts is an area of great interest. According to the preparation method of solid catalysts, their pore sizes are classified into three types:

1- Micropores ( pore size < 2nm)

2- Mesopores ( 2 nm <pore size < 50 nm)

3- Macropores ( pore size > 50 nm )

Pores can have regular or, more commonly, irregular shapes. Different techniques tend to show different results for the same sample. Therefore, it is essential to indicate the techniques by which the adsorption measurements were conducted.

One of the most appropriate adsorption techniques is nitrogen adsorption which is performed at 77 K. It has the ability to find out the type of adsorption isotherm. According to IUPAC, six types of isotherms can be distinguished, but only four types have been observed in catalyst characterisation. These are shown in Figure 2.1. In the nitrogen adsorption isotherm, the total coverage (θ) of adsorbate is dependent on the gas pressure [8].

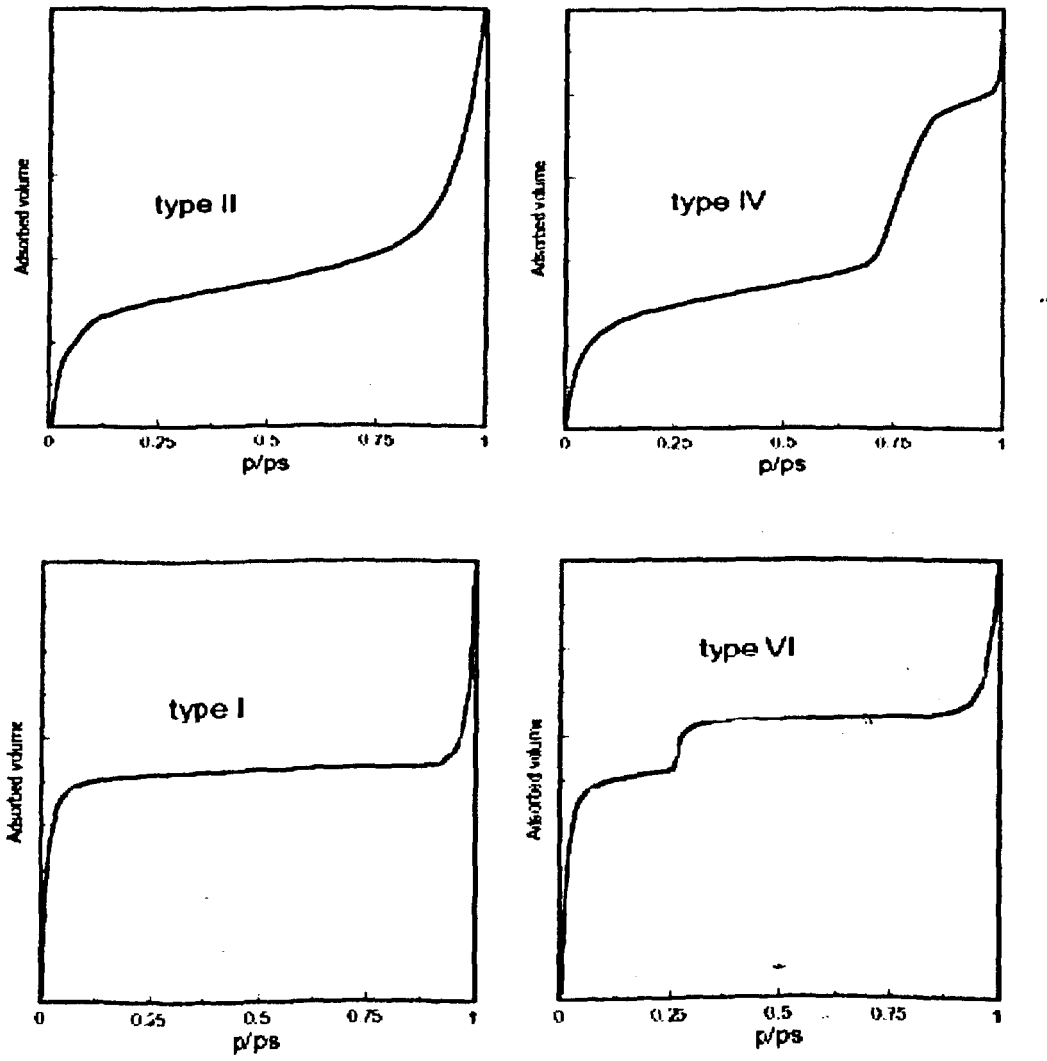


**Figure 2.1** The types of adsorption isotherm usually observed by nitrogen adsorption [8].

The description of these types is summarised as follows [8]:

• Type I indicates that the solid is microporous where adsorption occurs at very low relative pressures due to a strong interaction between the pore walls and the adsorbate. To fill all the pores, a higher pressure is required, which is favoured by an interaction between adsorbate molecules. When micropores are filled, the adsorption continues on the external surface, following the behaviour of macro- or mesoporous solids which are described below.

• Type II is a sign of macroporous solids on which a monolayer of adsorbed molecules is formed at low relative pressure, while at high relative pressures multilayer adsorption arises, demonstrating a dramatic increase in adsorbate thickness, to the point at which condensation pressure is achieved.

• Type IV states that the adsorption process is taking place on a mesoporous material. Similar to that which occurs with macroporous material, the adsorption initially happens at low relative pressure. Multilayer adsorption at a high relative pressure takes place until the condensation pressure is reached, giving a sharp rise in the adsorption volume.

• Type VI has been reported to be for uniform ultramicroporous solids. The adsorption pressure depends on the surface-adsorbate interaction. Therefore, if the solid is active and uniform, the whole process occurs at a well-defined pressure. If the surface has a lack of active uniform sites, a stepped isotherm should be observed in which each step indicates that the adsorption has occurred on only one group of sites. Due to the common heterogeneity obtained with solid catalyst surfaces, this type of isotherm has never been observed.

Pore size, pore volume and surface area can be measured using nitrogen adsorption. The major goal of carrying out nitrogen adsorption was to measure total surface area, pore volume, and pore size distributions of the catalysts prepared in this study.

**BET method (surface area)**

The well-known method used to determine the total surface area of porous solid is the Brunauer-Emmett-Teller (BET), method developed in the 1940s [37]. It is a volumetric method for the assessment of the surface area of porous and non-porous solids where multilayer (physical) adsorption takes place and isotherm types I, II or IV are identified.

The form of the BET equation which yields a linear plot, from which the surface area of the solid can be calculated, is given in equation 2.2.

$$\frac{P}{V(P_o - P)} = \frac{1}{V_m C} + \frac{(C-1)}{V_m C}\frac{P}{P_o} \qquad (2.2)$$

Here, **P** is the equilibrium pressure, $P_o$ is the saturated vapour pressure at 77 K, **V** is the total gas adsorbed volume, $V_m$ is the volume of gas adsorbed on the monolayer and **C** is a constant. The plot of $P/V\ (P_o-P)$ versus $P/P_o$ results in a straight line with the slope equal to $(C-1)/V_mC$ and the intercept equal to $1/VmC$.

From the slope and the intercept, the value of $V_m$ can be calculated and used in equation 2.3 to calculate the surface area ($A_s$).

$$A_s = \sigma V_m N_A / V_o \qquad (2.3)$$

In this Equation, $N_A$ is the Avogadro number ($6.023 \times 10^{23}$ $mol^{-1}$) and $V_o$ is the molar volume of $N_2$ (22,414 $dm^3$/mol at the standard temperature and pressure). It should

be pointed out that the linearity of the BET plot is usually restricted (**$0.05 < P/P_o < 0.35$**).

In this work, the BET method was used to determine surface areas of heteropoly acids and niobium oxide catalysts used in this study. The technique was also essential to confirm that the surface area of CPW was in the range of 110-140 $m^2/g$, which is an indication that the correct CsPW material was obtained.

**BJH method ( mesopore volume and mesopore size distribution)**

Mesopore volume and mesopore size for catalysts were calculated using the Barrett-Joyner-Halenda (BJH) model [9] which is based on the Kelvin equation and describes the adsorption-capillary condensation that takes place in the mesopores [8]. Capillary condensation occurs when $P/P_0 > \sim 0.4$, and each increase in pressure increases the thickness of the layer adsorbed on pore walls and also causes an increase in the capillary condensation in pores containing a core (empty space) of size $r_c$. This effect is defined by the Kelvin equation (2.4), where $r_c$ represents the radius of cylindrical pores, $\gamma$ is the distance between walls for slit shaped pores, $w_m$ is the molar volume and $\theta$ is the contact angle.

$$\ln (P/P_o) = -(2\gamma w_m \cos\theta)/RTr_c \qquad (2.4)$$

The model, assuming cylindrical or slit shape of the pores, gives a method of calculating the contribution of the thickness of the adsorbed film to the total adsorption and then the core volume. From these values, and assuming particular pore geometry, the core volume is transformed into the pore volume and the core size into the pore size.

The BET experiments in this study were conducted on a Micromeritics ASAP 2000 adsorption apparatus. Typically, a 0.10-0.15 g sample was packed into the sample tube and degassed at 250°C for 4-6 h to reach a vacuum of $10^{-3}$ Torr. After outgassing, the sample was allowed to cool to room temperature, and the tube was then immersed in liquid nitrogen. Finally, the gas pressure was allowed to reach equilibrium before subsequent dosing and then a series of 55 successive nitrogen doses were done in order to obtain an adsorption isotherm. At the end of analysis the sample was weighed and this weight was used for calculation of surface area and pore volumes.

### 2.4.4 Elemental analysis

The determination of elements such as carbon, hydrogen, nitrogen and sulfur in organic compounds is important for many chemical applications. Combustion analysis is a valuable tool for the calculation of C, N and H in given samples. As the catalysts are subjected to deactivation by coke formation, combustion analysis was used to measure the C and H content in spent catalysts.

The combustion analysis in this study was performed by S. G. Apter, on a Thermo Flash EA 1112 series analyzer.

### 2.4.5 $H_2$ chemisorption

The catalytic cycle in heterogeneous catalysis is known to take place on the surface of solid catalyst. The characterisation of metal components in supported metal catalysts is important for the catalyst design process and a full understanding of the catalyst behaviour. The highly dispersed state of metal at the surface of the support is vitally needed in catalytic process. Gas adsorption techniques are

commonly used for the determination of the surface areas, particle sizes and dispersion of metal [10]. Gas chemisorption ($H_2$, $O_2$ and $CO$) is a selective method for the measurement of metal dispersion on an inert support [10, 11].

A pulse $H_2$ chemisorption analysis is well-established procedure for the determination of metal dispersion which is, by definition, the ratio of the number of metal atoms present at the surface and the total number of metal atoms in the catalyst [12-15]. A more convenient and more sensitive variant of this analysis is the titration of oxygen adsorbed on metal sites (M) with $H_2$ [15]. This technique has previously been used for dispersion measurement of palladium [14], platinum [13], rhodium [16, 17], and ruthenium [18].

For $H_2$-$O_2$ titration experiments, the catalyst sample containing Ru, Pd, Pt or Rh was initially reduced at 250 °C with $H_2$ flow (20 mL/min) to ensure M was reduced to $M^0$. The reduced catalyst was then left for a period of 48 h in a desiccator exposed to air to allow $O_2$ to dissociatively adsorb onto M atoms on the surface at a $M_s$-O a ratio of 1:1. Where $M_s$ is the surface of M atom and O is oxygen that adsorbs without immediate desorption back into the atmosphere. A sample of the pretreated catalyst (typically 50 mg) was placed into the sample tube used for volumetric $H_2$ titration in a Micromeritics TPD/TPR 2900 analyzer fitted with a thermal conductivity detector (TCD). The sample was stabilised at 100 °C under nitrogen flow as a carrier gas for 1 h, which allowed TCD baseline to stabilise. 50 μL pulses of pure $H_2$ were injected in the flow in 3 minutes intervals until the catalyst was saturated with hydrogen. The stoichiometry of the $H_2$ titration is shown in Equation 2.5.

$$M_s\text{-}O + 3/2H_2 \longrightarrow M_s\text{-}H + H_2O \qquad (2.5)$$

The volume of $H_2$ adsorbed onto the surface was calculated through integrating areas under the peaks shown on the screen that were detected by the TCD. Then the ratio of the area of each peak where adsorption occurs compared to the area of the peaks where no adsorption occurred was calculated, and the total volume of $H_2$ adsorbed at 348 K. the dispersion and average M particle diameter were calculated using equations 2.6- 2.9 [19].

$$V_{348K} = \Sigma \{50 - [(PA_{ads}/PA_{av}) \times 50]\} \quad (2.6)$$

In Equation 2.6, $V_{348K}$ is the total Volume adsorbed of $H_2$ (μL) with a temperature of 75 °C (348 K), $PA_{ads}$ is the peak area with $H_2$ adsorption, $PA_{av}$ is the mean average peak area of injections with no adsorption.

$$V_{273\,K} = V_{348K} \times (273/348) \quad (2.7)$$

In Equation 2.7, $V_{273\,K}$ is the total volume (μL) adsorbed of $H_2$ at 0 °C (273 K).

$$D = \frac{V_{273K}(mL) \times A_r}{M_{cat}(g) \times 22414\ (mL) \times C_M \times 1.5} \quad (2.8)$$

In Equation 2.8, $D$ is the dispersion, $A_r$ is the relative atomic mass of M, $m_{cat}$ is the mass of catalyst used (g), 22414 represents the volume of one mole of $H_2$ gas at 273 K, $C_M$ is the concentration of M as a fraction of the catalyst mass, and 1.5 is the

The volume of $H_2$ adsorbed onto the surface was calculated through integrating areas under the peaks shown on the screen that were detected by the TCD. Then the ratio of the area of each peak where adsorption occurs compared to the area of the peaks where no adsorption occurred was calculated, and the total volume of $H_2$ adsorbed at 348 K. the dispersion and average M particle diameter were calculated using equations 2.6- 2.9 [19].

$$V_{348K} = \Sigma \{50 - [(PA_{ads}/PA_{av}) \times 50]\} \quad (2.6)$$

In Equation 2.6, $V_{348K}$ is the total Volume adsorbed of $H_2$ (μL) with a temperature of 75 °C (348 K), $PA_{ads}$ is the peak area with $H_2$ adsorption, $PA_{av}$ is the mean average peak area of injections with no adsorption.

$$V_{273\,K} = V_{348K} \times (273/348) \quad (2.7)$$

In Equation 2.7, $V_{273\,K}$ is the total volume (μL) adsorbed of $H_2$ at 0 °C (273 K).

$$D = \frac{V_{273K}(mL) \times A_r}{M_{cat}(g) \times 22414\ (mL) \times C_M \times 1.5} \quad (2.8)$$

In Equation 2.8, $D$ is the dispersion, $A_r$ is the relative atomic mass of M, $m_{cat}$ is the mass of catalyst used (g), 22414 represents the volume of one mole of $H_2$ gas at 273 K, $C_M$ is the concentration of M as a fraction of the catalyst mass, and 1.5 is the

stoichiometry of $H_2$ adsorbed to M adsorbent. The particle size, $d_s$ (nm), was calculated using the empirical Equation (2.9) [14].

$$d = 0.9/D_2 \qquad (2.9)$$

## 2.4.6 Ultraviolet (UV) spectroscopy

Most UV spectrometers operate on the double-beam basis, with one beam passing through the sample and the other through a reference cell [20]. After passing through the monochromator and the cells, the light from the source arrives at the detector which measures the ratio of the intensity of the reference beam (the incident intensity, $\mathbf{I_0}$) to the intensity of the sample beam (the transmitted intensity, **I**). On most machines the output from detector is automatically converted into the absorbance $\mathbf{A = \log I_0/I = \log 1/T}$. The absorbance of a sample is proportional to its concentration, **c**, and to the path length, $\boldsymbol{\ell}$, and is given by an equation, usually called the Lambert-Beer law:

$$\mathbf{A = \varepsilon c \ell} \qquad (2.10)$$

Typically, a standard UV cell with $\boldsymbol{\ell}$ = 1 cm is used, hence $\mathbf{A = \varepsilon c}$. The constant $\boldsymbol{\varepsilon}$ (molar extinction coefficient) is a measure of how well the compound absorbs at a given wavelength. Provided that the concentration of the sample is known, $\boldsymbol{\varepsilon}$ is readily calculated. Conversely, if the $\boldsymbol{\varepsilon}$ value for a compound is known at a given wavelength, measuring the absorbance at this wavelength permits the determination of the concentration of the sample. Absorption maxima and molar extinction coefficient are characteristics of an absorption spectrum [20].

UV spectroscopy was used in this project to investigate the catalyst leaching under reaction conditions by measuring the UV absorption characteristic of Keggin anions $[PW_{12}O_{40}]^{-3}$ which appear in the region of (260-270 nm). 0.2 g of catalyst was used under reaction conditions. After the separation of the solid catalyst, 1 mL of reaction mixture was diluted in 24 mL of $H_2SO_4$ (1 N). The use of $H_2SO_4$ was to keep pH below 2 in order to maintain the Keggin structure which has been found to form lacunary (defect) species in aqueous solution at appropriate pH. For example, $[PW_{12}O_{40}]^{3-}$ forms the lacunary anion $[PW_{11}O_{39}]^{7-}$ at the pH 2 in aqueous solution. The amount of $H_3PW_{12}O_{40}$ in 1 N $H_2SO_4$ aqueous solution was measured with the VARIAN Cary 50 UV spectrophotometer in 1 cm quartz cuvette at a wavelength of 265 nm. The UV spectrum of the $PW_{12}O_{40}^{3-}$ anion in aqueous solution usually consists of one broad peak (Figure. 2.2).

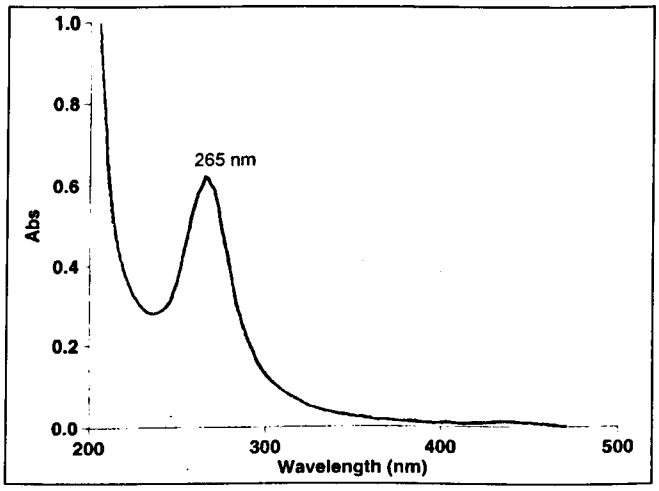


**Figure 2.2** UV spectrum for aqueous solution of $H_3PW_{12}O_{40}$ in 1 N $H_2SO_4$.

## 2.4.7 Fourier transform infrared spectroscopy (FTIR)

FT-IR experiments were conducted on $Ru/Cs_{2.5}PW$ samples before and after catalytic reaction to determine the structural stability of the heteropoly acid compound. FTIR of adsorbed pyridine on the catalyst surface was also used to investigate the presence of Lewis and Brønsted sites. It is a widely used technique for obtaining information on the structural framework of materials [21].

Infrared radiation (in the region 400-4000 $cm^{-1}$) is used to probe the vibrational modes of sample chemical bonds. The infrared radiation is absorbed by chemical bonds and bending and stretching of the bonds is induced. The frequency of the radiation needed to excite the vibrational modes and the intensity of this absorption is dependant on the strength and chemical environment of the bonds existing within the sample. The sample is scanned with infrared radiation across the spectral region and when there is absorption of the radiation, the transmitted infrared beam is weakened. The resultant spectrum (a plot of intensity *vs* wave number) can be shown in either transmission or absorption mode.

For heteropoly acid compounds, the fingerprint region of the spectrum (1200-500 $cm^{-1}$) is of most interest, revealing information about their primary structure. For the investigation of heteropoly acid primary structure for fresh and spent catalysts used in this study, samples were prepared by drying in vacuum at 150 °C for 1.5 h. Then 2 mg of the catalyst was mixed with 100 mg of KBr and ground thoroughly to create a diffusely scattering matrix that lowers absorption and hence increases the throughput of the beam, enhancing the resolution for analysis. The experiments were performed at room temperature under a dry nitrogen flow. FT-IR studies were carried out in absorbance mode using a Nicolet NEXUS FT-IR spectrometer.

Diffuse reflectance infrared Fourier transform (DRIFT) spectra of adsorbed pyridine were obtained using the same instrument equipped with a controlled environment chamber (Spectra-Tech model 0030-101). Catalyst samples were diluted with KBr powder (10 wt% in KBr), then loaded into the environmental chamber and pretreated at 100 °C and 20 mTorr for 1 h. Then the background DRIFT spectra were recorded at 100 °C and 20 mTorr. The samples were then exposed to pyridine vapour at 15 Torr pressure and 100 °C for 0.5 h, followed by pumping out at 100 °C and 20 mTorr pressure for 0.5 h. The DRIFT spectra of adsorbed pyridine were recorded at 100 °C and 20 mTorr against the background spectra and displayed in the absorbance mode [6].

### 2.4.8 Powder X-ray diffraction

X-rays have wavelengths equivalent to the spacing of atoms in crystals and can therefore be diffracted by them, resulting in a diffraction pattern. Powder X-ray diffraction was developed by Peter Debye and Paul Scherrer, and independently by Albert Hull [22]. Powdered solids contain randomly orientated particles, and when a fraction of the particles from crystalline materials are orientated so as to have a crystal plane at the correct angle for constructive interference to occur, and thus obeying Bragg's law (Equation 2.11), a diffractogram will result. In Equation 2.10, $n$ is the order of the reflection (an integer value), $\lambda$ is the incident X-ray wavelength, $d$ is the lattice planar spacing, $\theta$ is the diffraction angle.

$$n\lambda = 2d\mathrm{Sin}\theta \qquad (2.11)$$

placed in the medium part of the tubes (since the cylindrical sample crucible is completely surrounded by the detector, all heat exchange is evaluated and hence gives very accurate measurements). The calorimetric block is fixed on a vertical stand, and a symmetrical balance is sat above. The suspensions of the balance are brought into line with the axis of each experimental tube. The crucibles, hooked at the ends of the suspensions, are driven in the detection zone of the DSC by sliding the balance.

In this study, the fresh samples were pre-treated under a flow of dry helium (30 ml/min) at 300°C for one hour (heating rate 5°C/min) to remove all water. The temperature was then lowered to 100°C. After stabilisation of the sample weight at 100°C (about 2 h), the analysis was performed by successive injections of ammonia carried by flow of helium. Sufficient time (20 min) was allowed after each injection for the ammonia to be absorbed and equilibrium to be reached. Weight gain and corresponding heat of adsorption were recorded.

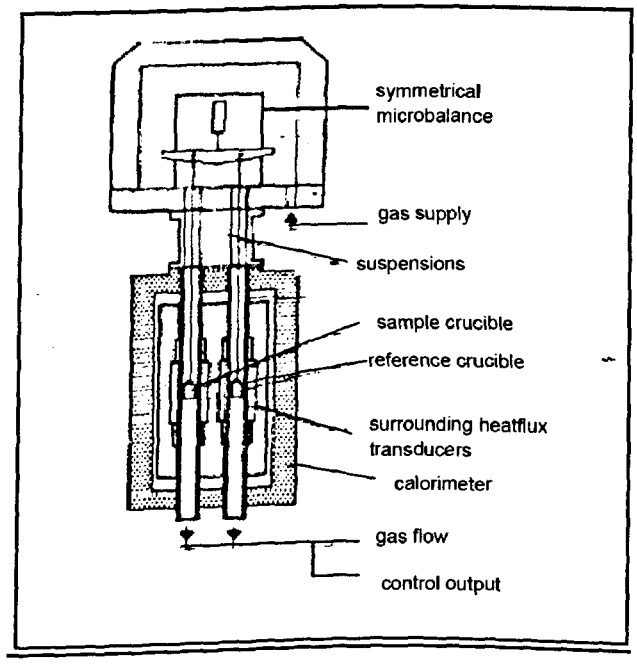


**Figure 2.3** TG-DSC schematic cross section [25].

## 2.5 Catalytic reaction studies

### 2.5.1 Liquid phase reactions

The liquid phase hydrogenolysis of glycerol was carried out in a 45-mL Parr 4714 stainless steel autoclave equipped with a magnetic stirrer. The reaction mixture contained 5.0 mL of an aqueous solution of glycerol and 0.10-0.40 g catalyst. The autoclave was purged with $H_2$ three times, then pressurised with $H_2$ (3–14 bar) and placed in the oil bath preheated to the required temperature. Figure 2.4 shows the equipment setup for the liquid phase reactions.

After reaction completion, the autoclave was cooled to 0°C, depressurised and opened. The catalyst was then separated by centrifugation. The liquid products and the unreacted glycerol were weighed and 0.25 g of n-butanol was added as an external standard.

Products were analysed by off-line GC. Products mixture of 0.5 µl was injected into GC column (GC conditions are given in Section 2.6.1). Method described in section 2.6.1 and equation 2.16 were used for the quantitative analysis of the reaction products. Individual product selectivities were calculated as the molecular percentage of all organic products obtained. The conversion of glycerol was calculated as the ratio of moles of all products to the total moles of glycerol initially present.

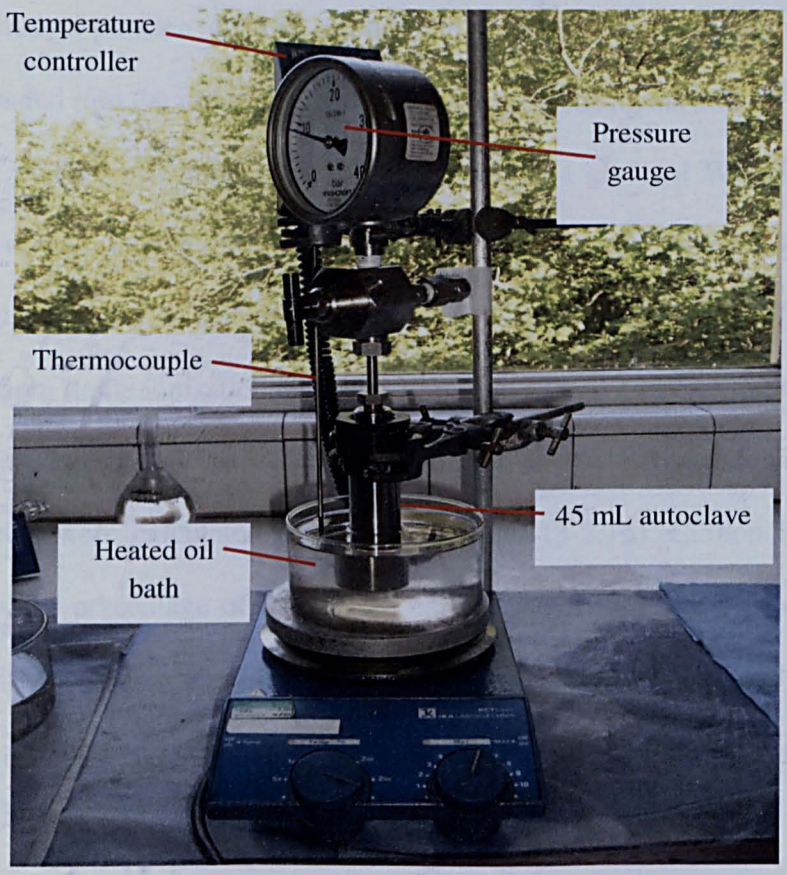


**Figure 2.4** Liquid phase reaction equipment setup.

## 2.5.2 Gas phase reactions

Dehydration of glycerol was carried out in a vertical down-flow fixed-bed Pyrex tubular reactor of 28 cm length and 0.8 cm internal diameter with a catalyst bed set at the middle of reactor length. Figure 2.5 shows a schematic presentation for the gas phase glycerol dehydration process. A glass wool plug was placed in the top of reactor to enhance evaporation of the liquid glycerol feed before reaching the catalyst bed. The reactor was placed in an electrically heated furnace. The temperature was controlled by a thermocouple which was located near the catalyst bed. Nitrogen or hydrogen was used as a carrier gas at a flow rate of 15 mL $min^{-1}$ which was controlled by Brooks mass flow controllers. The reactor was packed with

0.30 g of catalyst powder (45–180 μm particle size). A glycerol–water (10:90 w/w) solution was fed into the top of reactor by a Kontron Instruments 422 HPLC pump at a flow rate of 0.14 mL $min^{-1}$, which corresponds to a glycerol WHSV of 2.8 $h^{-1}$. Reaction products, together with unconverted glycerol, were collected hourly in an ice trap (0 °C) and subjected to offline GC analysis (Varian CP-3800 gas chromatograph, flame ionisation detector, 30 m × 0.32 mm CPWAX 52 CB capillary column) using ethanol as a standard. Glycerol conversion, product selectivities and product yields were calculated using Equations (2.13-2.15). Carbon balance was estimated as the percentage of the reacted carbon atoms found in organic products. Typically, it was close to 100% within ±5% experimental error. Non-analysed gaseous by-products and coke deposited on the catalyst had little effect on the carbon balance and are neglected unless stated otherwise.

$$\text{Conversion of glycerol (\%)} = \frac{\text{Moles of glycerol reacted}}{\text{Moles of glycerol fed}} \times 100 \qquad (2.13)$$

$$\text{Product yield (\%)} = \frac{\text{Moles of products}}{\text{Moles of glycerol fed}} \times 100 \qquad (2.14)$$

$$\text{Product selectivity (\%)} = \frac{\text{Product yield}}{\text{Glycerol conversion}} \times 100 \qquad (2.15)$$

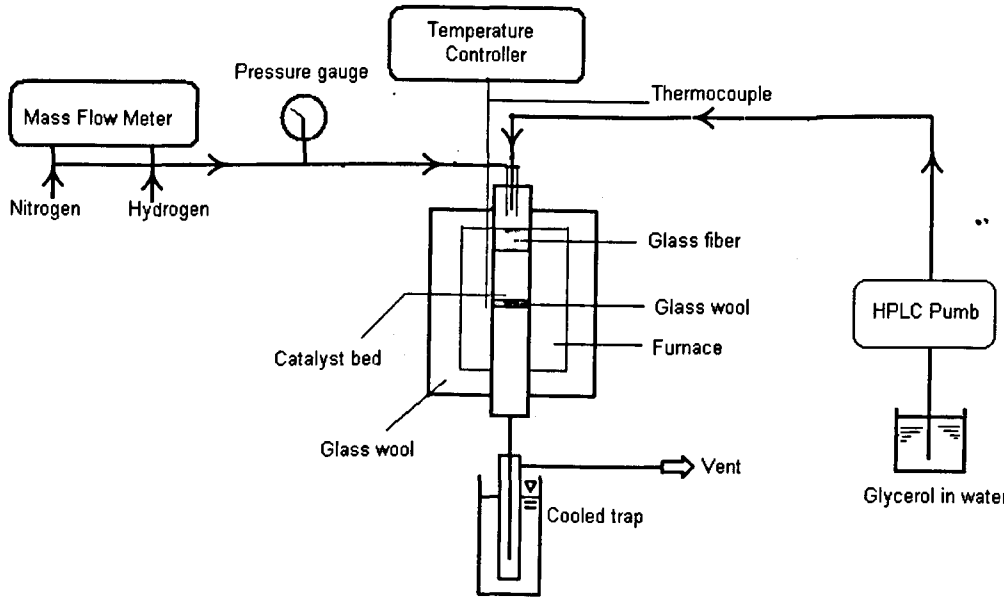


**Figure 2.5** Experimental set-up for gas-phase dehydration of glycerol to acrolein.

## 2.6 Product analysis

### 2.6.1 Gas chromatography

Gas chromatography is a method for separating components of mixtures of volatile compounds by transferring them in a gas stream as a mobile phase through a column containing a liquid or solid phase. Figure 2.6 shows the content of GC chromatography. Compounds migrate through the column according to their boiling points, solubility or adsorption. The mobile phase is known as a carrier gas and should be inert to the column and components of the mixture. Typical examples are helium, argon, nitrogen and hydrogen [7, 26].

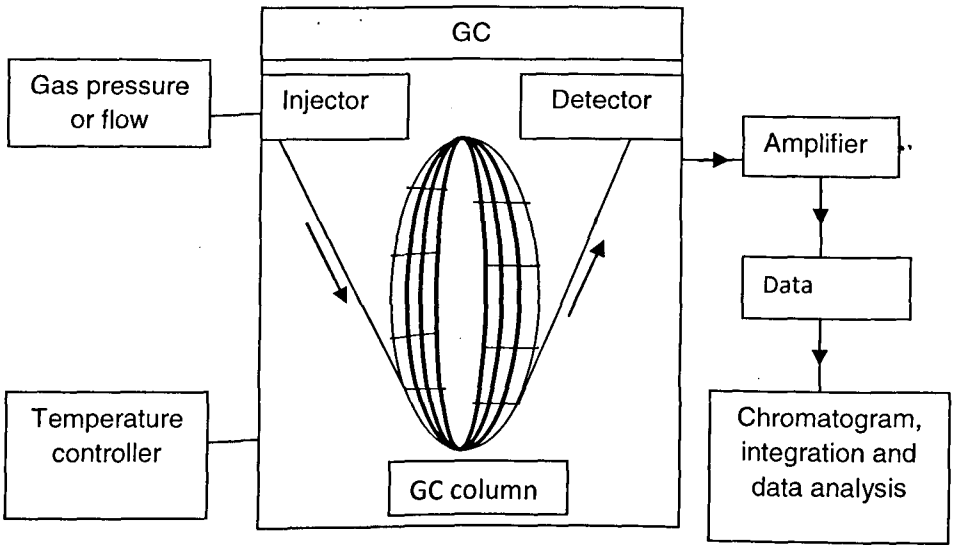


**Figure 2.6** Schematic diagram of gas chromatograph.

The separation process takes place in a column such as a capillary column, which is the one most widely used. This column consists of a coil of stainless steel, glass or quartz tubing. It can also be used in different lengths of up to 100 m thereby providing a high level of efficiency, particularly for complex mixtures. On the internal wall of the column the liquid or solid stationary phase are coated or chemically bonded. The high thickness of the stationary phase results in a high level of efficiency but low sample capacity. The most important properties of the stationary phase are that it should be non-volatile, chemically and thermally stable over a wide range of temperatures, and nonreactive with the separating compounds. Furthermore, it should have similar polarities to the samples [7, 26].

Regarding the sample injection, there are a variety of injection methods and injection ports but the type of column used determines the appropriate port to use. Due to the use of a capillary column in our case, the split/splitless injector was employed in order to reduce the amount of compounds entering the column.

There are many types of detectors. A common one is the flame ionization detector (FID) which is highly sensitive and responsive to all organic solutes except formaldehyde, formic acid and fully halogenated compounds. In this detector, the gas mixture which has been transferred from the column is mixed with hydrogen and air and burnt at a small metal jet. A 150-200 V potential is applied between the burner jet (positive) and a collector electrodes (negative) which is just above the micro-flame. The electrodes are linked to an external route where the signal can be amplified and recorded. Extracted solutes are burnt to produce ions which increase the electrical conductivity of the flame and the current, which is proportional to the concentration of ions derived from the solutes, is recorded.

**Quantitative analysis of products**

Different methods can be used to perform quantitative gas chromatographic analysis. The internal or external standard is widely used. This method relies on the addition of a known concentration of a selected standard compound to the mixture. Therefore, the ratios of the compounds peak areas or heights to that of the standard depend only on their concentrations and not on their actual amounts injected. For more accurate results, the standard should be eluted very closely to the components to be analysed and its peak area should be similar to theirs. This method enables us to quantify compounds involved in the analysis by using Equation (2.16):

$$M/M_o = K.S/S_o \qquad (2.16)$$

In this equation, $M/M_o$ is the molar ratio of analysed compound and internal or external standard, $S/S_o$ is the ratio of peak areas of compound and the standard and K is the molar calibration factor which can be obtained from the linear plot of Equation (2.16). It should be noted that the concentration of the standard is kept

constant and that the calibration factor differs for each compound. In our study, the calibration factors were measured using external standards, n-butanol for the liquid phase reactions and ethanol for the gas phase reactions. The retention times and the calibration factors for the products observed in this study are given in Table 2.2.

**Table 2.2** Retention times and molar calibration factors for all components involved in the liquid and gas phase reactions of glycerol.

| Compound | Molecular weight (g/mol) | Boiling point (°C) | Retention time (min) | Calibration factor (K) |
|---|---|---|---|---|
| Glycerol | 92.09 | 290 | 8.71 | 1.72 |
| Acetol | 74.08 | 146 | 3.39 | 1.52 |
| 1,2-Propanediol | 76.09 | 188 | 5.12 | 1.35 |
| 1,3-Propanediol | 76.09 | 212 | 6.03 | 1.04 |
| n-Butanol | 74.11 | 117 | 2.32 | - |
| 1-Propanol | 60.10 | 97 | 1.86 | 1.04 |
| 2-Propanol | 60.10 | 82 | 1.56 | 2.50 |
| Ethylene glycol | 62.07 | 197 | 5.35 | 1.86 |
| Ethanol | 46.07 | 78 | 1.46 | 2.15 |
| Acrolein | 56.06 | 53 | 1.34 | 1.37 |

The typical GC traces for liquid-phase glycerol hydrogenolysis are shown in Figure 2.7. The column and detector conditions are also provided in Figure 2.8. The calibration plots (Equation 2.16) from which the molar calibration factors for the main products involved in the liquid phase hydrogenolysis of glycerol and gas phase dehydration of glycerol are shown in Figure 2.9. The GC traces for glycerol dehydration products are presented in Figure 2.10.

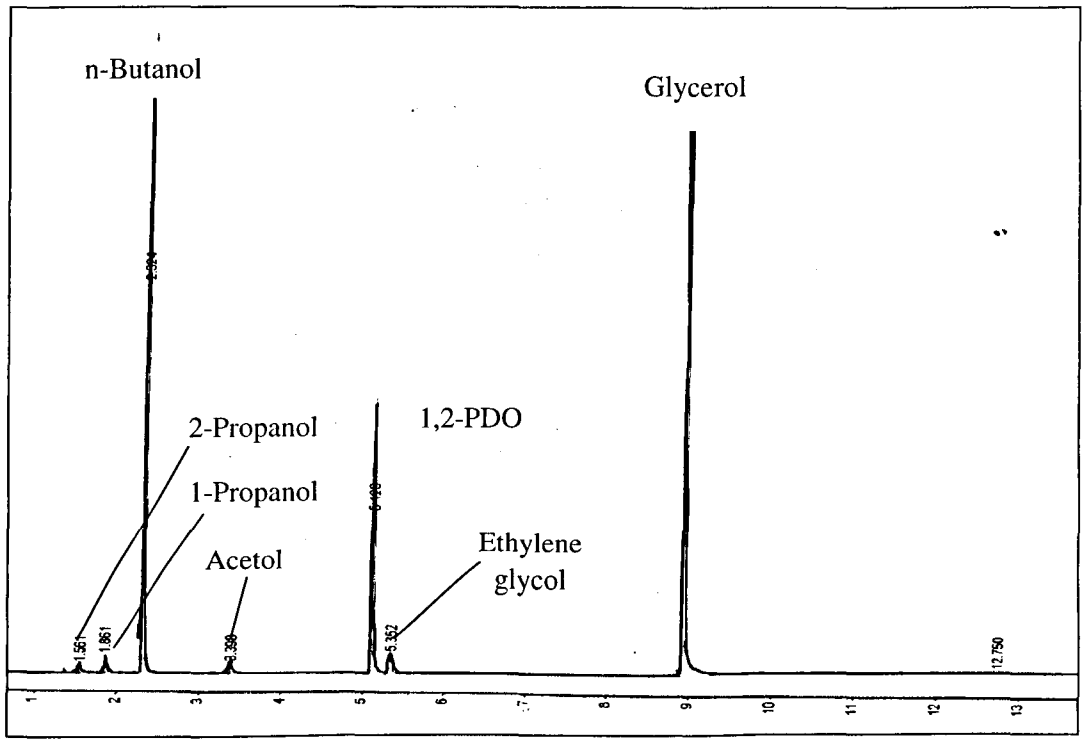


**Figure 2.7** GC traces of glycerol hydrogenolysis reaction products.

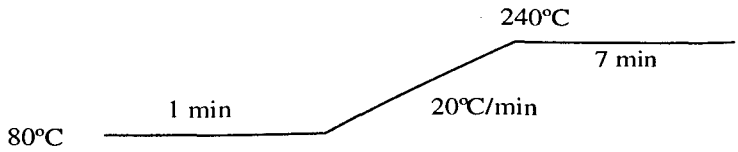


Injector temperature = 280°C

Detector Temperature = 300°C

**Figure 2.8** Conditions of GC analysis for glycerol hydrogenolysis.

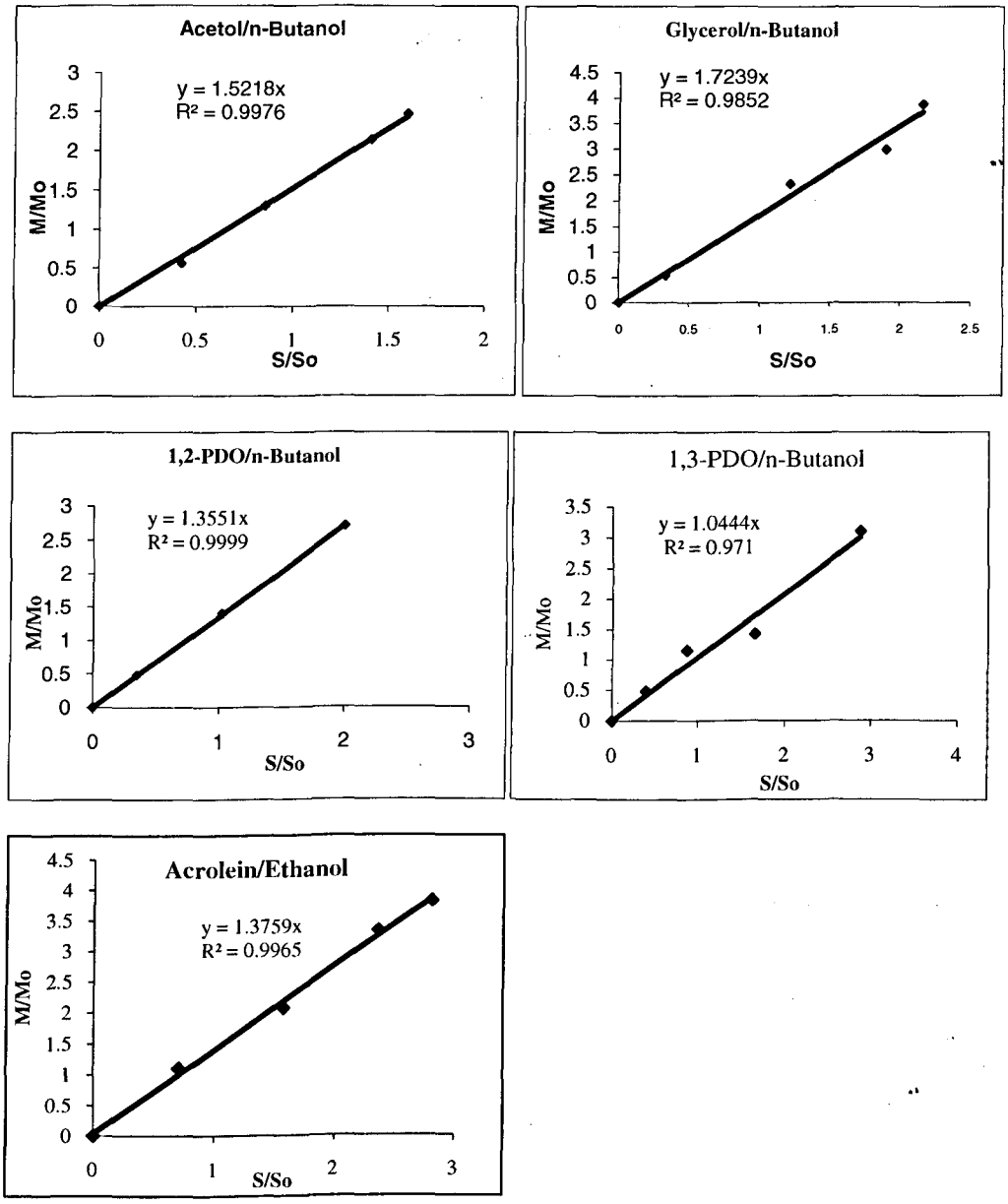


**Figure 2.9** Calibration plots for the main products observed in liquid-phase hydrogenolysis of glycerol and gas-phase dehydration of glycerol.

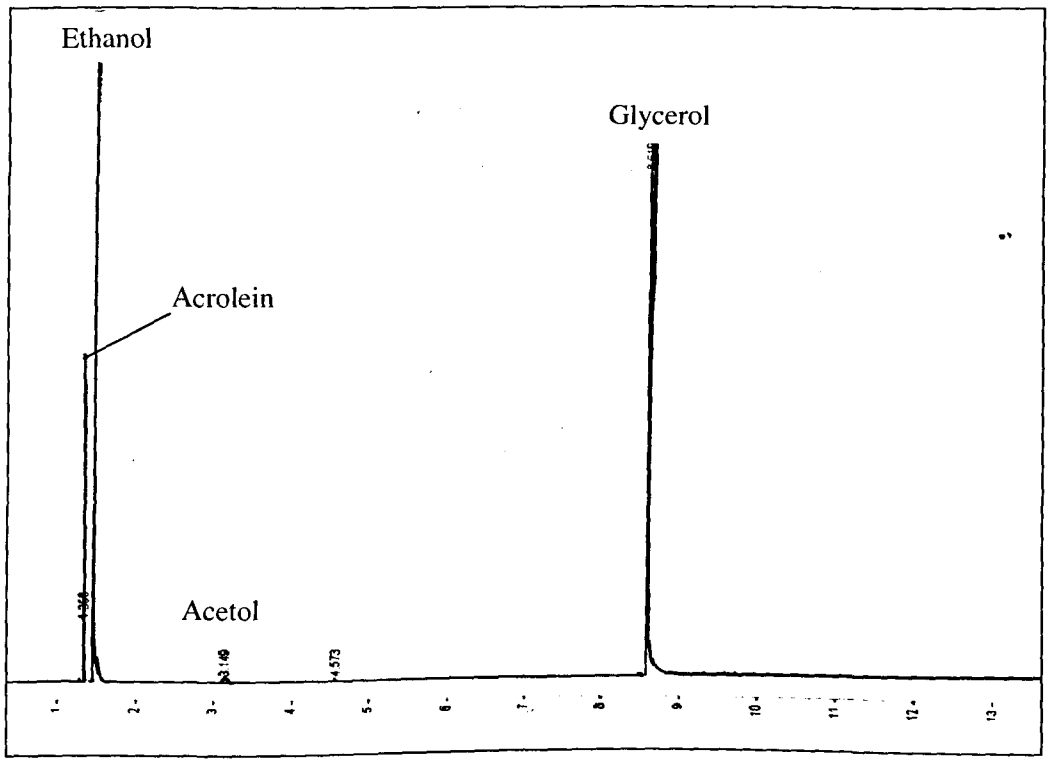


**Figure 2.10** GC traces for products observed in gas-phase glycerol dehydration.

## 2.6.2 Gas chromatography-mass spectrometry (GC-MS)

In mass spectrometry the material under examination is vaporised using a high vacuum, and a high-energy electron beam bombards the vapour [20, 21]. Many molecules in the vapour phase undergo fragmentation and produce an array of ions of various sizes. These ions are detected by accelerating them in an electric field and then deflecting them into a magnetic field where they will follow paths dictated by their mass/charge ratio.

Each kind of ion gives a peak in the mass spectrum. Non-volatile inorganic materials can be examined by vaporising them using a high-voltage electric spark. Mass spectrometry is particularly useful for establishing the structure of organic compounds, but it requires pure substances for optimum results. Even simple

mixtures tend to produce complicated spectra that may be difficult to interpret. The use of mass spectrometry as a detector for chromatographic methods allows identification of each compound as it elutes from the chromatograph.

A TRIO-1000 GC-MS spectrometer was employed to identify compounds in liquid phase hydrogenolysis of glycerol and the gas phase dehydration of glycerol. The samples were analysed by Alan Mills and Moya McCarron. The results for the main products in liquid and gas phase are shown in Figures 2.11-2.16.

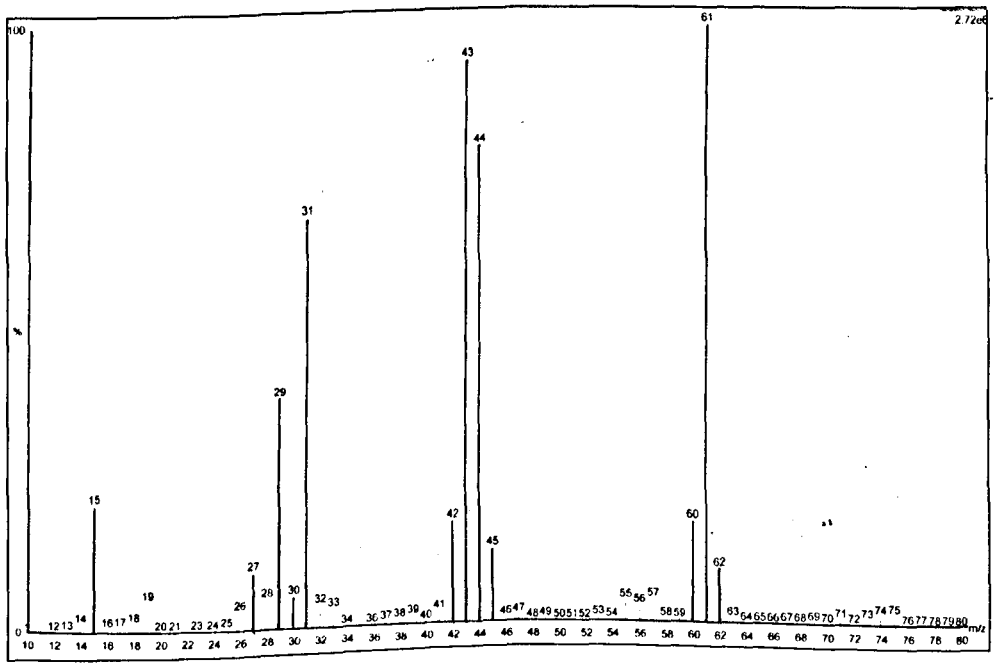


**Figure 2.11** Mass spectrum of glycerol. Relative molecular mass = 92.09.

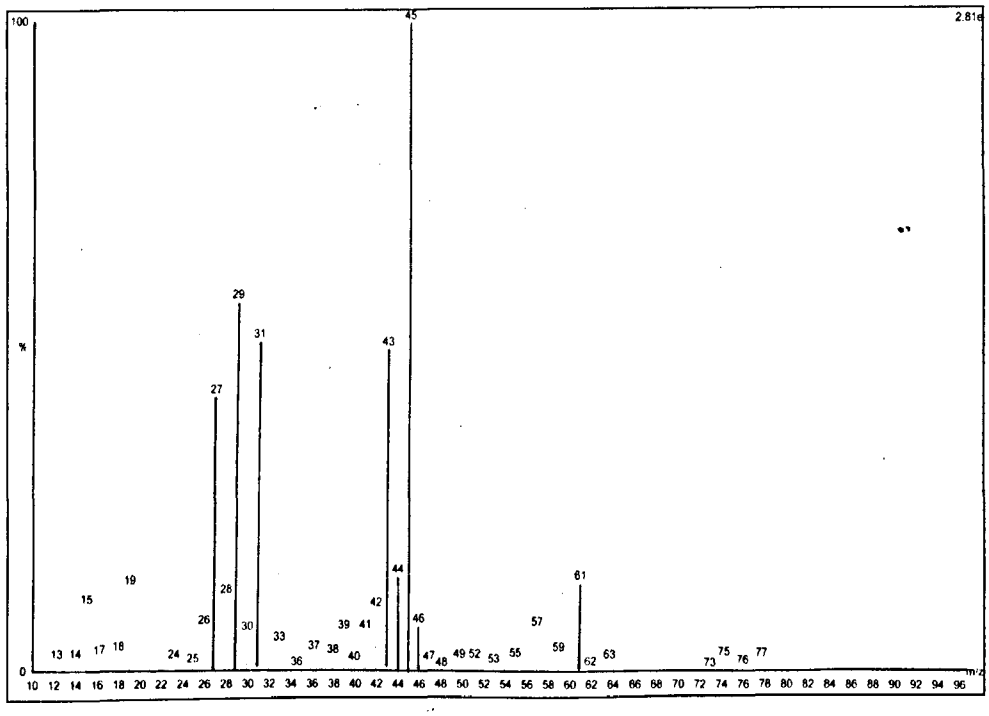


**Figure 2.12** Mass spectrum of 1,2-propanediol. Relative molecular mass = 76.09.

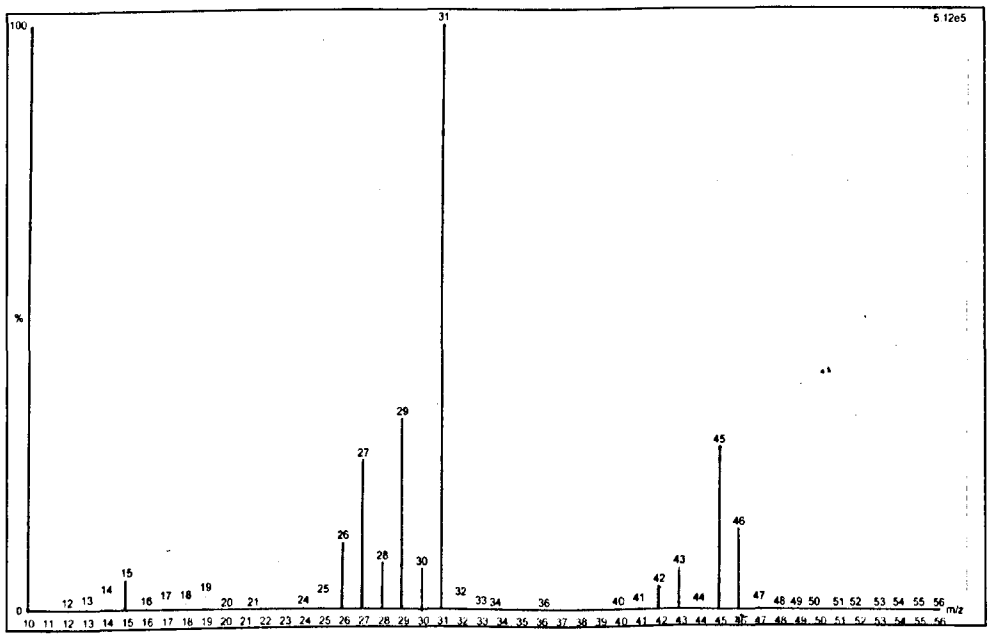


**Figure 2.13** Mass spectrum of ethanol. Relative molecular mass = 46.07.

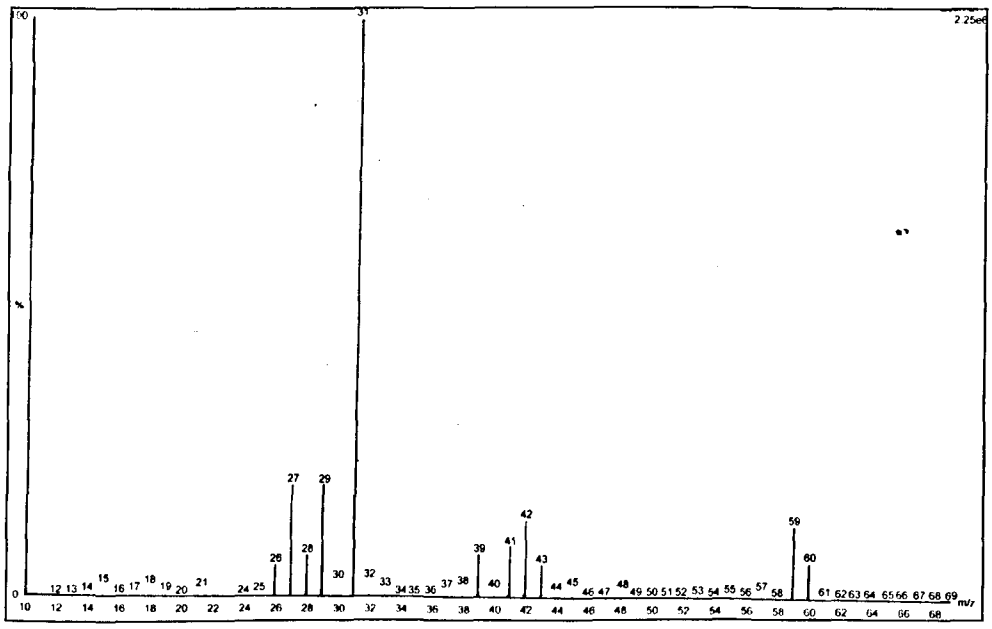

**Figure 2.14** Mass spectrum of 1-propanol. Relative molecular mass = 62.07.

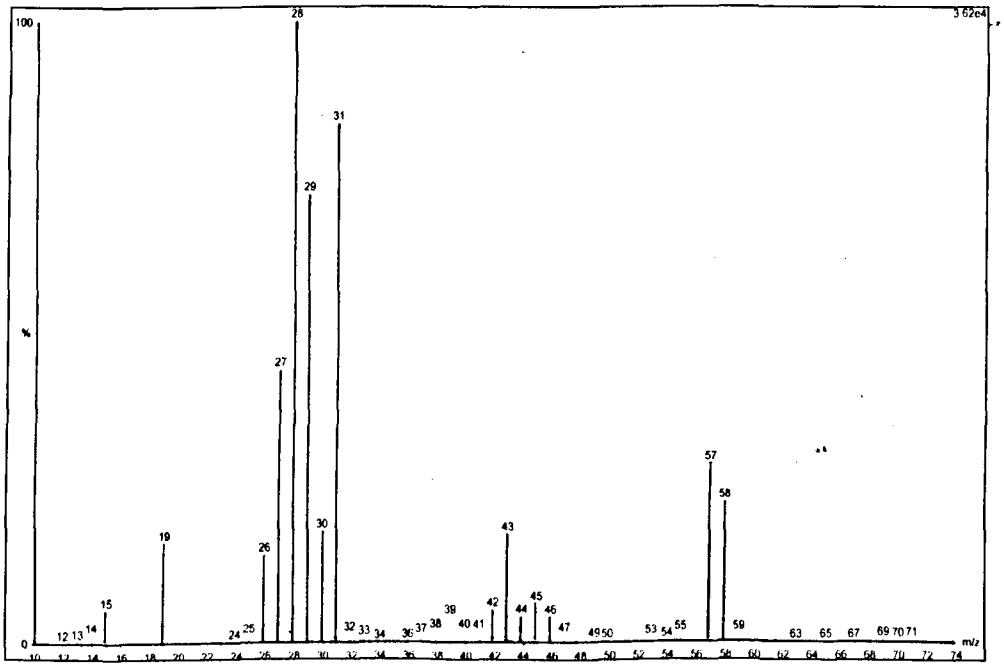

**Figure 2.15** Mass spectrum of 1,3-propanediol. Relative molecular mass = 76.09.

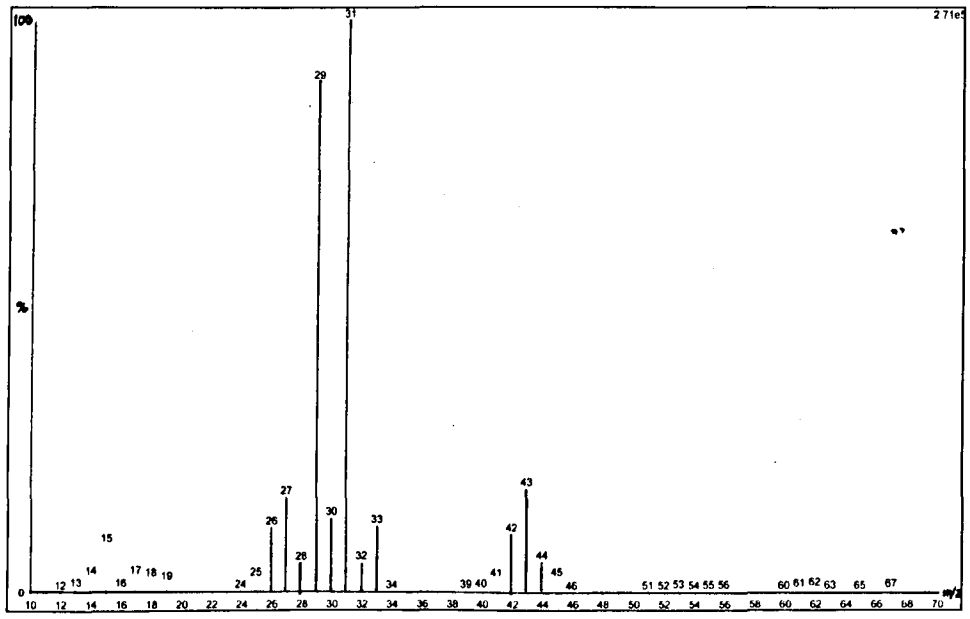

**Figure 2.16** Mass spectrum of ethylene glycol. Relative molecular mass = 76.09.

## References


[1] S. Tatematsu, T. Hibi, T. Okuhara, M. Misono, Chem. Lett. (1984) 865.

[2] Y. Izumi, M. Ono, M. Kitagawa, M. Yoshida, K. Urabe, Microporous Mater. 5 (1995) 255.

[3] I. V. Kozhevnikov, Catalysts For Fine Chemical Synthesis, Catalysis by Polyoxometalates Wiley 2002.

[4] E. F. Kozhevnikova, E. Rafiee, I. V. Kozhevnikov, Appl. Catal. A 260 (2004) 25.

[5] M. R. H. Siddiqui, S. Holmes, H. He, W. Smith, E. N. Coker, M. P. Atkins, I. V. Kozhevnikov, Catal. Lett. 66 (2000) 53.

[6] F. Al-Wadaani, E. F. Kozhevnikova, I. V. Kozhevnikov, J. Catal. 257 (2008) 199.

[7] D. Kealy, D. J. Haines, Analytical Chemistry, Bio scientific Ltd, Oxford, UK, 2002.

[8] G. Leofanti, M. Padovan, G. Tozzola, B. Venturelli, Catal. Today. 41 (1998) 207.

[9] E. P. Barrett, L. G. Joyner, P. P. Halenda, J. Am. Chem. Soc. 73 (1951) 373.

[10] J. H. Sinfelt, Rev. Mod. Phys. 51 (1979) 569.

[11] F. Pinna, Catal. Today. 41 (1998) 129.

[12] P. Carlo, V. Pierluigi, Catal. Today. 34 (1997) 281.

[13] J. E. Benson, M. Boudart, J. Catal. 4 (1965) 704.

[14] J. E. Benson, M. Boudart, J. Catal. 30 (1973) 146.

[15] G. C. Bond, Metal-Catalysed Reactions of Hydrocarbons, Springer, New York, 2005.

[16] S. E. Wanke, Doughart.Na, J. Catal. 24 (1972) 367.

[17] C. Blanco, R. Ruiz, C. Pesquera, F. Gonzalez, Appl. Organomet. Chem. 16 (2002) 84.

[18] K. C. Taylor, J. Catal. 38 (1975) 299.

[19] TPD/TPR 2900 analyser, Operator's manual, VI.02, April 1993.

[20] L. M. Harwood, C. J. Moody, J. M. Percy, Experimental Organic Chemistry: Standard and Microscale, Blackwell Science, 2001.

[21] G. Schwedt, The Essential Guide to Analytical Chemistry John Wiley and Sons, Chichester, England, 1997.

[22] P. W. Atkins, Physical Chemistry, Oxford University Press, 1998.

[23] F. Lefebvre, F.X. Liucai, A. Auroux, J. Mater. Chem. 4 (1994) 125.

[24] V. Rakic, V. Dondur, U. Mioc, D. Jovanovic, Top. Catal. 19 (2002) 241.

[25] P. Leparlouer, J. Mercier, B. Jalon, Thermochimica Acta. 103 (1986) 21.

[26] F. W. Fifield, D. Kealy, Principles and practice of analytical chemistry, ($5^{th}$ ed) Blackwell Science Ltd, 2000.

# 3. Catalyst characterisation

## 3.1 Introduction

In this chapter, the results of catalyst characterisation are presented and discussed. The catalysts under study are caesium heteropoly salt, $Cs_{2.5}H_{0.5}PW_{12}O_{40}$ (CsPW), Pd, Ru and Rh doped CsPW, $Cs_{3.5}H_{0.5}SiW_{12}O_{40}$, niobium oxide ($Nb_2O_5$) and Ru, Rh doped $Nb_2O_5$. Catalyst texture including surface area, pore diameter and pore volume, the state of metals on the catalyst surface, catalyst crystallinity, and the nature and the strength of acid sites were investigated using different techniques: nitrogen adsorption, IR (infrared spectroscopy), XRD (X-ray diffraction), hydrogen chemisorptions and DSC (differential scanning calorimetry).

## 3.2 Thermogravimetric analysis

### 3.2.1 $Cs_{2.5}H_{0.5}PW_{12}O_{40}$

TGA analysis was used to determine the content of water in catalysts and their thermal stability. The acidic $Cs^+$ salt of the heteropolyacid $H_3PW_{12}O_{40}$, $Cs_{2.5}H_{0.5}PW_{12}O_{40}$ (CsPW), has been found to be a water-tolerant solid acid catalyst with hydrophobic surface and is stable up to 600 °C [1, 2]. Figures 3.1-3.3 show the thermal analysis of CsPW, 5 wt% Ru/CsPW and 0.5 wt%Pd/CsPW. All TGA experiments were carried out using a heating rate of 20 mL/min in a $N_2$ flow, and 15-25 mg samples pretreated at 150 °C at a pressure of 0.5 Torr.

As shown in Figure 3.1, up to 3% weight loss was observed at temperatures up to 300 °C for the CsPW catalyst corresponding to the departure of 3 to 4 molecules of physisorbed water and/or crystallisation water per Keggin unit [3]. 5.0 wt%

Ru/CsPW and 0.5 wt%Pd/CsPW as illustrated in Figure 3.2 and 3.3, respectively, exhibited smaller weight loss than the parent CsPW. This is probably due to the reduction treatment of these catalysts prior to TGA analysis. The second weight loss was observed between 500 and 600°C. This loss may be due to a deprotonation step and corresponds to 0.25 $H_2O$ molecules per Keggin unit. From XRD studies carried out with thermally treated parent $H_3PW_{12}O_{40}$, it was deduced that the water is formed from the extraction of oxygen from the anion by the protons without collapse of the Keggin structure [1]. This mechanism is shown in Equation 3.1.

$$H_3PW_{12}O_4 \longrightarrow PW_{12}O_{38.5} + 1.5\ H_2O \qquad (3.1)$$

The use of TGA/TPO (temperature-programmed oxidation) for the characterisation of the nature of coke during the use of HPA catalysts is well established [4-6]. Figures 3.4 and 3.5 show the TGA/TPO profiles of the spent 5.0 wt%Ru/CsPW and 0.5 wt%Pd/CsPW catalysts after reactions in the liquid and gas phase respectively. For comparison, the fresh catalyst loses hydration water below 300 °C and exhibits no further weight loss up to 620 °C. The TPO for the spent catalyst provides an insight into the presence and the nature of coke as a deactivation cause. The TPO profile of 5.0 wt% Ru/CsPW used in liquid-phase glycerol hydrogenolysis shows no weight loss between 300 and 620 °C, indicating that no formation of carbonaceous deposits took place. In contrast, the TPO profile of 0.5 wt%Pd/CsPW used in the gas phase process of glycerol dehydration shows a broad combustion peak in the temperature range of 350– 550 °C, indicating that this coke is a mixture of aliphatic (easier to burn) and polyaromatic (more difficult to burn) carbonaceous deposits [7, 8].

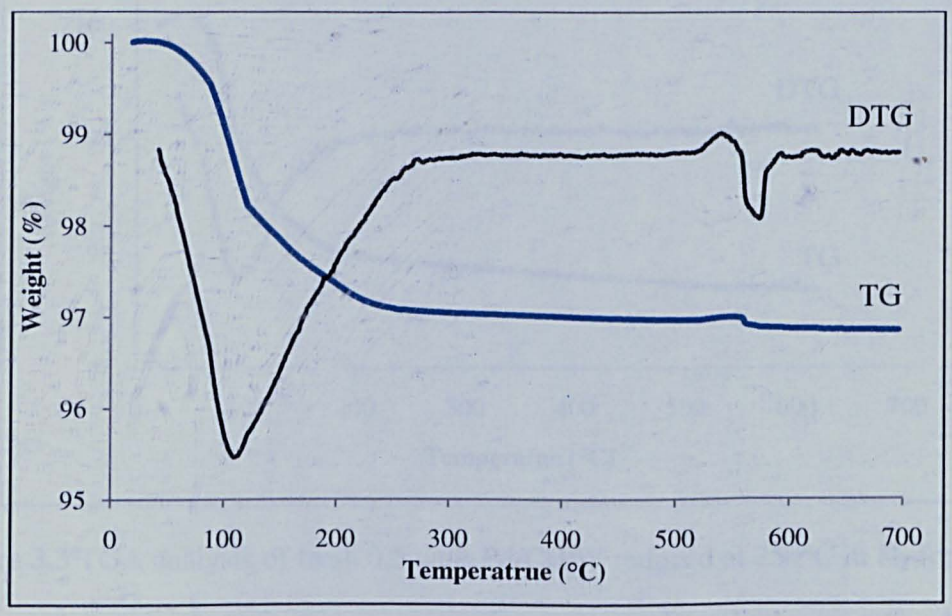


**Figure 3.1** TGA analysis of fresh CsPW calcined at 150°C under vacuum for 1.5 h.

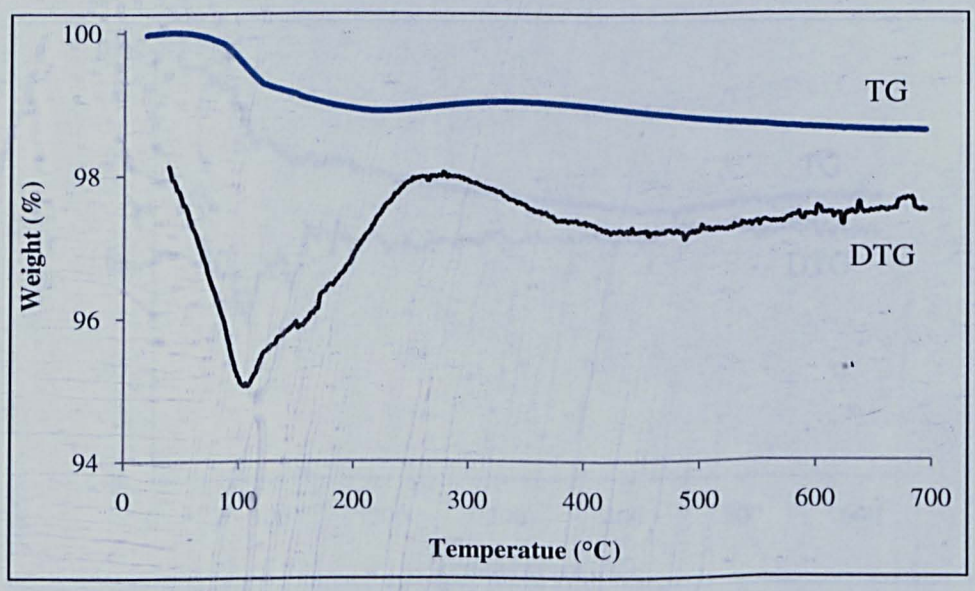


**Figure 3.2** TGA analysis of fresh 5.0 wt% Ru/CsPW reduced at 250°C in $H_2$ for 2 h.

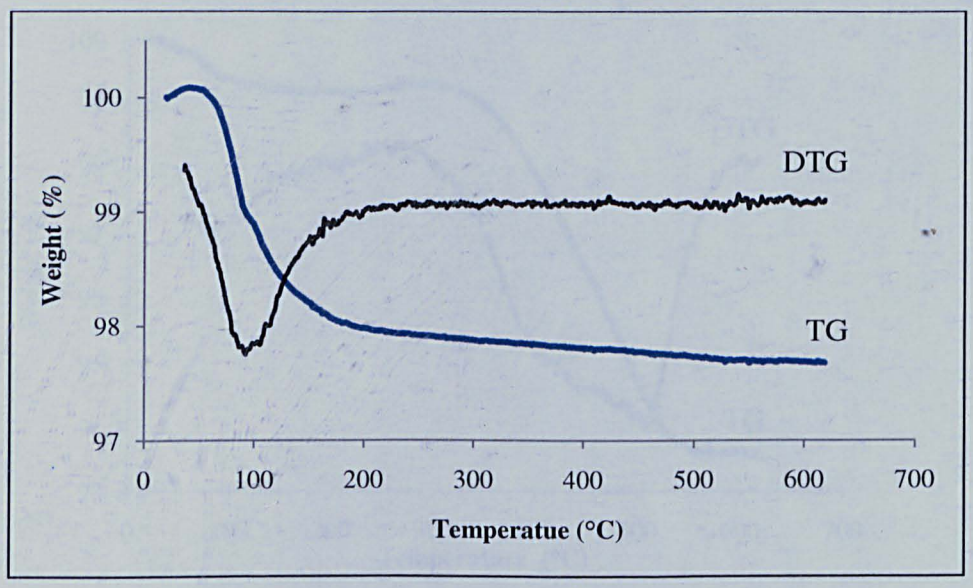


**Figure 3.3** TGA analysis of fresh 0.5 wt% Pd/CsPW reduced at 250°C in $H_2$ for 2 h.

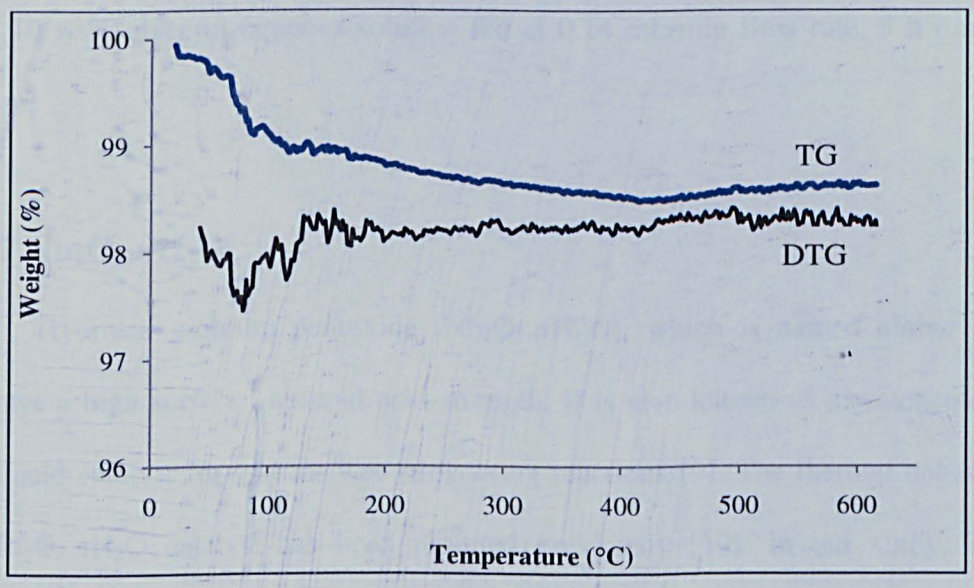


**Figure 3.4** TGA/TPO of 5.0 wt% Ru/CsPW after use in liquid-phase glycerol hydrogenolysis. After separation, the catalyst was left to dry in open air for few days prior to analysis. Reaction conditions: 180 °C, 5 bar $H_2$, 10 h, 20 wt% glycerol aqueous solutions and 0.2 g catalyst.

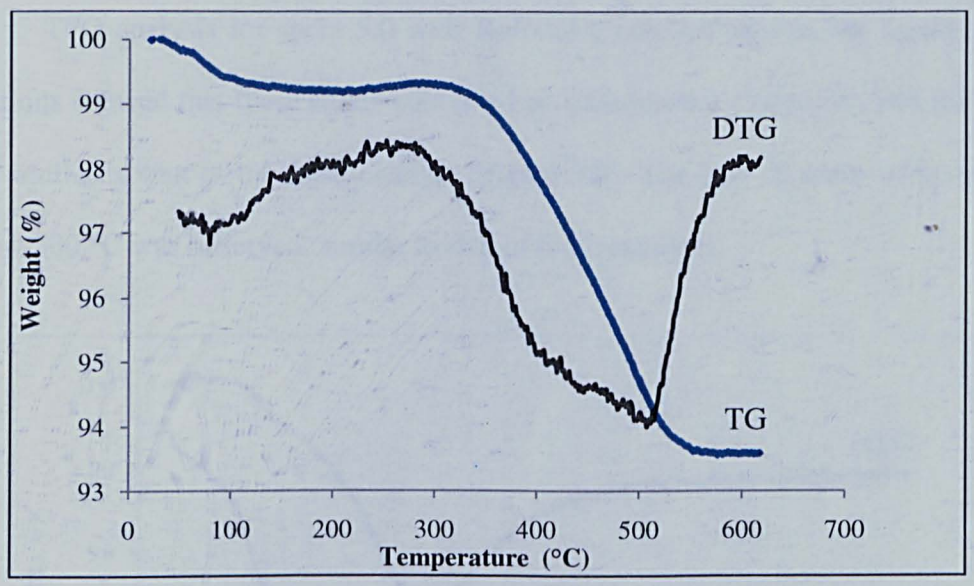


**Figure 3.5** TGA/TPO experiments for 0.5%Pd/CsPW after use in gas-phase glycerol dehydration. After separation, the catalyst was left to dry in the open air for few days prior to analysis. Reaction conditions: 275 °C, 0.30 g catalyst, 15 mL/min $H_2$ flow rate, 10 wt% glycerol aqueous solution fed at 0.14 mL/min flow rate, 5 h time on stream.

### 3.2.2 $Nb_2O_5.nH_2O$

Hydrated niobium pentoxide ($Nb_2O_5.n$H2O), which is named niobic acid, displays a high surface area and acid strength. It is also known as a water-tolerant solid acid catalyst for various water-involving reactions [9]. The thermal behaviour of $Nb_2O_5.nH_2O$ catalyst has been reported previously [10]. In our study, TGA analysis was carried out to investigate the thermal stability of bulk $Nb_2O_5.nH_2O$ and 5.0 wt%Ru/ $Nb_2O_5$, the results are shown in Figures 3.5 and 3.6. For the bulk $Nb_2O_5.nH_2O$, calcined at 100 °C overnight, a weight loss (up to 8%) attributable to the elimination of adsorbed and crystallization water was observed. On further heating of the samples above 350 °C, no weight loss occurred. These results are in agreement with those reported in the literature [11].

TPO analysis for spent 5.0 wt% $Ru/Nb_2O_5$ catalyst used in the liquid phase reactions showed that these solids contained no carbonaceous materials and the TPO was similar to that of the fresh catalyst (Figure 3.8). The loss of water of hydration below 300 °C was observed, similar to that of fresh catalysts.

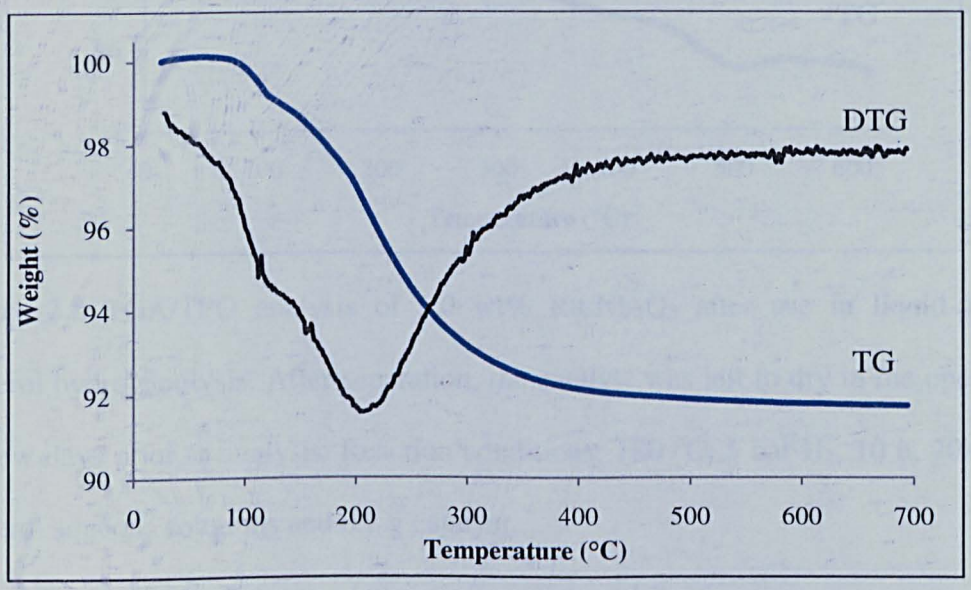


**Figure 3.6** TGA analysis of fresh $Nb_2O_5nH_2O$ calcined 100°C overnight.

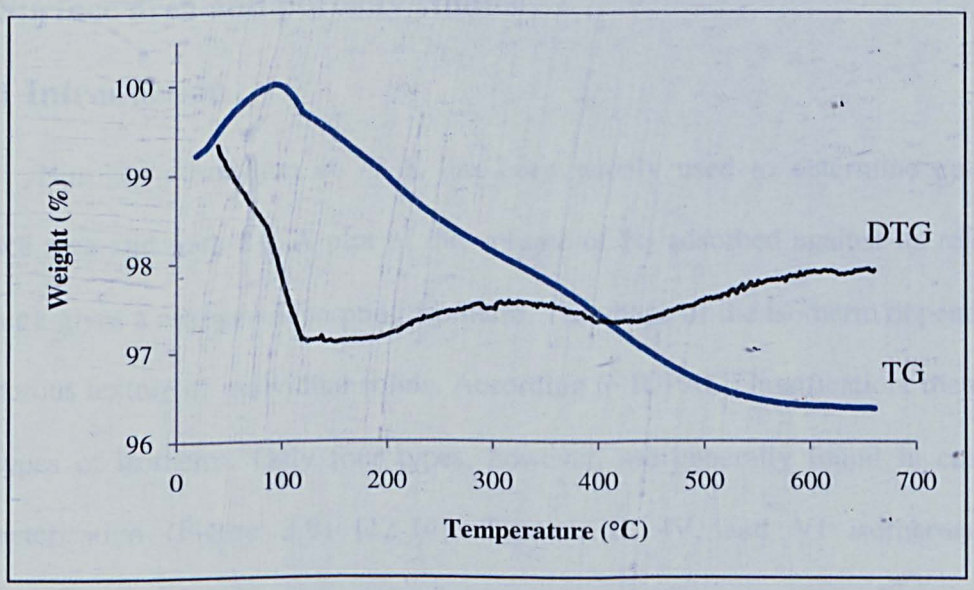


**Figure 3.7** TGA analysis of fresh 5.0 wt% $Ru/Nb_2O_5$ reduced at 250 °C in $H_2$ for 2 h.

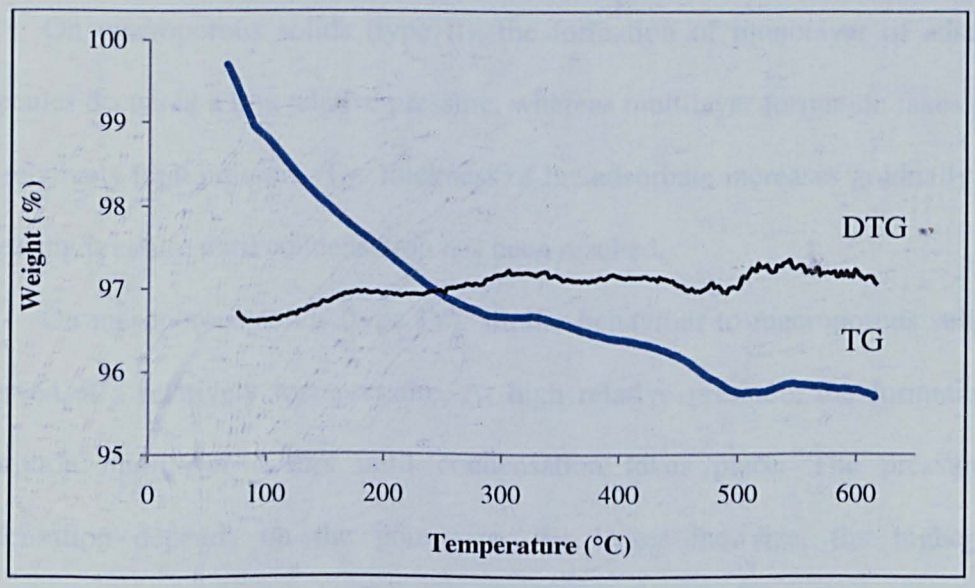


**Figure 3.8** TGA/TPO analysis of 5.0 wt% $Ru/Nb_2O_5$ after use in liquid-phase glycerol hydrogenolysis. After separation, the catalyst was left to dry in the open air for few days prior to analysis. Reaction conditions: 180 °C, 5 bar $H_2$, 10 h, 20 wt% glycerol aqueous solutions and 0.2 g catalyst.

## 3.3 Surface area and porosity studies

### 3.3.1 Introduction

Nitrogen adsorption at 77 K has been widely used to determine catalyst surface area and porosity. A plot of the volume of $N_2$ adsorbed against its relative pressure gives a nitrogen adsorption isotherm. The shape of the isotherm depends on the porous texture of individual solids. According to IUPAC classification, there are six types of isotherm. Only four types, however, are generally found in catalyst characterisation (Figure 3.9) [12-14]. Type I, II, IV, and VI isotherms are representative of microporous, macroporous, mesoporous and uniform ultramicroporous solids, respectively.

On macroporous solids (type II), the formation of monolayer of adsorbed molecules occurs at a low relative pressure, whereas multilayer formation takes place at a relatively high pressure. The thickness of the adsorbate increases gradually with increasing pressure until condensation has been reached.

On mesoporous solids (type IV), similar behaviour to macroporous solids is observed at a relatively low pressure. At high relative pressure, the formation of adsorption multilayer occurs until condensation takes place. The pressure of condensation depends on the pore size, the larger the size, the higher the condensation pressure. As mesopores are filled, the adsorption continues on the external surface. Most catalysts belong to this class of solids.

On microporous solids (Type I), a strong interaction between the pore walls and the adsorbate occurs. Therefore, the adsorption takes place at relatively very low pressures. A higher pressure favoured by interaction between adsorbed molecules is required to complete the filling of the pores. After the micropores have been filled, the adsorption continues on the external surface as is the case with mesopores. Active carbons and zeolites are typical examples of this type.

Type VI (uniform ultramicroporous solids) has been included recently, with the advent of well-defined single crystal substrates, where such behaviour was observed. Each step in the isotherm corresponds to the completion of the first, second, etc., monolayers.

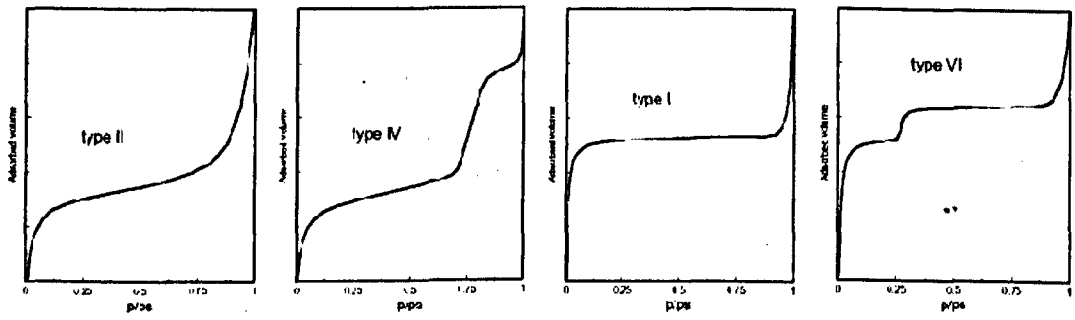


**Figure 3.9** The four types of adsorption isotherm found with the $N_2$ adsorption [15].

When saturation is reached, desorption of adsorbate occurs in the opposite process to that of adsorption. However, on mesoporous solids, evaporation usually takes place at a pressure lower than that of capillary condensation giving a hysteresis loop. Figure 3.10 shows the four hysteresis types that have been classified by IUPAC [15].

Types H1 and H2 hysteresis isotherms are shown when the solids consist of particles crossed by nearly cylindrical channels or made by aggregates (consolidated) or agglomerates (unconsolidated) that are spheroidal in shape. Type H1 samples have pores with uniform size and shape, while type H2 samples have pores of non-uniform size and shape. Theses hystereses are owing to different size of pore mouth and pore body (e.g. ink-bottle shaped pores) and/or a different behaviour in adsorption and desorption in near cylindrical pores. Most mesoporous catalysts show Type H1 and H2 hysteresis adsorption isotherms [15].

Types H3 and H4 hysteresis isotherms are found when the solids consist of aggregates or agglomerates of particles forming slit shaped pores (plates or edged particles similar to cubes), with non-uniform and uniform size and/or shape, respectively. These hystereses are due to the different behaviour in adsorption and desorption. Active carbon and zeolites are examples of this class.

The absence of adsorption isotherm hysteresis indicates that the solids possess blind cylindrical, cone-shaped and/or wedge shaped pores. However, as catalyst pores are usually irregular, only solids with a much reduced hysteresis loop will be observed.

Closure of a hysteresis loop in nitrogen adsorption generally occurs at a relative pressure of 0.42 owing to liquid adsorbate properties and irrespectively of the adsorbent or the pore size distribution.

The general procedure for the measurement of surface area and porosity is described in Section 2.4.3. The total surface area of the catalysts was calculated using the Brunauer-Emmett-Teller (BET) method [16]. The pore size distribution and the total pore volumes were both determined using the Barrett, Joyner and Halenda (BJH) method [17].

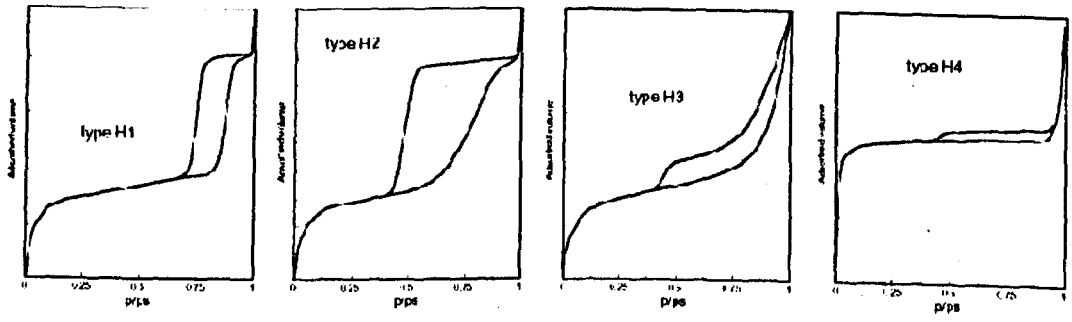


**Figure 3.10** The four hysteresis types usually observed with $N_2$ adsorption [15].

### 3.3.2 $Cs_{2.5}H_{0.5}PW_{12}O_{40}$

The porosity and surface area of bulk heteropolyacids are very low, typically in the range of 1-10 $m^2/g$ reflecting their high solubility in water [1, 18, 19]. Salts of HPA with rather small cations are similar to the parent HPAs; they are readily soluble in water, nonporous, and possess surface areas under 10 $m^2\ g^{-1}$. In contrast, water-insoluble salts with large monovalent cations, such as $NH_4^+$, $K^+$, $Cs^+$, etc., have

a rigid microporous/mesoporous structure and surface areas over 100 $m^2 g^{-1}$ [1]. In addition, they possess high thermal stability and low solubility in polar solvents [18].

Misono et al. [20] reported the preparation procedure of CsPW. Extensive studies using $^{31}P$ NMR, XRD, electron diffraction, atomic force microscopy (AFM) and scanning electron microscopy (SEM), adsorption of $N_2$, etc, have been carried out to understand the microstructure of the acidic Cs salt of tungstophosphoric acid ($H_3PW_{12}O_{40}$). Misono et al. [21] stated that very fine precipitates of $Cs_3PW_{12}O_{40}$ are formed when the aqueous solution of HPW is titrated with $Cs_2CO_3$ at 298 K. The remaining HPW is adsorbed on $Cs_3PW_{12}O_{40}$, and as the titration proceeds the amount of HPW in the solution decreases, forming $Cs_3PW_{12}O_{40}$ precipitates. At a stoichiometry where x = 2, the precipitates are fine particles (10 nm diameter) of $Cs_3PW_{12}O_{40}$, where the surface is covered by a monolayer of HPW. The surface area at this stoichiometry is very low, ~1 $m^2/g$, which is ascribed to the fine particles sticking together densely after drying. No change is observed in the particle composition after heating. When the amount of $Cs^+$ exceeds the stoichiometry of 2, the surface area increases dramatically because most of the HPW precipitates as $Cs_3PW_{12}O_{40}$ and therefore the amount of HPW remaining in solution or adsorbed on the precipitate is reduced significantly. Micropores begin to develop which do not form at lower Cs stoichiometry, where HPW densely connects the nanoparticles together [21, 22]. The pores of the CsPW materials, as with many heteropoly acids, have been described as being interparticle and not intracrystalline based on TEM and previous $N_2$ adsorption studies [20, 22].

CsPW possesses a bimodal distribution of pores with micropores ranging from 0.5-1 nm (peak at 0.65 nm and mostly > than 0.75 nm), and mesopores (peak at 4-5 nm) [21]. It has been suggested that the micropores account for approximately 70 %

of the total surface area of CsPW and correspond to the spaces between the crystal plane [21]. The mesopores are formed from spaces between nanocrystallites (10-20 nm) and between aggregates in the region of 100-500 nm in size. Figure 3.11 is a schematic representation of the bimodal pore size distribution in CsPW [23].

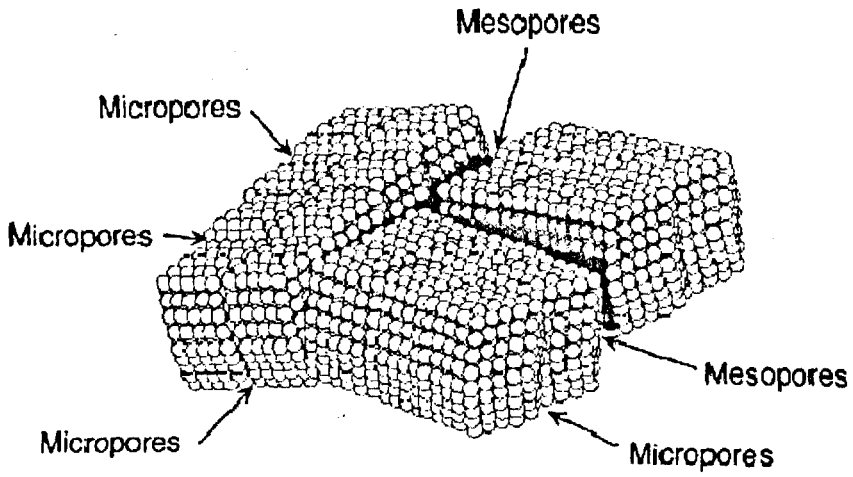


**Figure 3.11** The bimodal pore size distribution in $Cs_{2.5}H_{0.5}PW_{12}O_{40}$ [23, 24]

The BET isotherm and the pore size distribution for the CsPW used in our study are shown in Figures 3.12 and 3.13. $N_2$ adsorption isotherm type IV is observed for CsPW (Figure 3.12), which is a characteristic of mesoporous materials (2 nm < pore diameter < 50 nm). The hysteresis loop of the desorption isotherm type H2 is observed, indicating the presence of mesopores which are of non-uniform shape. In addition, the steep increase of the adsorption amount in the low pressure region observed for CsPW suggests the presence of micropores as well as mesopores. This isotherm for Cs salt is consistent with those reported in literature [2, 25, 26]. Figure 3.13 shows the mesopore-size distribution of CsPW derived from the desorption isotherm using the BJH (Barret- Joyner-Halenda) method. A sharp peak appeared at about 40 Å diameter. This compares well to previous research conducted on CsPW [2].

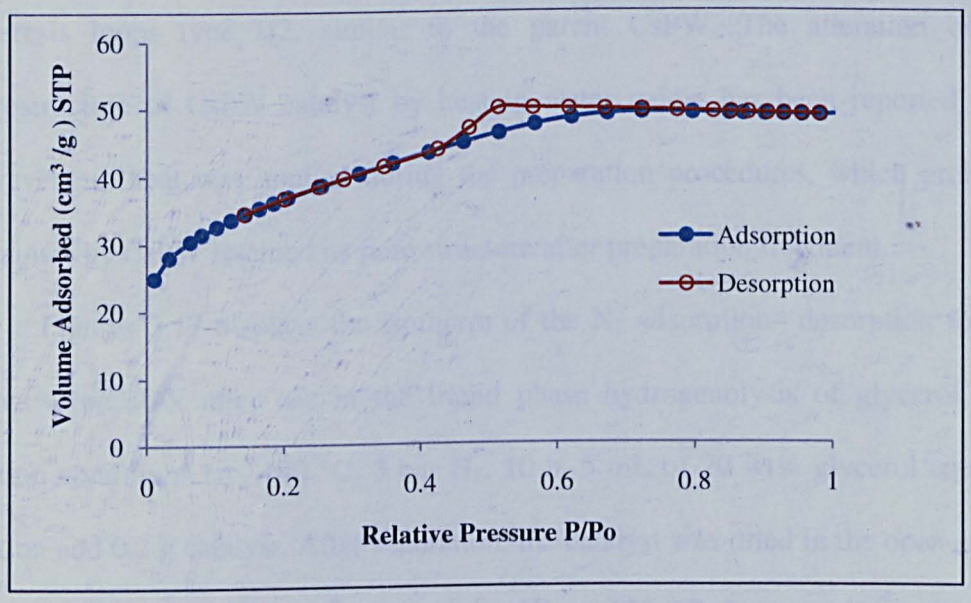


**Figure. 3.12** $N_2$ adsorption on CsPW at 77 K. The catalyst was pretreated at 250°C in vacuum.

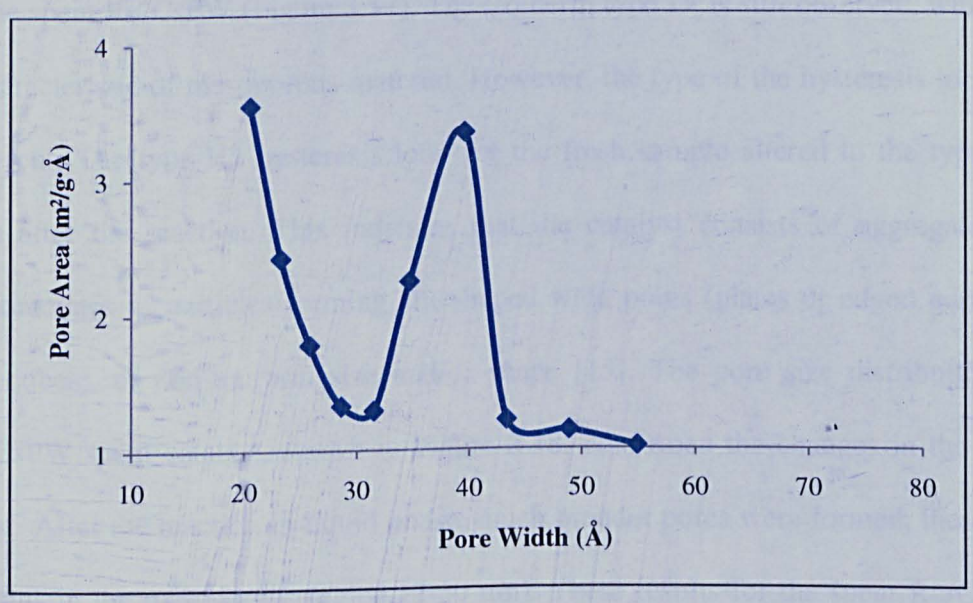


**Figure 3.13** Pore size distribution for $Cs_{2.5}H_{0.5}PW_{12}O_{40}$.

Figures 3.14-16 represent the effect of Ru, Rh and Pd loading on the adsorption isotherm of CsPW. Though the preparation of Ru and Rh catalysts involved treatment in water for 24 h at room temperature, no significant changes in the adsorption isotherms of modified samples are observed, all isotherms are classified into type IV. The desorption behaviour of modified catalysts shows

hysteresis loops type H2, similar to the parent CsPW. The alteration of the microstructure of CsPW catalyst by heat in water media has been reported [27]. However, no heat was applied during the preparation procedures, which probably explains why CsPW retained its pore structure after preparation treatment.

Figures 3.17 displays the isotherm of the $N_2$ adsorption– desorption for the 5.0 wt%Ru/CsPW after use in the liquid phase hydrogenolysis of glycerol. The reaction conditions are, 180 °C, 5 bar $H_2$, 10 h, 5 mL of 20 wt% glycerol aqueous solution and 0.2 g catalyst. After separation, the catalyst was dried in the open air for few days then pretreated in vacuum for 1.5 h at 150 °C. In contrast to the fresh Ru/CsPW, significant change in pore structure can be seen from the isotherm profile of the spent Ru/CsPW (Figure 3.17). The isotherm type IV is still observed, which is a characteristic of mesoporous material. However, the type of the hysteresis loops is different. The type H2 hysteresis loop for the fresh sample altered to the type H3 loop after the reaction. This indicates that the catalyst consists of aggregates or agglomerates of particles forming slit shaped wide pores (plates or edged particles like cubes), of non-uniform size and/or shape [15]. The pore size distribution of Ru/CsPW spent catalyst, shown in Figure 3.18, confirmed the changes in the pore sizes. After the reaction in liquid phase, much broader pores were formed, though it remains in the mesoporous region (2-50 nm). These results for the spent Ru/CsPW catalyst are consistent with that reported by Nakato et al. [27]. Pd/CsPW used in the gas phase dehydration of glycerol exhibited a similar tendency. Both fresh and spent Pd/CsPW show type IV isotherm (Figure 3.19). However, the hysteresis loop type H3 is also observed in the case of spent Pd/CsPW whereas fresh catalyst shows type H2.

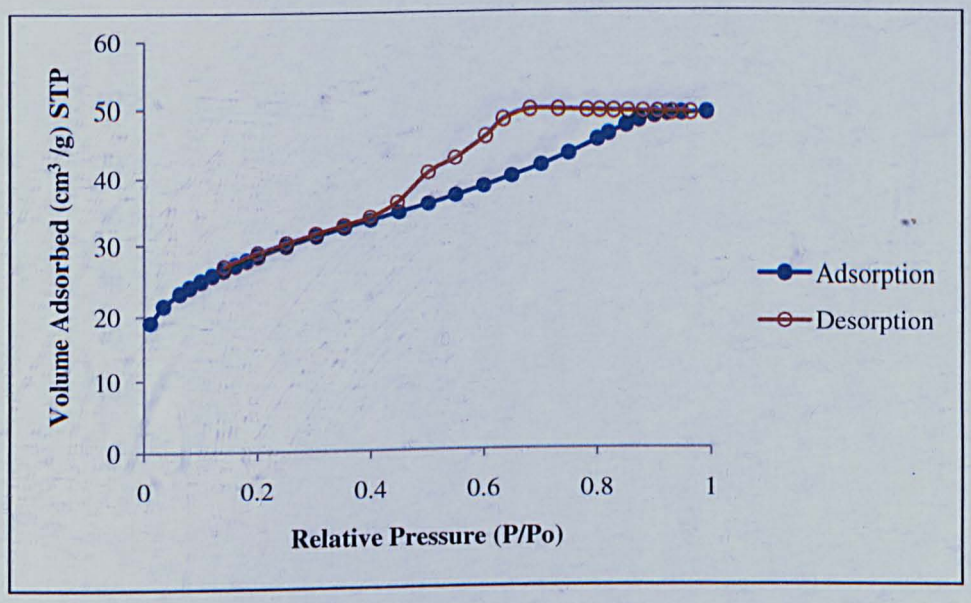


**Figure 3.14** $N_2$ adsorption on 5.0 wt%Ru/CsPW at 77 K. The catalyst was pretreated at 250°C in vacuum.

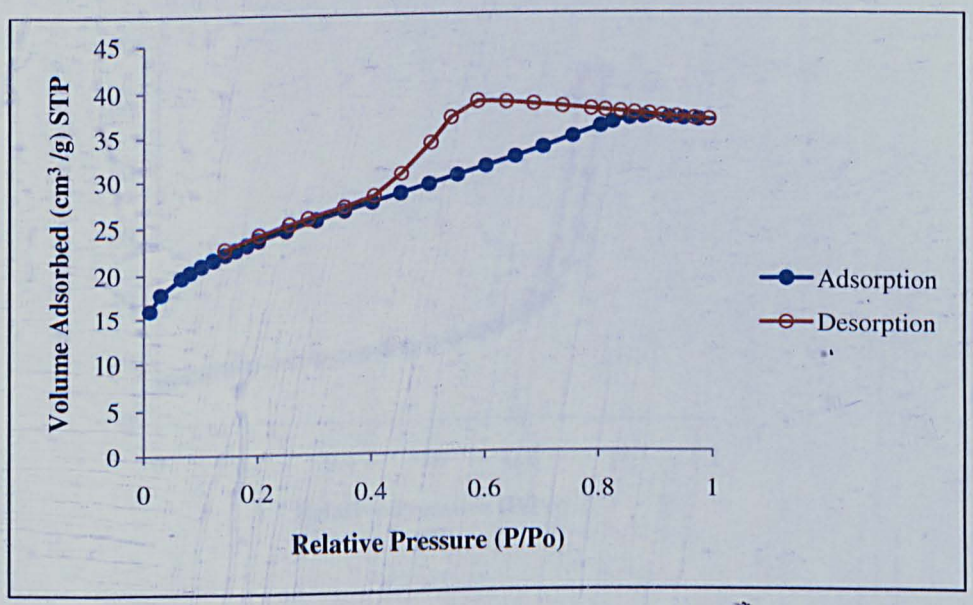


**Figure 3.15** $N_2$ adsorption on 5%Rh/CsPW at 77 K. The catalyst was pretreated at 250°C in vacuum.

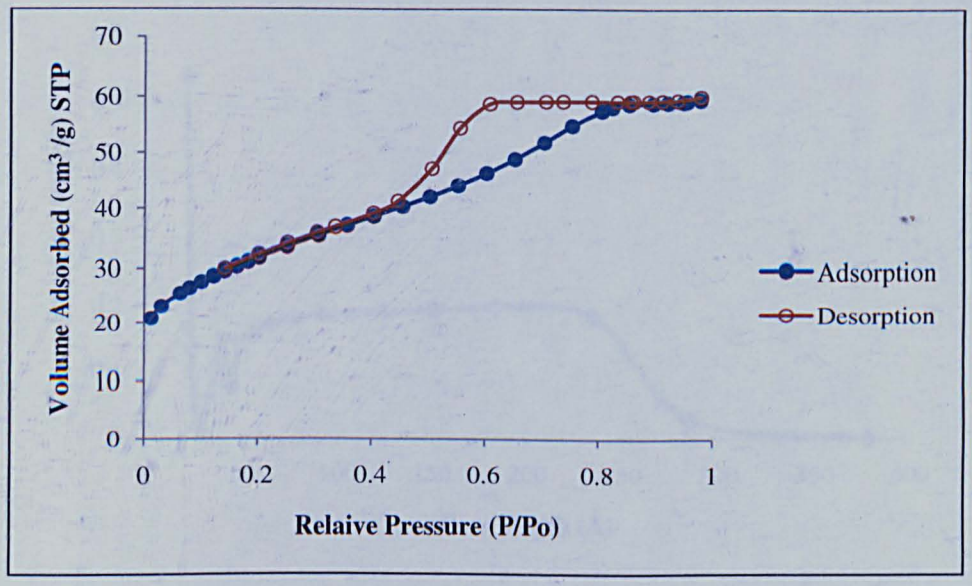


**Figure 3.16** $N_2$ adsorption on 0.5%Pd/CsPW at 77 K. The catalyst was pretreated at 250°C in vacuum.

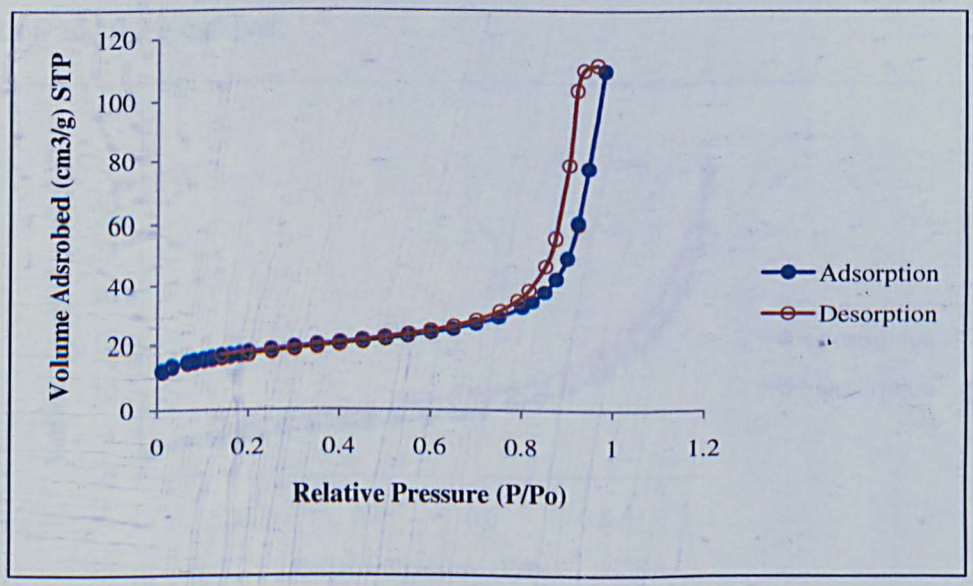


**Figure 3.17** $N_2$ adsorption on 5.0 wt%Ru/CsPW spent catalyst at 77 K. The catalyst separated after reaction was dried in air for few days, pretreated at 250 °C in vacuum. Reaction conditions: 180 °C, 5 bar $H_2$, 10 h, 5 mL of 20% glycerol aqueous solution and 0.2 g catalyst.

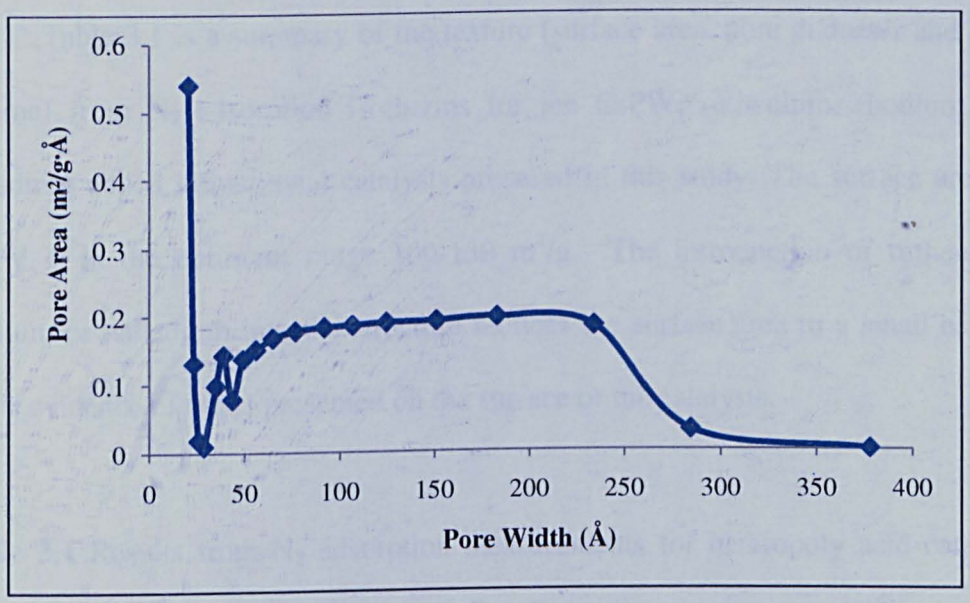


**Figure 3.18** Pore size distribution for 0.5 wt%Ru/CsHPW spent catalysts. The catalyst separated after reaction was dried in air for few days, pretreated at 250 °C in vacuum. Reaction conditions: 180 °C, 5 bar $H_2$, 10 h, 5 mL of 20% glycerol aqueous solution and 0.2 g catalyst.

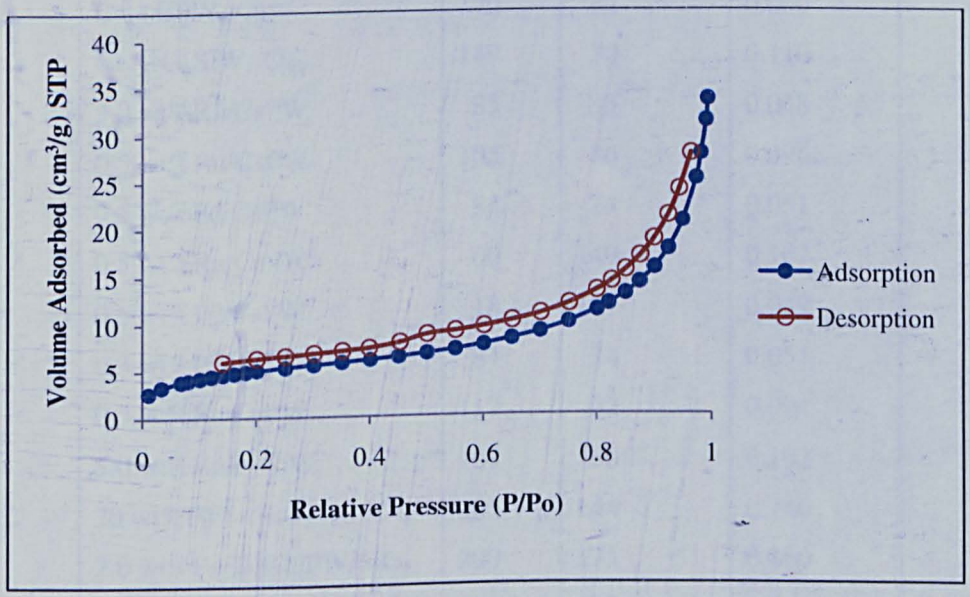


**Figure 3.19** $N_2$ adsorption on 0.5 wt%Pd/CsPW spent catalyst at 77 K. The catalyst separated after reaction was dried in air for few days, pretreated at 250 °C in vacuum. Reaction conditions: 180 °C, 5 bar $H_2$, 10 h, 5 mL of 20% glycerol aqueous solution and 0.2 g catalyst.

Table 3.1 is a summary of the texture (surface area, pore diameter and pore volume) from $N_2$ adsorption isotherms for the CsPW, ruthenium, rhodium and palladium doped bifunctional catalysts prepared in this study. The surface area of CsPW is in the optimum range 100-130 $m^2/g$. The introduction of ruthenium, rhodium or palladium into the structure reduces the surface area to a small extent, and is evidence of metal presented on the surface of the catalysts.

**Table 3.1** Results from $N_2$ adsorption measurements for heteropoly acid catalysts used in this study.

| **Catalyst** | **$S_{BET}$ ($m^2/g$)** | **Pore diameter[a] (A°)** | **Pore volume[b] ($cm^3/g$)** |
|---|---|---|---|
| $Cs_{2.5}H_{0.5}PW_{12}O_{40}$ | 127 | 24 | 0.076 |
| $Cs_{2..0}HPW_{12}O_{40}$ | 70 | 32 | 0.060 |
| $Cs_{3.5}H_{0.5}SiW_{12}O_{40}$ | 149 | 30 | 0.110 |
| 5.0 wt%Rh/CsPW | 85 | 33 | 0.048 |
| 0.5 wt%Ru/CsPW | 105 | 36 | 0.096 |
| 0.5 wt%Pd/CsPW | 84 | 24 | 0.051 |
| 0.5 wt%Ru/CsPW[c] | 60 | 149 | 0.167 |
| 0.5 wt%Pd/CsPW[d] | 18 | 121 | 0.049 |
| 0.3 wt%Pt/CsPW | 84 | 24 | 0.051 |
| 0.5 wt%Ru/CsPW | 117 | 32 | 0.094 |
| 5.0 wt%Ru/CsSiW | 101 | 36 | 0.102 |
| 20 wt%HPW/$SiO_2$ | 205 | 144 | 0.740 |
| 2.0 wt%Pd/20%HPW/$SiO_2$ | 200 | 175 | 0.860 |
| Zn-Cr (1:1) | 132 | 33 | 0.110 |
| 0.3 wt%Pd/Zn-Cr (1:1) | 112 | 35 | 0.090 |

a) Average BET pore diameter.

b) Single point total pore volume.

c) Catalyst spent in liquid-phase glycerol hydrogenolysis

d) Catalyst spent in gas-phase glycerol dehydration

### 3.3.3 $Nb_2O_5 \cdot nH_2O$

Hydrated niobium oxide, $Nb_2O_5 \cdot nH_2O$, is known to be a relatively strong solid acid exhibiting high catalytic activity and selectivity for hydration and dehydration reactions [10]. Depending on the preparation conditions, niobium oxide calcined at moderate temperatures of 100 – 300 °C showed high acidity, amorphous structure and high surface area. The surface area of niobium oxide dramatically decreases with increasing calcination temperatures above 500 °C, due to the formation of large $Nb_2O_5$ crystals from the heat treatment [10]. This decrease in the surface area is accompanied by a significant loss in the acidity after pretreatment above 500 °C. The decrease in acidity when increasing the pretreatment temperature can be attributed to the transformation of protonic sites to Lewis sites with the elimination of water. However this loss was attributed to a change from an amorphous to the crystalline form [10, 28].

The results of $N_2$ adsorption studies on bulk hydrated niobium oxide, Ru and Rh doped niobium oxide are demonstrated in Table 3.2. As previously reported [10, 28], the bulk hydrated niobium oxide exhibited high surface area when treated at low temperatures. The reduction in surface area when calcined at 500 °C was also observed. The catalyst texture was noticeably altered after impregnation of Ru and Rh metals. This is probably due to treatment in an aqueous solution during the impregnation stage and the subsequent reduction at 250 °C for 2 h. A shrinking of the $Ru/Nb_2O_5$ surface area down to 96 $m^2/g$ after reaction in the liquid phase was observed.

**Table 3.2** Results from $N_2$ adsorption measurements for niobium catalysts.

| Catalyst | Calcination Temp. (°C) | $S_{BET}$ ($m^2/g$) | Pore diameter[a] (A°) | Pore volume[b] ($cm^3/g$) |
|---|---|---|---|---|
| $Nb_2O_5$ | 100 | 201 | 39 | 0.200 |
| $Nb_2O_5$ | 500 | 99 | 69 | 0.170 |
| $Nb_2O_5$[c] | NA | 1 | 43 | 0.012 |
| 5.0 wt%Ru/ $Nb_2O_5$ | 100 | 126 | 51 | 0.160 |
| 5.0 wt%Rh/ $Nb_2O_5$ | 100 | 112 | 53 | 0.170 |
| 5.0 wt%Ru/ $Nb_2O_5$ | 500 | 52 | 108 | 0.140 |
| 5.0 wt%Ru/ $Nb_2O_5$[d] | 100 | 96 | 50 | 0.120 |

a) Average BET pore diameter.

b) Single point total pore volume.

c) Commercial catalyst.

d) Catalyst spent in liquid phase (180 °C, 10 h, 10 bar $H_2$, 5 mL of 20% glycerol aqueous solution, 0.2 g catalyst)

The $Nb_2O_5$ oxide possessing large surface area shows an adsorption isotherm of type IV characteristics of mesoporous materials (Figures 3.20 - 3.22). $Nb_2O_5$ and Ru/ $Nb_2O_5$ catalysts dried at 100 °C show a loop type H2 hysteresis, an indication of a non-uniform size and/or shape mesopores. Mesopores of 39 Å in diameter were found in the pore size distribution profile for these catalysts (Figure 3.23). The effect of increasing calcination temperature on the $N_2O_5$ catalysts can be seen in Figures 3.21 and 3.24. A similar adsorption isotherm (type IV) was obtained for catalyst calcined at 500 °C. A hysteresis loop (type H3) was observed, indicating the presence of mesopores. Figure 3.24 shows the pore size distribution for the catalyst calcined at 500 °C, which clearly shows that the pores became wider, 10 nm,

compared to 3.9 nm for the catalyst dried at 100 °C. These results are agreement with those reported by Paulis et al. [29].

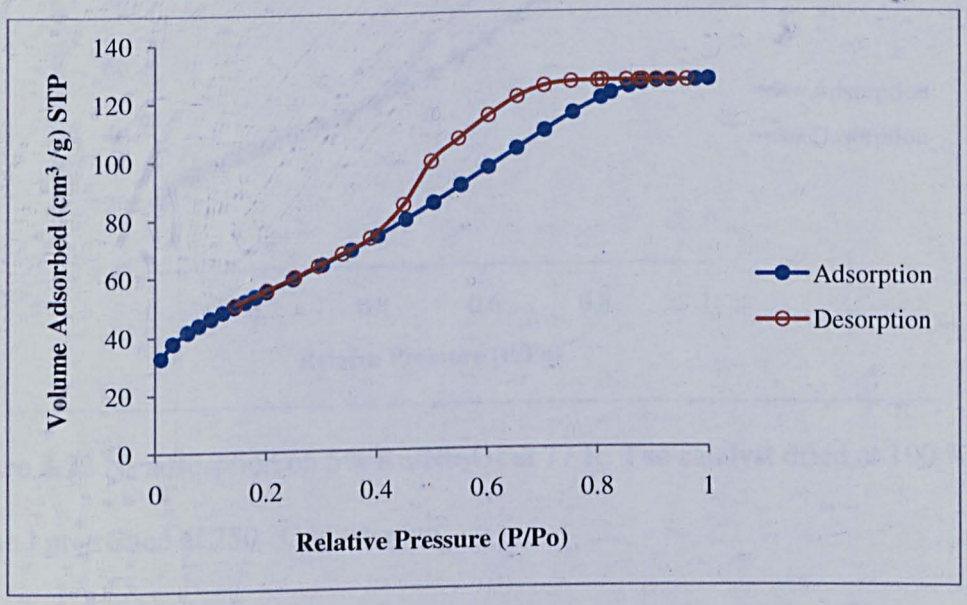


**Figure 3.20** $N_2$ adsorption on $Nb_2O_5$ at 77 K. The catalyst dried at 100 °C in air, and pretreated at 250 °C in vacuum.

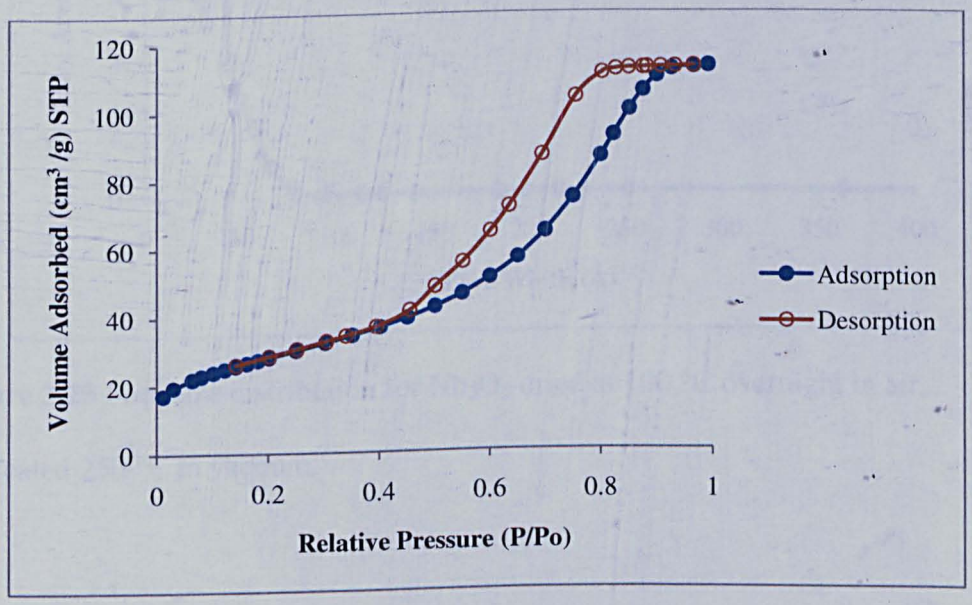


**Figure 3.21** $N_2$ adsorption on $Nb_2O_5$ at 77 K. The catalyst calcined at 500 °C in air, and pretreated at 250 °C in vacuum.

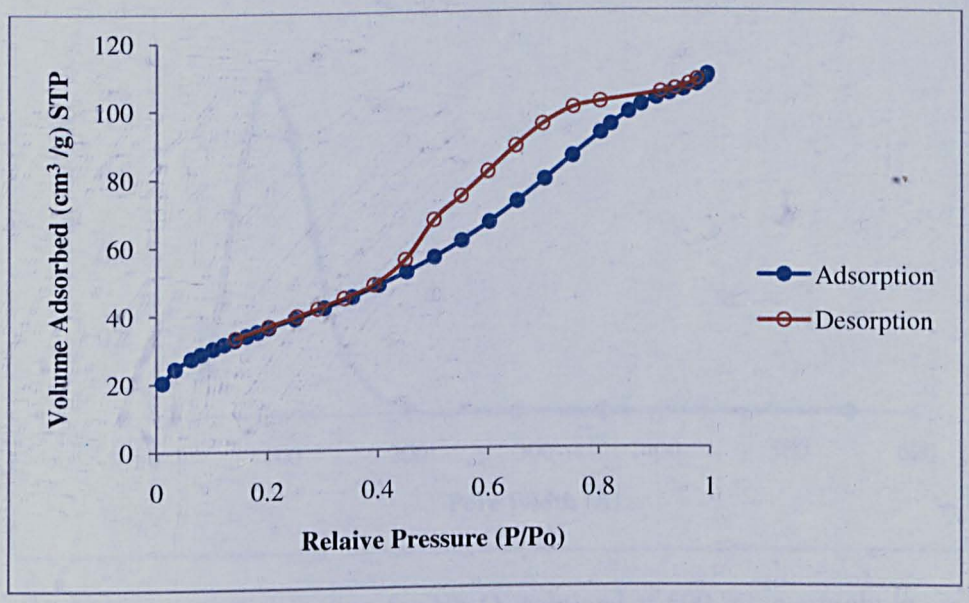


**Figure 3.22** $N_2$ adsorption on 5% $Ru/Nb_2O_5$ at 77 K. The catalyst dried at 100 °C in air, and pretreated at 250 °C in vacuum.

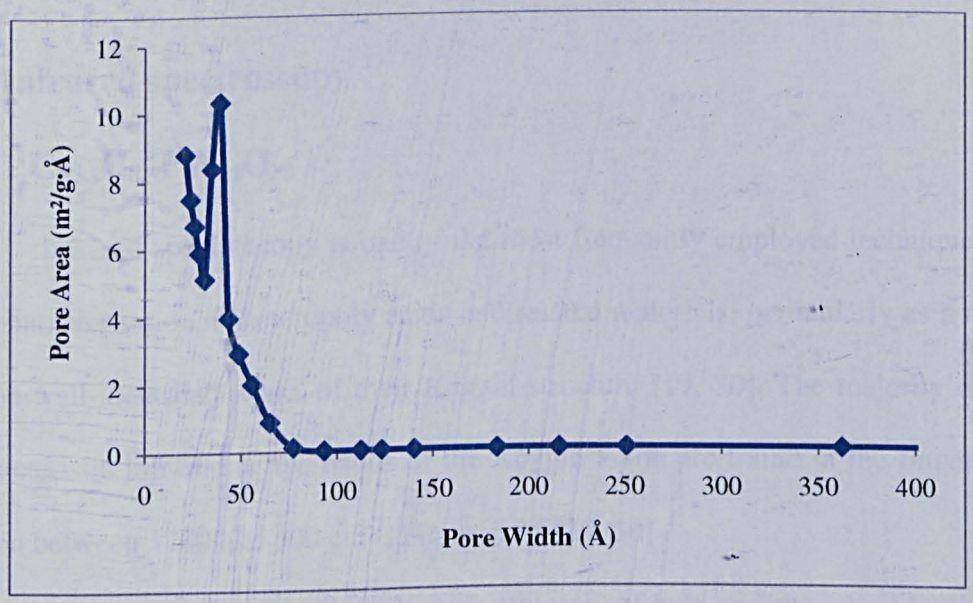


**Figure 3.23** Pore size distribution for $Nb_2O_5$ dried at 100 °C overnight in air, pretreated 250 °C in vacuum.

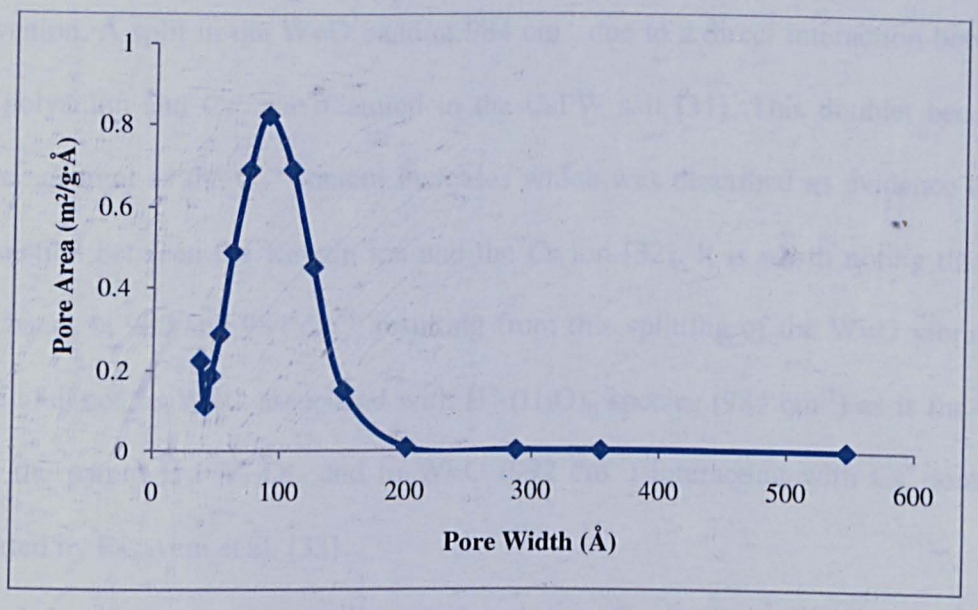


**Figure 3.24** Pore size distribution for $Nb_2O_5$ calcined at 500 °C overnight in air, pretreated 250 °C in vacuum.

## 3.4 Infrared spectroscopy

### 3.4.1 $Cs_{2.5}H_{0.5}PW_{12}O_{40}$

Infrared spectroscopy is one of the most frequently employed techniques for the characterisation of heteropoly acids and related materials, particularly as a result of the well-identified peaks of their Keggin structure [19, 30]. The majority of the characteristic infrared active bands of the Keggin anion are found in the fingerprint region between 1200 and 500 $cm^{-1}$, Figure 3.25 [19, 30] .

Choi et al.[31] examined the Keggin structure of bulk and supported HPW and $Cs_{2.5}PW$ using FTIR spectroscopy. Samples were prepared by calcining at 300 °C for 2 h and then pressing into a disk with 95% KBr [31]. The following infrared absorption bands were observed for the bulk tungstophosphoric acid $H_3PW_{12}O_{40}$ and the $Cs^+$ salt: 1080 $cm^{-1}$ (P-O in central tetrahedron), 984 $cm^{-1}$ (terminal W=O), 897 and 812 $cm^{-1}$ (W-O-W) associated with the asymmetric vibrations in the Keggin

polyanion. A split in the W=O band at 984 $cm^{-1}$ due to a direct interaction between the polyanion and $Cs^+$ was featured in the CsPW salt [31]. This doublet becomes more apparent as the $Cs^+$ content increases which was described as evidence of an interaction between the Keggin ion and the Cs ion [32]. It is worth noting that the two bands at 982 and 984 $cm^{-1}$, resulting from this splitting of the W=O vibration, were assigned as W=O associated with $H^+$ $(H_2O)_n$ species (984 $cm^{-1}$) as is the case with the parent $H_3PW_{12}O_{40}$ and to W=O (992 $cm^{-1}$) interacting with $Cs^+$ ions, as reported by Essayem et al. [33].

In our study, we examined the fresh and spent Ru, Pd doped CsPW catalysts in order to evaluate the catalyst preparation procedures and to detect any possible structure change during reactions of glycerol in the liquid and gas phase. The experimental procedure for our infrared measurements is described in section 2.4.7. The results are shown in Figures 3.26-3.27. All the spectra exhibited absorption bands characteristic of the Keggin structure at 1080, 985, 890 and 795 $cm^{-1}$ before and after use under reaction conditions, indicating that the primary structure of the catalysts was stable under reaction conditions. The split in the peak at 986 $cm^{-1}$, which is ascribed to interaction between $Cs^+$ and the polyanion, was observed in the spectrum of fresh 0.5 wt% Pd/CsPW and 5.0 wt%Ru/CsPW (Figures 3.26-27). However, this characteristic almost disappeared for the spent catalysts. The infrared spectra of Pd/CsPW and Ru/CsPW after gas and liquid phase reactions of glycerol show no sign of structural changes (Figure 3.26-27).

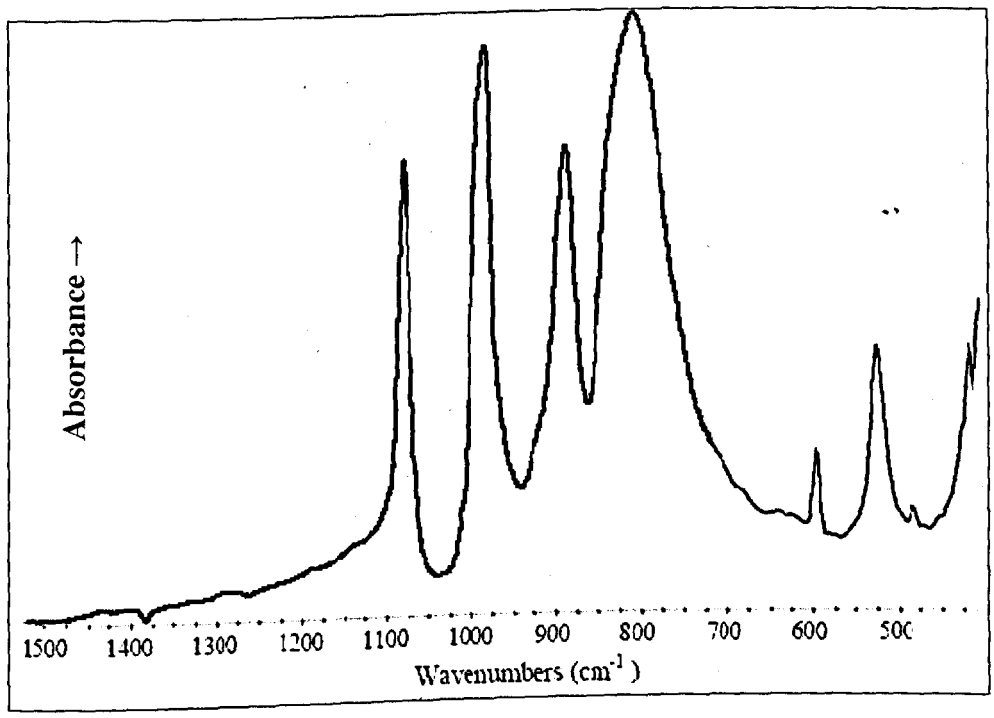


**Figure 3.25** FTIR spectrum of bulk $H_3PW_{12}O_{40}$.

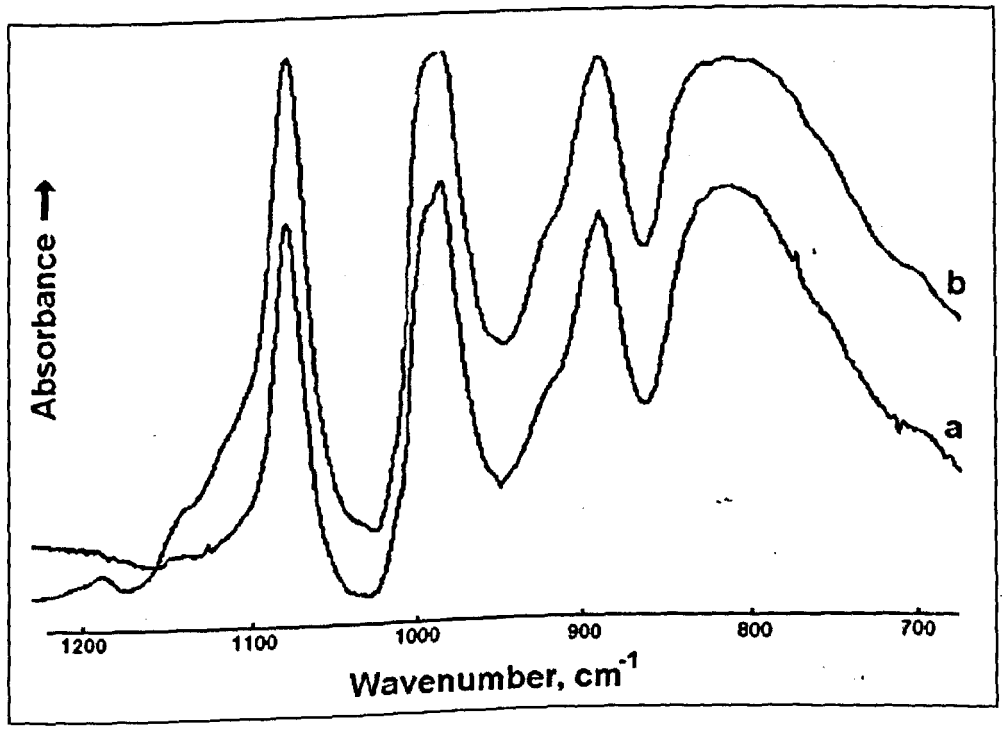


**Figure 3.26** DRIFT spectra for (a) fresh and (b) spent 0.5%Pd/CsPW catalyst.

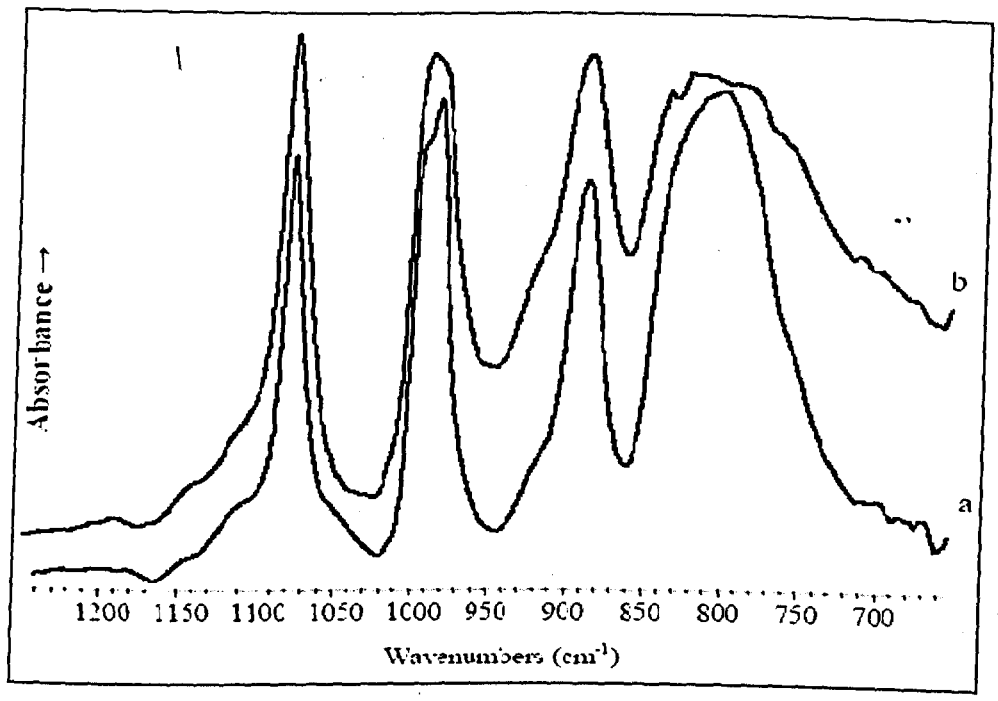


**Figure 3.27** DRIFT spectra for (a) fresh and (b) spent 5.0 %Ru/CsPW catalyst.

## 3.5 Ultraviolet (UV) spectroscopy

The stability of solid acid catalysts in water is a key factor. Few solid acids have been found to be water-tolerant. A number of heteropoly compounds are strong acids and they are active for various reactions such as acylation and alkylation in solid-liquid reaction systems. $C_{2.5}H_{0.5}PW_{12}O_{40}$ (CsPW) is known among heteropoly compounds as a water-tolerant catalyst [1, 23]. However, Keggin polyanions have been found to form lacunary (defect) species in aqueous solution at appropriate pH. For example, $[PW_{12}O_{40}]^{3-}$ forms the lacunary anion $[PW_{11}O_{39}]^{7-}$ at the pH 2 in aqueous solution [1]. The acidic CsPW forms colloidal suspension in water causing a recovery problem. In addition, the leaching of heteropoly anions in water under heat treatment was reported [27, 34]. UV spectroscopy has been used to detect the presence of heteropoly species in solution as the Keggin type $[PW_{12}O_{40}]^{3-}$ anion exhibits an absorption band at 265 nm [27, 35].

In our study, UV spectroscopy is used to investigate the CsPW leaching under reaction conditions by measuring the UV absorption characteristic of Keggin anions at 260 nm. The experimental procedures are described in Section 2.4.6. The leaching of Keggin anions detected by the UV spectra in the reaction mixture after catalyst separation is given in Table 3.3. In order to confirm the amount of leaching species estimated by UV spectra, the amount of W in the reaction solution was analysed by ICP. These results are also given in Table 3.3. The Ru/CsPW released up to 12 % of the heteropoly anions into the liquid phase during reaction at 180 °C for 10 h. On the other hand, the amount released by Ru/CsSiW was slightly higher than that of Ru/CsPW, although HSiW is suggested to possess higher hydrolytic stability than HPW, as mentioned earlier in section 1.2.3. The amount of released polyanions decreased with decreasing reaction temperature from 180 °C to 150 °C. No leaching of Ru species was observed.

**Table 3.3** The amount of $PW_{12}O_{40}^{-3}$ anions leached under reaction conditions[a].

| Catalyst | Reaction conditions | | UV (%) | ICP (%) |
|---|---|---|---|---|
| | T (°C) | $H_2$ (bar) | | |
| Ru/CsPW | 180 | 5 | 12.0 | 10.4 |
| | 150 | 5 | 10.3 | 10.9 |
| Ru/CsSiW | 180 | 5 | 12.8 | 11.5 |

a) Other reaction parameters: 0.2 g of catalyst, 5 mL of 20% glycerol solution, 10 h, 5 bar $H_2$.

Catalyst leaching is a common drawback in heterogeneous catalysis in the liquid phase. Different scenarios of a leaching situation can be distinguished: 1) leaching species form an active homogeneous catalyst; 2) the leaching species are not homogeneously active, 3) no leaching and the system is truly heterogeneous. To test the situation with Ru/CsPW, the catalyst was separated from reaction mixture,

and then the mixture was allowed to perform at the same reaction conditions. Indeed, we found that no further reaction took place. This may indicate that the leaching species are homogeneously inactive. The homogeneous $H_3PW_{12}O_{40}$ was also tested under reaction conditions, and again no activity was detected. This confirms the inactivity of leached heteropoly anions.

## 3.6 Powder X-ray diffraction

### 3.6.1. $Cs_{2.5}H_{0.5}PW_{12}O_{40}$

Powder X-ray diffraction is a widely applied technique in heterogeneous catalysis to identify phases present in catalysts. $Cs_{2.5}H_{0.5}PW_{12}O_{40}$ (CsPW) is an ordered crystalline material with a crystallite size close to 10 nm as estimated from the XRD line width using the Scherrer equation by Okuhara et al. [2]. The XRD pattern for CsPW is well-documented in the literature and is very similar to that of the parent heteropoly acid ($H_3PW_{12}O_{40}$) except for the broadening of the sharp diffraction lines of the hexahydrate, due to the removal of water of crystallisation upon drying of the CsPW [2, 32].

The XRD diffraction patterns for CsPW and 5.0 % Ru/ CsPW were recorded using the experimental process described in Section 2.4.8 and are shown in Figure 3.28. The XRD patterns are in good agreement with those observed for CsPW in the literature [32]. No changes in the diffraction patterns of CsPW upon the impregnation of ruthenium and the reduction pretreatment were observed. No diffraction pattern for the ruthenium metallic phase was observed either (2θ between 40 and 45°). This could probably be explained by the small average particle size of ruthenium.

The X-ray patterns for liquid phase spent catalysts were also recorded (Figure 3.2) from which it can be concluded that the catalysts maintained their crystalline structure under reaction conditions studied (180 °C, 5 bar $H_2$, 10 h, 20 wt% glycerol aqueous solution, 0.2 g catalyst).

$Cs_{3.5}H_{0.5}SiW_{12}O_{40}$ and 5.0 wt%Ru/CsSiW exhibited identical XRD patterns with those of CsPW and 5.0 wt%Ru/CsPW (Figure 3.29). No diffraction peaks were observed for Ru metallic phase.

The fresh CsPW and 0.5%Pd/CsPW as well as the spent 0.5%Pd/CsPW exhibited the same cubic XRD pattern characteristic of CsPW (Figure 3.30). It should also be noted that the XRD of Pd/CsPW, both fresh and used, did not show any pattern of Pd metal, thus the diffraction peak of Pd phase at $2\theta = 40.1$ is not seen in Figure 3.30. This is possibly due to a fine dispersion of Pd metal on the CsPW surface, which is discussed in following section.

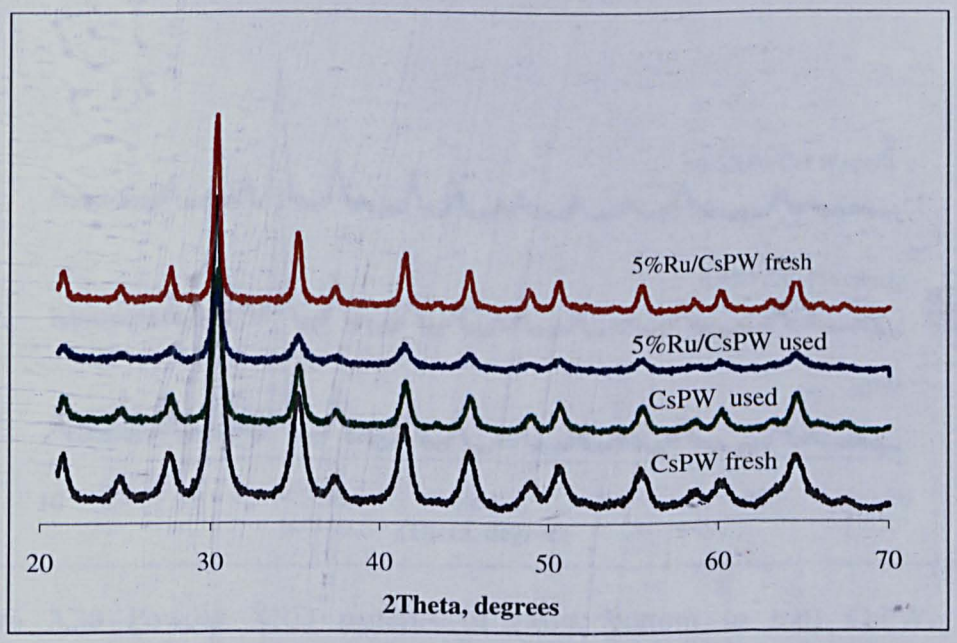


**Figure 3.28** XRD patterns for (from top to bottom) Ru/CsPW fresh, Ru/CsPW used, CsPW used and CsPW fresh. The X-ray source is Co Kα (λ = 1.788965 Å). Calcination temperature is 150°C, 1.5 h.

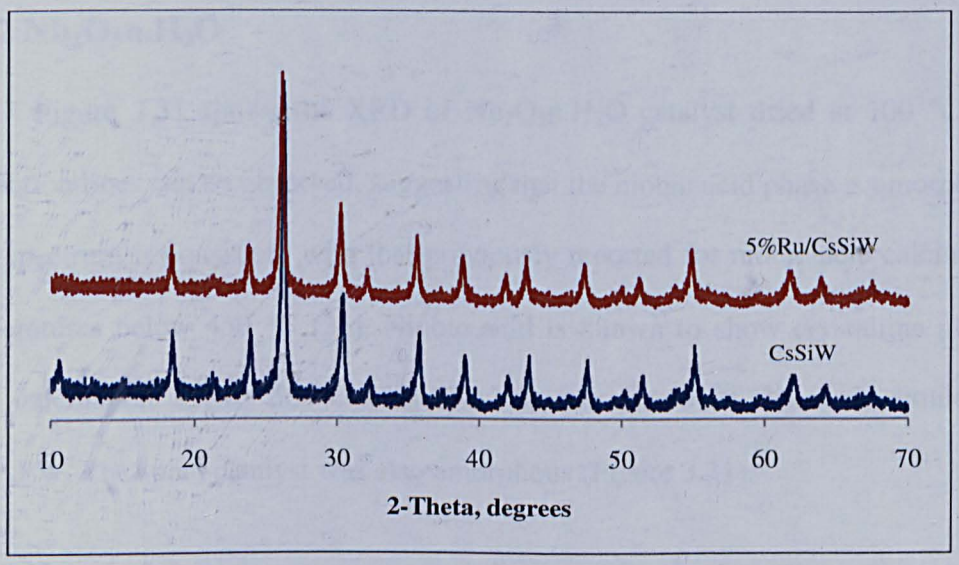


**Figure 3.29** XRD patterns for (top to bottom) CsSiW, (b) 5.0 %Ru/CsSiW. The X-ray source is Cu Kα (λ = 1.5406 Å). Calcination temperature 150 °C, 1.5 h.

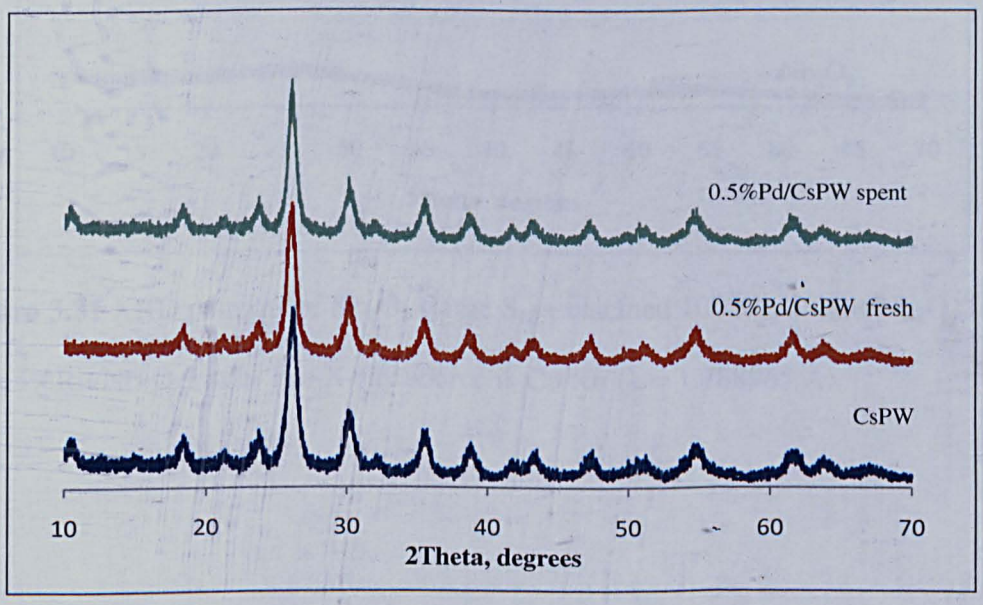


**Figure 3.30** Powder XRD patterns of (from bottom to top) CsPW, fresh 0.5%Pd/CsPW spent 0.5%Pd/CsPW. The X-ray source is Cu Kα (λ = 1.5406 Å). Calcination temperature 150 °C, 1.5 h.

### 3.6.2 $Nb_2O_5n.H_2O$

Figure 3.31 shows the XRD of $Nb_2O_5n.H_2O$ catalyst dried at 100 °C. No diffraction lines can be observed, suggesting that the niobic acid phase is amorphous. This spectrum is consistent with that previously reported for niobic acid calcined at temperatures below 450 °C [36]. Niobic acid is known to show crystalline phases after calcination above 500°C [37]. Ru (0) has not been detected, similar to Ru/CsPW. The spent catalyst was also amorphous (Figure 3.31).

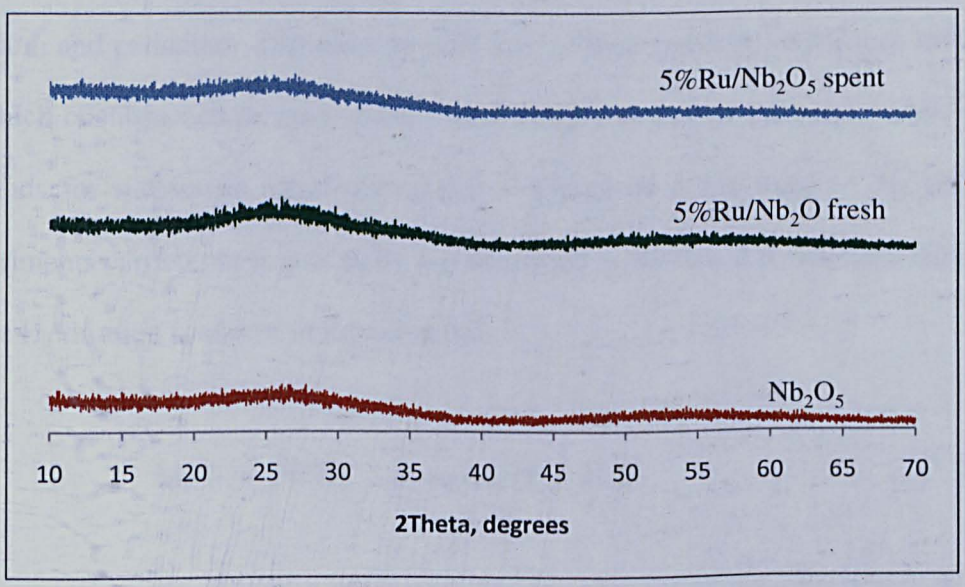


**Figure 3.31** XRD patterns of $Nb_2O_5$ (large $S_{BET}$ calcined 100°C), 5%Ru/$Nb_2O_5$ fresh large5%Ru/$Nb_2O_5$ used. The X-ray source is Co Kα (λ = 1.788965 Å).

## 3.7 Hydrogen chemisorption

### 3.7.1 Metal doped $Cs_{2.5}PW_{12}O_{40}$

A wide range of chemical and physical techniques are used for the determination of the local structures of nanocrystalline dispersed metal species: surface areas, particle sizes and dispersions. The catalytic activity of supported metals strongly depends on the metal dispersion. Moreover, the presence of metals on the surface of acid/base catalysts may also have an effect on the number of Brønsted acid sites in CsPW. It is thus of great interest to determine the ruthenium, rhodium and palladium dispersion and the size of their particles. Hydrogen titration, in which chemisorbed oxygen reacts with hydrogen is one of the most widely used methods for measuring metal dispersion of supported noble metals. $H_2$ titration experiments carried out in this study are described in Section 2.5. The stoichiometry of the $H_2$ titration is shown in Equation 3.2.

$$M_s\text{-}O + 3/2H_2 \longrightarrow M_s\text{-}H + H_2O \qquad (3.2)$$

This equation has previously been applied for dispersion measurements of palladium [38], platinum [39], rhodium [40, 41], and ruthenium [42]. The results of $H_2$ titration are listed in Table 3.4. No CsPW reduction was observed during $H_2$ adsorption, which rules out the hydrogen spillover. In addition, TPR study of HPA, carried out by by Katamura et al. [43] shows that the Pd-doped HPW is reduced by $H_2$ only above 300°C. The dispersion of ruthenium in the 5.0 wt%Ru/CsPW catalyst, $D = 0.11$, corresponds to an average metal particle diameter of 8 nm. For rhodium, these values were 0.88 and 1 nm, respectively, indicating a strong interaction of Rh with CsPW. Ruthenium average particle size (8 nm) is higher than that implied

through the absence of X-ray lines in the powder XRD study with the 5.0 wt% Ru/CsPW catalyst. To explain the low dispersion of Ru in this study, it should be noted that metal dispersion and particle size are critically dependent upon the preparation conditions and the metal precursor [44]. Ruthenium chloride ($RuCl_3xH_2O$) was used as Ru metal precursor, which is reduced to $Ru^0$ at 215 °C, as shown by Stuchinskaya et al. [45]. Thus, the reduction pretreatment of all Ru catalysts in our study were carried out at 250 °C for 2 h. In contrast, reduction temperatures of up to 450 °C for ruthenium catalysts were used in some previous reports [46, 47]. The low reduction temperature (250 °C) used in this study may result in incomplete reduction of $Ru^{3+}$ to $Ru^0$ leaving some $Cl^-$ species which could interfere with the adsorption of $H_2$ and hence lead to lower Ru dispersion [44]. As expected, decreasing Ru loading to 0.5% significantly increased the Ru dispersion, *D* = 0.54 for 0.5 wt%Ru/CsPW. At lower loadings, the reduction process could be more efficient at 250 °C, resulting in a higher dispersion.

Palladium and platinum dispersions, *D*, in 0.5 wt% Pd/CsPW and 0.3 wt%Pt/CsPW exhibited reasonably high values, 0.76 and 0.52 respectively. The estimated particle sizes of Pd and Pt are 1.2 and 1.7 nm respectively. These values are in agreement with those implied by the absence of Pd XRD patterns. A high dispersion of Pd was also obtained for 2.0 wt%Pd/HPW/$SiO_2$, close to that of 0.5% Pd on CsPW. This high dispersion, with high Pd loading, could be explained by the large surface area that $SiO_2$ provides for Pd particles. In addition, Pd particles in 2.0 wt%Pd/HPW/$SiO_2$ catalyst may react differently on $SiO_2$ which is already occupied by 20 wt%HPA.

**Table 3.4** Results of $H_2$ chemisorption experiments for Ru and Rh doped CsPW.

| Sample | Dispersion (D)[a] | Average Particle diameter (nm)[b] |
|---|---|---|
| CsPW | - | - |
| 5.0 wt% Ru/CsPW | 0.11 | 8.0 |
| 0.5 wt% Pd/CsPW | 0.76 | 1.2 |
| 5.0 wt% Rh/CsPW | 0.88 | 1.0 |
| 0.5 wt% Ru/CsPW | 0.54 | 1.6 |
| 0.3 wt%Pt/CsPW | 0.52 | 1.7 |
| 2.0 wt%Pd/HPW/$SiO_2$ | 0.66 | 1.4 |

a) $D = M_s/M_{total}$

b) Particle diameter, calculated using the equation, d=0.9/D [48].

### 3.6.2 $Nb_2O_5.nH_2O$

The $H_2$ titration experiments of Ru and Rh doped $Nb_2O_5$ are depicted in Table 3.5. The support ($Nb_2O_5$) in $H_2$ flow has been reported to be stable at temperatures up to 600 °C , much higher than our $H_2$ titration experiment conditions (100 °C) [49]. No hydrogen uptakes were detected for $Nb_2O_5$ suggesting that $Nb_2O_5$ is inactive towards $H_2$ adsorption at this temperature [50, 51]. For $Rh/Nb_2O_5$, it has been reported that no spillover of hydrogen occurs even at higher temperatures (500 °C). As shown in Table 3.5, $Rh/Nb_2O_5$ exhibited high metal dispersion, similar to Rh/CsPW. The dispersion of Ru on $Nb_2O_5$ surface was, $D$ = 0.17, higher than that obtained with Ru/CsPW, which can be explained by the higher surface area of $Nb_2O_5$. However, spillover of $H_2$ from metal to the support with $Ru/Nb_2O_5$ catalyst has been reported to take place at temperatures over 180 °C [49], higher than our experimental conditions (100 °C). The low Ru dispersion over $Nb_2O_5$ under our

conditions may be due to the insufficient reduction of Ru (III) to Ru (0), as stated earlier with Ru/CsPW.

**Table 3.5** Results of $H_2$ chemisorption experiments for Ru and Rh doped $Nb_2O_5.nH_2O$.

| Sample | Dispersion (D)[a] | Average Particle diameter (nm)[b] |
|---|---|---|
| $Nb_2O_5.nH_2O$ | - | - |
| 5.0 wt% $Ru/Nb_2O_5$ | 0.26 | 3.46 |
| 5.0 wt% $Rh/Nb_2O_5$ | 0.93 | 0.96 |

a) $D = M_s/M_{total}$

b) Particle diameter, calculated using the equation, d=0.9/D [48].

## 3.8 Acidity measurements

In this section, we aim to characterise the acidity of selected catalysts using various techniques: differential scanning calorimetry (DSC) of $NH_3$ adsorption in a gas-solid system to determine the strength of acid sites and Fourier transform infrared spectroscopy (FTIR) to determine the nature of acid sites (Brønsted and Lewis) by adsorption of pyridine. The experimental procedures for these measurements are described in Section 2.4.7 and 2.4.9.

### 3.8.1 Pulse ammonia adsorption analysis

The strength of acid sites in the catalysts was characterised by measuring the enthalpy ($\Delta H$) of ammonia adsorption at the gas-solid system. This technique does not differentiate between Brønsted and Lewis acid sites. The values of $\Delta H$ for the catalysts are given in Table 3.6. Figures 3.34-3.36 show the determination of the initial enthalpy of $NH_3$ adsorption, $\Delta H$, for $Cs_{2.5}H_{0.5}PW_{12}O_{40}$, $C_{3.5}H_{0.5}SiW_{12}O_{40}$ and

$Nb_2O_5$. Our ΔH values for the well-documented $Cs_{2.5}H_{0.5}PW_{12}O_{40}$ are in strong agreement with those reported previously by Okuhara [23]. As expected, $C_{3.5}H_{0.5}SiW_{12}O_{40}$ showed lower acidity strength compared to $Cs_{2.5}H_{0.5}PW_{12}O_{40}$ with ΔH being -119 kJ/mol [1]. Niobic acid calcined at 500 °C was observed to be strongly acidic giving a -123 kJ/mol as standard enthalpy of $NH_3$ adsorption. However, $Nb_2O_5$ calcined at lower temperatures reported to possess higher acidity strength [52]. The acid strength of catalysts decreases in the order: $Cs_{2.5}H_{0.5}PW_{12}O_{40}$ > $Nb_2O_5 \approx C_{3.5}H_{0.5}SiW_{12}O_{40}$.

**Table 3.6** Initial enthalpies of ammonia adsorption at 100 °C.

| **Catalyst** | **Calcination temperature (°C)** | **-ΔII (kJ/mol)** |
|---|---|---|
| $Cs_{2.5}H_{0.5}PW_{12}O_{40}$ | 300 | 162 |
| $Cs_{3.5}H_{0.5}SiW_{12}O_{40}$ | 300 | 119 |
| $Nb_2O_5$ | 500 | 123 |

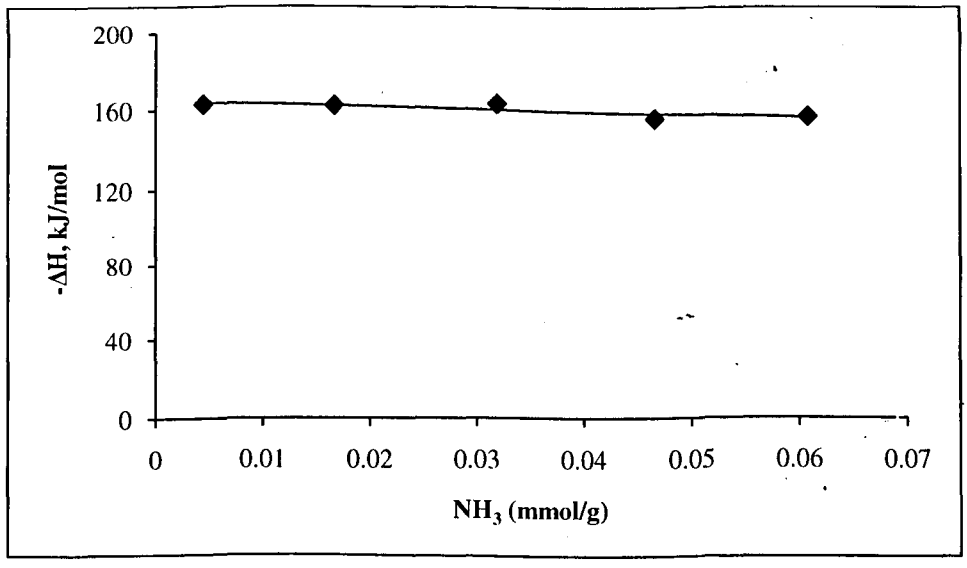


**Figure 3.34** The plot of enthalpy of $NH_3$ adsorption versus $NH_3$ uptake for $C_{2.5}H_{0.5}PW_{12}O_{40}$.

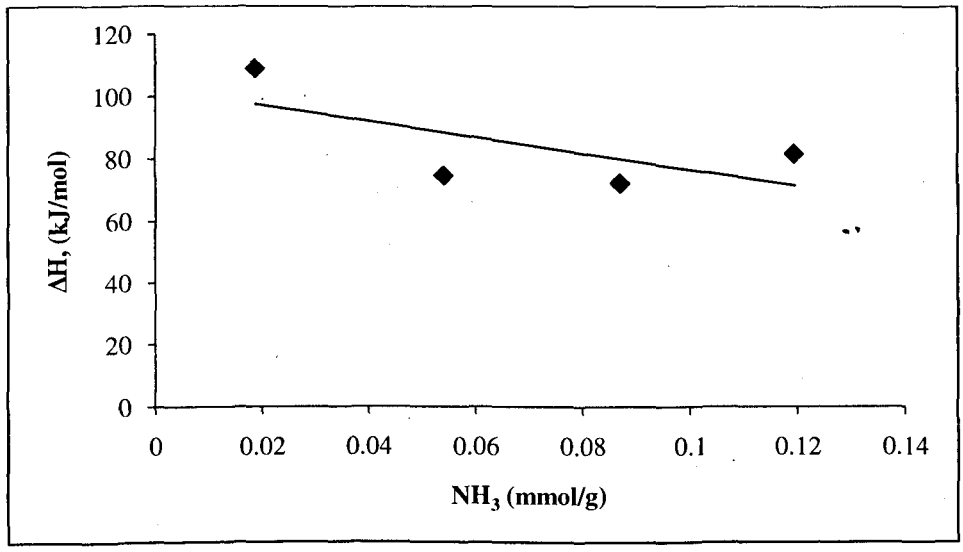


**Figure 3.35** The plot of enthalpy of $NH_3$ adsorption versus $NH_3$ uptake for $C_{3.5}H_{0.5}SiW_{12}O_{40}$.

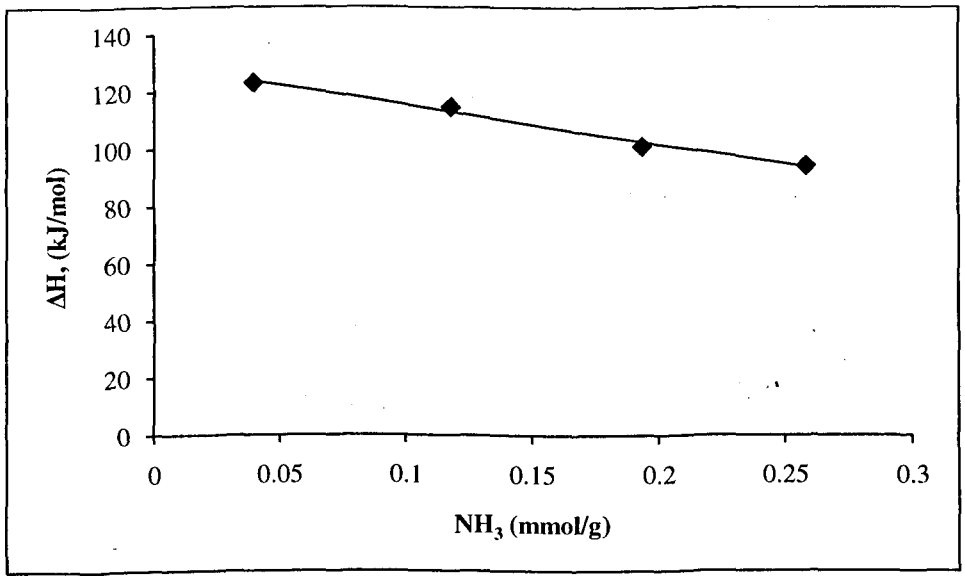


**Figure 3.36** The plot of enthalpy of $NH_3$ adsorption versus-$NH_3$ uptake for $Nb_2O_5$.

### 3.8.2 FTIR study of pyridine adsorption

The characterisation of surface acidity in heterogeneous catalysis is a fundamental stage towards understanding reaction mechanisms. Adsorption of pyridine as a base on the surface of solid acids is a powerful method for the characterisation of surface acidity [53-55]. The pyridinium ion exhibits a vibration at 1540 $cm^{-1}$ and enables identification of Brønsted acid sites. The pyridine co-ordinatively bonded shows absorption at 1440 $cm^{-1}$ which is a characteristic of Lewis acid sties [55].

The FTIR spectra of adsorbed pyridine were used to characterise the type of acid sites available on the surface of CsPW and hydrated $Nb_2O_5$, the results are shown in Figures 3.37-3.41. These spectra were measured as described in Section 2.4.7. The physisorbed pyridine shows a band at ~ 1440 $cm^{-1}$, which can be misinterpreted as Lewis sites. Therefore, care has been taken to remove it by pumping it out at 100-150 °C. Figure 3.37 shows that the $Cs_{2.5}H_{0.5}PW_{12}O_{40}$ pre-treated at temperatures below 300°C possesses strong Brønsted acid sites, as confirmed by strong IR band at 1540 $cm^{-1}$. This was previously reported for bulk $H_3PW_{12}O_{40}$ and $Cs_{2.5}H_{0.5}PW_{12}O_{40}$ [1, 19]. In contrast, Zn-Cr '(1:1) mixed oxide displays purely Lewis acid sites proved by the band at 1440 $cm^{-1}$, in agreement with a study by Al-Wadaani et al. [56]. $Cs_{3.5}H_{0.5}SiW_{12}O_{40}$ exhibited similar behaviour as CsPW of possessing Brønsted acid sites, as appears in Figure 3.38. Hydrated $Nb_2O_5$ catalyst possesses both Brønsted and Lewis acid sites, as confirmed by strong IR bands at 1540 and 1450 $cm^{-1}$, respectively (Figure 3.39). This is consistent with previous studies [57, 58].

FTIR pyridine adsorption spectra of spent Ru/CsPW and Ru/ $Nb_2O_5$ catalysts are shown in Figures 3.40 and 3.41. In both catalysts, the intensities of band at 1540

$cm^{-1}$, which is a distinctive of Brønsted acid sites, are obviously reduced. This indicates that the surface acidities of both catalysts are altered by reaction conditions (180 °C, 10 h, 20 wt% glycerol aqueous solution). This change in the catalyst acidity is probably explained by the decrease in the density of acid sites rather than the acid strength. Nakato et al. [27] investigated the effect of heat treatment in water on the catalyst acidity. The calorimetric study of ammonia adsorption showed that the water treatment reduced the number of acid sites, whereas the acid strength was little affected [27].

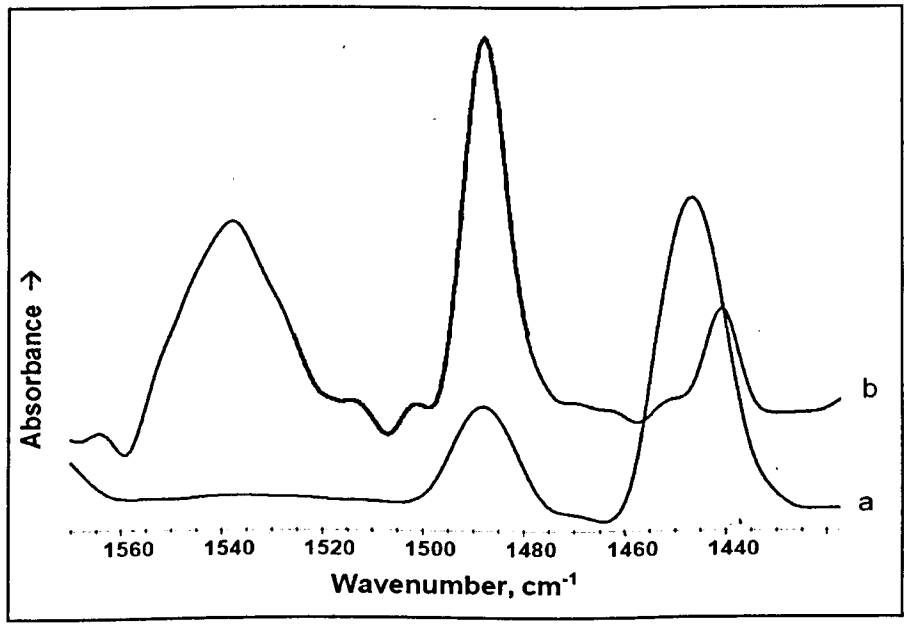


**Figure 3.37** DRIFT spectra of pyridine adsorbed on (a) Zn-Cr (1:1) mixed oxide and (b) CsPW.

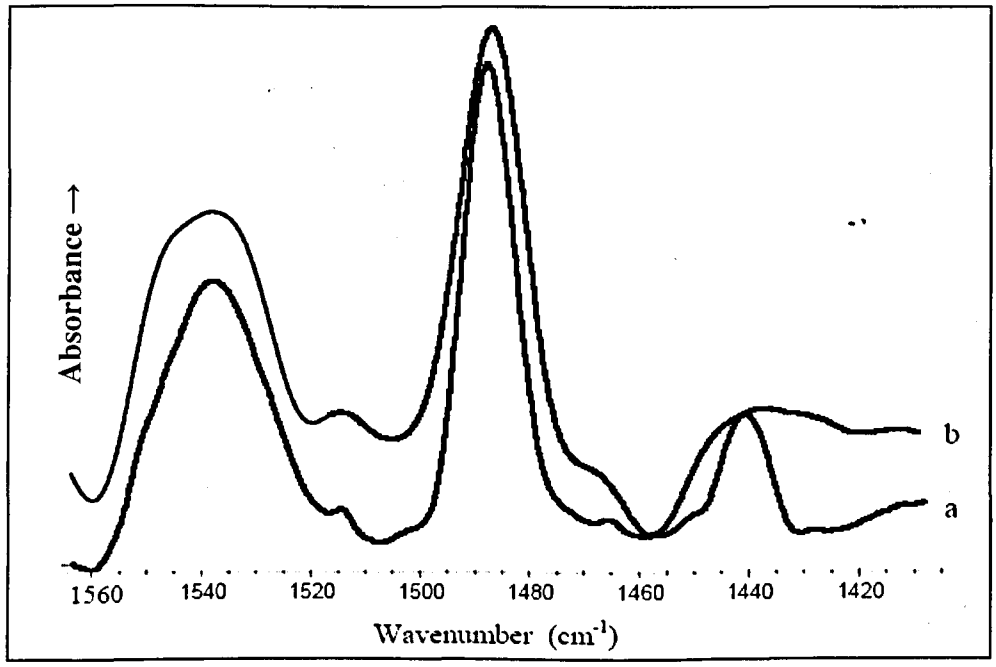


**Figure 3.38** DRIFT spectra of pyridine adsorbed on (a) CsPW vs. (b) CsSiW.

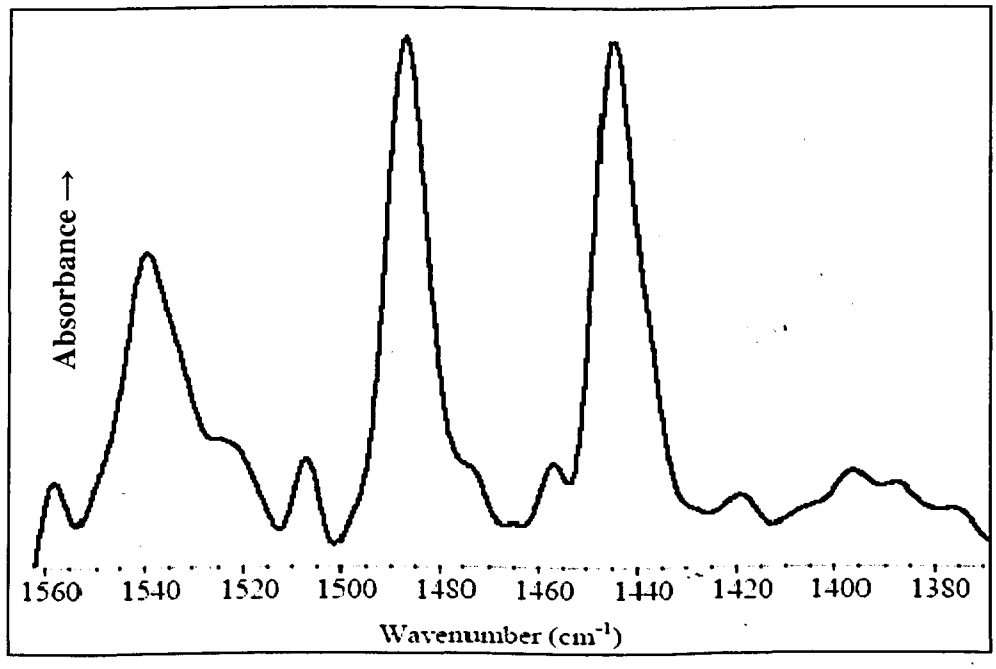


**Figure 3.39** DRIFT spectrum of pyridine adsorbed on $Nb_2O_5$ calcined at 100°C.

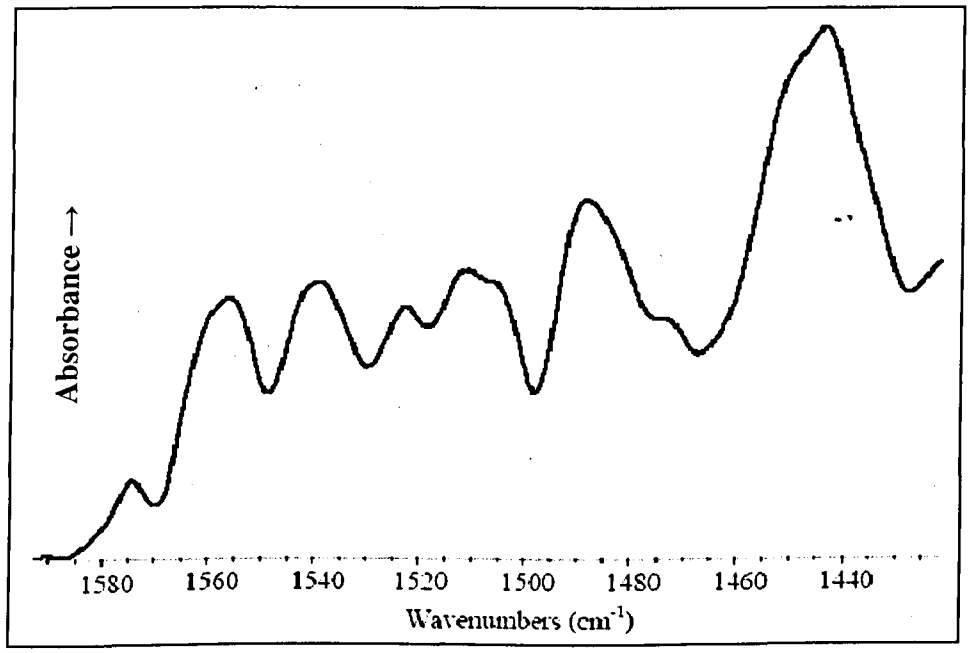


**Figure 3.40** DRIFT spectrum of pyridine adsorbed on Ru/CsPW after use in liquid-phase glycerol hydrogenolysis.

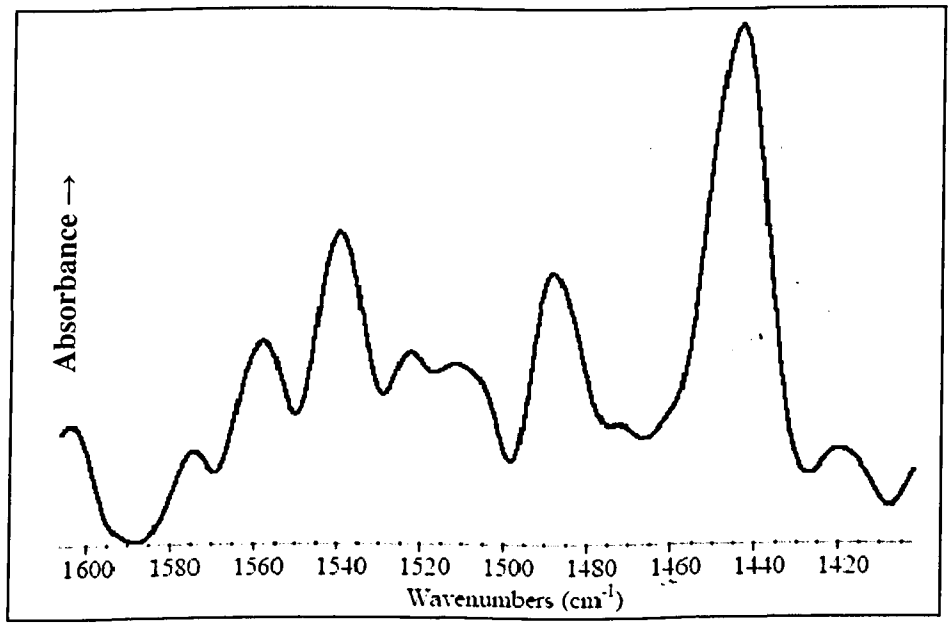


**Figure 3.41** DRIFT spectrum of pyridine adsorbed on Ru/ $Nb_2O_5$ after use in liquid-phase glycerol hydrogenolysis.

## 3.9 Conclusions

The texture of catalysts was characterised by $N_2$ physisorption. All the catalysts under study were mesoporous materials with high surface areas (200 – 85 $m^2/g$) and average pore diameters of 24 – 175 Å. FTIR study showed that all HPA catalysts maintained their primary structure after use in liquid phase glycerol hydrogenolysis and gas-phase dehydration of glycerol. UV spectroscopy and ICP analysis confirmed the leaching of heteropoly anions into solution in liquid phase glycerol hydrogenolysis. The XRD measurements showed that CsPW and CsSiW catalysts are crystalline and no diffraction lines were recorded for Ru, Rh and Pd metals, which suggests the presence of these metals in high dispersion on the catalyst surface. $Nb_2O_5$ dried at 100 °C was amorphous, and again no Ru and Rh metallic phases were detected.

Hydrogen titration experiments demonstrated the presence of Rh, Pd and Pt metals in high dispersion state compared to Ru metal, which could probably be due to insufficient reduction of the metal precursor ($RuCl_3$) to Ru metallic phase ($Ru^0$). CsPW and CsSiW were found to possess purely Brønsted acid sites whereas $Nb_2O_5$ contain both Brønsted and Lewis sites. Zn-Cr (1:1) mixed oxide exhibited only Lewis acid sites, as evidenced by FTIR study of pyridine adsorption. From ammonia adsorption calorimetry, the acid strength of catalysts under study decreases in the order: $Cs_{2.5}H_{0.5}PW_{12}O_{40} > Nb_2O_5 \approx C_{3.5}H_{0.5}SiW_{12}O_{40}$.

## References


[1] I. V. Kozhevnikov, Catalysts For Fine Chemical Synthesis, Catalysis by Polyoxometalates, Wiley 2002.

[2] T. Okuhara, H. Watanabe, T. Nishimura, K. Inumaru, M. Misono, Chem. Mater. 12 (2000) 2230.

[3] N. Essayem, G. Coudurier, M. Fournier, J.C. Vedrine, Catal. Lett. 34 (1995) 223.

[4] M. R. H. Siddiqui, S. Holmes, H. He, W. Smith, E. N. Coker, M. P. Atkins, I. V. Kozhevnikov, Catal. Lett. 66 (2000) 53.

[5] I. V. Kozhevnikov, S. Holmes, M. R. H. Siddiqui, Appl. Catal. A 214 (2001) 47.

[6] E. F. Kozhevnikova, E. Rafiee, I. V. Kozhevnikov, Appl. Catal. A 260 (2004) 25.

[7] J. Barbier, Stud. Surf. Sci. Catal. 34 (1987) 1.

[8] J. Barbier, Applied Catalysis. 23 (1986) 225.

[9] K. Tanabe, Catal. Today. 78 (2003) 65.

[10] I. Nowak, M. Ziolek, Chem. Rev. 99 (1999) 3603.

[11] C. X. Guo, Z. H. Qian, Catal. Today. 16 (1993) 379.

[12] S. J. Gregg, K. S. W. Sing, Adsorption, Surface Area and Porosity, Academic Press, London, 1982.

[13] K. K. Unger, J. Roquerol, K. S. W. Sing, H. Kral (Eds.), Charactersation of Porous Solids I, Elsevier, Amsterdam, 1988.

[14] J. Roquerol, F. Rodriguez-Reinoso, K.S.W. Sing, K.K.Uger (Eds.), Charactersation of Porous Solids III, Alservier, Amsterdam 1994.

[15] G. Leofanti, M. Padovan, G. Tozzola, B. Venturelli, Catal. Today. 41 (1998) 207.

[16] S. Brunauer, P. H. Emmett, E. Teller, J. Am. Chem. Soc. 60 (1938) 309.

[17] E. P. Barrett, L. G. Joyner, P.P. Halenda, J. Am. Chem. Soc. 73 (1951) 373.

[18] N. Mizuno, M. Misono, Chem. Rev. 98 (1998) 199.

[19] T. Okuhara, N. Mizuno, M. Misono, Adv. Catal. 41 (1996) 113.

[20] S. Tatematsu, T. Hibi, T. Okuhara, M. Misono, Chem. Lett. (1984) 865.

[21] M. Misono, Chem. Commun. (2001) 1141.

[22] N. Mizuno, M. Misono, Chem. Lett. (1987) 967.

[23] T. Okuhara, Chem. Rev. 102 (2002) 3641.

[24] T. Okuhara, Catal. Today. 73 (2002) 167.

[25] T. Yamada, Y. Yoshinaga, T. Okuhara, Bull. Chem. Soc. Jpn. 71 (1998) 2727.

[26] T. Nakato, Y. Toyoshi, M. Kimura, T. Okuhara, Catal. Today. 52 (1999) 23.

[27] T. Nakato, M. Kimura, S. Nakata, T. Okuhara, Langmuir. 14 (1998) 319.

[28] M. Ziolek, Catal. Today. 78 (2003) 47.

[29] M. Paulis, M. Martin, D.B. Soria, A. Diaz, J.A. Odriozola, M. Montes, Appl. Catal. A 180 (1999) 411.

[30] J. B. Moffat, Metal-Oxygen Clusters. The Surface and Catalytic Properties of Heteropoly Oxometalates, Kluwer, New York, 2001.

[31] S. M. Choi, Y. Wang, Z. M. Nie, J. Liu, C.H.F. Peden, Catal. Today. 55 (2000) 117.

[32] J. A. Dias, E. Caliman, S.C.L. Dias, Microporous. Mesoporous Mater. 76 (2004) 221.

[33] N. Essayem, A. Holmqvist, P. Y. Gayraud, J.C. Vedrine, Y. Ben Taarit, J. Catal. 197 (2001) 273.

[34] T. Okuhara, M. Kimura, T. Kawai, Z. Xu, T. Nakato, Catal. Today. 45 (1998) 73.

[35] P. Villabrille, G. Romartelli, P. Vazquez, C. Caceres, Appl. Catal. A 334 (2008) 374.

[36] V. S. Braga, J. A. Dias, S. C.L. Dias, J. L. de Macedo, Chem. Mater. 17 (2005) 690.

[37] S. H. Chai, H. P. Wang, Y. Liang, B.Q. Xu, J. Catal. 250 (2007) 342.

[38] J. E. Benson, M. Boudart, J. Catal. 30 (1973) 146.

[39] J. E. Benson, M. Boudart, J. Catal. 4 (1965) 704.

[40] S. E. Wanke, Doughart.Na, J. Catal. 24 (1972) 367.

[41] C. Blanco, R. Ruiz, C. Pesquera, F. Gonzalez, Appl. Organomet. Chem. 16 (2002) 84.

[42] K. C. Taylor, Journal of Catalysis. 38 (1975) 299.

[43] K. Katamura, T. Nakamura, K. Sakata, M. Misono, Y. Yoneda, Chem. Lett. (1981) 89.

[44] G. C. Bond, Metal-Catalysed Reactions of Hydrocarbons, Springer, New York 2005.

[45] T. L. Stuchinskaya, M. Musawir, E. F. Kozhevnikova, I. V. Kozhevnikov, J. Catal. 231 (2005) 41.

[46] D. K. Sohounloue, C. Montassier, J. Barbier, React. Kinet. Catal. Lett. 22 (1983) 391.

[47] S. Sayan, M. Kantcheva, S. Suzer, D. O. Uner, J. Mol. Struct. 481 (1999) 241.

[48] J. E. Benson, H. S. Hwang, M. Boudart, J. Catal. 30 (1973) 146.

[49] K. V. R. Chary, C. S. Srikanth, V. V. Rao, Catal. Commun. 10 (2009) 459.

[50] D. A. G. Aranda, F. B. Noronha, M. Schmal, F. B. Passos, Appl. Catal. A 100 (1993) 77.

[51] F. B. Passos, D. A. G. Aranda, R.R. Soares, M. Schmal, Catal. Today. 43 (1998) 3.

[52] J. C. Vedrine, G. Coudurier, A. Ouqour, P. G. P. de Oliveira, J. C. Volta, Catal. Today. 28 (1996) 3.

[53] B. M. Devassy, S. B. Halligudi, J. Catal. 236 (2005) 313.

[54] B. M. Devassy, F. Lefebvre, S. B. Halligudi, J. Catal. 231 (2005) 1.

[55] B. H. Davis, R. A. Keogh, S. Alerasool, D. J. Zalewski, D. E. Day, P. K. Doolin, J. Catal. 183 (1999) 45.

[56] F. Al-Wadaani, E. F. Kozhevnikova, I. V. Kozhevnikov, J. Catal. 257 (2008) 199.

[57] K. Tanabe, M. Misono, Y. Ono, H. Hattori, New Solid Acids and Bases: Their Catalytic Properties, Kodansha, Tokyo, 1989.

[58] T. Iizuka, K. Ogasawara, K. Tanabe, Bull. Chem. Soc. Jpn. 56 (1983) 2927.

# 4. Liquid - phase hydrogenolysis of glycerol to propanediols using Ru-doped $Cs_{2.5}H_{0.5}PW_{12}O_{40}$

## 4.1 Introduction

The development of biodiesel production by transesterification of vegetable oils makes large amounts of glycerol available as a reaction by-product, ca. 10 wt% of the biodiesel produced [1]. The availability and low price of glycerol make it a promising feedstock for producing a wide range of value-added chemicals. Synthesis of propanediols, 1,2-PDO and 1,3-PDO, from glycerol has attracted significant interest [2-7]. 1,2-PDO and 1,3-PDO are currently produced from petroleum derivatives by chemical catalytic routes: 1,2-PDO from propylene oxide and 1,3-PDO from ethylene oxide or acrolein [8]. These diols can be produced by an alternative route involving hydrogenolysis of glycerol.

A number of patents and papers have disclosed the hydrogenolysis of glycerol in the presence of homogeneous and heterogeneous catalysts ([2-7] and references therein). This reaction has been carried out in liquid-phase batch systems at 110–260 °C and an $H_2$ pressure up to 300 bar yielding 1,2- and 1,3-PDO together with 1- and 2-propanol, ethylene glycol, ethanol and methane as byproducts. More efficient hydrogenolysis procedures that have been reported recently employ CuO–ZnO (200 °C, 42 bar, 12 h) [2, 6], copper chromite (200 °C, 14 bar, 24 h) [3] as heterogeneous catalysts. These procedures, however, have serious drawbacks such as high temperature and pressure of the process, low selectivity to propanediols, and low catalyst activity hence low glycerol conversion and long reaction times.

The hydrogenolysis of glycerol to 1,2-PDO and 1,3-PDO is suggested to proceed via dehydration of glycerol to acetol and 3-hydroxypropanal by acid catalysis followed by catalytic hydrogenation , which has been supported by the observation of acetol amongst the reaction products and its selective hydrogenation to 1,2-PDO [3-5]. Alternatively, dehydrogenation of glycerol to glyceraldehyde followed by dehydration to 2-hydroxyacrolein and hydrogenation to yield 1,2-PDO has been suggested [7, 9]. These mechanisms suggest that bifunctional acid/hydrogenation catalysis should be effectively employed to carry out glycerol hydrogenolysis in one-pot system.

Multifunctional catalysis is considered an important future direction of sustainable organic synthesis to effect multi-step reactions in one-pot systems without separating intermediate products [10]. Recently, Miyazawa et al. [4, 5] have used a mixture of 5%Ru/C as a hydrogenation catalyst and Amberlyst-15 acid resin as an acid catalyst for glycerol hydrogenolysis in one-pot system. However, catalyst performance was rather low: 1,2-POD together with 1,3-POD were obtained with 55 and 5% selectivity, respectively at 13% glycerol conversion. A serious drawback to Amberlyst-15 was its decomposition above 120 °C [4]. In this system, Rh/C also exhibited some catalytic activity, whereas Pd/C and Pt/C were practically inactive. The aim of this work is to study the hydrogenolysis of glycerol to propanediols using Ruthenium supported over the acidic heteropoly salt, $Cs_{2.5}H_{0.5}PW_{12}O_{40}$ (CsPW), as an efficient bifunctional catalyst. CsPW is well known as a water-insoluble strong Brønsted acid and a versatile solid acid catalyst possessing considerable thermal stability (≥ 500 °C) [11-13].

## 4.2 Catalytic performance of Ru-doped CsPW for liquid-phase hydrogenolysis of glycerol

The hydrogenolysis of glycerol was carried out in a 45-mL Parr 4714 stainless steel autoclave equipped with a magnetic stirrer. The reaction mixture contained 5.0 mL of an aqueous solution of glycerol and 0.20 g catalyst unless stated otherwise. The autoclave was purged with $H_2$ then pressurised with $H_2$ (3 –14 bar) and placed in the oil bath preheated to the required temperature. After reaction completion, the autoclave was cooled to 0 °C, depressurised and opened. The catalyst was separated by centrifugation. The reaction products were identified via a combination of gas phase chromatography coupled with mass spectroscopy (GC/MS) and by comparing the retention times of the reaction products with the retention times of the pure compounds. The reaction products were then quantified by a GC equipped with flame ionisation detector, using the method detailed in section 2.6.1.

Table 4.1 shows representative results for the hydrogenolysis of glycerol. The CsPW acidic salt itself was not active in the formation of propanediols, providing only a trace of acetol. With water in large excess, the formation of acetol by acid-catalysed dehydration of glycerol is probably limited by unfavourable equilibrium. The Ru/CsPW catalyst showed excellent performance in glycerol hydrogenolysis at an unprecedented low hydrogen pressure of 5 bar, producing selectively 1,2-PDO with only traces of 1,3-PDO under the reaction conditions studied. Acetol, 1- and 2-propanol (1-PO and 2-PO), ethylene glycol (EG) and methane were found amongst byproducts, similar to the previous reports [2-7, 14, 15]. The Ru/CsPW catalyst is much more selective than the Ru/C + Amberlyst-15 [4, 5, 14]. It provides 88% 1,2-PDO selectivity (at 5 bar $H_2$) compared to 55% (at 80 bar $H_2$) [4] at similar glycerol

conversions, other reaction conditions being 120 °C, 10 h, 20 wt% glycerol aqueous solution.

**Table 4.1** Hydrogenolysis of glycerol over 5%Ru/CsPW and 5%Rh/CsPW[a].

| Catalyst | Temp. (°C) | Conv. (%) | TOF[b] ($h^{-1}$) | Selectivity (%) | | | | | |
|---|---|---|---|---|---|---|---|---|---|
| | | | | 1,2-PDO | 1,3-PDO | Acetol | 1-PO | EG | 2-PO |
| CsPW | 120 | <1 | - | 0.0 | 0.0 | 0.0 | 0.0 | 0.0 | 0.0 |
| Cs/PW[c] | 180 | <1 | - | 0.0 | 0.0 | trace | 0.0 | 0.0 | 0.0 |
| Ru/CsPW[d] | 180 | 5 | - | 11.0 | 0.0 | 70 | 0.0 | 0.0 | 0.0 |
| Ru/CsPW | 120 | 9.8 | 9.8 | 88.0 | 0.0 | 0.0 | 3.5 | 0.0 | 8.5 |
| Ru/CsPW | 150 | 21 | 21.0 | 95.8 | 0.0 | 0.0 | 4.2 | 0.0 | 0.0 |
| Ru/CsPW | 180 | 23 | 23.0 | 73.6 | 0.0 | 5.7 | 4.3 | 11.9 | 4.5 |
| Ru/CsPW | 200 | 27 | 27.0 | 67.7 | 0.0 | 8.6 | 5.1 | 14.0 | 4.6 |
| Rh/CsPW | 180 | 6.3 | 0.82 | 65.4 | 7.1 | 0.0 | 27.5 | 0.0 | 0.0 |
| Ru/CsSiW | 180 | 17 | 17 | 69.0 | 0.0 | 0.0 | 10.0 | 16 | 5.0 |

[a] Reaction conditions: 5 bar $H_2$ pressure, 0.2 g catalyst (4 wt%), 20 wt% glycerol aqueous solution (5 mL), 10 h. [b] TOF as the number of glycerol molecules converted per one surface Ru or Rh atom per 1 hour at 10 h reaction time. [c] Reaction in the absence of $H_2$. [d] 2 bar of nitrogen.

Temperature has a significant effect on the overall yield of propanediols as reported in the literature [3, 4, 6, 7, 15-17]. Experiments were carried out on the liquid-phase reaction over 5%Ru/CsPW catalyst at 120, 150, 180, 200 °C and at 5 bar pressure of hydrogen. Table 4.1 and Figure 4.1 show the effect of temperature on the conversion and selectivity of the reaction. The glycerol conversion of 27% was obtained at a maximum reaction temperature of 200°C. Our best results were obtained at 150 °C and 5 bar $H_2$ pressure: 96% 1,2-PDO selectivity at 21% glycerol conversion (20% yield of 1,2-PDO) with 4 wt% catalyst amount (Table 4.1).

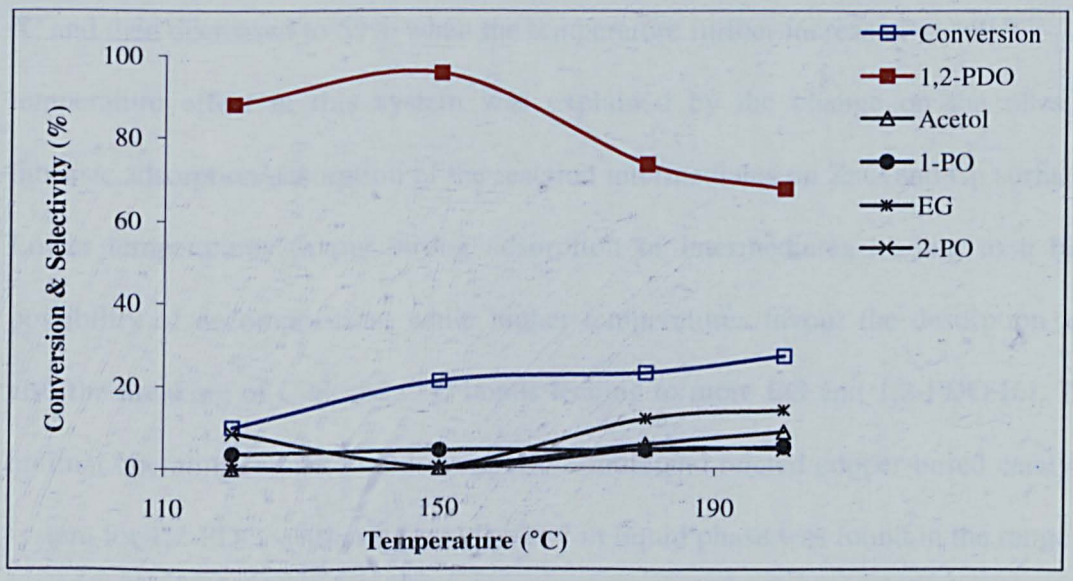


**Figure 4.1** Effect of reaction temperature on glycerol conversion and product selectivity (5 bar of $H_2$, 0.2 g of catalyst, 5 mL of 20% of glycerol solution and 10 h).

As the temperature increases from 120 to 200 °C, the glycerol conversion increases from 9.8 to 27%, with 1,2-PDO selectivity decreasing to 65% mainly due to the formation of ethylene glycol. The latter has been suggested to form by C–C bond cleavage on ruthenium [4, 5, 7]. At lower temperatures (120-150 °C) no acetol was observed, indicating a complete hydrogenation to 1,2-PDO which was seen with very high selectivity. This indicates that a high temperature is necessary to enhance the rate of acetol formation, as the reaction intermediate, which would improve both conversion of glycerol and 1,2-PDO selectivity. As the temperature increased, acetol was formed with considerable selectivity which requires $H_2$ for the hydrogenation to 1,2-PDO.

It appears that higher temperatures promote more by-product formation. Therefore, the reaction should be carried out at lower temperatures, similar to that reported in the literature [18]. However, with Cu/ZnO [6], the selectivity of 1,2-PDO increased sharply from 16% to 81% when the temperature increased from 180 to 220

°C and then decreased to 59% when the temperature further increased to 240 °C. The temperature effect in this system was explained by the change on the rates of intrinsic adsorption/desorption of the reaction intermediates on ZnO and Cu surfaces. Lower temperatures favour strong adsorption of intermediates leading to a high possibility of decomposition, while higher temperatures favour the desorption and also the breaking of C-C and C-O bonds leading to more EG and 1,2-PDO [6]. The optimal operating temperature in copper-chromite and related copper-based catalytic system for 1,2-PDO synthesis from glycerol in liquid phase was found in the range of 200-220 °C, whereas the Ru-based catalytic systems favour considerably lower temperatures, 150-180 °C. This suggests that the reaction, in these systems, may obey different reaction routes that involve different reaction intermediates.

Table 4.1 demonstrates that the catalyst turnover frequency (TOF) is 21 $h^{-1}$, as estimated from the Ru dispersion. 5%Rh/CsPW catalyst was found considerably less active than the 5%Ru/CsPW catalyst (Table 4.1). The TOF value for the Rh catalyst is 28 times lower that that for the Ru catalyst at 180 °C. However, the Rh catalyst was more selective to 1,3-PDO and 1-propanol (7.1% and 27.5% selectivity, respectively at 180 °C). The main product with the Rh catalyst was 1,2-PDO (65% selectivity), as with Ru catalyst (Table 4.1). No ethylene glycol was found, indicating that Rh in contrast to Ru was inactive in C–C bond cleavage. Similar results have been obtained by Miyazawa et al. [4]. In contrast to the Ru and Rh catalysts, 2%Pd/CsPW and 1%Pt/CsPW (not shown in Table 4.1) exhibited practically no activity in glycerol hydrogenolysis, confirming the literature results that clearly show the superior activity of Ru metal with different supports.

## 4.3 The effect of hydrogen pressure

In the hydrogenolysis of glycerol to propanediols, it is well known that hydrogen is necessary for the hydrogenation of intermediates such as acetol and 3-hydroxypropanal to form propanediols. It indicates that the addition of hydrogen would increase the yield of propanediols.

Figure 4.2 shows the effect of the initial hydrogen pressure on glycerol conversion and product selectivity for the reaction over Ru/CsPW. Unexpectedly, in contrast to other catalysts such as Ru/C + Amberlust-15 [4, 5], copper chromite [3], Cu:Al [19], $Cu/Al_2O_3$ [20] and Co/MgO [17], the conversion of glycerol over Ru/CsPW instead of a monotonous growth passes a maximum at 5 bar $H_2$ pressure. The selectivity to ethylene glycol exhibits a similar trend, whereas the selectivity to acetol decreases monotonously with increasing $H_2$ pressure. The decrease in acetol selectivity can be explained by the facile hydrogenation of acetol at higher $H_2$ pressure 1,2-PDO resulting in an increase of 1,2-PDO selectivity. The lower selectivity of EG at high $H_2$ pressure was also reported [4]. The decrease in catalyst activity above 5 bar $H_2$ pressure may be explained by the reduction of tungsten (VI) in CsPW which could lead to a decrease in catalyst acidity [13, 21]. The reduction of W (VI) under reaction conditions was observed by the presence of tungsten blues at higher $H_2$ pressures after the reaction and once it is exposed to air, re-oxidation of W (IV) takes place.

Regardless of the decline in the activity of Ru/CsPW catalyst due to catalyst deactivation at high hydrogen pressure, it is widely accepted that the conversion of glycerol increases with the increased availability of $H_2$. Similar trends have been reported for 1,2-PDO selectivity such as with copper-chromite catalyst [3]. A small

effect on 1,2-PDO selectivity at higher $H_2$ pressures has been observed in some cases, for example: Ru/C [4, 15], Ni/NaX [22], $Cu/Al_2O_3$ [20] and Cu:Al [19].

**Table 4.2** The effect of $H_2$ pressure on glycerol hydrogenolysis.

| $H_2$ (bar) | Conversion (%) | Selectivity (%) | | | | | |
|---|---|---|---|---|---|---|---|
| | | 1,2-PD | 1,3-PD | Acetol | 1-PO | EG | 2-PO |
| 3 | 14 | 77 | 0 | 7 | 3 | 12 | 0 |
| 5 | 24 | 72 | 0 | 3 | 4 | 15 | 3 |
| 7.5 | 20 | 81 | 1 | 0 | 4 | 12 | 0 |
| 14 | 9 | 90 | 0 | 0 | 9 | 0 | 0 |

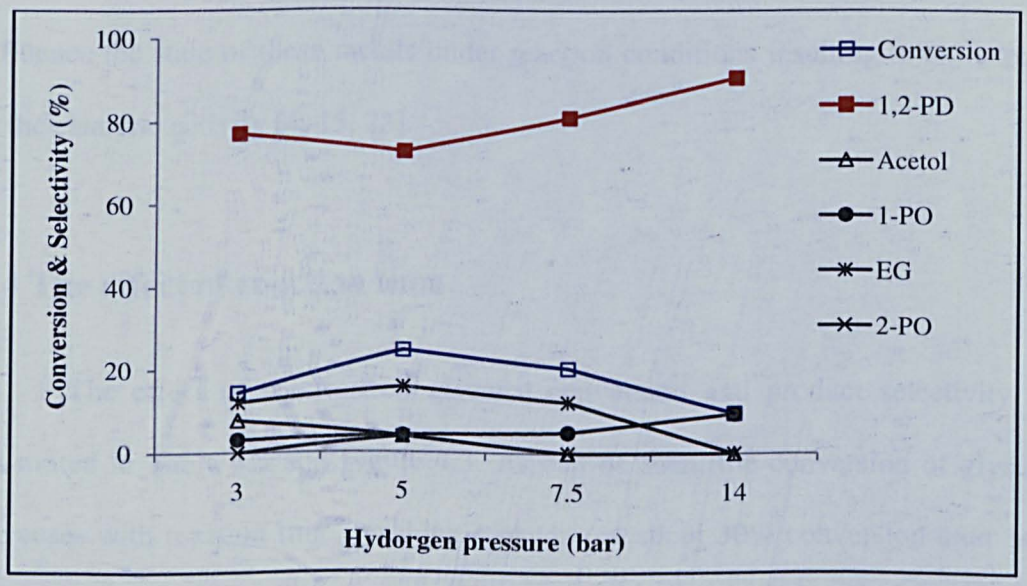


**Figure 4.2** The effect of $H_2$ pressure on glycerol hydrogenolysis (5 mL 20 wt% glycerol aqueous solution, 180°C, 10 h, 0.2 g of Ru/CsPW).

In this study, as Figure 4.2 illustrates, after the maximum conversion of glycerol was reached, at 5 bar of $H_2$, the selectivity to 1,2-PDO increased from 74% to 90% as $H_2$ pressure further increased to 14 bar but with a low glycerol conversion of 10%, compared to 23% at 5 bar $H_2$. The selectivity to 1-PO slightly increased at pressures higher than 5 bar.

When $H_2$ pressure increased beyond the optimum values, at which the best selectivity of 1,2-PDO was achieved, the selectivity to 1,2-PDO decreased along with increasing lower alcohols (1-PO, 2-PO) selectivity, in particular 1-PO [15]. This indicates that a further hydrogenolysis of 1,2-PDO may occur at high $H_2$ pressure.

The increased activity of a catalyst at higher $H_2$ pressure might be due to an increase in $H_2$ concentration in the liquid phase which would increase acetol and/or 3-hydroxypropanal hydrogenation to 1,2- and 1,3-PDO driving the overall reaction equilibrium toward the side of propanediol formation. As metals such as Ru, Cu, Rh play a key role in the hydrogenolysis process, hydrogen may also positively influence the state of these metals under reaction conditions resulting in an increase in the catalytic activity [4, 15, 23].

## 4.4 The effect of reaction time

The effect of reaction on glycerol conversion and product selectivity are illustrated in Table 4.3 and Figure 4.3. As can be seen, the conversion of glycerol increases with reaction time, reaching a plateau at about 30% conversion after 14 h (Figure 4.3). This may be due to the abovementioned catalyst deactivation. The product selectivity depends weakly on the reaction time. Likewise, with $Cu/Al_2O_3$ catalyst, the selectivity toward 1,2-PDO remained constant with time, irrespective of the remarkable increase in the conversion [20]. In contrast, little improvements in the selectivity trend with respect to reaction time have been reported for a number of catalysts, including $Ru/Al_2O_3 + Re_2(CO)_{10}$ [16], $Ru/C + Nb_2O_5$ [24] and Ni/NaX [22]. However, a slight decrease in the selectivity of 1,2-PDO at longer reaction times has been observed over Ni/NaX [22] suggesting that the decomposition of 1,2-PDO my take place [22].

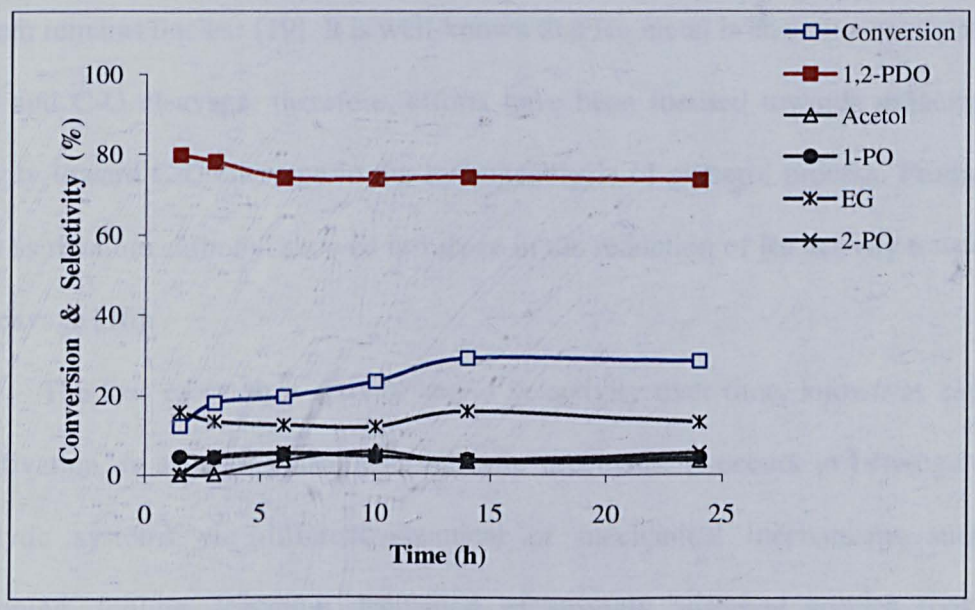


**Figure 4.3** The effect of reaction time on glycerol hydrogenolysis (5 mL 20% glycerol aqueous solution, 180 °C, 5 bar $H_2$, 0.2 g of Ru/CsPW).

**Table 4.3** The effect of reaction time on glycerol conversion and product selectivity.

| Time (h) | Conversion (%) | Selectivity (%) | | | | |
|---|---|---|---|---|---|---|
| | | 1,2-PDO | Acetol | 1-PO | EG | 2-PO |
| 1.5 | 12 | 79 | 0 | 4 | 15 | 0 |
| 3 | 18 | 78 | 0 | 4 | 13 | 4 |
| 6 | 19 | 73 | 3 | 5 | 12 | 5 |
| 10 | 23 | 73 | 5 | 4 | 11 | 4 |
| 14 | 29 | 74 | 3 | 3 | 15 | 3 |
| 24 | 28 | 73 | 3 | 4 | 13 | 5 |

It should be noted that 1,2-PDO and ethylene glycol form in parallel rather than consecutive reactions (Figure 4.3), suggesting that the ethylene glycol mainly forms by the cleavage of C–C bond in glycerol or 1,2-PDO precursors rather than in 1,2-PDO itself. Similar results have been obtained with Ru/C + $Nb_2O_5$ [24] and Ni/NaX [22]. On the other hand, over $Ru/Al_2O_3$ [16], EG selectivity decreased with time in the presence of $Re_2(CO)_{10}$ as a promoter. It was also reported that increasing

the amount of $Re_2(CO)_{10}$ greatly decreased the EG selectivity. The role of Re in this system remains unclear [19]. It is well-known that Ru metal is an active candidate for C-C and C-O cleavage; therefore, efforts have been focused towards reducing Ru activity toward C-C cleavage in the hydrogenolysis of glycerol process. Promoters, such as rhenium carbonyl showed influence in the reduction of Ru activity toward C-C cleavage [16].

The loss of catalyst activity and/or selectivity over time, known as catalyst deactivation, is a major concern in catalytic processes. It occurs in heterogeneous catalytic systems via different chemical or mechanical mechanisms such as poisoning, fouling, leaching, deposition of strongly adsorbed species (coking), sintering etc. [25, 26]. In our study, as Figure 4.3 shows, no further increase in glycerol conversion over time which indicates that there is a deactivation of probably both, the acidic support (CsPW) and the metal (Ru). Deactivation of solid heteropoly acid catalysts during liquid and gas phase organic reactions because of the formation of carbonaceous deposit (coke) on the catalyst surface is well known [27, 28].

The TGA/TPO analysis of 5%Ru/CsPW spent in the liquid phase (Figure 3.4) shows no combustion peak in temperature range 350-650 °C which indicates that coke, as a deactivation cause, was not probably formed during the reaction. Therefore, the cause of catalyst deactivation in our catalytic system is probably the heat (180 °C) and water treatment (wt 94%) which Ru/CsPW catalyst encountered during 10 h reaction time. The BET surface area of the spent 5%Ru/CsPW was reduced by 40%. Also, FTIR pyridine adsorption spectrum of spent Ru/CsPW (Figure 3.40) shows considerable reduction in the intensity of band Brønsted acid sites bands of CsPW at 1540 $cm^{-1}$, These results confirm the reduction of surface acidity of catalysts under reaction conditions. This is in agreement with the result

reported by Nakato et al. which state that the surface area, pore structure and the acidity of CsPW are influenced by heat (120 °C) and water treatment (wt 92%) [29]. The leaching of heteropoly anions from CsPW catalyst under reaction condition was reported in Chapert 3.5, which could be another possible reason for catalyst deactivation. The deactivation of Ru metal by sintering, deposition of inactive species or impurities is likely [25], although no investigation was carried out for Ru in spent 5%Ru/CsPW.

## 4.5 The effect of glycerol concentration

In the liquid-phase hydrogenolysis of glycerol, it is always preferable to eliminate water from the reaction system to drive the equilibrium toward the propanediol formation as the initial step is expected to be the dehydration of glycerol to reaction intermediates, acetol and/or 3-hydroxypropanal. Additionally, large amounts of energy are necessary for the removal of water by distillation for propanediols isolation. The effects of glycerol concentration on the conversion of glycerol and product distribution tend to vary according to the catalytic system and reaction conditions.

Table 4.4 and Figure 4.4 provide a summary of the effect of glycerol concentration on glycerol conversion and product selectivity using 5%Ru/CsPW catalyst. As can be seen in Figure 4.4, the conversion of glycerol decreased with increasing glycerol concentration in the reaction mixture. The 1,2-PDO selectivity remains practically constant within the glycerol concentration range from 5 to 50 wt%, slightly decreasing at higher glycerol concentrations, with a simultaneous increase in selectivity to 1-propanol. The selectivity to acetol increased with glycerol concentration reaching 8% at 80% glycerol concentration. This can be explained by the more favourable equilibrium for acetol formation at a lower water concentration.

It should be underlined that the decrease in glycerol conversion with increasing glycerol concentration over Ru/CsPW catalyst is in accordance with literature findings, particularly, over bifunctional catalytic systems such as Ru/C + Amberlyst [4], $Rh/SiO_2$ [15, 30], Ru/C + $Nb_2O_5$ [24] and Co/MgO [17]. The selectivity of 1,2-PDO was almost unchanged over these catalysts. It can be implied that the conversion of glycerol is dependent on the number of available catalytic active sites [17, 24]. However, in the case of using $Ru/Al_2O_3$ catalyst [31], there was almost no change in the conversion of glycerol, but an increase in 1,2-PDO selectivity was observed with the glycerol concentration increasing from 10 wt% to 40 wt%. In contrast, glycerol conversion increased with an increase in glycerol concentration when rhenium carbonate was present in the catalytic system [31]. It has been observed that the optimum glycerol concentration in terms of both conversion and product yields is in range of 10-40 wt%. For Ru/CsPW, 20wt% glycerol aqueous solution was chosen for further investigation.

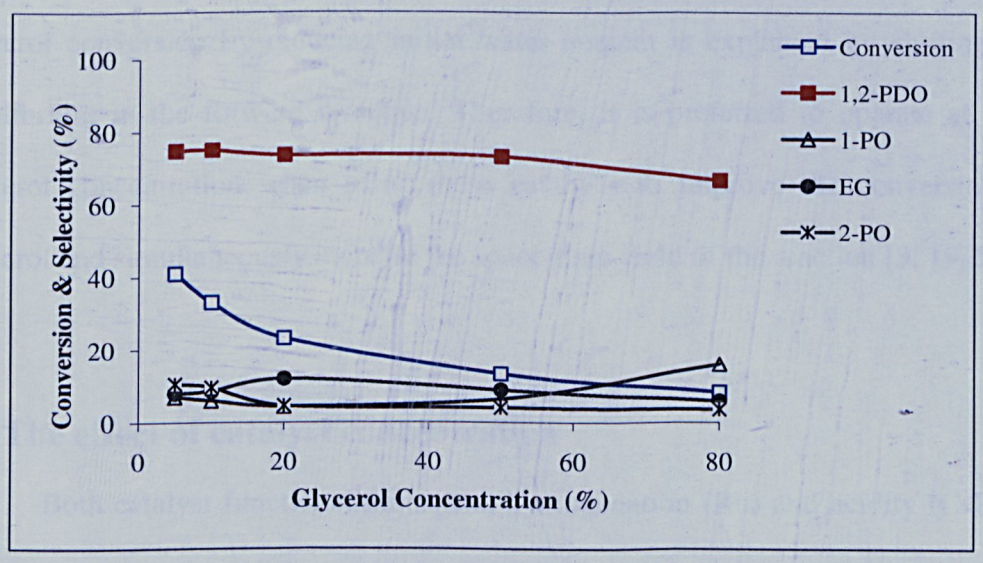


**Figure 4.4** The effect of glycerol concentration on glycerol hydrogenolysis (180 °C, 5 bar $H_2$, 10 h, 0.2 g of Ru/CsPW).

**Table 4.4** The effect of glycerol concentration on glycerol conversion and product selectivity.

| Glycerol concentration (wt%) | Conversion (%) | Selectivity (%) | | | | |
|---|---|---|---|---|---|---|
| | | 1,2-PDO | Acetol | 1-PO | EG | 2-PO |
| 5 | 40 | 75 | 0 | 7 | 7 | 11 |
| 10 | 33 | 76 | 0 | 6 | 8 | 10 |
| 20 | 23 | 74 | 6 | 4 | 11 | 5 |
| 50 | 13 | 73 | 7 | 7 | 8 | 5 |
| 80 | 8 | 66 | 9 | 15 | 5 | 5 |

In contrast, copper-containing catalysts demonstrated different performance in terms of conversion and selectivity with increasing glycerol concentration. Both glycerol conversion and 1,2-PDO yield presented a significant increase when glycerol concentration increased from 10 to 100% over copper-chromite [3], $Cu/Al_2O_3$ [20] and Cu-Al [19]. A decline in glycerol conversion beyond 60 wt% was detected over nano Cu-Al catalyst [19]. It should be noted that the reaction mechanism for glycerol hydrogenolysis using copper-containing catalysts was validated via dehydration step to form acetol intermediate. Therefore, the increase in glycerol conversion by reducing initial water content is explained by shifting the equilibrium in the forward direction. Therefore, it is preferred to operate at high glycerol concentration when using these catalysts to improve the conversion of glycerol and simultaneously increase the space-time yield of the reaction [3, 19, 20].

## 4.6 The effect of catalyst concentration

Both catalyst functionalities, metal hydrogenation (Ru) and acidity (CsPW), are essential for the efficiency of the Ru/CsPW catalyst, acting synergistically in glycerol hydrogenolysis to yield 1,2-PDO. Without ruthenium, CsPW is not active. In the absence of CsPW, ruthenium (e.g. Ru/C) exhibits some activity in 1,2-PDO

formation [4, 5]. Doping ruthenium with CsPW greatly enhances its activity in this reaction. These results suggest that sufficient amounts of both acid and metal catalysts are required to achieve the optimum conversion and selectivity.

To examine the effect of 5%Ru/CsPW amount on the conversion of glycerol and the selectivity of 1,2-PDO, we carried the reaction by changing both the catalyst content at 150 and 180 °C, 5 bar of $H_2$, 10 h and 5 mL glycerol aqueous solution; the results are shown in Table 4.5 and Figures 4.5 and 4.6. It was found that the conversion of glycerol increased with respect to an increase in catalyst loading from 4 to 15 wt% at 180 °C (Figure 4.5). At 150 °C, the conversion reached a maximum value (31%) when 6 wt% of catalyst was used. This result indicates that lowering reaction temperature along with increasing catalyst amount could improve the operation at milder reaction conditions. The positive effect of increasing catalyst amount on glycerol conversion was also reported previously [3, 4, 14, 19, 20, 24]. This result can be explained by the increase in the number of active sites available for the reaction as the catalyst amount increases.

As regards the 1,2-PDO selectivity (Figure 4.5), at 180 °C, the selectivity remained almost unchanged (73%) while at 150 °C (Figure 4.6) a small decrease (from 95% to 80%) was observed. This could probably be understood in terms of acetol formation, at 180 °C, more acetol was formed as glycerol conversion increases and, therefore, more subsequently hydrogenation to 1,2-PDO took place. However, at 150 °C, as the conversion remained constant no more acetol was formed resulting in more 1-PO which is expected to form from further hydrogenolysis of 1,2-PDO.

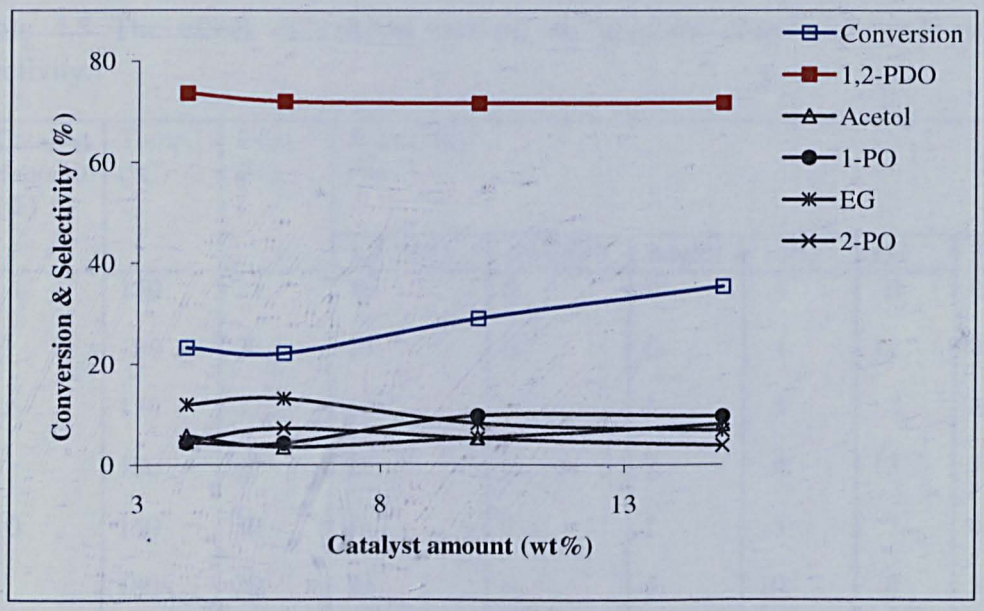


**Figure 4.5** The effect of catalyst amount on glycerol conversion and product selectivity (5 bar of $H_2$, 180°C, 5 mL of 20% glycerol, 10 h).

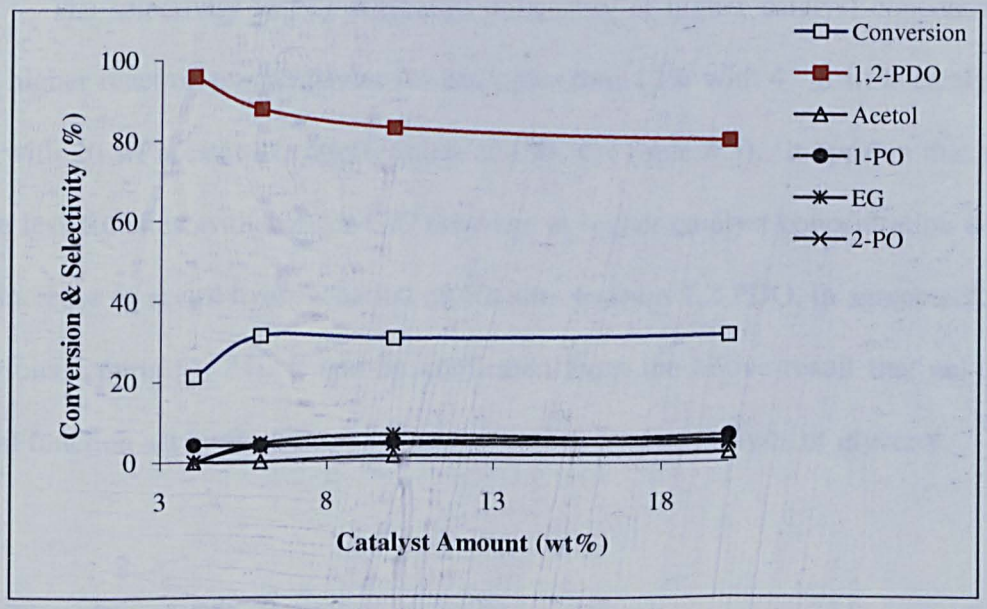


**Figure 4.6** The effect of catalyst amount on glycerol conversion and product selectivity (5 bar of $H_2$, 150°C, 5 mL of 20% glycerol aqueous solution, 10 h).

**Table 4.5** The effect of catalyst amount on glycerol conversion and product selectivity.

| Catalyst amount (%) | Temp. (°C) | Conv. (%) | Selectivity (%) | | | | | |
|---|---|---|---|---|---|---|---|---|
| | | | 1,2-PDO | 1,3-PDO | Acetol | 1-PO | EG | 2-PO |
| 4 | 150 | 21 | 96 | 0 | 0 | 4 | 0 | 0 |
| | 180 | 23 | 74 | 0 | 6 | 4 | 12 | 4 |
| 6 | 150 | 31 | 87 | 0 | 0 | 5 | 4 | 4 |
| | 180 | 22 | 73 | 0 | 3 | 4 | 13 | 7 |
| 10 | 150 | 30 | 83 | 0 | 1 | 5 | 7 | 4 |
| | 180 | 29 | 72 | 0 | 5 | 10 | 8 | 5 |
| 20 | 150 | 31 | 80 | 0 | 3 | 7 | 5 | 5 |
| 15 | 180 | 35 | 72 | 0 | 8 | 9 | 7 | 4 |

The selectivity to EG decreased noticeably at higher catalyst concentration and higher reaction temperatures, for example from 12% with 4 - 6 wt% catalyst to 6% with 20 wt% catalyst concentration at 180 °C (Table 4.5). It appears that there were less Ru sites available for C-C cleavage at higher catalyst concentration due to the increase of acetol hydrogenation on Ru sites to form 1,2-PDO, in agreement with previous reports [4, 24]. It can be confirmed from the above result that acid and metal function act synergistically in a bifunctional hydrogenolysis of glycerol.

## 4.7 The effect of Ru loading

Ruthenium has demonstrated a critical function in the catalytic process of glycerol hydrogenolysis to propanediols. Many attempts have been made to understand the role of Ru in the hydrogenolysis process. Ru has been involved in the hydrogenation of acetol, the proposed reaction intermediate, to the desirable 1,2-PDO [4]. In this study, CsPW was inactive itself indicating that Ru plays a key role

in the initial step of the hydrogenolysis reaction using Ru/CsPW. To gain insight into the effect of Ru loading on the conversion of glycerol and product selectivity, the reaction was carried out using different Ru loadings under our optimum reaction conditions (5 bar, 180 °C, 10 h, 5 mL 20 wt% glycerol aqueous solution). The results are given in Table 4.6 and Figure 4.7.

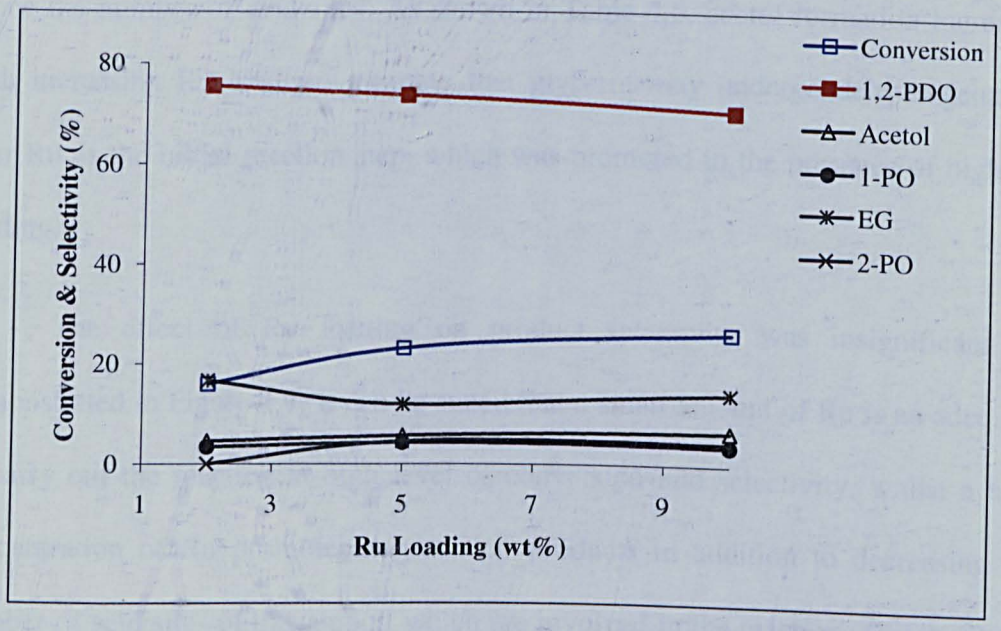


**Figure 4.7** The effect of Ru loading on glycerol conversion and product selectivity (5 bar of $H_2$, 180°C, 5 mL of 20% glycerol aqueous solution, 10 h, 0.2 g catalyst).

**Table 4.6** The effect of Ru loading on glycerol conversion and product selectivity.

| Ru (%) | Conversion (%) | Selectivity (%) | | | | |
|---|---|---|---|---|---|---|
| | | 1,2-PDO | Acetol | 1-PO | EG | 2-PO |
| 2 | 16 | 75 | 4 | 3 | 16 | 0 |
| 5 | 23 | 73 | 6 | 4 | 12 | 4 |
| 10 | 26 | 70 | 7 | 4 | 14 | 4 |

As can be seen in Figure 4.7, the conversion of glycerol increased with an increase in metal content up to 10 wt%. This is consistent with what was previously stated with the Ru/C catalyst [4, 24]. Although with the Ru/C catalyst, the increase in the conversion was larger. This difference could be due to the constant content of acid, Amberlyst or $Nb_2O_5$, used in a combination with the Ru/C system. In our case however, increasing the loading of Ru-doped CsPW decreased the surface area and hence the number of acid sites. As shown in Table 4.6, acetol formation increased with increasing Ru loading, meaning that glycerol may undergo dehydrogenation over Ru as the initial reaction step, which was promoted in the presence of high Ru loading.

The effect of Ru loading on product selectivity was insignificant, as demonstrated in Figure 4.7. It can be stated that a small amount of Ru is an adequate to carry out the reaction at high level of conversion and selectivity, whilst a high concentration of Ru promotes degradation products in addition to decreasing the number of acid sites of the support which are involved in the reaction. This results in a lack of improvement in the overall reaction conversion and selectivity. Moreover, using a high concentration of metals usually leads to the formation of bigger particles and hence low metal dispersion. Therefore, the ratio of Ru to CsPW should be optimised to achieve a higher selectivity of the propanediols. In this study, 5 wt% of Ru has been found to be the optimum loading with respect to glycerol conversion and product selectivity.

## 4.8 The effect of pH

The effect of pH on the reaction of glycerol hydrogenolysis to propanediols has been reported [4, 6, 7]. According to Montassier et al. [9, 32] as discussed in Section 1.1.6, the first step in the reaction of glycerol over a transition metal catalyst is the dehydrogenation of glycerol to form glyceraldehyde intermediate. In this mechanism, the cleavage of C–C bonds is proposed to occur through a base-catalysed retro-aldol reaction, whereas C–O cleavage occurs through a base-catalysed dehydration reaction. This suggestion was supported later by Wang et al. [33] through investigating the hydrogenolysis of 1,3-diol model compounds. Therefore, the addition of base should increase the conversion of glycerol to both EG and 1,2-PDO because the retro-aldol and dehydration reactions are both catalysed by the adsorbed hydroxyl.

Davis et al. [7] have found that both NaOH and CaO addition enhanced the rate of glycerol hydrogenolysis over Ru/C and Pt/C. However the extent of enhancement is greater over Pt/C than Ru/C. This result is consistent with the speculation mentioned earlier. In the absence of base, Ru/C was more active than Pt/C for the hydrogenolysis of glycerol. Under neutral conditions, Ru favors the formation of ethylene glycol over propylene glycol. Because the rate of ethylene glycol formation was not enhanced significantly in the presence of base, C–C cleavage is thought to occur over Ru primarily via a metal-catalysed reaction instead of base-catalysed. 1,2-PDO formation however, could occur through two possible routes: (1) metal-catalysed and (2) base-catalysed. These results reported by Davis et al. stated the effect of pH conditions on the rate of hydrogenolysis reaction as well as reaction routes.

Liu et al. [6] has claimed that increasing pH values for the reaction solution increases glycerol conversion and 1,2-PDO and EG selectivity. The effect of pH was not due to related to the reaction pathways but to the effect on the catalyst structure because at higher pH values smaller particles are formed.

In our study, $H_2SO_4$ and NaOH were used to adjust the pH of the reaction solution, in order to explore the pH effect on glycerol conversion and product selectivity over Ru/CsPW. After reaction, the pH was neutral. The results are shown in Table 4.8 and Figure 4.7. The maximum conversion of glycerol was achieved at neutral conditions, inconsistent with that reported by Liu [6] and Davis [34]. Under neutral conditions, EG formation was higher, whereas no EG was observed at pH 12 and 2. Comparable conversion of glycerol was obtained under acidic and basic conditions. Tomishige et al. [4] compared the activity of Ru/C + $H_2SO_4$ and Ru/C + Amberlyst and found that the Ru/C + $H_2SO_4$ combination gave much lower conversion of glycerol than that of the Ru/C + Amberlyst. Our result showed a similar trend where Ru/CsPW was more active without $H_2SO_4$ addition. As CsPW itself was not active, the initial step of glycerol hydrogenolysis over Ru/CsPW catalyst may take place over Ru. As result, the presence of protons in solution may reduce the possibility of reactant (glycerol and hydrogen) adsorption on Ru sites and hence decrease glycerol conversion. C-C cleavage is well known to occur over Ru and the absence of EG in basic and acidic conditions further supports the reduction of Ru activity under such conditions.

**Table 4.7** The effect of pH on glycerol conversion and product selectivity.

| pH | Conversion (%) | Selectivity (%) | | | | |
|---|---|---|---|---|---|---|
| | | 1,2-PDO | Acetol | 1-PO | EG | 2-PO |
| 2 | 11 | 100 | 0 | 0 | 0 | 0 |
| 6 | 23 | 74 | 3 | 5 | 12 | 6 |
| 12 | 11 | 96 | 0 | 4 | 0 | 0 |

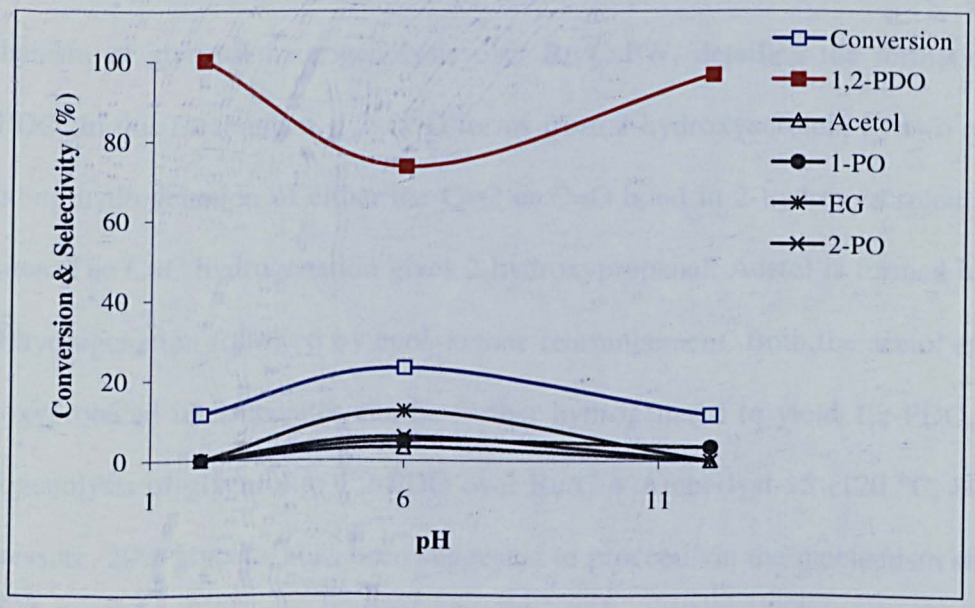


**Figure 4.8** The effect of pH on glycerol conversion and product selectivity (5 bar of $H_2$, 180°C, 10 hrs and 5 mL of 20% glycerol aqueous solution).

## 4.9 Reaction mechanism over Ru/CsPW

Both catalyst functionalities, metal hydrogenation (Ru) and acidity (CsPW), are essential for the efficiency of Ru/CsPW catalyst, acting synergistically in glycerol hydrogenolysis to yield 1,2-PDO. Without ruthenium, CsPW is not active. In the absence of CsPW, ruthenium (e.g. Ru/C, $Ru/SiO_2$, $Ru/Al_2O_3$, $Ru/ZrO_2$) exhibits good activity in 1,2-PDO formation [4, 7, 16, 24, 34, 35]. Supporting ruthenium on the CsPW greatly enhances its activity in this reaction.

Regarding the reaction mechanism, the absence of acetol amongst the products when the reaction is carried out with CsPW without Ru present, although does forms in the presence of Ru/CsPW (Table 4.1), is inconsistent with the mechanism of 1,2-PDO formation presented in Scheme 4.1. The alternative mechanism shown in Scheme 4.2 is, therefore, more likely. The question is how does acetol form in the presence of Ru/CsPW? Scheme 4.2 shows the proposed mechanism of glycerol hydrogenolysis over Ru/CsPW, detailing the formation of 1,2-PDO. In this mechanism, 1,2-PDO forms from 2-hydroxyacrolein by two routes including hydrogenation of either the C=C or C=O bond in 2-hydroxyacrolein over Ru sites. The C=C hydrogenation gives 2-hydroxypropanal. Acetol is formed by the C=O hydrogenation followed by enol–ketone rearrangement. Both the acetol and 2-hydroxypropanal intermediates can be further hydrogenated to yield 1,2-PDO. The hydrogenolysis of glycerol to 1,2-PDO over Ru/C + Amberlyst-15 (120 °C, 80 bar $H_2$ pressure, 20% glycerol) has been suggested to proceed via the mechanism shown in Scheme 4.1[4, 5, 14], although only traces of acetol (0.01% yield) have been observed. It is conceivable that this reaction also occurs via Scheme 4.2 like in our case, and the negligible acetol yield may be due to the much higher $H_2$ pressure in this system.

In contrast, with copper-chromite catalyst (200 °C, 14 bar $H_2$, 80% glycerol), 1,2-PDO is evidenced to form via Scheme 4.1 (acetol route) because in this case acetol has been obtained with a high yield by interaction of glycerol with copper-chromite catalyst in the absence of $H_2$ and further selectively hydrogenated to 1,2-PDO [3, 36]. The formation of 1,2-PDO through acetol intermediate has been reported in all copper-containing catalysts reported so far in both liquid and gas phase processes [6, 19, 20, 37-40].

Amberlyst [4], CsPW (strong acid) and $TiO_2$ (moderate acid) [35] have shown almost no reaction, indicating that these solid catalysts themselves cannot catalyse the hydrogenolysis of glycerol, and the initial step is probably taking place over Ru metal. Ru itself has been considerably active with a large number of supports [16, 24, 35]. This result seems to be in agreement with that reported by Montassier et al. [9, 32, 41] and Davis et al. [7] where the hydrogenolysis of glycerol is initiated by the dehydrogenation of glycerol to glyceraldehyde over metal.

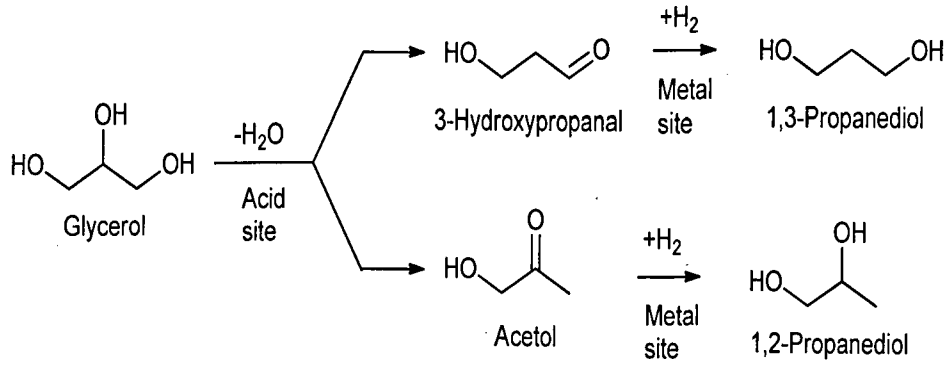


**Scheme 4.1** Hydrogenolysis of glycerol (dehydration + hydrogenation) to 1,2-PDO and 1,3-PDO.

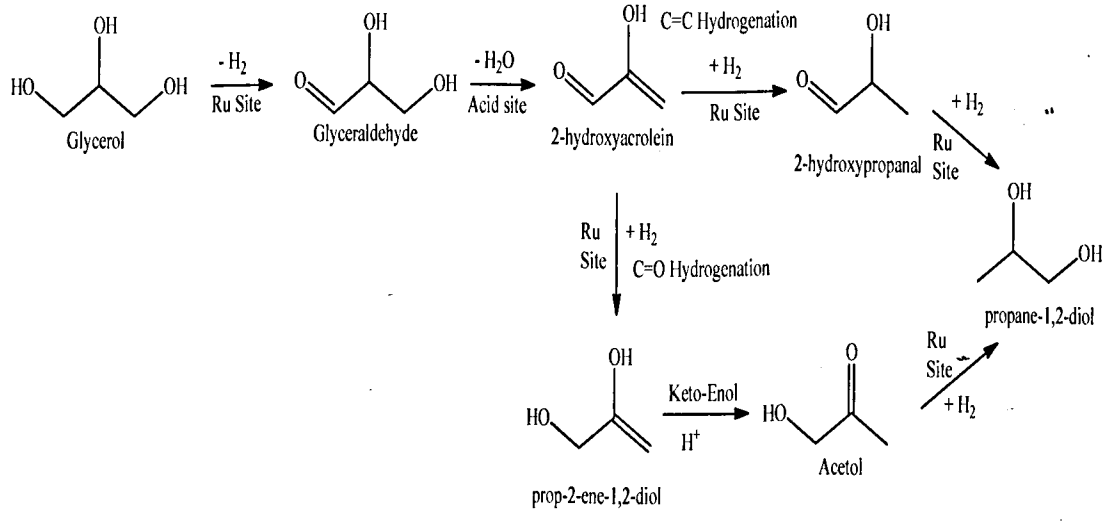


**Scheme 4.2** Hydrogenolysis of glycerol through dehydrogenation step over Ru/CsPW [32].

The presence of acetol as a reaction product over Ru/CsPW catalyst confirms also the role of acid CsPW in this reaction. This statement is consistent with the observation by others that the presence of solid acid greatly influences the conversion of glycerol during its hydrogenolysis over Ru metal. Tomishige et al. [14, 42] studied glycerol hydrogenolysis over Ru/C using different acids such as zeolites, $H_2WO_4$ and Amberlyst. They found remarkable enhancement in catalyst activity when the acidic Amberlyst was used. Moreover, Balaraju et al. [24] have proved the dependence of glycerol conversion on the total acidity of the catalysts involved and there exists a linear correlation between the conversion and the acidity.

Solid acid plays an additional major function in the formation of the desirable product. In our study, CsPW shows excellent selectivity to 1,2-PDO (Table 4.1). The reaction is speculated to occur in two parallel directions: (1) C-O cleavage, via dehydrogenation to glyceraldehyde to finally produce 1,2-PDO, (2) C-C cleavage resulting in EG as a by-product. The presence of strong solid acid catalysts promote the reaction route to 1,2-PDO. This can be seen by the low selectivity of EG (12%) with Ru/CsPW compared to (22%) with Ru/C in the absence of solid acid catalyst [4]. The addition of strong acidic resin, Amberlyst-15, increased glycerol conversion as well as decreasing EG selectivity from 22% to 13% [4]. Feng et al. [35] also reported that under a given condition, the support material can influence the reaction routes in the presence of a metal catalyst. Among tested catalysts, Ru/C, $Ru/Al_2O_3$, Ru/NaY and $Ru/TiO_2$ have exhibited considerably higher selectivity to EG [35], compared to our catalyst (Ru/CsPW) and Ru/C + Amberlyst [4] probably because of their weak acidity compared to CsPW and Amberlyst.

To investigate the reactivity of reaction products, 10 wt% aqueous solution of acetol, 1,2-PDO, 1,3-PDO and EG were tested separately under our optimum

reaction conditions, 5 bar $H_2$, 180 °C, 10 h, 0.2 g of 5 wt%Ru/CsPW. The results are shown in Table 4.8. As can be seen from Table 4.8, the order of the reactivity is: acetol > 1,3-PDO > EG > 1,2-PDO. This indicates that 1,2-PDO has the lowest reactivity, which explains the high selectivity of this product in glycerol hydrogenolysis. This is consistent with that observed with Ru/C + Amberlyst combination [4, 14]. 1,2- and 1,3-PDO are the primary products of glycerol hydrogenolysis, and the lower alcohols, 1-PO and 2-PO, are formed by the subsequent hydrogenolysis of propanediols. From Table 4.8, it can be noticed that 1-PO selectivity is much higher than 2-PO selectivity. Acetol is the most reactive molecule under given conditions producing mainly 1,2-PDO. This confirms the formation of 1,2-PDO from glycerol hydrogenolysis via acetol intermediate. EG has not been observed with 1,2- and 1,3-PDO hydrogenolysis confirming the formation of EG in glycerol hydrogenolysis in a parallel pathway directly from glycerol. Ethanol, methanol and methane were detected during the reaction of EG.

**Table 4.8** Reactivity test for glycerol hydrogenolysis products.

| **Reactant** | **Conversion** | **selectivity (%)** | | | | | |
|---|---|---|---|---|---|---|---|
| | **(%)** | **1,2-PDO** | **Acetol** | **1-PO** | **2-PO** | **MeOH** | **EtOH** |
| Acetol | 44 | 98 | 0 | 2 | 0 | 0 | 0 |
| 1,2-PDO | 7 | 0 | 11 | 58 | 31 | 0 | 0 |
| 1,3-PDO | 30 | 0 | 0 | 72 | 27 | 0 | 0 |
| EG[a] | 20 | 0 | 0 | 0 | 0 | 15 | 45 |

a)There is a loss in mass balance due to gases formed during EG reaction.

Reaction conditions: 10 wt% aqueous solution of reactant, 5 bar $H_2$, 180 °C, 10 h, 0.2 g of 5 wt%Ru/CsPW.

## 4.10 Conclusions

Ruthenium supported on the heteropoly salt $Cs_{2.5}H_{0.5}PW_{12}O_{40}$ was studied as a bifunctional catalyst for the hydrogenolysis of glycerol under mild conditions. 1,2-propanediol was obtained with 96% selectivity at 21% conversion at 150 °C and low hydrogen pressure of 5 bar. The effects of reaction temperature, glycerol concentration, hydrogen pressure, reaction time, catalyst amount, pH and Ru loading have been established in order to arrive at the optimum conditions, which were 150 °C, 10 h, 0.2 g catalyst, 5 mL 20% glycerol aqueous solution. Catalyst deactivation particularly above 5 bar $H_2$ was observed which could probably be explained by the reduction of tungsten (VI) in CsPW. Leaching of polyanions in the reaction media may also be another cause of catalyst deactivation. 5%Rh/CsPW catalyst was found considerably less active than the 5%Ru/CsPW catalyst. However, the Rh catalyst was more selective to 1,3-PDO and 1-propanol. The main product with the Rh catalyst was 1,2-PDO (65% selectivity), as with Ru catalyst. No ethylene glycol was found, indicating that Rh in contrast to Ru was inactive in C–C bond cleavage.

Both functionalities, metal hydrogenation (Ru) and acidity (CsPW), are essential for the reaction to proceed. Without Ru, CsPW was inactive while Ru showed considerable activity in the absence of acidic support such as Ru/C. The absence of acetol amongst the products when the reaction is carried out with CsPW without Ru present, although it forms in the presence of Ru/CsPW, suggests that the reaction is more likely to proceed via glyceraldehyde intermediate by dehydrogenation of glycerol on Ru site. In this mechanism, 1,2-PDO forms from 2-hydroxyacrolein by two routes including hydrogenation of either the C=C or C=O bond in 2-hydroxyacrolein on Ru sites. The C=C hydrogenation gives 2-

hydroxypropanal. Acetol is formed by the C=O hydrogenation followed by enol–ketone rearrangement. Both acetol and 2-hydroxypropanal intermediates can be further hydrogenated to yield 1,2-PDO.

In the absence of hydrogen, acetol and 1,2-PDO were obtained in the presence of Ru-doped CsPW catalyst. In this system, $H_2$ was supplied by the liquid phase reforming of glycerol over Ru. Hydrogen was further consumed in the hydrogenation of acetol to form 1,2-PDO.

## References


[1] A. Strivastava, R. Prasad, Renwable Sustainable Energy Rev. 4 (2000) 111.

[2] J. Chaminand, L. Djakovitch, P. Gallezot, P. Marion, C. Pinel, C. Rosier, Green Chem. 6 (2004) 359.

[3] M. A. Dasari, P. P. Kiatsimkul, W. R. Sutterlin, G. J. Suppes, Appl. Catal. A. 281 (2005) 225.

[4] T. Miyazawa, Y. Kusunoki, K. Kunimori, K. Tomishige, J. Catal. 240 (2006) 213.

[5] T. Miyazawa, S. Koso, K. Kunimori, K. Tomishige, Appl. Catal.A. 318 (2007) 244.

[6] S. Wang, H.C. Liu, Catal. Lett. 117 (2007) 62.

[7] E. P. Maris, R. J. Davis, J. Catal. 249 (2007) 328-337.

[8] K. Weissermel, H.-J. Arpe, Industrial Organic Chemistry Wiley-VCH, 1997.

[9] C. Montassier, J. C. Menezo, L. C. Hoang, C. Renaud, J. Barbier, J. Mol. Catal. 70 (1991) 99.

[10] A. Bruggink, R. Schoevaart, T. Kieboom, Org. Process Res. Dev. 7 (2003) 622.

[11] T. Okuhara, N. Mizuno, M. Misono, Adv. Catal. 41 (1996) 113.

[12] I. V. Kozhevnikov, Chem. Rev. 98 (1998) 171.

[13] I. V. Kozhevnikov, Catalysts For Fine Chemical Synthesis, Catalysis by Polyoxometalates Wiley 2002.

[14] T. Miyazawa, S. Koso, K. Kunimori, K. Tomishige, Appl. Catal. A. 329 (2007) 30.

[15] I. Furikado, T. Miyazawa, S. Koso, A. Shimao, K. Kunimori, K. Tomishige, Green Chem. 9 (2007) 582.

[16] L. Ma, D.H. He, Z.P. Li, Catal. Commun. 9 (2008) 2489.

[17] X. H. Guo, Y. Li, R. J. Shi, Q. Y. Liu, E. S. Zhan, W. J. Shen, Appl. Catal.A. 371 (2009) 108.

[18] C. W. Chin, A. Tekeei, J. M. Ronco, M. L. Banks, G. J. Suppes, Ind. Eng. Chem. Res. 47 (2008) 6878.

[19] R. B. Mane, A. M. Hengne, A. A. Ghalwadkar, S. Vijayanand, P. H. Mohite, H. S. Potdar, C. V. Rode, Catal. Lett. 135 (2010) 141.

[20] L. Y. Guo, J. X. Zhou, J. B. Mao, X. W. Guo, S. G. Zhang, Appl. Catal. A. 367 (2009) 93.

[21] M. T. Pope, Heteropoly and Isopoly Oxometalates, (1983) ed., Springer, Berlin.

[22] J. Zhao, W. Q. Yu, C. Chen, H. Miao, H. Ma, J. Xu, Catal. Lett. 134 (2010) 184.

[23] C. Montassier, J.M. Dumas, P. Granger, J. Barbier, Appl. Catal. A. 121 (1995) 231.

[24] M. Balaraju, V. Rekha, P. S. S. Prasad, B. L. A. P. Devi, R. B. N. Prasad, N. Lingaiah, Appl. Catal. A. 354 (2009) 82.

[25] M. Besson, P. Gallezot, Catal. Today. 81 (2003) 547.

[26] C. H. Bartholomew, Appl Catal a-Gen. 212 (2001) 17-60.

[27] E. F. Kozhevnikova, J. Quartararo, I. V. Kozhevnikov, Appl. Catal.A. 245 (2003) 69.

[28] B. H. Jeong, J. S. Han, S. W. Ko, J. H. Lee, B. J. Lee, J. Ind. Eng. Chem. 13 (2007) 310.

[29] T. Nakato, M. Kimura, S. Nakata, T. Okuhara, Langmuir. 14 (1998) 319.

[30] Y. Shinmi, S. Koso, T. Kubota, Y. Nakagawa, K. Tomishige, Appl. Catal. B. 94 (2010) 318.

[31] L. Ma, D. H. He, Top. Catal. 52 (2009) 834.

[32] C. Montassier, D. Giraud, J. Barbier, Stud. Surf. Sci. Catal. 41 (1988) 165-170.

[33] K. Y. Wang, M. C. Hawley, T. D. Furney, Ind. Eng. Chem. Res. 34 (1995) 3766.

[34] E. P. Maris, W. C. Ketchie, M. Murayama, R. J. Davis, J. Catal. 251 (2007) 281.

[35] J. Feng, H. Y. Fu, J. B. Wang, R. X. Li, H. Chen, X. J. Li, Catal. Commun. 9 (2008) 1458.

[36] C. W. Chin, M. A. Dasari, G.J. Suppes, W. R. Sutterlin, AIChE J. 52 (2006) 3543.

[37] Z. Yuan, J. Wang, L. Wang, W. Xie, P. Chen, Z. Hou, X. Zheng, Bioresour. Technol. 101 (2010) 7088.

[38] J. Zheng, W. C. Zhu, C. X. Ma, Y. Z. Hou, W. X. Zhang, Z. L. Wang, Reaction Kinetics Mechanisms and Catalysis. 99 (2010) 455.

[39] S. Sato, M. Akiyama, R. Takahashi, T. Hara, K. Inui, M. Yokota, Appl. Catal. A. 347 (2008) 186.

[40] M. Akiyama, S. Sato, R. Takahashi, K. Inui, M. Yokota, Appl. Catal. A. 371 (2009) 60.

[41] C. Montassier, D. Giraud, J. Barbier, J. P. Boitiaux, Bull. Soc. Chim. Fr. (1989) 148.

[42] Y. Kusunoki, T. Miyazawa, K. Kunimori, K. Tomishige, Catal. Commun. 6 (2005) 645.

# 5. Liquid-phase hydrogenolysis of glycerol using Ru-doped $Nb_2O_5$

## 5.1 Introduction

Niobium-based materials have been widely employed as catalysts in numerous catalytic applications [1, 2]. There are various functions of niobium compounds in heterogeneous catalysis [1]. Niobic acid can be used as promoters, supports, and as unique solid acid catalysts [2, 3]. Niobic acid ($Nb_2O_5.nH_2O$) is known as a typical strong metal-support interacting (SMSI) oxide [4]. It has been used as a water-tolerant solid acid catalyst for various water-involving reactions, such as esterification, hydrolysis, dehydration, and hydration[2].

According to the reaction mechanism of the hydrogenolysis of glycerol to 1,2-PDO discussed in Sections 1.1.6 and 4.10, we can deduce that a solid bifunctional catalyst consisting of metal and acidic (or basic) functions would be an effective course to carry out the glycerol hydrogenolysis in one-pot system.

In the present investigation, Ru and Rh were supported on $Nb_2O_5$ using impregnation method. The reaction conditions, including temperature, pressure, time, glycerol concentration, were optimised in order to achieve the best catalyst activity that produces the most effective balance of glycerol conversion and propanediols selectivity.

## 5.2 Catalytic performance of $Ru/Nb_2O_5$ catalyst in liquid-phase hydrogenolysis of glycerol

The hydrogenolysis of glycerol was carried out using similar procedure described in Section 4.2. The catalytic performance of $Nb_2O_5$-based catalysts was tested in the hydrogenolysis of glycerol and the results are summarised in Table 5.1. $Ru/Nb_2O_5$ gave only 29% conversion and 69% 1,2-PDO selectivity. 1- and 2-propanol (PO), ethylene glycol (EG) and ethanol were among reaction by-products. At higher hydrogen pressures $Ru/Nb_2O_5$ was more active than Ru/CsPW, which is probably due to the limited stability of CsPW at elevated hydrogen pressures. It can be seen from Table 5.1 (entry 1,2 and 3) that the preparation procedures of $Nb_2O_5$ could affect the performance of the $Nb_2O_5$ catalysts. In-house made $Nb_2O_5$ showed higher catalytic activity than the commercial $Nb_2O_5$ (Table 5.1, entry 1 and 2). This can be explained by the low surface area ($S_{BET}$ = 1 $m^2/g$) of the commercial catalyst compared to the In-house made catalyst ($S_{BET}$ = 201 $m^2/g$). Another possible reason for the low activity of the commercial $Nb_2O_5$ catalyst is the reduced surface acidity which is essentially required for the bifunctional catalysis in glycerol hydrogenolysis.

With Ru doped commercial $Nb_2O_5$, significant amount of EG was formed, 42% of EG selectivity compared to 8% with the in-house made $Ru/Nb_2O_5$. As proposed in Section 4.4, the C-C breaking in glycerol hydrogenolysis process occurs over Ru in parallel with the hydrogenolysis route. As a result of the low acidity of $Ru/Nb_2O_5$ (commercial), the C-C breaking is facilitated over Ru, thus producing more EG. The calcination temperature of the in-house made $Nb_2O_5$ catalyst seemed to influence that catalytic activity of Ru-doped $Nb_2O_5$. $Ru/Nb_2O_5$ calcined at 500 °C exhibited lower catalytic activity than the catalyst dried at 100 °C. This is probably due to the reduction of surface acidity of $Nb_2O_5$ upon increasing the calcination

temperature, as reported in Section 1.3.2. With the reduction of $Nb_2O_5$ acidity, the selectivity to 1,2-PDO decreased and more EG was formed indicating that the conversion of glycerol to 1,2-PDO depends on the acidity of the catalyst. Comparing the results obtained using Ru/CsPW (Section 4.2) and results of $Ru/Nb_2O_5$ (Table 5.1) we can conclude that the order of catalyst activity in glycerol conversion is as follows: $Nb_2O_5$ (dried at 100 °C) > Nb2O5 (calcined at 500 °C) ≈ CsPW > CsSiW > $Nb_2O_5$ (commercial). In terms of 1,2-PDO selectivity, the following order was observed: CsPW > $Nb_2O_5$ (dried at 100 °C) ≈ CsSiW > $Nb_2O_5$ (calcined at 500 °C) > $Nb_2O_5$ (commercial). Although CsPW is known to possess stronger acidity than $Nb_2O_5$, the conversion of glycerol using Ru/CsPW is lower than with $Ru/Nb_2O_5$. This could be due to the higher total acidity (number of acid sites) of the $Nb_2O_5$ support. These results suggest that moderate acidity of catalyst is sufficient to obtain higher glycerol conversion, and that the total acidity plays a key role in the hydrogenolysis of glycerol. The influence of catalyst acidity on glycerol conversion indicates that the dehydration of glycerol occurs on acid sites to form acetol followed by hydrogenation on Ru sites. The presence of acetol as a reaction product in the absence of hydrogen proves the role of acid catalysts in this reaction. Reduction in catalyst acidity causes an increase in the formation of EG and other degradation products over Ru.

Balaraju et al. [5] investigated the effect of solid acids as co-catalysts on glycerol hydrogenolysis over Ru/C. $Nb_2O_5$ (CBMM Brazil), $H_3PW_{12}O_{40}$ (HPW) supported on zirconia ($ZrO_2$), $Cs_2HPW$, $CsPW/ZrO_2$ were used. The authors have found the following order of catalytic activity for these catalysts in glycerol hydrogenolysis: $Nb_2O_5$ (CBMM Brazil) > $HPW/ZrO_2$ > $Cs_2HPW$ > $CsPW/ZrO_2$. A linear relation between the acidity of these catalysts and the glycerol conversion was

observed. They suggest that the total acidity of the catalyst (acid site density) has greater influence on the overall conversion of glycerol than the acid strength. A synergistic effect between solid acids and Ru/C catalyst towards glycerol conversion and selectivity to 1,2-PDO was observed. The synergistic effect between acid/base and metal functions in the liquid phase hydrogenolysis of glycerol has also been reported with supported metal catalysts and acid co-catalysts [6-10].

**Table 5.1** Hydrogenolysis of glycerol in the liquid phase using $Ru/Nb_2O_5$ catalysts.

| Catalyst | Conv. (%) | Selectivity (%) | | | | | | |
|---|---|---|---|---|---|---|---|---|
| | | 1,2-PDO | Acetol | 1-PO | EG | 2-PO | EtOH | 1,3-PDO |
| 1) 5%Ru/ $Nb_2O_5$ | 29 | 69 | 0 | 12 | 8 | 2 | 7 | 0 |
| 2) 5%Ru/ $Nb_2O_5$[a] | 13 | 41 | 0 | 3 | 42 | 0 | 11 | 0 |
| 3) 5%Ru/ $Nb_2O_5$[b] | 24 | 65 | 0 | 2 | 25 | 2 | 4 | 0 |
| 4) 5%Rh/$Nb_2O_5$ | 17 | 61 | 0 | 21 | 6 | 0 | 6 | 3 |
| 5) 5%Ru/ $Nb_2O_5$[c] | 6 | 11 | 71 | 0 | 0 | 0 | 0 | 0 |
| 6) $Nb_2O_5$ | 1 | 0 | traces | 0 | 0 | 0 | 0 | 0 |
| 7) $Nb_2O_5$[d] | 5 | 73 | 0 | 27 | 0 | 0 | 0 | 0 |
| 8) Acetol[e] | 62 | 96 | 0 | 4 | 0 | 0 | 0 | 0 |

Reaction conditions: 180°C,10 h, 5 mL of 20 wt% glycerol solution, 10 bar of $H_2$, and 0.2 g catalyst. (a) commercial $Nb_2O_5$; (b) calcined $Nb_2O_5$ 500°C in air; (c) under 2 bar $N_2$ in the absence of $H_2$; (d) 5 bar $H_2$. (e) 5 wt% acetol aqueous solution at similar conditions.

5%Rh/$Nb_2O_5$ catalyst was found considerably less active than 5%Ru/$Nb_2O_5$ catalyst (Table 5.1). This is similar to that observed with Ru/CsPW, as mentioned in section 4.2. The Rh catalyst was more selective to 1,3-PDO and 1-propanol (4% and 21% selectivity, respectively at 180 °C). The main product with the Rh catalyst was 1,2-PDO (61% selectivity), as with Ru catalyst (Table 5.1). No ethylene glycol was

found, indicating that Rh in contrast to Ru was inactive in C–C bond cleavage. The promoting effect of Rh metal towards 1,3-PDO formation has been observed previously [8, 10]. The conversion of glycerol and 1,2-PDO selectivity have been found to depend on the reaction temperature, hydrogen pressure, reaction time and glycerol concentration. Therefore, a more detailed study of the optimum reaction conditions using 5%$Ru/Nb_2O_5$ catalyst was undertaken, and the results are shown and discussed in the following sections.

## 5.3 The effect of hydrogen pressure

The reaction mechanisms proposed for glycerol hydrogenolysis to propanediols along with empirical evidence have illustrated that the hydrogen pressure is vital for the hydrogenation of reaction intermediates such as acetol, 1,3-hydroxypropanal and glycidol to 1,2-PDO and/or 1,3-PDO [10-13]. The influence of $H_2$ on the hydrogenolysis of glycerol over 5%$Ru/Nb_2O_5$ was studied by carrying out the reaction at various pressures from 5 to 20 bar at constant temperature (180 °C) and reaction time (10 h). Figure 5.1 and Table 5.2 show the effect of hydrogen pressure on the hydrogenolysis of glycerol and product selectivity over $Ru/Nb_2O_5$.

It can be seen from Figure 5.1 and Table 5.2 that the glycerol conversion increased with increasing $H_2$ pressure up to 20 bar. The increased activity of $Ru/Nb_2O_5$ at high $H_2$ pressure demonstrates a better stability of this catalyst at high hydrogen pressure compared to Ru/CsPW. A maximum glycerol conversion of 40% was obtained at 20 bar. Some reported catalysts such as Ru/C + Amberlust-15 [14, 15], copper-chromite [11], Cu-Al nanocatalyst [16], $Cu/Al_2O_3$ [17] and Co/MgO [18] have shown similar performance $H_2$ pressure increase. The selectivity to 1,2-PDO decreased to some extent at high $H_2$ pressure, which is possibly due to the formation

of more EG and further hydrogenolysis of 1,2-PDO to generate more 2-PO, as can be noticed from Table 5.2. Acetol was detected at lower $H_2$ pressures indicating insufficient hydrogen availability to carry out its hydrogenation to 1,2-PDO. This result is in agreement with the results obtained using Ru/CsPW catalyst, which implies that acetol is one of the reactive intermediates of liquid phase hydrogenolysis of glycerol to 1,2-PDO. The rate of formation of lower alcohols (1-PO and 2-PO) and EG was enhanced at high $H_2$ pressure; comparable results were observed with Ru/C + $Nb_2O_5$ system [5].

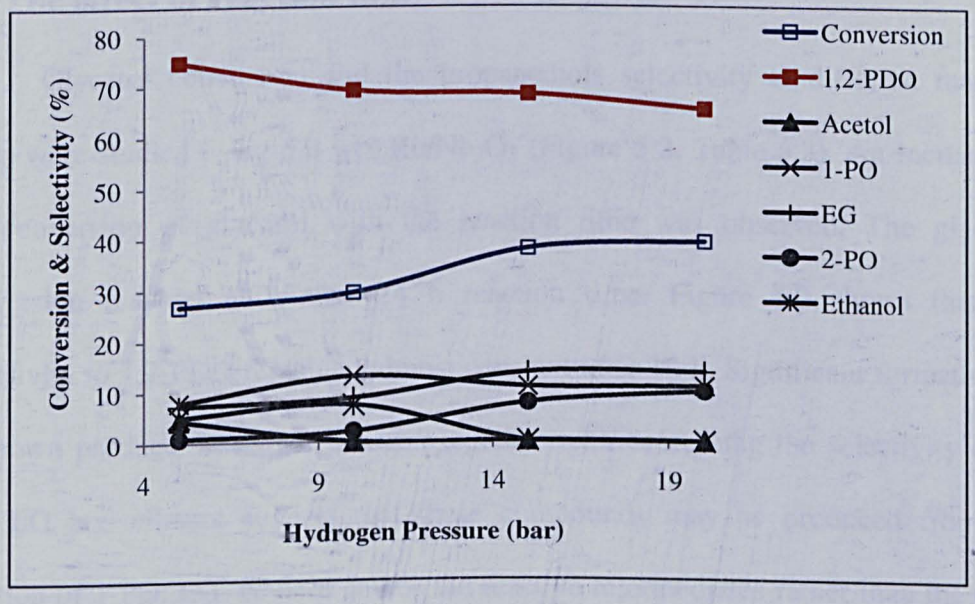


**Figure 5.1** The effect of initial hydrogen pressure on conversion and selectivity of glycerol hydrogenolysis. Reaction conditions: 180°C, 10 h, 5 ml of 20 wt% glycerol solution and 0.2 g of Ru/$Nb_2O_5$.

**Table 5.2** The effect of initial hydrogen pressure on conversion and selectivity of glycerol hydrogenolysis.

| $H_2$ (bar) | Conv. (%) | Selectivity (%) | | | | | |
|---|---|---|---|---|---|---|---|
| | | 1,2-PDO | Acetol | 1-PO | EG | 2-PO | Ethanol |
| 5 | 26 | 74 | 4 | 8 | 7 | 2 | 5 |
| 10 | 29 | 69 | 0 | 12 | 8 | 2 | 7 |
| 15 | 37 | 68 | 0 | 10 | 13 | 7 | 0 |
| 20 | 40 | 65 | 0 | 10 | 13 | 9 | 0 |

Reaction conditions: 180°C, 10 h, 5 mL of 20 wt% glycerol solution and 0.2 g of $Ru/Nb_2O_5$.

## 5.4 The effect of reaction time

Glycerol conversion and the propanediols selectivity at different reaction times were studied using 5.0 wt%$Ru/Nb_2O_5$ (Figure 5.2, Table 5.3). An increase in the conversion of glycerol with the reaction time was observed. The glycerol conversion reached 44% after 24 h reaction time. Figure 5.2 shows that the selectivity to 1,2-PDO remained almost constant after 10 h. Significant formation of unknown products at longer reaction together with decreasing the selectivity of 1-PO, EG and ethanol suggest that these compounds may be produced from the reaction of 1-PO, EG, ethanol and/or the reactive intermediates rather than the from 1,2-PDO, whose selectivity remained constant.

In another study, the performance of Ru/C + $Nb_2O_5$ system has been found to exhibit a similar relation with reaction time [5]. Higher glycerol conversion (51%) was achieved within 12 h and then remained constant with further increase in the reaction time [5]. The increasing conversion of glycerol with time has been also observed with several catalytic systems such as $Ru/Al_2O_3$ [19], Ni/NaX [20] and

$Cu/Al_2O_3$ [17]. However, at longer reaction times, the conversion of glycerol slightly decreased in some cases, indicating the possibility of catalyst deactivation.

In contrast, Ru/CsPW catalyst (Section 4.4) reached a plateau at about 30% conversion after 14 h due to catalyst deactivation, whereas $Ru/Nb_2O_5$ achieved 34% conversion after 15 h and 44% after 24 h suggesting that $Ru/Nb_2O_5$ is more stable than Ru/CsPW under reaction conditions.

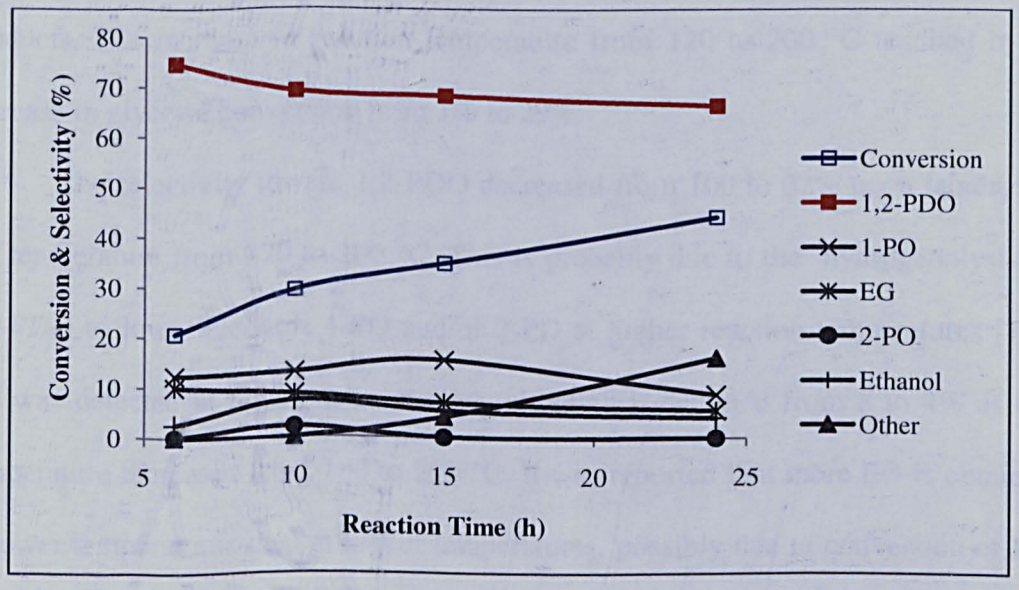


**Figure 5.2** The effect of reaction time on glycerol conversion and product selectivity. Reaction conditions: 180°C, 10 h, 5 ml 20% wt of glycerol solution, 10 bar of $H_2$, and 0.2 g of $Ru/Nb_2O_5$.

**Table 5.3** The effect of reaction time on glycerol conversion and product selectivity.

| Reaction time (h) | Conv. (%) | Selectivity (%) | | | | | | |
|---|---|---|---|---|---|---|---|---|
| | | 1,2-PDO | Acetol | 1-PO | EG | 2-PO | Ethanol | unknown |
| 6 | 20 | 74 | 0 | 12 | 10 | 0 | 2 | 0 |
| 10 | 29 | 69 | 0 | 12 | 8 | 2 | 7 | 0 |
| 15 | 34 | 68 | 0 | 15 | 6 | 0 | 5 | 4 |
| 24 | 44 | 66 | 0 | 8 | 5 | 0 | 3 | 16 |

Reaction conditions: 180°C, 10 h, 5 ml of 20% wt glycerol solution, 10 bar of $H_2$, and 0.2 g of $Ru/Nb_2O_5$.

## 5.5 The effect of reaction temperature

Temperature has a significant effect on glycerol reactivity and product selectivity over a wide range of reported catalytic systems [8, 11, 12, 14, 18, 19, 21]. To investigate the effect of temperature on the $Ru/Nb_2O_5$ catalyst, experiments were carried out on the liquid-phase reaction over $5\%Ru/Nb_2O_5$ catalyst at 120, 150, 180 and 200 °C and at 10 bar pressure of hydrogen. Table 5.4 and Figure 5.3 show the effect of temperature on the conversion of glycerol and the selectivity reaction products. The increase in reaction temperature from 120 to 200 °C resulted in an increase in glycerol conversion from 1% to 29%.

The selectivity toward 1,2-PDO decreased from 100 to 62% upon increasing the temperature from 120 to 200 °C. This is probably due to the hydrogenolysis of 1,2-PDO to lower alcohols 1-PO and/or 2-PD at higher reaction temperatures [11]. EG was detected at higher temperatures, although it declined from 8 to 4% as the temperature increased from 180 to 200 °C. It was reported that more EG is obtained at lower temperatures than at higher temperatures, possibly due to conversion of EG to other products such as ethanol [22].

At lower temperatures (120-180 °C) acetol was not observed, which indicates its complete hydrogenation to 1,2-PDO. With the Ru/CsPW catalyst (Section 4.2), considerable amount of acetol was formed at 180-200 °C which is possibly due to the low hydrogen pressure (5 bar) used in this system. This indicates that a high temperature is necessary to enhance acetol formation and, in turn, improve both the conversion of glycerol and 1,2-PDO selectivity. However, as can be seen in Figure 5.3 and Table 5.4, high temperatures promote the formation of by-products. The optimum temperature found for the $Ru/Nb_2O_5$ catalyst is 180 °C, similar to that for Ru/CsPW.

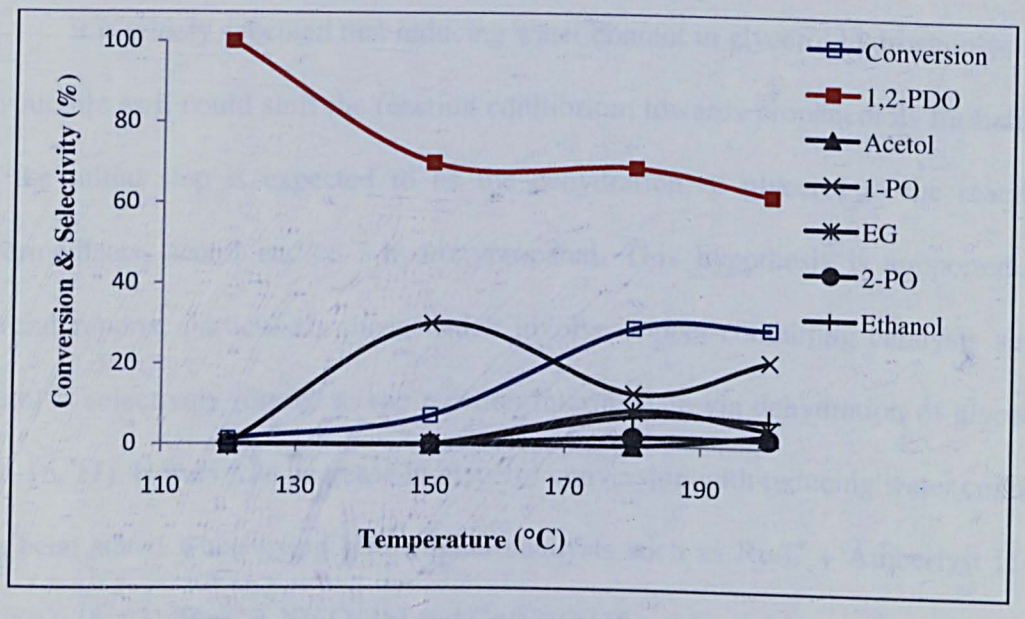


**Figure 5.3** The effect of temperature on glycerol conversion and product selectivity. Reaction conditions: 10 h, 5 ml of 20% wt glycerol solution, 10 bar of $H_2$, and 0.2 g of $Ru/Nb_2O_5$.

**Table 5.4** The effect of temperature on glycerol conversion and product selectivity.

| T (°C) | Conv. (%) | Selectivity (%) | | | | | |
|---|---|---|---|---|---|---|---|
| | | 1,2-PDO | Acetol | 1-PO | EG | 2-PO | Ethanol |
| 120 | 1.5 | 100 | 0 | 0 | 0 | 0 | 0 |
| 150 | 7.0 | 70 | 0 | 30 | 0 | 0 | 0 |
| 180 | 29.0 | 70 | 0 | 12 | 8 | 3 | 7 |
| 200 | 29.0 | 62 | 3 | 21 | 4 | 2 | 6 |

Reaction conditions: 10 h, 5 ml of 20% wt of glycerol solution, 10 bar of $H_2$, and 0.2 g of $Ru/Nb_2O_5$.

## 5.6 The effect of glycerol concentration

The effects of glycerol concentration or (water content) on glycerol hydrogenolysis were studied. The results are presented in Figure 5.4 and Table 5.5. Considerable decrease in glycerol conversion was noticed with the increase in glycerol concentration. Others have reported similar effects of glycerol concentration [8, 23].

It is widely accepted that reducing water content in glycerol hydrogenolysis is favourable as it could shift the reaction equilibrium towards propanediols formation, as the initial step is expected to be the dehydration of glycerol to the reaction intermediates, acetol and/or 3-hydroxypropanal. This hypothesis is supported by several reports, particularly those which involve copper-containing catalysts since acetol is selectively formed as the reaction intermediate via dehydration of glycerol [11, 16, 17]. However, a decrease in glycerol conversion with reducing water content has been stated when using bifunctional catalysts such as Ru/C + Amberlyst [14], $Rh/SiO_2$ [8, 23], Ru/C + $Nb_2O_5$ [5] and Co/MgO [18].

The 1,2-PDO selectivity over $Ru/Nb_2O_5$ remains practically constant within the glycerol concentration range from 10 to 50%, decreasing at higher glycerol concentrations, with a simultaneous increase in selectivity of 1-PO. The selectivity of acetol increases with glycerol concentration, reaching 4% at 50-80% glycerol concentration. This could be explained by the more favourable equilibrium for acetol formation at low water content.

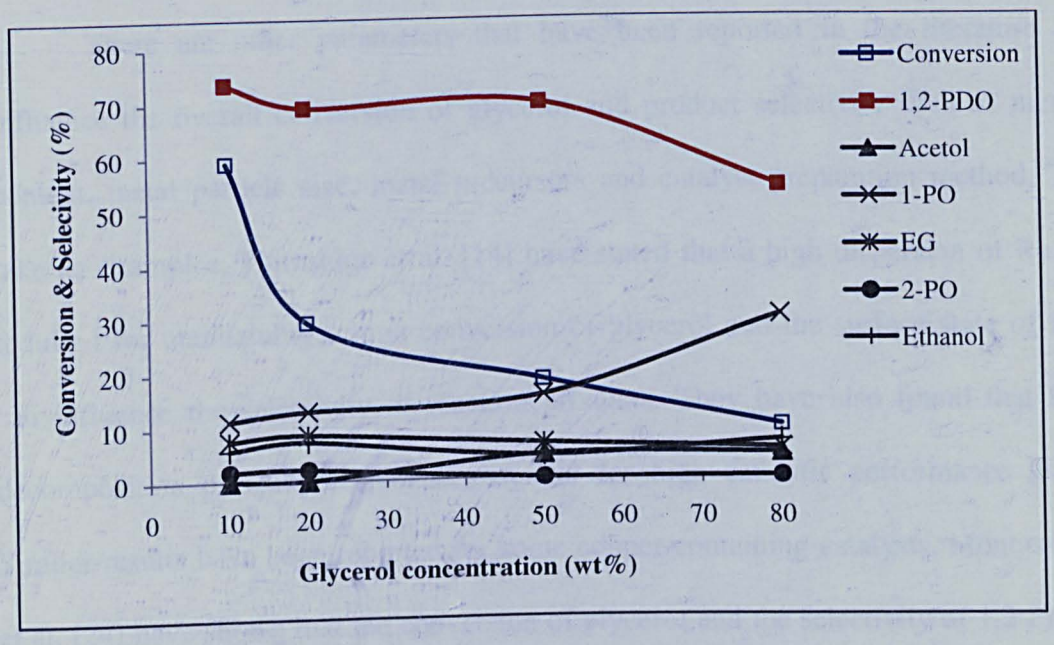


**Figure 5.4** The effect of glycerol concentration on glycerol conversion and product selectivity. Reaction conditions: 10 h, 5 ml glycerol solution, 10 bar of $H_2$, and 0.2 g of $Ru/Nb_2O_5$, 180 °C.

**Table 5.5** The effect of glycerol concentration on glycerol conversion and product selectivity.

| Glycerol concentration (wt%) | Conversion (%) | Selectivity (%) | | | | | |
|---|---|---|---|---|---|---|---|
| | | 1,2-PDO | Acetol | 1-PO | EG | 2-PO | Ethanol |
| 10 | 59 | 74 | 0 | 11 | 8 | 2 | 5 |
| 20 | 29 | 70 | 0 | 13 | 8 | 2 | 7 |
| 50 | 18 | 69 | 4 | 16 | 7 | 0 | 5 |
| 80 | 9 | 54 | 5 | 29 | 6 | 0 | 6 |

Reaction conditions: 10 h, 5 ml glycerol solution, 10 bar of $H_2$, and 0.2 g of $Ru/Nb_2O_5$, 180 °C.

There are other parameters that have been reported in the literature to influence the overall conversion of glycerol and product selectivity such as metal content, metal particle size, metal precursors and catalyst preparation method. To take an examples, Tomishige et al. [14] have stated that a high dispersion of Ru is required for maintaining a high conversion of glycerol and the surface state of Ru can influence the selectivity of reaction products. They have also found that the decomposition of Ru precursor is essential for high catalytic performance [15]. Similar results have been reported for some copper-containing catalysts. Montassier et al. [24] have shown that the conversion of glycerol and the selectivity of 1,2-PDO increase gradually with increasing hydrogen pressure as a result of increasing the amount of metallic copper with a simultaneous decrease in the amount of Cu (I) hydroxide species. Glycerol conversion and 1,2-PDO selectivity have been realised to be dependent on the particle size of Cu and ZnO in the Cu-ZnO catalyst [12].

The effect of using different Ru precursors for catalyst preparation has been examined using $Al_2O_3$, $ZrO_2$ and $SiO_2$ as supports [25]. The catalysts have been prepared using two different precursors ($RuCl_3$ and $RuNO(NO_3)_3$) by the wet impregnation method and then calcined in synthetic air for 3 h at 500 °C. The results obtained show that different metal precursors influence the activity of the catalyst when supported on $\gamma$-$Al_2O_3$. The selectivity to 1,2-PDO decline significantly when the chloride precursor is used while the conversion of glycerol is much higher when the catalyst is prepared with the nitrate precursor. This increasing activity is explained by the presence of incorporated $Cl^-$ ions into the structure of $\gamma$-$Al_2O_3$, which increases the acidity of the catalyst, as confirmed by TEM-EDS and acidiy measurements. In this work, it has been observed that the yield of the hydrogenolysis

products depends on the total acidity of catalysts, which is in good agreement with other literature results [5].

In another study by Tomishige et al. [15], the effect of different Ru precursors ($RuCl_3$, $Ru(NO)(NO_3)_3$, Ru(acac)) using active carbon as a support has been investigated. The non-pre-treated catalysts show very low or no activity for glycerol hydrogenolysis. On the other hand, the catalytic activity has increased remarkably with increasing pre-treatment temperatures up to 300 °C. Ru/C prepared from $Ru(NO)(NO_3)_3$ has exhibited the best activity, which is explained by the decomposition of the precursor salt during the pretreatment. The presence of intact salt species in the catalyst could suppress the hydrogenolysis activity [15].

Catalyst preparation methods have been found to influence glycerol conversion and product selectivity, as demonstrated by Balaraju et al. [26]. Ru supported on titania has been prepared by two different methods, the deposition-precipitation (DP) and the conventional impregnation (IM). Both catalysts were reduced in $H_2$ at 300 °C. The catalysts prepared by the DP method have shown higher conversion compared to the catalysts prepared by the IM method, which is related to the state of Ru on the surface. The high activity of the DP catalyst is explained by the well-dispersed nanosized Ru particles on titania. Larger particles of Ru and residual $Cl^-$ remaining on the catalyst surface are detrimental to the hydrogenolysis of glycerol over $Ru/TiO_2$ [25, 27].

In our study, the bifunctional catalysts were prepared by conventional impregnation method using $RuCl_3$ as a metal precursor. The standard reduction conditions involved catalyst treatment at 250 °C for 2 h in $H_2$ flow. As discussed in Section 3.7, the dispersion of Ru is low compared to the literature results meaning that Ru particles were quite large, also some $Cl^-$ may have remained on the catalyst

surface due to the low reduction temperature. Considering all the above, it is clear that the state of Ru on the surface of catalysts synthesised and tested in our work was probably the cause of the low catalytic activity compared to the most recent studies. Therefore, further investigation into Ru/CsPW and $Ru/Nb_2O_5$ preparation methods and characterisation of the state of Ru on the catalyst surface is required.

## 5.7 Reaction mechanism over $Ru/Nb_2O_5$

$Ru/Nb_2O_5$ catalyst is a bifunctional catalyst consisting of acid (Brønsted & Lewis) sites and metal (Ru) sites. To investigate the role of each catalytic active site, the reaction was conducted in the abesence of Ru at the standard reaction conditions (180 °C 10 h 5 mL of 20 wt% glycerol aqueous solution, 0.2 g catalyst, 5 bar of $H_2$ or in the absence of $H_2$). The results presented in Table 5.1. (entry 6) revleal that $Nb_2O_5$ itself was inactive for glycerol hydrogenolysis to 1,2-PDO. Only traces of acetol were obtained, which formed 1,2-PDO in the presence of hydrogen leading to a slightly higher conversion of glycerol (Table 5.1 entry 7). These results are in a good agreement with those obtained using CsPW, Section 4.2. Amberlyst (strong acid) [14], CsPW (strong acid) and $TiO_2$ (moderate acid) [7] are almost inactive, indicating that these solid acid catalysts themselves cannot catalyse the hydrogenolysis of glycerol, and the initial step is probably taking place over Ru metal. Ru itself has been found considerably active with a large number of supports [5, 7, 19]. This seems to be in agreement with Montassier et al. [28-30] and Davis et al. [21], who suggested that the hydrogenolysis of glycerol is initiated by glycerol dehydrogenation on metal sites to form glyceraldehyde (Scheme 1.1.6.1.2.2 and 4.10).

When Ru was added to the $Nb_2O_5$ catalyst, in 5 wt% loading, the conversion of glycerol increased significantly to almost 30% in the presence of $H_2$. 1,2-PDO was obtained with high selectivity (69%). Acetol was detected in some reactions, particularly at high glycerol concentrations and high temperatures. The presence of acetol and 1,2-PDO when Ru present confirms the role of acidic $Nb_2O_5$ in this reaction, similar to CsPW catalyst. Selective hydrogenation of pure acetol (5 wt% aqueous solution) to 1,2-PDO in the presence of $Ru/Nb_2O_5$ catalyst under hydrogenolysis conditions was achieved suggesting that acetol is a possible reaction intermediate for the formation of 1,2-PDO, Table 5.1 (entry 8). Ru/CsW and Ru/C + Amberlyst [13, 14] were also active and selective for acetol hydrogenation to 1,2-PDO.

The results for both Ru/CsPW and $Ru/Nb_2O_5$ show that the hydrogenolysis of glycerol requires the presence of a bifunctional catalyst, i.e., the presence of both acid and metal functions. Using our results and the published data as a guidance, the three possible reaction routes involved in the liquid-phase hydrogenolysis of glycerol over $Ru/Nb_2O_5$ are summarised in Scheme 5.1 The hydrogenolysis route involves dehydrogenation, dehydration and then hydrogenation to form 1,2-PDO, which could also undergo hydrogenolysis process to form 1- and 2-PO (Section 4.10). In the second reaction pathway, the reforming of glycerol may take place producing hydrogen and $CO_2$. This route was confirmed by conducting the hydrogenolysis of glycerol in the absence of added hydrogen which was then detected among reaction products. 1,2-PDO is a relatively stable product and EG was not detected when 1,2-PDO was tested under reaction conditions (Section 4.10) [14]. Therefore, EG is likely to form directly from C-C cleavage of glycerol over Ru. Ethanol can be formed during the hydrogenolysis of EG [14].

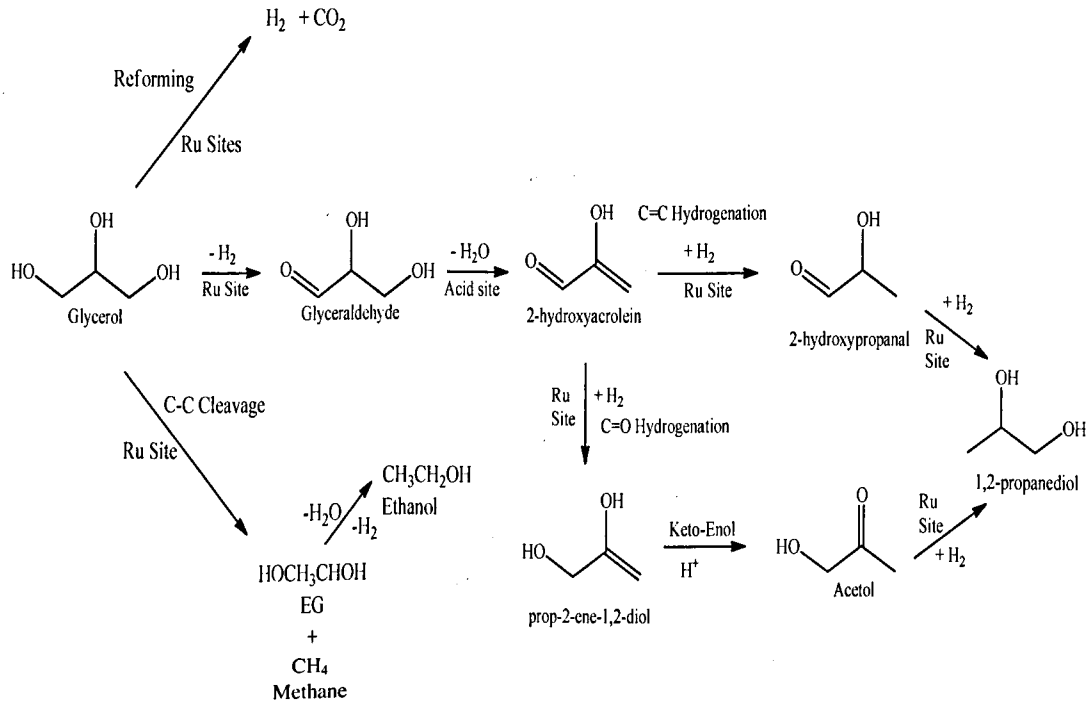


**Scheme 5.1** Proposed reaction network for glycerol hydrogenolysis over $Ru/Nb_2O_5$.

Recent work reported by Vasiliadou et al. [25] has emphasised that the presence of metal is a key for the activation of glycerol. They have found that supports such as $Al_2O_3$, $SiO_2$ and $ZrO_2$ in the absence of Ru show very low activity for the hydrogenolysis of glycerol, although they exhibit much higher acidity than the Ru samples. They concluded that the dehydration of glycerol is the first reaction step, which proceeds on the acid sites and also requires the presence of Ru metal as well. No further explanation for the role of Ru in the dehydration of glycerol was given [25].

## 5.8 Hydrogenolysis – aqueous phase reforming of glycerol: An integrated approach

As reported in Section 1.1.3, aqueous phase reforming (APR) of glycerol is a process that utilises glycerol for the formation of synthesis gas. APR of glycerol takes place according to the following equations [31]:

$$\text{Reforming:} \quad C_3H_8O_3 \longrightarrow 3CO + 4H_2$$

$$\text{Water-gas shift} : 3CO + 3H_2O \rightleftharpoons 3CO_2 + 3H_2$$

$$\text{Overall reaction:} \quad C_3H_8O_3 \longrightarrow 3CO_2 + 3H_2$$

The aqueous phase reforming (APR) of oxygenated hydrocarbons for hydrogen production has been well-established by several researchers [31-34]. This process has been carried out in the presence of metals such as Ru, Pt, Pd, Rh Ni, Ir using various supports including $Al_2O_3$, C, $SiO_2$, $ZrO_2$, $CeO_2/ZrO_2$, and $MgO/ZrO_2$ at relatively low temperatures (150-250 °C) and pressures (16–60 bar) [35]. Dumesic et al. [34] have studied the APR of ethylene glycol as a model reaction and observed that the overall catalytic activity for ethylene glycol reforming, as measured by the rate of $CO_2$ production at 210 °C, decreases in the following order for silica-supported metals: Pt > Ni > Ru > Rh > Pd > Ir. In contrast to Pt and Pd, Ru, Rh and Ni show low selectivity to $H_2$ production and high selectivity to alkane formation. The selectivity of $H_2$ formation over Pt-based catalysts improves in the following order: glucose < sorbitol < glycerol < ethylene glycol < methanol [33, 34]. Large oxygenated molecules such as glucose, sorbitol and glycerol may undergo parallel reactions that take place in aqueous solution leading to the consumption of formed $H_2$, and hence result in low $H_2$ selectivity.

In general, the catalysts active for APR are those that possess high catalytic activity for the water gas shift reaction and C-C bond cleavage. Catalysts active for C-O hydrogenation lead to lower hydrogen selectivity. The acidic supports of active metals favour dehydration/dehydrogenation reactions consuming hydrogen [31]. Among the different noble metals tested for the APR of glycerol, Ru has shown considerable activity. However, Pt was the most selective catalyst for hydrogen formation [31]

In our study, it was interesting to reveal that Ru/CsPW and $Ru/Nb_2O_5$ were active for glycerol hydrogenolysis without external use of hydrogen (Table 4.1 and 5.1). In this reaction, 1,2-PDO and acetol were obtained as the main products. Other by-products such as propanoic acid, butanoic acid, isobutane and other unknown products were formed with total selectivity of 18%. The reaction was carried out at our standard hydrogenolysis conditions (180 °C, 10 h, 5 mL of 20 wt% glycerol aqueous solution, 0.2 g catalyst) without hydrogen and 5 bar of nitrogen was used as a carrier gas. The presence of 1,2-PDO, which is mainly formed via hydrogenation of acetol, clearly proved the in-situ generation of hydrogen by APR of glycerol. This hydrogen is further consumed in the hydrogenation of acetol to 1,2-PDO. The presence of hydrogen among reaction products was confirmed by a GC equipped with TCD.

Regardless of the low conversion of glycerol and $H_2$ selectivity in our system, this result is significant for the utilisation of glycerol and related chemistry. The external hydrogen supply for glycerol hydrogenolysis makes this process dependent on fossil fuels [36]. A new promising approach involves coupling hydrogenolysis and reforming processes to allow in-situ formation of 1,2-PDO from glycerol without external hydrogen supply. It is beyond the scope of our study to carry out any further

investigations into this process. However, the relevant recent literature publications are reported here for clarity.

Very recently, D'Hondt et al. [36], Wawrzetz et al.[35], Roy et al. [37] and Gandarias et al. [38] established a new catalytic process for glycerol transformation to propanediols without externally added hydrogen. The catalysts under investigation were Pt/NaY, $Pt/Al_2O_3$, mixture of $Pt/Al_2O_3$ and $Ru/Al_2O_3$ and Pt supported on amorphous silica-alumina. Their results have demonstrated that both metal and acid functions are necessary for the conversion of glycerol to propanediols and the reforming process. It has been claimed that acid sites of the supports are responsible for the dehydration of glycerol to acetol and/or 3-hydroxypropanal and metal (Pt/Ru) sites catalyse hydrogenation of these intermediates to 1,2-PDO and 1,3-PDO. The reforming of glycerol is suggested to occur via catalytic cleavage of C-C bonds over metal sites. It has been reported that acetol formation is more pronounced in the presence of metals (Ru/Pt), in agreement with our results. Therefore, it is conceivable to suggest that glycerol is first dehydrogenated over metal site to glyceraldehyde which is then further dehydrated to acetol over acid sites. This is consistent with early reports [21, 30, 40] which suggested the dehydrogenation of glycerol to glyceraldehyde occurs on the metal surface. Wawrzetz et al. [35] conducted ATR-IR spectroscopic study for the surface species during the aqueous phase reforming of glycerol over $Pt/Al_2O_3$ at 160-225 °C and 29 bar of $H_2$ [35]. The results revealed the presence of keto and aldehyde groups in the temperature range 190-225 °C, which probably belong to glyceraldehyde and acetol. Glyceraldehyde was also identified in some hydrogenolysis experiments by Roy et al. [37].

Another kinetic study conducted by Wawrzetz et al.[35], has disclosed a new mechanistic approach towards understanding the bifunctional catalysis in the hydrogenolysis of glycerol. It has been claimed in the presence of bifunctional catalysts that possess metal and acid/base functionalities, alcohols undergo both dehydrogenation and dehydration reactions. Gas and liquid products are formed through subsequent reactions such as decarbonylation, water gas shift, Cannizzaro/Tishchenko type disproportionation and decarboxylation. In Wawrzetz's study, acetol is the main intermediate detected and is suggested to form by the dehydration of glycerol over acid sites of the support, similar to the literature results [14]. However, the unsupported Pt was active for acetol formation from glycerol, with 1,2-PDO, $CO_2$, and EG as by-products. The question is how does acetol form over Pt surface in the absence of acid? The authors assumed that under the reaction conditions Pt black might act as an acid. D'Hondt et al. [36] have also observed acetol using the non-acidic Pt/NaY catalyst. Their answer to the above question is that $CO_2$ forms via liquid phase reforming dissolves in the aqueous medium, generating $H_2CO_3$, which could dissociate providing free protons. Roy et al. [37] also reported the same phenomenon in the transformation of pyruvaldehyde to lactic acid during glycerol hydrogenolysis process.

## 5.9 Conclusions

Our findings demonstrate that $Ru/Nb_2O_5$ is an effective catalyst for the liquid-phase hydrogenolysis of glycerol to produce 1,2-PDO. 29% conversion of glycerol and 69% 1,2-PDO selectivity were achieved at 180 °C, 10 h and 10 bar of $H_2$. The catalyst performance is significantly affected by the catalyst calcination temperature

and preparation method. In-house made $Nb_2O_5$ provides more active catalyst than the commercial $Nb_2O_5$. This can be explained by the higher surface area and total acidity of the in-house made $Nb_2O_5$ compared to the commercial one. $Nb_2O_5$ dried at 100 °C exhibits higher catalytic activity than that calcined at 500 °C, which is possibly due to the reduction in surface acidity upon increasing the calcination temperature. The order of catalysts activity in the liquid-phase hydrogenolysis of glycerol is: $Nb_2O_5$ (dried at 100 °C) > $Nb_2O_5$ (calcined at 500 °C) ≈ CsPW > CsSiW > $Nb_2O_5$ commercial. This indicates that moderate rather than strong acidity of catalyst is required for glycerol conversion and it is the total catalyst acidity rather than the acid strength that plays a key role in this reaction.

The $Ru/Nb_2O_5$ catalyst is more stable than Ru/CsPW under reaction conditions. $Nb_2O_5$ itself is not active for glycerol hydrogenolysis, similar to the CsPW catalyst. Ru itself is moderately active on non-acidic supports. However, when Ru is supported on $Nb_2O_5$, the conversion of glycerol increases significantly. This implies that the hydrogenolysis of glycerol vitally requires a bifunctional catalyst which involves both metal and acid functionalities. The same has been observed for strong acids such as Amberlys -15, as well as moderate acids such as $Al_2O_3$, $SiO_2$, $ZrO_2$ and $TiO_2$ [14, 25]. These results suggest that the initial step in the hydrogenolysis of glycerol is the dehydrogenation of the primary hydroxyl group on metal sites of the catalysts.

A reaction network for glycerol hydrogenolysis over $Ru/Nb_2O_5$ catalyst consisting of three parallel pathways can be constructed. These include: (1) dehydrogenation of glycerol to glyceraldehyde followed by dehydration to acetol which is further hydrogenated to 1,2-PDO; (2) reforming of glycerol; and (3) C-C cleavage to form EG and C1 products.

The reforming of glycerol was confirmed by the presence of $H_2$ among reaction products when the reaction was carried out without externally added hydrogen. 1,2-PDO and acetol were the main products of this reaction. This result allows the formation of 1,2-PDO without external hydrogen supply by integrating the hydrogenolysis process with liquid phase reforming of glycerol. This is a new emerging process and requires further investigations.

## References


[1] I. Nowak, M. Ziolek, Chem. Rev. (1999) 3603.

[2] K. Tanabe, Catal. Today. 78 (2003) 65.

[3] K. Tanabe, Catal. Today. 8 (1990) 1.

[4] E. I. Ko, J. M. Hupp, F. H. Rogan, N. J. Wagner, J. Catal. 84 (1983) 85.

[5] M. Balaraju, V. Rekha, P. S. S. Prasad, B. L. A. P. Devi, R. B. N. Prasad, N. Lingaiah, Appl. Catal. A 354 (2009) 82.

[6] Y. Kusunoki, T. Miyazawa, K. Kunimori, K. Tomishige, Catal. Commun. 6 (2005) 645.

[7] J. Feng, H. Y. Fu, J. B. Wang, R. X. Li, H. Chen, X. J. Li, Catal. Commun. 9 (2008) 1458.

[8] I. Furikado, T. Miyazawa, S. Koso, A. Shimao, K. Kunimori, K. Tomishige, Green Chem. 9 (2007) 582.

[9] Z. L. Yuan, P. Wu, J. Gao, X. Y. Lu, Z. Y. Hou, X. M. Zheng, Catal. Lett. 130 (2009) 261.

[10] J. Chaminand, L. Djakovitch, P. Gallezot, P. Marion, C. Pinel, C. Rosier, Green Chem. 6 (2004) 359.

[11] M. A. Dasari, P. P. Kiatsimkul, W. R. Sutterlin, G. J. Suppes, Appl. Catal. A 281 (2005) 225.

[12] S. Wang, H. C. Liu, Catal. Lett. 117 (2007) 62.

[13] T. Miyazawa, S. Koso, K. Kunimori, K. Tomishige, Appl. Catal. A 329 (2007) 30.

[14] T. Miyazawa, Y. Kusunoki, K. Kunimori, K. Tomishige, J. Catal. 240 (2006) 213.

[15] T. Miyazawa, S. Koso, K. Kunimori, K. Tomishige, Appl. Catal. A 318 (2007) 244.

[16] R. B. Mane, A. M. Hengne, A. A. Ghalwadkar, S. Vijayanand, P. H. Mohite, H. S. Potdar, C. V. Rode, Catal. Lett. 135 (2010) 141.

[17] L. Y. Guo, J. X. Zhou, J. B. Mao, X. W. Guo, S. G. Zhang, Appl. Catal. A 367 (2009) 93.

[18] X. H. Guo, Y. Li, R. J. Shi, Q. Y. Liu, E. S. Zhan, W. J. Shen, Appl. Catal. A 371 (2009) 108.

[19] L. Ma, D. H. He, Z. P. Li, Catal. Commun. 9 (2008) 2489.

[20] J. Zhao, W. Q. Yu, C. Chen, H. Miao, H. Ma, J. Xu, Catal. Lett. 134 (2010) 184.

[21] E. P. Maris, R. J. Davis, J. Catal. 249 (2007) 328.

[22] C. W. Chin, A. Tekeei, J. M. Ronco, M. L. Banks, G. J. Suppes, Ind. Eng. Chem. Res. 47 (2008) 6878.

[23] Y. Shinmi, S. Koso, T. Kubota, Y. Nakagawa, K. Tomishige, Appl. Catal. B 94 (2010) 318.

[24] C. Montassier, J. M. Dumas, P. Granger, J. Barbier, Appl. Catal. A 121 (1995) 231.

[25] E. S. Vasiliadou, E. Heracleous, I. A. Vasalos, A. A. Lemonidou, Appl. Catal. B 92 (2009) 90.

[26] M. Balaraju, V. Rekha, B. L. A. P. Devi, R. B. N. Prasad, P. S. S. Prasad, N. Lingaiah, Appl. Catal. A 384 (2010) 107.

[27] N. Li, C. Descorme, M. Besson, Appl Catal B 71 (2007) 262.

[28] C. Montassier, J. C. Menezo, L. C. Hoang, C. Renaud, J. Barbier, J. Mol. Catal. 70 (1991) 99.

[29] C. Montassier, D. Giraud, J. Barbier, Stud. Surf. Sci. Catal. 41 (1988) 165.

[30] C. Montassier, D. Giraud, J. Barbier, J. P. Boitiaux, Bull. Soc. Chim. Fr. (1989) 148.

[31] R. R. Davda, J. W. Shabaker, G. W. Huber, R. D. Cortright, J. A. Dumesic, Appl. Catal. B 56 (2005) 171.

[32] R. R. Soares, D. A. Simonetti, J. A. Dumesic, Angew. Chem. Int. Ed. 45 (2006) 3982.

[33] R. D. Cortright, R. R. Davda, J. A. Dumesic, Nature. 418 (2002) 964.

[34] R. R. Davda, J. W. Shabaker, G. W. Huber, R. D. Cortright, J. A. Dumesic, Appl. Catal. B 43 (2003) 13.

[35] A. Wawrzetz, B. Peng, A. Hrabar, A. Jentys, A. A. Lemonidou, J. A. Lercher, J. Catal. 269 (2010) 411.

[36] E. D'Hondt, S. V. de Vyver, B. F. Sels, P. A. Jacobs, Chem. Commun. (2008) 6011.

[37] D. Roy, B. Subramaniam, R. V. Chaudhari, Catal. Today. 156 (2010) 31.

[38] I. Gandarias, P. L. Arias, J. Requies, M. B. Guemez, J. L.G. Fierro, Appl. Catal. B 97 (2010) 248.

# 6. Gas-phase dehydration of glycerol to acrolein catalysed by caesium heteropoly salt

## 6.1 Introduction

The development of an alternative environmentally benign process for the production of acrolein based on the biomass-derived glycerol as a sustainable feedstock is a real challenge [1-5, 8]. One of the most important directions for the utilisation of glycerol is its dehydration to acrolein. Acrolein is an important intermediate for the chemical and agricultural industries, which is currently produced by oxidation of petroleum derived propene [1]. It can also be obtained from glycerol via acid-catalysed dehydration in the gas or liquid phase [8].

The dehydration of glycerol to acrolein has been known since the nineteenth century [3, 4, 8]. Homogeneous and heterogeneous acid catalysts, as well as biocatalysts, have been used for this reaction [5-7]. Due to technical and environmental advantages, heterogeneous catalysis appears to be much more attractive. A number of solid acid catalysts for the dehydration of glycerol have been reported including metal sulphates and phosphates, zeolites, supported mineral acids, niobia, sulphated zirconia and heteropoly acids [8]. The synthesis of acrolein is an endothermic reaction with a standard enthalpy of 4.34 $kcalmol^{-1}$ for a gas-phase process. Typically, the reaction is carried out in the temperature range of 260 – 350°C using an aqueous glycerol as a feedstock. Since much steam is present in the gas flow, the catalyst should have good water tolerance. The catalyst efficiency in acrolein synthesis is enhanced with increasing catalyst acidity [3, 4, 8]. Supported Keggin heteropoly acids, possessing very strong Brønsted acidity, have been found

amongst the most efficient catalysts for glycerol-to-acrolein conversion in the gas phase [9-12]. In particular, with the 12-tungstosilicic acid, $H_4SiW_{12}O_{40}$, which possesses a higher water tolerance compared to other Keggin heteropoly acids, acrolein yields of ≥80% have been achieved at an optimum temperature of 275°C [9].

As regards to the reaction mechanism, the dehydration of glycerol on acid catalysts is suggested to proceed via the formation of 3-hydroxypropanal, with 1-hydroxyacetone (acetol) formed as a relatively stable by-product (Scheme 1) [8, 9, 12-14]. Acetol is the main product (>90% selectivity) in the gas-phase dehydration of glycerol on mixed-oxide catalysts, such as copper chromite [15], and supported metal catalysts, e.g., $Cu/Al_2O_3$ [16]. This may indicate that Lewis acid sites and metal sites are important for the formation of acetol, whereas the formation of 3-hydroxypropanal followed by its dehydration to acrolein is favoured in the presence of strong Brønsted acid sites.

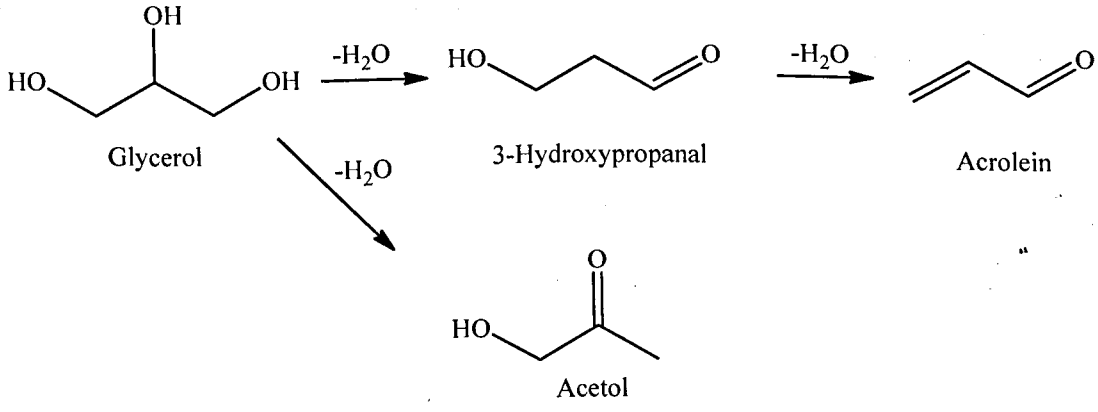


**Scheme 6.1** Dehydration of glycerol over acid catalysts.

The major drawback to the gas-phase dehydration of glycerol on acid catalysts is catalyst deactivation due to extensive coke deposition on the catalyst surface as well as the difficulty of direct usage of the crude glycerol obtained from biodiesel production [8]. Catalyst regeneration by combustion of coke has been

attempted [8], either in-situ continuously [17, 18] or ex-situ periodically [19], although both with limited success. Glycerol dehydration using a fluidised catalyst bed with catalyst circulation between the reactor and regenerator similar to the fluidised catalytic cracking process has also been demonstrated [14]. It should be noted that regeneration of heteropoly acid catalysts by combustion of coke is difficult because of the relatively low thermal stability of heteropoly acids [20].

The acidic heteropoly salt, caesium 12-tungstophosphate $Cs_{2.5}H_{0.5}PW_{12}O_{40}$ (CsPW) is well known as a water-insoluble strong Brønsted acid and a versatile solid acid catalyst possessing high thermal stability ($\geq 500^{o}C$) and water tolerance [21-23]. Therefore, CsPW is investigated as a potentially efficient catalyst for the dehydration of glycerol to acrolein in the gas phase. We also attempt to enhance catalyst lifetime and reduce coke deposition by doping CsPW with platinum group metals (PGM), such as Ru, Pd and Pt, and co-feeding hydrogen to the reaction system. This approach, involving bifunctional acid-metal catalysis, has already been effectively used in petrochemical industry for alkane hydroisomerisation [24, 25]. Finally, new mechanistic evidence is presented regarding the nature of acid sites required for the dehydration of glycerol to acrolein.

## 6.2 Glycerol dehydration over CsPW

The first entry in Table 6.1 shows the performance of CsPW bulk heteropoly salt in glycerol dehydration in the gas phase at an optimum temperature of 275 °C and 1 bar pressure. Previously, the same optimum temperature has been established for supported heteropoly acids [9, 10]. It should be noted that the reaction was carried out in the presence of a large excess of steam as a result of using 10 wt% glycerol aqueous solution as a feed. The molar ratio of [glycerol]:[$N_2$]:[$H_2O$] in the

incoming gas flow was 1:4.4:46 and the glycerol WHSV 2.8 $h^{-1}$, corresponding to the glycerol molar flow rate of 30 mmol $h^{-1}g_{cat}^{-1}$. Nitrogen was used as a carrier gas. To withstand severe steaming the catalyst should have strong steam resistance. The results presented here show that the bulk CsPW salt was fit for the purpose.

The CsPW catalyst exhibited high initial activity, with the glycerol conversion amounting to 100% at 98% acrolein selectivity after 1 h on stream. The conversion, however, decreased sharply with the time on stream, down to ~40% after 6 h, without impairing acrolein selectivity (Figure 6.1). A significant amount of coke (8.9 wt%, Table 6.1) was deposited on the catalyst surface during the reaction, which was the likely cause of catalyst deactivation [8, 9-12]. Similar deactivation has been reported previously for supported heteropoly acids [9-12], as well as for other solid acid catalysts [8]. With CsPW, despite catalyst deactivation, the selectivity of acrolein remained high for a long time, 92% after 12 h on stream. Acetol was the main by-product, but with only 2 – 3% selectivity. Amongst other by-products were found acetone, acetaldehyde, propanal and propanoic acid together with traces of other unidentified compounds.

Acidic caesium 12-tungstosilicate, $Cs_{3.5}H_{0.5}SiW_{12}O_{40}$, performed quite similar to CsPW, but with a lower glycerol conversion and a faster catalyst deactivation (Table 6.1). Within the Misono's classification of mechanisms of heteropoly acid catalysis (i.e., bulk-type and surface-type mechanisms), which have been described in Section 4.3 [21], the dehydration of glycerol on the water-insoluble and rather hydrophobic CsPW can be viewed as a surface-type acid-catalysed reaction occurring on the accessible surface proton sites of CsPW.

**Table 6.1** Gas-phase dehydration of glycerol to acrolein using caesium heteropoly salt.[a]

| Catalyst | Gas flow | Conversion[b] (%) | Selectivity[b] (%) | | | |
|---|---|---|---|---|---|---|
| | | | Acrolein | Acetol | Others[c] | C[d] (wt%) |
| $Cs_{2.5}H_{0.5}PW_{12}O_{40}$ | $N_2$ | 41 (100) | 94 (98) | 2.4 | 3.6 | 8.9 |
| $Cs_{3.5}H_{0.5}SiW_{12}O_{40}$ | $N_2$ | 21 (91) | 94 (97) | 3.3 | 2.7 | - |

a) Reaction conditions: 275 °C, 0.30 g catalyst powder of 45-180 μm particle size, 15 $mLmin^{-1}$ gas flow rate ($N_2$ or $H_2$), 10 wt% glycerol aqueous solution fed at 0.14 $mLmin^{-1}$ flow rate (2.8 $h^{-1}$ glycerol WHSV), 5 h time on stream.

b) In brackets, glycerol conversion and acrolein selectivity after 1 h on stream.

c) A mixture of organic by-products including acetaldehyde, acetone, propanal, propanoic acid and other unidentified components.

d) Carbon content in spent catalyst after reaction (5-6 h on stream) from combustion analysis.

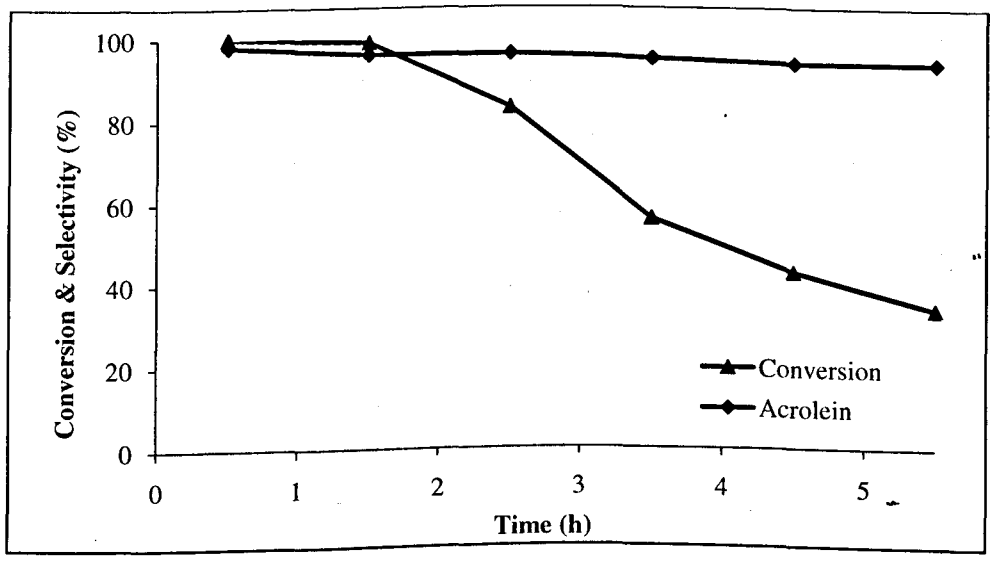


**Figure 6.1** Time course for glycerol dehydration over CsPW at 275 °C in $N_2$ flow.

### 6.2.1 Turnover frequency (TOF)

Turnover frequency (TOF) is a more accurate measure of catalyst activity, which is directly related to the strength of acid sites. It is defined as the number of molecules reacted per catalytic site per unit time [22]. From the results in Table 6.2, we can estimate the turnover frequency (TOF) for glycerol conversion on this catalyst using $S_{BET}$ = 130 $m^2g^{-1}$ for the fresh catalyst and assuming a Keggin unit cross section of 144 $Å^2$, and that all surface protons are equally accessible for reaction [21, 23]. This gives an initial TOF of 405 $h^{-1}$ per one surface proton site at 1 h time on stream. After 5 h on stream, this value decreases to 166 $h^{-1}$ due to catalyst deactivation. These are approximate figures because the catalyst surface area was shrinking during reaction down to 97 $m^2g^{-1}$ after 5 h on stream, which would lead to higher TOF values. The corresponding values of the specific rate of acrolein production are 30 and 12 mmol $h^{-1}g_{cat}^{-1}$ for 1 and 5 h time on stream respectively. These compare well with the best values reported for supported heteropoly acid catalysts: 5.1 mmol $h^{-1}g_{cat}^{-1}$ at 275°C and 5 h time on stream for 30%$H_4SiW_{12}O_{40}/SiO_2$ and 10.5 mmol $h^{-1}g_{cat}^{-1}$ at 315°C and 9 – 10 h time on stream for 10%$H_3PW_{12}O_{40}/ZrO_2$ [11, 12], which are calculated per total catalyst mass.

In contrast to CsPW, heteropoly acids, for example the parent acid $H_3PW_{12}O_{40}$, are readily water-soluble and highly hydrophilic compounds [21-24]. Therefore, the above heteropoly acid catalysts are most likely to dehydrate glycerol via the bulk-type mechanism by the Misono's classification [21], which would mean that all heteropoly acid protons are available for reaction. With that in mind, the following TOF values for glycerol conversion were calculated for these catalysts: 14.3 $h^{-1}$ for 30%$H_4SiW_{12}O_{40}/SiO_2$ (275 °C, 5 h) and 148 $h^{-1}$ for 10%$H_3PW_{12}O_{40}/ZrO_2$ (315 °C, 9 – 10 h). These values are lower than our TOF value 166 $h^{-1}$ (275 °C, 5 h)

for CsPW. This result can be explained by suggesting that under our reaction conditions in the presence of a large excess of steam the hydrophobic CsPW has less hydrated hence stronger proton sites as compared to the hydrophilic heteropoly acids. It should be pointed out that in the absence of water CsPW is a weaker acid than the bulk parent $H_3PW_{12}O_{40}$ as measured by ammonia adsorption calorimetry and ammonia TPD [24, 34], with the values of initial $NH_3$ adsorption enthalpy -162 and -195 $kJmol^{-1}$ and $NH_3$ desorption temperature 557 °C and 577 °C for CsPW and $H_3PW_{12}O_{40}$ respectively [24]. It should be noted, however, that supported heteropoly acids have weaker acid sites compared to bulk ones [23].

## 6.3 Glycerol dehydration over PGM-doped CsPW

As demonstrated above, the bulk CsPW catalyst shows high initial activity in glycerol dehydration, but, like other solid acid catalysts, suffers from rapid deactivation due to coke formation. Regeneration of heteropoly acid catalysts has been reviewed recently [20]. Traditional regeneration by coke combustion, which is typically carried out at ~500 °C, is difficult because of insufficient thermal stability of heteropoly acids. Doping heteropoly acid catalysts with platinum group metals (PGM) such as Pd and Pt improves their regeneration by reducing the combustion temperature to ~350 °C [20]. However, the disadvantage of such regeneration is that the catalytic process must be discontinued.

Here we attempted to enhance catalyst lifetime and reduce coke deposition by doping CsPW with PGM such as Ru, Pd and Pt and co-feeding hydrogen into the reaction system. This approach has been effectively used in the industrial hydroisomerisation of alkanes, which is carried out on PGM-doped alumina or zeolite in the presence of hydrogen [25, 26]. The metal additives, on the one hand,

promote bifunctional metal-acid mechanism of alkane isomerisation and, on the other, reduce catalyst coking by hydrogenating coke precursors. Solid Keggin heteropoly acids such as $H_3PW_{12}O_{40}$ doped with Pd and Pt have been reported as bifunctional catalysts for alkane hydroisomerisation [35-38].

Two types of PGM-doped CsPW catalysts were tested: (i) catalysts obtained by impregnation of CsPW with a PGM precursor followed by reduction with $H_2$ and (ii) mechanical mixtures of CsPW with carbon-supported PGM (5% Ru/C, 10% Pt/C and 10% Pd/C). The first type had 0.3 – 0.5 wt% metal loading and the second 0.5 wt%. Representative results on their performance in glycerol dehydration are shown in Table 6.1.

First, the supported PGM catalysts (0.5%Ru/CsPW, 0.3%Pt/CsPW and 0.5%Pd/CsPW) were tested using the same procedure as for the undoped CsPW above, i.e., at 275 °C in $N_2$ flow. Under such conditions, their performance was similar to that of the undoped CsPW. Then they were tested in $H_2$ flow, whereupon they showed considerable improvement in their stability to deactivation compared to CsPW (Table 6.2, Figure. 6.2). This improvement, however, strongly depended on the metal dopant. Thus the Ru and Pt catalysts exhibited a relatively small enhancement at longer times on stream (Figure 6.1 and Figure 6.2 (A, B)). In contrast, the Pd catalyst, 0.5%Pd/CsPW, provided significant enhancement of catalyst performance (Figure 6.2 (C)). It is important to note that PGM doping had little (Pd and Pt) or no effect (Ru) on acrolein selectivity (Table 6.2, Figure 6.2). It should be noted, however, that in the initial stage of reaction (1 h time on stream), Pd and Pt reduced the selectivity to acrolein to 83 and 87% respectively, which then increased to 95 – 96% (Figure 6.2 (B, C)). It was found that the drop in selectivity was due to an increased formation of propanoic acid in the initial stage of reaction.

This effect of Pd on the selectivity of acrolein was also observed with 2%Pd/20%HPW/$SiO_2$, Figure 6.3. This selectivity trend with Pd and Pt may suggest that these metals promote the formation of by-products, mainly propanoic acid, from reaction intermediates at the initial stage of reaction, when strong metal and acid sites are present. However, when deactivation by coking takes place (after 1 h time on stream), these strong sites are most likely to deactivate resulting in a decrease in the formation of propanoic acid which in turn increases the formation of acrolein (Figure 6.2 and 6.3). When CsPW and 20%HPW/$SiO_2$ were used in the absence of metals (Figure 6.1 and 6.3 A), the main dehydration route which forms acrolein, is more promoted, maintaining a high selectivity of acrolein throughout 5 h time on stream. Ru metal shows practically no effect towards coke inhibition and so towards propanoic acid formation, therefore selectivity behaviour of Ru/CsPW, during 1 h time on stream, is similar to the undoped CsPW (Figure 6.2A).

**Table 6.2** Glycerol dehydration over PGM-doped CsPW[a].

| Catalyst | Gas flow | Conversion[b] (%) | Selectivity[b] (%) | | | |
|---|---|---|---|---|---|---|
| | | | Acrolein | Acetol | Others[c] | C[d] (wt%) |
| 0.3%Pt/CsPW | $H_2$ | 51 (100) | 94 (97) | 2.8 | 3.2 | 6.8 |
| 0.5%Ru/CsPW | $H_2$ | 47 (100) | 95 (87) | 2.5 | 2.5 | 8.0 |
| 0.5%Pd/CsPW | $H_2$ | 79 (97) | 96 (83) | 1.4 | 2.6 | 4.5 |

a) Reaction conditions: 275 °C, 0.30 g catalyst powder of 45-180 μm particle size, 15 $mLmin^{-1}$ gas flow rate ($N_2$ or $H_2$), 10 wt% glycerol aqueous solution fed at 0.14 $mLmin^{-1}$ flow rate (2.8 $h^{-1}$ glycerol WHSV), 5 h time on stream.

b) In brackets, glycerol conversion and acrolein selectivity after 1 h on stream.

c) A mixture of organic by-products including acetaldehyde, acetone, propanal, propanoic acid and other unidentified components.

d) Carbon content in spent catalysts after reaction (5 – 6 h on stream) from combustion analysis.

The PGM doping combined with $H_2$ supply was found to reduce the amount of coke deposited on the catalyst surface (Table 6.1), which is in line with the enhancement of catalyst stability towards deactivation. Thus Ru and Pt had only small effect on the amount of coke formed, whereas Pd had a pronounced effect, reducing the amount of coke by half, down to 4.5%, which constitutes only 0.8% of carbon supplied into the reactor with the feed. This shows that the enhancing effect of PGM in glycerol dehydration is related to their coke inhibition, with Pd being the most effective dopant.

Figure 3.5 (Section 3.1.1) shows the TGA/TPO (temperature programmed oxidation) of the spent 0.5%Pd/CsPW catalyst after 6 h on stream in $H_2$ at 275°C and, for comparison, the TGA for the fresh catalyst (Figure 3.1, Section 3.1.1).

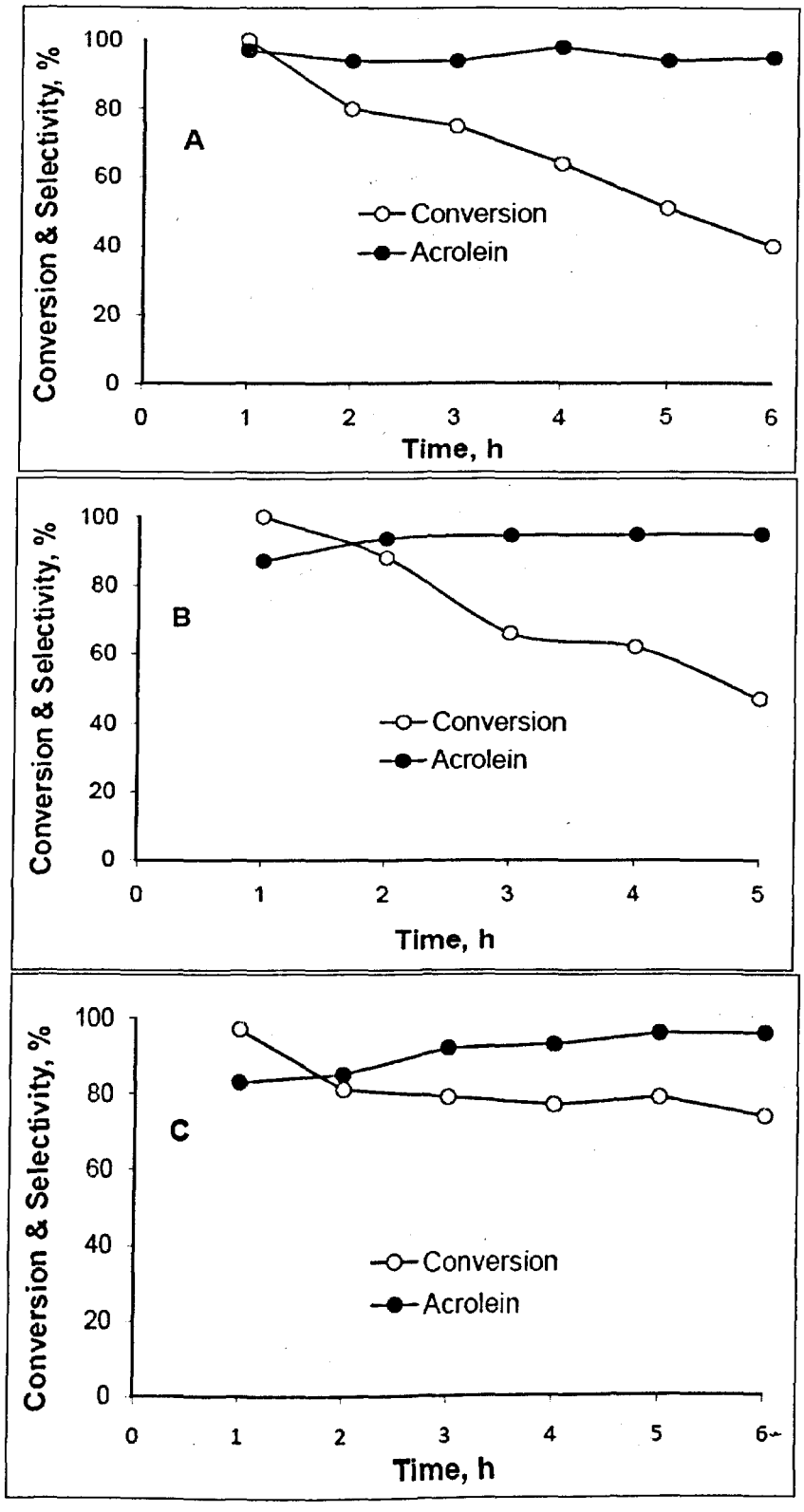


**Figure 6.2** Time course for glycerol dehydration over (A) 0.5%Ru/CsPW, (B) 0.3%Pt/CsPW and (C) 0.5%Pd/CsPW at 275 °C in $H_2$ flow.

The fresh catalyst looses hydration water below 200°C and exhibits no further weight loss up to 620°C. The TPO for the spent catalyst provides an insight into the nature of coke formed. The TPO profile shows a broad combustion peak in the temperature range of 350 – 550°C, indicating that this coke is a mixture of aliphatic (easier to burn) and polyaromatic (more difficult to burn) carbonaceous deposits [39].

Therefore, doping CsPW with PGM together with co-feeding $H_2$ improves catalyst stability to deactivation without impairing the high selectivity to acrolein. The enhancing effect of PGM increases in the order: Ru ~ Pt < Pd. The catalyst 0.5%Pd/CsPW gives 96% acrolein selectivity at 79% glycerol conversion (76% yield) at 275 °C and 5 h time on stream. It performs with an average TOF of 320 $h^{-1}$ (estimated, as for the undoped CsPW above, using $S_{BET}$ = 84 $m^2g^{-1}$ for the fresh catalyst). Again, this is an approximation because the catalyst surface was shrinking during reaction down to 68 $m^2g^{-1}$ after 5 h on stream, which would lead to a higher TOF value. For this catalyst, the specific rate of acrolein production amounts to 23 mmol $h^{-1}g_{cat}^{-1}$ at 5 h on stream, exceeding that reported for supported heteropoly acids.

The performance of catalysts prepared by mechanical mixing of CsPW with carbon-supported PGM is also presented in Table 6.3. The Ru catalyst, 5%Ru/C + CsPW (1:10), showed very similar results to those for the supported Ru catalyst 0.5%Ru/CsPW, albeit with a slightly lower glycerol conversion and acrolein selectivity. The Pt and Pd catalysts behaved quite differently, however. These two catalysts gave high glycerol conversions, but very low acrolein selectivities, especially in the initial stage of reaction. Instead, these catalysts produced large amounts of propanoic acid, which was identified by GC-MS. Moreover, significant

loss of carbon balance was observed: 75 – 90% and 14 – 50% for the Pt and Pd catalyst respectively, depending on the time on stream. Larger carbon losses were observed in the initial stage of reaction, decreasing with the time on stream. Since the catalyst weight did not change significantly after reaction, these carbon losses cannot be explained by coking. It can be suggested that these catalysts produced gaseous products such as $H_2$, CO and $CO_2$ by steam reforming of glycerol. This would be similar to aqueous phase reforming (APR) of polyols documented by Dumesic et al. [6]. Pt and Pd are active catalysts in the APR, with Pt being the most active one [6]. However, as regards to the dehydration of glycerol to acrolein, these catalysts have no advantage over the supported PGM catalysts discussed above, therefore no attempt was made to study them in more detail.

**Table 6.3** The performance of catalysts prepared by mechanical mixing of CsPW with carbon-supported PGM.[a]

| Catalyst | Gas flow | Conversion[b] (%) | Selectivity[b] (%) | | |
|---|---|---|---|---|---|
| | | | Acrolein | Acetol | Others[c] |
| 5%Ru/C + CsPW (1:10)[d] | $H_2$ | 50 (95) | 92 (94) | 3.5 | 4.5 |
| 10%Pt/C + CsPW (1:20)[d] | $H_2$ | 74 (100) | 5.8 (0) | 3.3 | 15 |
| 10%Pd/C + CsWP (1:20)[d] | $H_2$ | 83 (100) | 31 (4) | 2.9 | 52 |

**a)** Reaction conditions: 275 °C, 0.30 g catalyst powder of 45-180 μm particle size, 15 $mLmin^{-1}$ gas flow rate ($N_2$ or $H_2$), 10 wt% glycerol aqueous solution fed at 0.14 $mLmin^{-1}$ flow rate (2.8 $h^{-1}$ glycerol WHSV), 5 h time on stream.

**b)** In brackets, glycerol conversion and acrolein selectivity after 1 h on stream.

**c)** A mixture of organic by-products including acetaldehyde, acetone, propanal, propanoic acid and other unidentified components.

**d)** Mechanical mixtures of CsPW with PGM/C in weight ratios shown in brackets with a total PGM content of 0.5 wt%. 75-90% and 14-50% loss of carbon balance was observed for the Pt and Pd catalyst respectively, indicating the formation of gaseous products (CO and $CO_2$).

For comparison, we also tested silica-supported $H_3PW_{12}O_{40}$ (HPW) catalysts 20%HPW/$SiO_2$ and 2%Pd/20%HPW/$SiO_2$ under the same conditions (Table 6.4, Figure 6.3). The performance of the undoped catalyst in $N_2$ at 275°C was similar to that of CsPW regarding acrolein selectivity and even better regarding glycerol conversion: 60% conversion at 5 h compared to 41% for CsPW. As a result, 20%HPW/$SiO_2$ gave a higher specific rate of acrolein production of 17 mmol $h^{-1}g_{cat}^{-1}$ (5 h) per total catalyst mass and 85 mmol $h^{-1}g_{HPW}^{-1}$ per HPW mass. Assuming that all protons of HPW were available for the reaction, the TOF values were calculated to be 147 $h^{-1}$ at 1 h and 88 $h^{-1}$ at 5 h. The Pd-doped catalyst 2%Pd/20%HPW/$SiO_2$, similarly to 0.5%Pd/CsPW, showed considerable improvement regarding its stability to deactivation compared to 20%HPW/$SiO_2$ (Figure 6.3). At 5 h on stream, it gave 94% acrolein selectivity at 72% conversion (68% yield), with an acrolein production rate of 21 mmol $h^{-1}g_{cat}^{-1}$ (105 mmol $h^{-1}g_{HPW}^{-1}$) and a TOF value of 106 $h^{-1}$. Although these results are not as good as those for 0.5%Pd/CsPW (see above), they are still better than those reported for supported heteropoly acids previously [11, 12].

**Table 6.4** Glycerol dehydration on silica-supported $H_3PW_{12}O_{40}$ (HPW)[a].

| Catalyst | Gas flow | Conversion[b] (%) | Selectivity[b] (%) | | |
|---|---|---|---|---|---|
| | | | Acrolein | Acetol | Others[c] |
| 20%HPW/$SiO_2$ | $N_2$ | 60 (100) | 95 (97) | 3.6 | 1.4 |
| 2%Pd/20%HPW/$SiO_2$ | $H_2$ | 72 (100) | 94 (85) | 3.3 | 2.7 |

**a)** Reaction conditions: 275 °C, 0.30 g catalyst powder of 45-180 μm particle size, 15 $mLmin^{-1}$ gas flow rate ($N_2$ or $H_2$), 10 wt% glycerol aqueous solution fed at 0.14 $mLmin^{-1}$ flow rate (2.8 $h^{-1}$ glycerol WHSV), 5 h time on stream.

**b)** In brackets, glycerol conversion and acrolein selectivity after 1 h on stream.

**c)** A mixture of organic by-products including acetaldehyde, acetone, propanal, propanoic acid and other unidentified components.

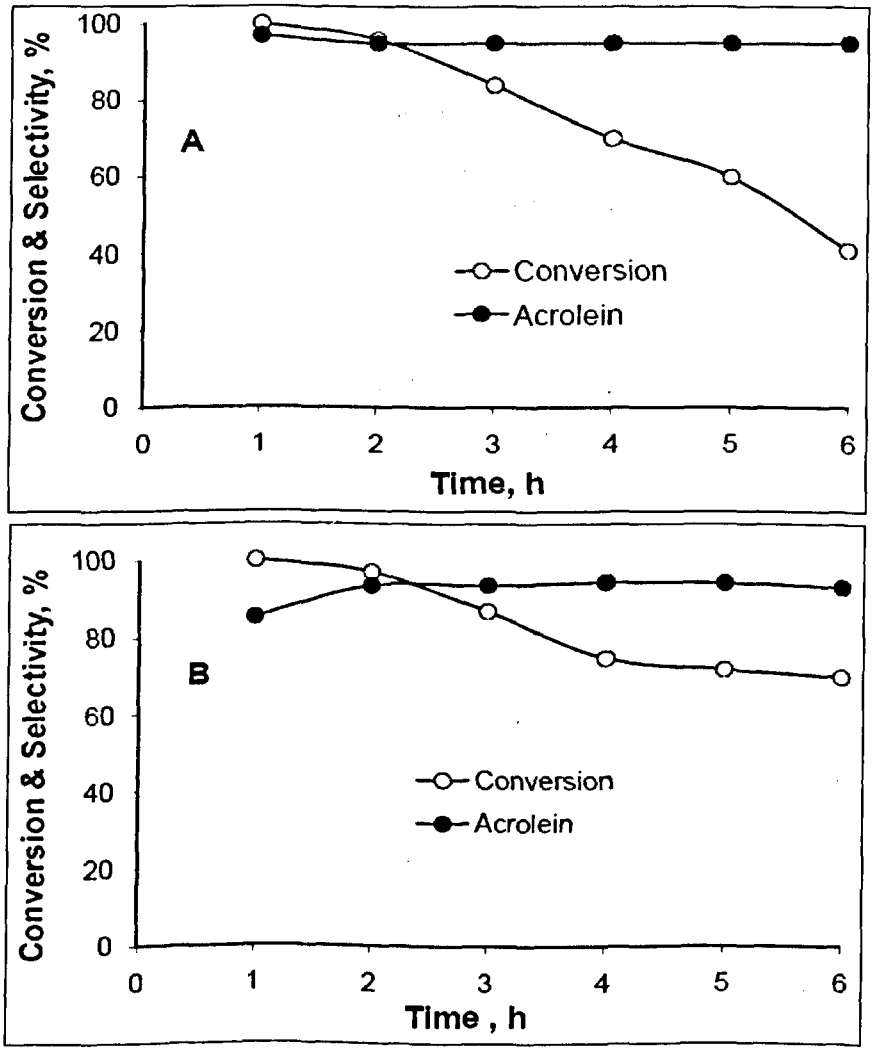


**Figure 6.3** Time course for glycerol dehydration at 275 °C over (A) 20%HPW/$SiO_2$ in $N_2$ flow and (B) 2%Pd/20%HPW/$SiO_2$ in $H_2$ flow.

It should be noted that Pt is usually more active than Pd in alkane hydroisomerisation over bifunctional catalysts. Therefore, the question arises why is Pd more active than Pt in our case? The reason for this could be that the nature of the coke formed is different in these reactions. In alkane hydroisomerisation, the coke is mainly formed by olefin polymerisation, hence it has a hydrocarbon composition. In glycerol-to-acrolein dehydration, the coke is likely to form by acrolein polymerisation and, therefore, comprises of oxygenated hydrocarbons. It is

conceivable; therefore, that Pd is more effective than Pt in inhibiting the formation of oxygenated coke.

## 6.4 Mechanistic considerations

It has been suggested that the dehydration of glycerol to acrolein proceeds through the formation of 3-hydroxypropanal and acetol as the primary products, with the former further dehydrated to acrolein, whereas the latter is a relatively stable by-product (Scheme 6.1) [8-14]. We tested the reactivity of acetol in our conditions at 275°C passing 5 wt% aqueous solution of acetol over CsPW in $N_2$ flow and over 0.5%Pd/CsPW in $H_2$ flow (acetol WHSV = 1.4 $h^{-1}$). Neither of these tests showed any conversion of acetol, thus confirming that acetol indeed is a relatively stable by-product in our system. Notably, we did not observe any hydrogenation of acetol to 1,2-propanediol with Pd/CsPW, although this reaction has been reported to occur in other systems [15]. This result can be explained by the large excess of steam in our system. Another conclusion that can be drawn from the lack of acetol conversion is that in our system the coke is mainly originated from acrolein and maybe to some extent from 3-hydroxypropanal (Scheme 6. 2).

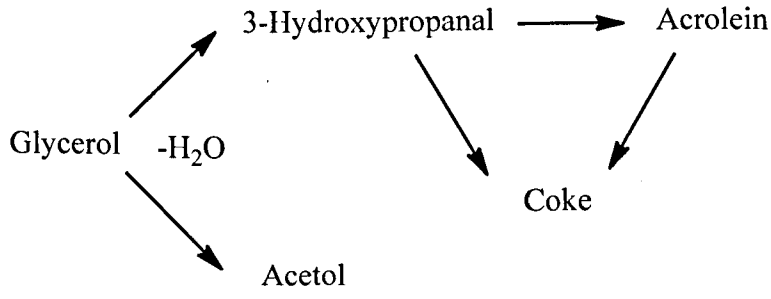


**Scheme 6.2** Reaction pathway for glycerol dehydration to acrolein.

Previous work on glycerol dehydration suggests that acrolein forms on strong Brønstead acid sites [8-14]. Consequently, tungsten heteropoly acids such as $H_3PW_{12}O_{40}$ and $H_4SiW_{12}O_{40}$ and the CsPW heteropoly salt presented here, which are all strong, purely Brønsted acids, are amongst the most efficient catalysts for the synthesis of acrolein. In this context, it was interesting to test a purely Lewis solid acid catalyst for the synthesis of acrolein. As such, we tested Zn(II)-Cr(III) (1:1) mixed oxide and its Pd-doped derivative 0.3%Pd/Zn-Cr. Recently, these catalysts have been found active for dehydroisomerisation of α-pinene to p-cymene [41] and hydrogenation of acetone to methyl isobutyl ketone [30], and the acid properties of Zn-Cr oxide have been characterised in detail [30].

Figures 3.25 and 3.6 (Section 3.7.2) show the DRIFT spectra of pyridine adsorbed on CsPW and Zn-Cr (1:1) oxide, which give clear evidence of the nature of acid sites in these catalysts. As expected, the CsPW possesses Brønsted acid sites as indicated by the strong band at 1540 $cm^{-1}$. In contrast, the Zn-Cr oxide possesses only Lewis acid sites as evidenced by the strong band at 1450 $cm^{-1}$. These Lewis sites have been found to be of moderate acid strength with an enthalpy of $NH_3$ adsorption of 155 $kJmol^{-1}$ [30].

Table 6.5 and Figure 6.4 show the performance of Zn-Cr and 0.3%Pd/Zn-Cr catalysts in acrolein dehydration. In contrast to CsPW, these catalysts were not active at 275°C due to their weaker acidity, but showed a moderate activity at 300 – 350°C, with good performance stability for 5 – 6 h on stream (Fig. 8). The important result is that these catalysts gave acetol as the main product with the selectivity (31 – 42%) greater than, or equal to, that of acrolein (30 – 34%).

**Table 6.5** Glycerol dehydration over Zn-Cr (1:1) mixed oxide catalyst[a]

| Catalyst | Gas flow | T (°C) | Conversion (%) | Selectivity (%) | | |
|---|---|---|---|---|---|---|
| | | | | Acrolein | Acetol | Others |
| Zn-Cr | $N_2$ | 275 | ≤ 1 | | | |
| Zn-Cr | $N_2$ | 300 | 9 (13) | 34 (38) | 42 (40) | 24 |
| Zn-Cr | $N_2$ | 350 | 18 (25) | 30 (30) | 40 (32) | 30 |
| 0.3%Pd/Zn-Cr | $H_2$ | 350 | 49 (44) | 32 (23) | 31 (22) | 37 |

a) Reaction conditions as in Table 2. Glycerol conversion and product selectivity are after 5 h time on stream, in brackets after 1 h on stream.

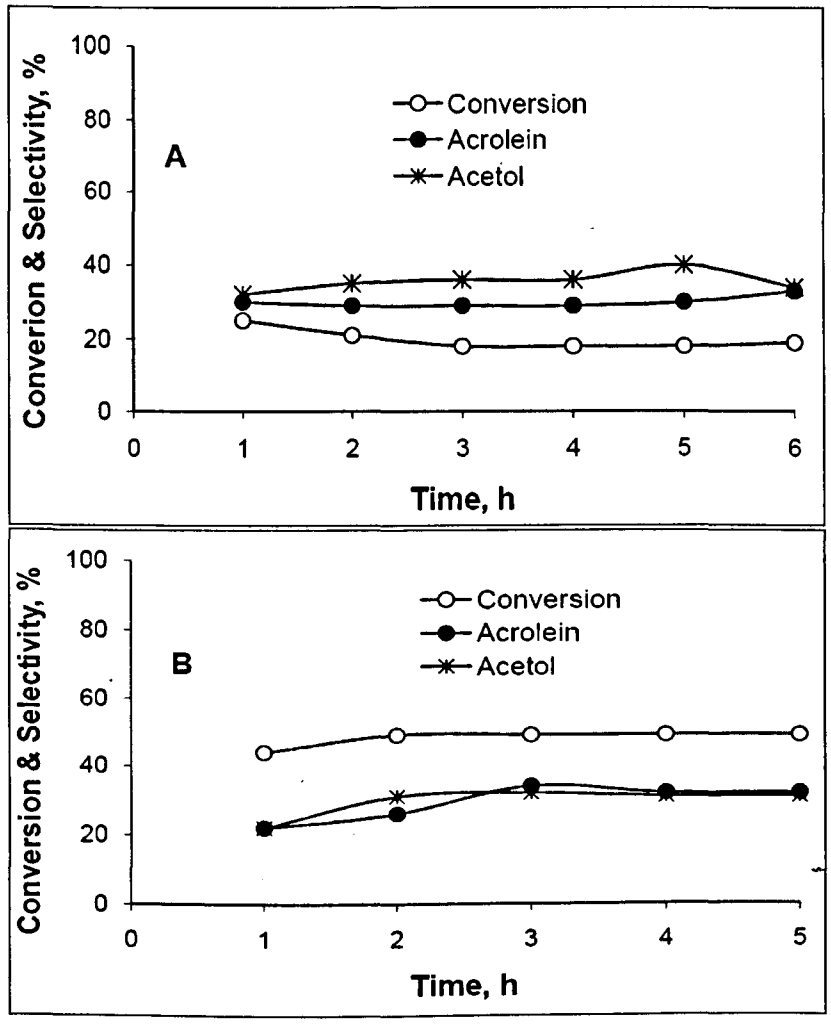


**Figure 6.4** Time course for glycerol dehydration at 350 °C over (A) Zn-Cr (1:1) in $N_2$ flow and (B) 0.3%Pd/Zn-Cr (1:1) in $H_2$ flow.

It is logical, therefore, to suggest that acetol was formed on Lewis acid sites whereas acrolein on Brønsted acid sites. Although Brønsted sites were not available in the fresh Zn-Cr oxide, they could be generated by interaction of the Lewis sites with steam present in the system to give rise to the acrolein formation.

We propose the following mechanistic schemes to explain these results. Scheme 6.3 represents glycerol dehydration on strong Brønsted proton sites and Scheme 6.4 on Lewis sites. Since proton transfer is not limited by steric constrains, interaction of glycerol with a proton site should mainly lead to the protonation of the internal oxygen in the glycerol molecule, which possesses a higher negative charge compared to the terminal oxygens (Scheme 6.3). Subsequent steps involve elimination of $H_3O^+$ to give 1,3-dihydroxypropene and its tautomerisation to 3-hydroxypropanal. The latter undergoes further acid-catalysed dehydration to yield acrolein. Finally, the proton site is regenerated by the interaction of its conjugate base with $H_3O^+$. Similar mechanism for acrolein formation has been suggested previously [8-14].

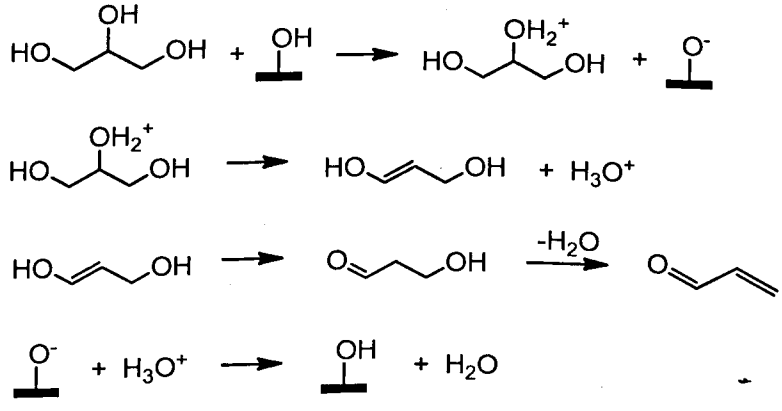

**Scheme 6.3** Mechanism of glycerol dehydration on Brønsted acid sites.

Interaction of glycerol with Lewis acid sites occurs differently, as indicated by our results with Zn-Cr oxide. This interaction, in contrast to the glycerol protonation above, is bound to be affected by steric constrains. As a result, it is the terminal OH group of glycerol rather than the internal one that is more likely to interact with Lewis acid site as shown in Scheme 6.4, where two oxo-bridged metal ions (M) represent the Lewis acid site in the Zn-Cr oxide. Concerted transfer of the terminal OH group of glycerol to the M and migration of the $H^+$ from the internal carbon atom to the bridging O atom of the oxide gives 2,3-dihydroxypropene together with the hydrated active site in the catalyst. The 2,3-dihydroxypropene is then tautomerised to yield acetol, and the Lewis acid site is regenerated by thermal dehydration of its hydrated form.

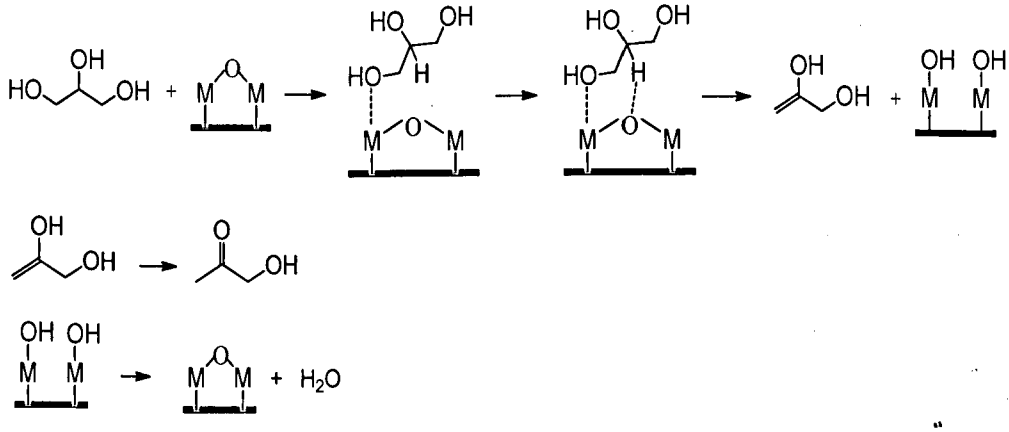


**Scheme 6.4** Mechanism of glycerol dehydration on Lewis acid sites.

The proposed mechanisms (Scheme 6.3 and 6.4) adequately represent the dehydration of glycerol on Brønsted and Lewis acid sites. New evidence presented here regarding the nature of acid sites required for the dehydration of glycerol to acrolein supports the importance of strong Brønsted sites for this reaction.

## 6.5 Conclusions

This study has demonstrated that the water-insoluble Cs heteropoly salt, $Cs_{2.5}H_{0.5}PW_{12}O_{40}$ (CsPW), possessing strong Brønsted acid sites and high water tolerance is an active catalyst for the dehydration of glycerol to acrolein in the gas-phase process at 275°C and 1 bar pressure. The catalyst exhibits high initial activity, with a glycerol conversion of 100% at 98% acrolein selectivity. The activity, however, decreases significantly with the time on stream due to catalyst coking, without impairing acrolein selectivity. It has been found that doping CsPW with platinum group metals (PGM) together with co-feeding hydrogen improves catalyst stability to deactivation, while maintaining high selectivity to acrolein. The enhancing effect of PGM increases in the order: Ru ~ Pt < Pd. The catalyst 0.5%Pd/CsPW performs with a turnover frequency of 320 $h^{-1}$ at 275°C and 5 h time on stream and gives 96% acrolein selectivity at 79% glycerol conversion (76% yield). It provides a specific rate of acrolein production of 23 mmol $h^{-1}g_{cat}^{-1}$, which exceeds the specific rates reported in the literature for supported Keggin heteropoly acids (5 – 11 mmol $h^{-1}g_{cat}^{-1}$ per total catalyst mass). New mechanistic evidence has also been obtained regarding the nature of acid sites required for the dehydration of glycerol to acrolein, which supports the importance of strong Brønsted sites for this reaction.

## References


[1] A. Corma, S. Iborra, A. Velty, Chem. Rev. 107 (2007) 2411.

[2] M. Pargliaro, R. Ciriminna, H. Kimura, M. Rossi, C. Della Pina, Angew. Chem. Int. Ed. 46 (2007) 4434.

[3] C. Zhou, J.N. Beltramini, Y. Fan, G. Q. Lu, Chem. Soc. Rev. 37 (2008) 527.

[4] Y. Zheng, X. Chen, Y. Shen, Chem.Rev. 108 (2008) 5253.

[5] A. Behr, J. Eilting, K. Irawadi, J. Leschinski, F. Lindner, Green Chem. 10 (2008) 13.

[6] G. W. Huber, J. W. Shabaker, J. A. Dumesic, Science 300 (2003) 2075.

[7] K. Weissermel, H. J. Arpe, Industrial Organic Chemistry, 3rd ed., Wiley, 1997.

[8] B. Katryniok, S. Paul, M. Capron, F. Dumeignil, Chem. Sus. Chem. 2 (2009) 719.

[9] E. Tsukuda, S. Sato, R. Takahashi, T. Sodesawa, Catal. Commun. 8 (2007) 1349.

[10] H. Atia, U. Armbruster, A. Martin, J. Catal. 258 (2008) 71.

[11] S. H. Chai, H. P. Wang, Y. Liang, B .Q. Xu, Green Chem. 10 (2008) 1087.

[12] S. H. Chai, H. P. Wang, Y. Liang, B.Q. Xu, Appl. Catal. A 353 (2009) 213.

[13] W. Suprun, M. Lutecki, T. Haber, H. Papp, J. Mol. Catal. A 309 (2009) 71.

[14] A. Corma, G.W. Huber, L. Sauvanaud, P. O'Connor, J. Catal. 257 (2008) 163.

[15] C. W. Chiu, M. A. Dasari, G. J. Suppes, W. R. Sutterlin, AIChE J. 52 (2006) 3543.

[16] S. Sato, M. Akiyama, R. Takahashi, T. Hara, K. Inui, M. Yokota, Appl. Catal. A 347 (2008) 186.

[17] J. L. Dubois, C. Duquenne, W. Hoelderich, J. Kervennal, WO 2006087084 (2006).

[18] H. Kasuga, M. Okada, JP 2008137950 (2008).

[19] Y. Arita, H. Kasuga, M. Kirishiki, JP 2008110298 (2008).

[20] I. V. Kozhevnikov, J. Mol. Catal. A 305 (2009) 104.

[21] T. Okuhara, N. Mizuno, M. Misono, Adv. Catal. 41 (1996) 113.

[22] M. Boudart, Chem. Rev. 95 (1995) 661.

[23] I. V. Kozhevnikov, Chem. Rev. 98 (1998) 171.

[24] T. Okuhara, Chem. Rev. 102 (2002) 3641.

[25] J. A. Moulijn, P. W. N. M. van Leeuwen, R. A. van Santen (Eds.), Catalysis, Elsevier, Amsterdam, 1993.

[26] A. Chica, A. Corma, J. Catal. 187 (1999) 167.

[27] Y. Izumi, M. Ono, M. Kitagawa, M. Yoshida, K. Urabe, Microporous Mater. 5 (1995) 255.

[28] A. Alhanash, E. F. Kozhevnikova, I. V. Kozhevnikov, Catal. Lett. 120 (2008) 307.

[29] E. F. Kozhevnikova, E. Rafiee, I. V. Kozhevnikov, Appl. Catal. A 260 (2004) 25.

[30] F. Al-Wadaani, E.F. Kozhevnikova, I.V. Kozhevnikov, J. Catal. 257 (2008) 199.

[31] K. Katamura, T. Nakamura, K. Sakata, M.Misono, Y. Yoneda, Chem. Lett. (1981) 89.

[32] J. E. Benson, M. Boudart, J. Catal. 4 (1965) 704.

[33] J. E. Benson, H.S. Hwang, M. Boudart, J. Catal. 30 (1973) 146.

[34] E. F. Kozhevnikova, I. V. Kozhevnikov, J. Catal. 224 (2004) 164.

[35] T. Baba, Y. Hasada, M. Nomura, Y. Ohno and Y. Ono, J. Mol. Catal. A 114 (1996) 247.

[36] T. Okuhara, Appl. Catal. A 256 (2003) 213.

[37] N. Essayem, Y. Ben Taârit, P. Y. Gayraud, G. Sapaly, C. Naccache, J. Catal. 204 (2001) 157.

[38] N. Essayem, Y. Ben Taârit, C. Feche, P. Y. Gayraud, G. Sapaly, C. Naccache, J. Catal. 219 (2003) 97.

[39] J. Barbier, Stud. Surf. Sci. Catal. 34 (1987) 1.

[40] T. Okuhara, H. Watanabe, T. Nishimura, K. Inumaru, M. Misono, Chem. Mater. 12 (2000) 2230.

[41] F. Al-Wadaani, E. F. Kozhevnikova, I. V. Kozhevnikov, Appl. Catal. A 363 (2009) 153.

# 7. Conclusions

The current worldwide concerns about the finite nature of fossil fuel, the present energy source, and the global warming issue have made the synthesis of fuel and chemicals from catalytic transformation of bio-sustainable resources a global challenge. Biodiesel fuel, as an example, has received a much attention as a substitute for fossil fuel, and the worldwide production of biodiesel by transesterification of plant oils and animal fats has increased drastically. This has created a large surplus of glycerol, the by-product of biodiesel process with approximately 10% of the total product by mass. Therefore, it is of great industrial interest to utilise glycerol as renewable feedstock for the synthesis of value-added chemicals. Due to its rich functionality, glycerol can be used to produce a large number of value-added chemicals. Catalysis represents a fundamental approach towards the development of green utilisation of glycerol. Multifunctional catalysis, in particular, is a promising direction, not only for technologies that use glycerol but also for sustainable organic synthesis, to effect multi-step reactions in one-pot system without intermediate separations.

1,2-PDO is an important commodity chemical, which finds use as an antifreeze, aircraft deicer and lubricant. 1,3-PDO is copolymerised with terephthalic acid to produce polyesters, which are used for manufacturing carpet and textile fibres exhibiting strong chemical and light resistance. 1,2-PDO and 1,3-PDO are currently produced from petroleum derivatives by chemical catalytic routes: 1,2-PDO from propylene oxide and 1,3-PDO from ethylene oxide or acrolein. These diols can be produced by an alternative route involving hydrogenolysis of glycerol. The

hydrogenolysis of glycerol to 1,2-PDO and 1,3-PDO is suggested to proceed via dehydration of glycerol to acetol and 3-hydroxypropanal by acid catalysis followed by catalytic hydrogenation. This mechanism is supported by the observation of acetol amongst the reaction products and its selective hydrogenation to 1,2-PDO. Alternatively, dehydrogenation of glycerol to glyceraldehyde followed by dehydration to 2-hydroxyacrolein and then hydrogenation to yield 1,2-PDO is also suggested. These mechanisms imply that bifunctional acid/hydrogenation catalysis should be an effective course to carry out the hydrogenolysis of glycerol in one-pot system.

Acrolein is an important intermediate for the chemical and agricultural industries and is currently produced by oxidation of petroleum-derived propene. It can also be obtained from glycerol via acid-catalysed dehydration in the gas or liquid phase. The development of an alternative environmentally benign process for the production of acrolein based on the biomass-derived glycerol as a sustainable feedstock is highly desirable. The dehydration of glycerol using acid catalysts is suggested to occur via the formation of 3-hydroxypropanal, with 1-hydroxyacetone (acetol) formed as a relatively stable by-product. This may indicate that Lewis acid sites and metal sites are important for the formation of acetol, whereas the formation of 3-hydroxypropanal followed by its dehydration to acrolein is favoured in the presence of strong Brønsted acid sites.

The aim of this work is to study the liquid-phase hydrogenolysis of glycerol to propanediols and the gas-phase dehydarion of glycerol to acrolein using multifunctional catalysis by heteropoly salts modified with ruthenium, platinum, palladium and rhodium. Polyoxometalates (POMs), especially those of Keggin structure, have found numerous applications as catalysts. These are inherently

multifunctional compounds. Solid POMs allow for considerable alteration of their texture and can be modified to introduce another chemical function, e.g. metal function. Among POM materials, caesium 12-tungstophosphate $Cs_{2.5}H_{0.5}PW_{12}O_{40}$ (CsPW) is well known as a water-insoluble strong Brønsted acid and a versatile solid acid catalyst possessing considerable thermal stability (≥ 500 °C). This project aims also to investigate liquid-phase hydrogenolysis of glycerol using bifunctional catalysis by niobium oxide doped with ruthenium and rhodium. Hydrated niobium oxide is also known to be relatively strong solid acid catalyst and is water-tolerant in water-involving organic reactions.

The catalysts under study were prepared according to the literature procedures and characterised by number of physical and chemical techniques. The characterisation results confirmed that all catalysts under study are mesoporous materials with high surface areas (200 – 85 $m^2/g$) and average pore diameters of 24 – 175 Å. FTIR and XRD measurements reveal that catalysts maintained their structure after use in the liquid phase glycerol hydrogenolysis and gas phase dehydration of glycerol. However, UV spectroscopy and ICP analysis show that in the case of CsPW catalyst leaching of heteropoly anions into solution of liquid phase glycerol hydrogenolysis can occur. Hydrogen titration experiments demonstrated the presence of Rh, Pd and Pt metals in high dispersion state compared to Ru metal, which could probably be due to insufficient reduction of metal precursor ($RuCl_3$) to Ru metallic phase ($Ru^0$). CsPW and CsSiW were found to possess purely Brønsted acid sites whereas $Nb_2O_5$ contain both Brønsted/Lewis sites, as presented by FTIR study of pyridine adsorption. On the other hand, Zn-Cr (1:1) mixed oxide show only Lewis sites. From ammonia adsorption calorimetry, the acid strength of catalysts under study decreases in the order: $Cs_{2.5}H_{0.5}PW_{12}O_{40} > Nb_2O_5 \approx C_{3.5}H_{0.5}SiW_{12}O_{40}$.

Ru/CsPW is an active bifunctional catalyst for the hydrogenolysis of glycerol providing 1,2-propanediol with 96% selectivity at 21% conversion under mild conditions, 150 °C and very low hydrogen pressure of 5 bar. This result is significant as it shows that the hydrogenolysis of glycerol can be carried out under very low pressure of hydrogen, compared to the high pressure that has been traditionally applied. Our results demonstrate that liquid-phase glycerol hydrogenolysis proceeds even in the absence of externally-added hydrogen. In this system, $H_2$ is supplied by the liquid phase reforming of glycerol over Ru metal. Hydrogen can further be consumed in the hydrogenation of acetol to 1,2-PDO. The recent literature publications established number of catalytic processes for glycerol transformation to propanediols without externally added hydrogen.

Rh catalyst is more selective to 1,3-PDO and 1-propanol. The main product with the Rh catalyst was 1,2-PDO (65% selectivity), as with Ru catalyst. Both functionalities, metal hydrogenation (Ru, Rh) and acidity (CsPW), are essential for the hydrogenolysis reaction to proceed. Without Ru, CsPW was inactive, while Ru showed moderate activity in the absence of acidic support such as Ru/C. The absence of acetol amongst products when the reaction is carried out with CsPW without Ru present, although it forms in the presence of Ru/CsPW, suggests that the reaction is more likely to proceed via glyceraldehyde intermediate by dehydrogenation of glycerol over Ru sites.

Comparable results were obtained using $Ru/Nb_2O_5$ catalyst. However, $Ru/Nb_2O_5$ was more active and stable in contrast to Ru/CsPW. 29% conversion of glycerol and 69% 1,2-PDO selectivity were achieved with $Ru/Nb_2O_5$ at 180 °C, 10 h and 10 bar of $H_2$. The catalyst performance was significantly affected by the catalyst calcination temperature and preparation method. This is because the acidity of $Nb_2O_5$

decreases with increasing calcination temperature. Commercial $Nb_2O_5$ that possesses very low BET surface area showed poor activity for glycerol hydrogenolysis. The order of catalyst activity in glycerol conversion is: $Nb_2O_5$ (dried at 100 °C) > $Nb_2O_5$ (calcined at 500 °C) ≈ CsPW > CsSiW > $Nb_2O_5$ commercial. This order indicates that moderate rather than strong acidity of catalyst is required for glycerol conversion and it is the total catalyst acidity rather than the acid strength that plays a key role in this reaction. $H_2$ was also generated in-situ when reaction was carried out over $Ru/Nb_2O_5$ in the absence of externally added hydrogen. This is again due the reforming activity of Ru under such conditions. $Nb_2O_5$ itself was inactive but with Ru present, a high activity was achieved. This suggests that hydrogenolysis of glycerol by Ru-doped acidic supports may be initiated by glycerol dehydrogenation over Ru sites to produce glyceraldehyde, as proposed by Montassier et al.

A reaction network for glycerol hydrogenolysis over $Ru/Nb_2O_5$ catalyst consisting of three parallel pathways can be constructed as follows:

1) Dehydrogenation of glycerol to glyceraldehyde, which is dehydrated to 2-hydroxyacrolein. 1,2-PDO forms from 2- hydroxyacrolein by two routes including hydrogenation of either the C=C or C=O bond in 2-hydroxyacrolein over Ru sites. The C=C hydrogenation gives 2-hydroxypropanal. Acetol is formed by the C=O hydrogenation followed by enol–ketone rearrangement. Both the acetol and 2-hydroxypropanal intermediates can be further hydrogenated to yield 1,2-PDO.
2) Reforming of glycerol. This reaction was confirmed by the presence of $H_2$ among reaction products when the reaction was carried out over Ru/CsPW and $Ru/Nb_2O_5$ without externally added hydrogen.

3) C-C cleavage to form EG and C1 products. EG can undergo hydrogenolysis and reforming to form ethanol, $H_2$ and other gaseous products.

The dehydration of glycerol to acrolein in the gas-phase occurs over CsPW catalyst at 275 °C and 1 bar pressure. In contrast, as reported by others, metal oxide catalysts such as copper-containing catalysts selectively form 1,2-PDO via acetol intermediate in the liquid as well as the gas phase. The CsPW catalyst exhibits high initial activity, with a glycerol conversion of 100% at 98% acrolein selectivity. The activity, however, decreases significantly with the time on stream due to catalyst coking, without impairing acrolein selectivity. It has been found that doping CsPW with platinum group metals (PGM) together with co-feeding hydrogen improves catalyst stability to deactivation, while maintaining high selectivity to acrolein. The enhancing effect of PGM increases in the order: Ru ~ Pt < Pd. The catalyst 0.5%Pd/CsPW performs with a turnover frequency of 320 $h^{-1}$ at 275°C and 5 h time on stream and gives 96% acrolein selectivity at 79% glycerol conversion (76% yield). New mechanistic evidence has been obtained regarding the nature of acid sites required for the dehydration of glycerol to acrolein, which supports the importance of strong Brønsted sites for acrolein formation from glycerol in gas phase.